Università degli Studi di Milano

Department of Biosciences

PhD Course in Environmental Sciences

THE ROLE OF PLASTICS AS CARRIER OF ENVIRONMENTAL POLLUTANTS: AN INTEGRATED APPROACH TO ASSESS TOXICITY ON AQUATIC AND TERRESTRIAL SPECIES

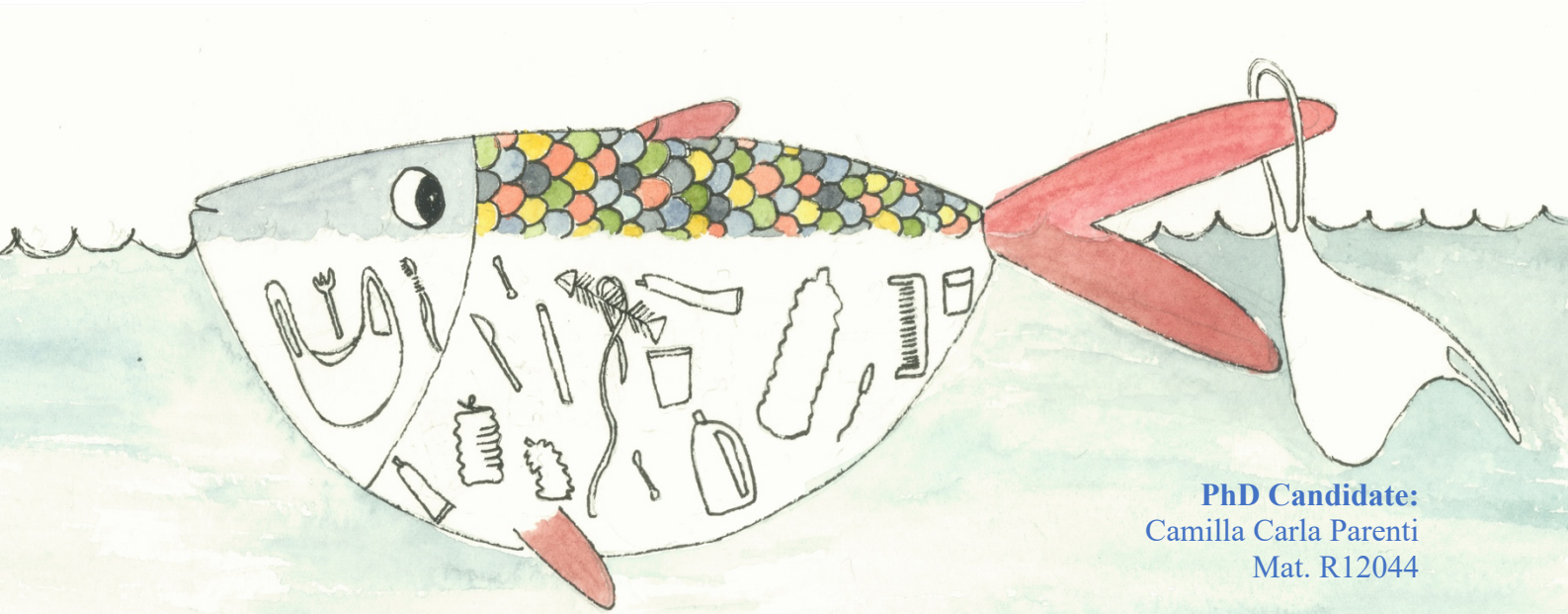

PhD Candidate:
Camilla Carla Parenti
Mat. R12044

Academic Tutor:
Prof. Andrea Binelli

XXXIII Cycle
Academic year 2019-2020

I would like to thank all the students that helped me during these three years,
I hope that their dedication and their enthusiasm will make them go far,
and Margherita for her amazing hand and watercolours.

ABSTRACT

The uniqueness of plastic is given by its several advantages, including low cost, lightweight, flexibility and resistance. These properties exponentially increased the global demand for plastic in the last 70 years, turning this revolutionary material into a global environmental threat. Indeed, the mismanagement of plastic waste, most of which is still sent to landfills or directly littered in the environment by human improper behaviour, is becoming a serious threat for ecosystems. The effects of plastic dispersal in the environment potentially increase when considering the fragments of smaller dimension, which derive from the degradation of macroplastics or are intentionally produced for industrial applications. A lower dimension may therefore enhance the plastic fragment capacity to accumulate at tissue level, but also to act as vector for chemical contaminants. The project was aimed at evaluating the environmental impact due to the presence of micro- and nanoplastics, exposing aquatic and terrestrial species and observing the potential adverse effects using multi-tiered approaches. Several laboratory experiments were conducted using both freshwater model species, the vertebrate *Danio rerio* and the invertebrate *Dreissena polymorpha*, and, for the first time, the terrestrial model *Bombyx mori*. Moreover, the role of plastics as carrier of environmental contaminants was investigated on zebrafish larvae. All organisms showed the accumulation of plastics and their infiltration in different tissues. The biochemical analyses highlighted only slight effects of micro- and nanoplastic exposures, while more relevant results emerged from behavioural tests, which deserve further studies. Furthermore, the effects at individual level, combined with proteomic analyses, pointed out a shift in the toxicity of plastics and chemical contaminants when co-administered, suggesting a more complicated relationship then an additive or synergistic effect. Finally, the study paves the way for the use of *B. mori* larva as model organism for the evaluation of the effects of plastic particles on terrestrial ecosystems, which are still largely unknown.

TABLE OF CONTENT

1. INTRODUCTION

1.1 The Plastic Age

Nowadays, plastic has become almost irreplaceable, being the most cheap and resistant material in commerce (Frias and Nash, 2019). We are living in the so-called "Plastic Age", with plastic infrastructure, and industrial and consumer products that are prevalent and play a crucial role across every aspect of our daily life (Osborn and Stojkovic, 2014). The development of plastic materials began in the 19th century with the use of some materials, such as chewing gum or shellac, that naturally display plastic properties (Harrison and Hester, 2018). Then, the development of plastic industry really expanded, giving birth to a huge range of types of polymers, including chemically modified natural materials (rubber, nitrocellulose, collagen) and the modern synthetic materials, such as thermoset plastics and thermoplastics (Andrady and Neal, 2009). Nowadays, within the multitude of plastic materials commercially available, six polymers account for about the 80% of the total plastic demand (Fig. 1), namely polypropylene (PP), polyethylene (PE), polyvinyl chloride (PVC), polyurethanes (PUR), polyethylene terephthalate (PET) and polystyrene (PS).

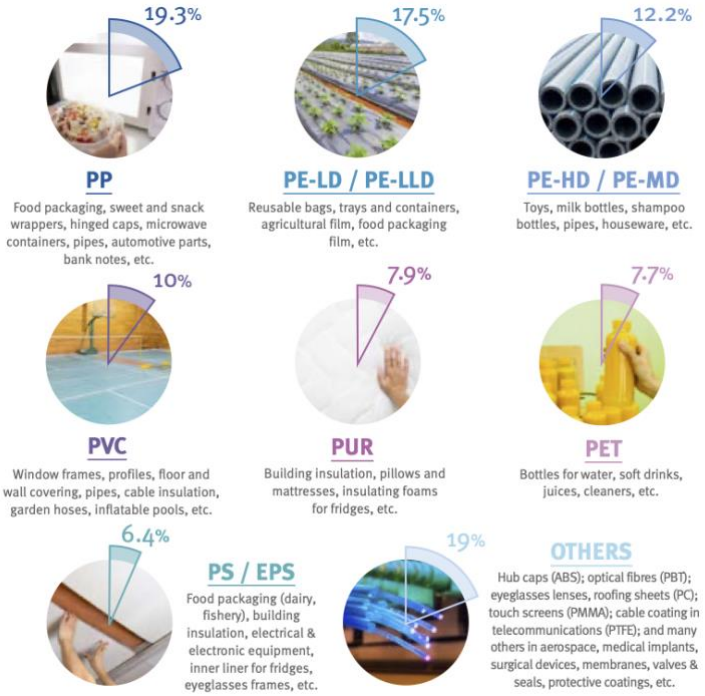

Fig. 1. European plastic demand by polymer type in 2018 (PlasticsEurope, 2019). (PP = polypropylene; PE-LD = low-density polyethylene; PE-LLD = linear low-density PE; PE-HD = high-density PE; PE-MD = branched medium-density PE; PVC = polyvinyl chloride; PUR = polyurethane; PET = polyethylene terephthalate; PS, EPS = polystyrene and expanded PS).

All existing plastic polymers are classified in two main groups: thermoplastics and thermosets. The former become soft when heated and, after production, they can be re-heated and will soften and melt again (Rhodes, 2018). For this reason, this type of plastic can be recycled. On the contrary, thermosets can no longer be melted down once they have been produced (Rhodes, 2018).

In detail, PP and PE, two of the principal thermoplastics, are included in the family of polyolefins, a class of synthetic resins prepared by the polymerization of olefins. Their versatility is reflected by a huge range of possible applications, from packaging, automotive and building, to medical and consumer products. PE is further classified into several categories based on its density, which strictly depends on branching: high-density PE (HDPE), branched low-density PE (LDPE), medium-density PE (MDPE, and linear low-density PE (LLDPE) (Okamura, 2014).

PVC is a synthetic resin made from vinyl chloride and it is included in the family of vinyls (Takeoka, 2014). It is one of the earliest thermoplastic materials and, being a very flexible material, it is widely used for flooring, electrical insulations and roofing membranes (Harrison and Hester, 2018).

PUR are a versatile class of thermoset plastic materials containing multiple carbamate functional groups in the polymer chain (Barksby et al., 2014). They are highly resistant, flexible and durable, and these features lend themselves to differing applications, from building insulation, to electrical appliances, to automotive (Nicholson, 2017).

PET is a synthetic semi-aromatic polyester belonging to the thermoplastic group (Ohishi and Otsuka, 2014). The high resistance and toughness make it suitable for a huge range of recreation and household goods and one of the main plastic materials used for food and drink packaging (Kint and Munoz-Guerra, 1999).

PS is one of the most popular thermoplastic resins (Terashima, 2014). Its commercial production began in 1930 and it is now globally used for the production of several goods essential for our daily life (food packaging, electronics, insulation panels, medical items, etc.) (Ho et al., 2018).

The properties of these polymers, together with their low cost, make the public demand for plastic materials constantly increasing, as showed by data on global plastic production, which raised from 2

million tonnes in 1950 to 360 million tonnes in 2018 (PlasticsEurope, 2019). Future previsions report that this amount is expected to quadruple by 2050 (Suaria et al., 2016).

Even if the invention of plastic has brought several advantages, its overexploitation and mismanaged waste turned this revolutionary material into a global environmental threat. Challenges concerning plastic waste management combined with the continuously increased demand for plastic materials pose a serious threat to the environment and have now become one of the most debated environmental issues (Thompson et al., 2009). Essentially, there are three different fates for plastic waste: recycling, incineration and disposal (Geyer et al., 2017). Even if the rate of plastic recycling is extremely variable among countries (Jambeck et al., 2015), it is still the lower percentage (less than 20%) compared to the amount of plastic waste that is incinerated or discarded (Geyer et al., 2017). Moreover, pre-established recycling systems do not exist for all polymers (d'Ambrières, 2019), and several plastic waste fractions (derived from packaging, electronics, or transport and construction sectors) need high cost and intensive sorting to re-obtain high-quality recycled resins that can substitute raw materials (Hahladakis et al., 2018). Energy recovery from waste plastics is another alternative to reduce landfill volumes, but it does not reduce the demand for fossil fuels and hazardous chemicals are released in the environment during the process (Alabi et al., 2019).

However, the development of suitable polymers and the implementation of these alternatives is a slow process and, in 2018, more than 7 million tons of European plastic waste (more than 3 million tons deriving from plastic packaging), were still sent to landfills (PlasticsEurope, 2019). Plastic waste present in landfills or dumpsites will persist in the environment and potentially release chemical additives in the surrounding areas (Teuten et al., 2009). The inadequate disposal of plastic waste includes also plastic litter generated by improper human behavior, mostly coming from people living in coastal areas (Jambeck et al., 2015).

The scientific interest was firstly focused on plastic pollution in marine ecosystems, whose inputs reaches 8 million tons per year, following the most recent estimate made by Jambeck et al. (2015) (Fig. 2).

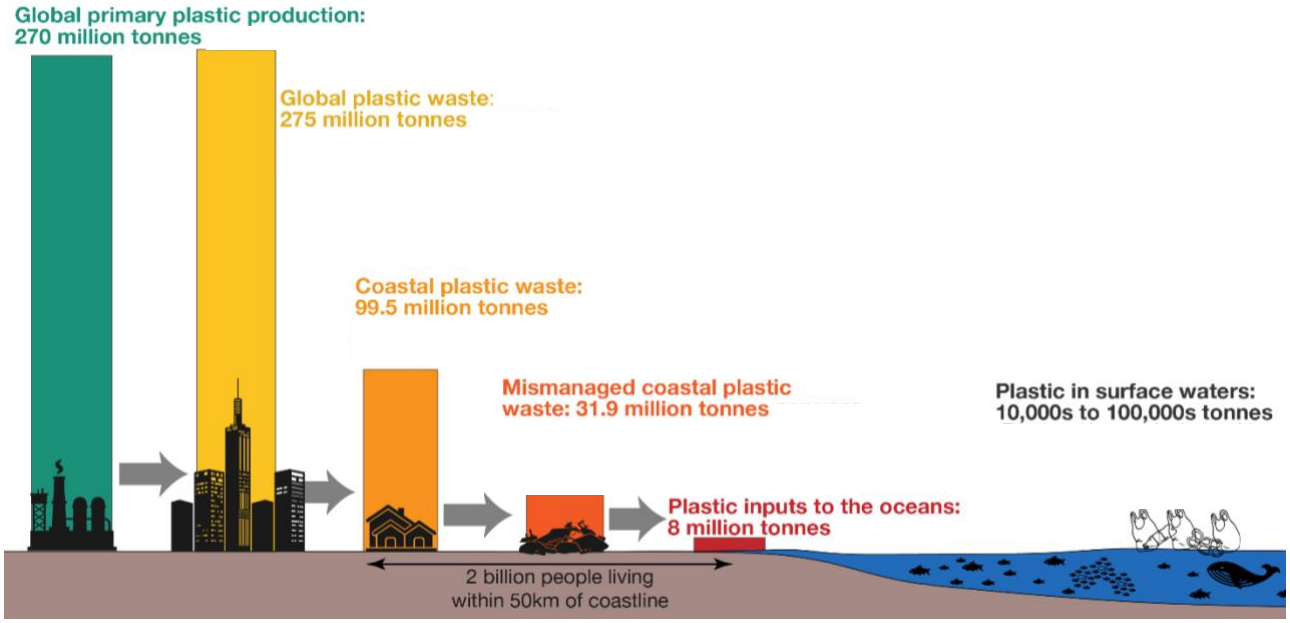

Fig. 2. Estimates of global plastic input into the world's oceans from land-based sources, in 2010 (based on Jambeck et al., 2015).

Once in the oceans, floating plastic debris are transported passively by currents (Li et al., 2020). The highest concentrations are found offshore in the main subtropical ocean gyres, where converging surface currents create real plastic islands (Law and Thompson, 2014). Floating debris are obviously the most visible impacts of plastic contamination, but the different physical properties of plastic particles enable them to be distributed also in the water column, beached in coastal areas or deposited into deep-sea sediments (Galgani et al. 2015). The same degree of plastic contamination is observed in freshwater ecosystems, as showed by a huge variety of sampling data collected in lakes, rivers, and estuaries (Zeng, 2018). Even if aquatic ecosystems are the most studied with regard to plastic occurrence, the 80% of plastic marine waste comes from terrestrial sources (Andrady, 2011), where plastic contamination is widespread in different environmental compartments, including sediments, soils, and air (Shen et al., 2019).

The ubiquitous distribution in marine and freshwater ecosystems is due to their natural conditions, particularly currents, solar radiation, abrasion, and interactions with vessels and organisms, which cause the degradation and fragmentation of plastic items into smaller particles (Frias and Nash, 2019). These smaller plastic debris are considered persistent pollutants and, thanks to their size and physical-

chemical properties, such as lightweight, durability and buoyancy, they have a high dispersion potential that makes the spread into the environment constant and inevitable (Karbalaei et al., 2020).

1.2 Plastic debris: definitions and properties

Plastic debris can be classified based on their origin, size, shape and polymer type (Hartmann et al., 2019). As regard to origins, they can be divided in two classes. The primary plastic particles derive from the manufacturing process of some products for cleaning and personal hygiene, such as hand and facial cleansers, cosmetics, toothpastes, and industrial scrubbers (Cole et al., 2011). Secondary plastic particles derive from the deterioration of larger plastic items, both in sea and land. There are many processes responsible for the creation of secondary plastic particles, which include weathering by physical stress, and photo- and microbial degradation (Andrady, 2011). All these processes reduce the size of plastic to particles and can also change the surface and structural properties of plastic waste, making them potentially more toxic (ter Halle et al., 2016).

Until now there is not a clear consensus on size-related classification of plastic particles, namely the upper and lower dimension limits of macro-, meso-, micro-, and nanoplastics (Fig. 3).

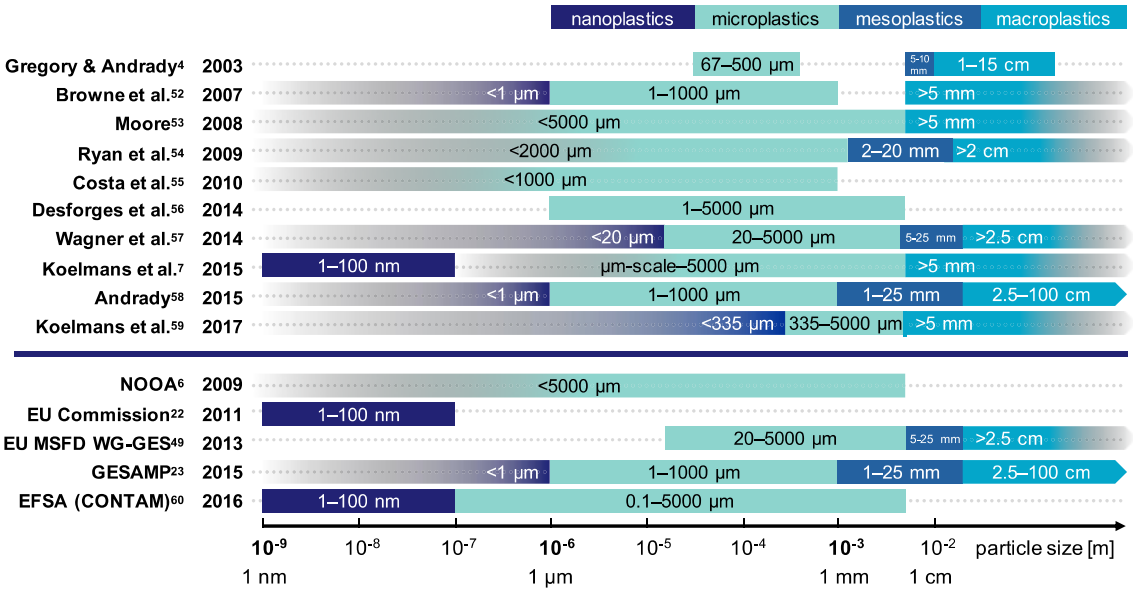

Fig. 3. Examples of different classifications of plastic debris based on size (Hartmann et al., 2019).

One of the most recent and clear classifications proposed by Hartmann et al. (2019) defines macroplastics as particles of size ≥ 1 cm, mesoplastics from 1 to 10 mm, microplastics from 1 to <1000 µm, and nanoplastics from 1 to <1000 nm.

Plastic debris are also sorted by shape and polymer composition (Fig. 4). The shapes most commonly found in the environment are fragments, fibers, pellets and sheets (Hidayaturrahman and Lee, 2019), whereas the most frequently detected polymers are PE, PP, PS, PVC, PC, PET, polyamides (PA), and polyesters (PES) (Rezania et al., 2018).

Different particles present a different sinking behavior in the aquatic environment, which is mostly related to their densities (de Haan et al., 2019), but also to particle sizes and shapes, and water salinity (Kowalski et al., 2016). PE and PP, having lower densities than seawater, tend to float on the sea surface and, being also the highest produced plastic materials, they are the predominant forms of sampled plastics in Mediterranean surface waters (Suaria et al., 2016).

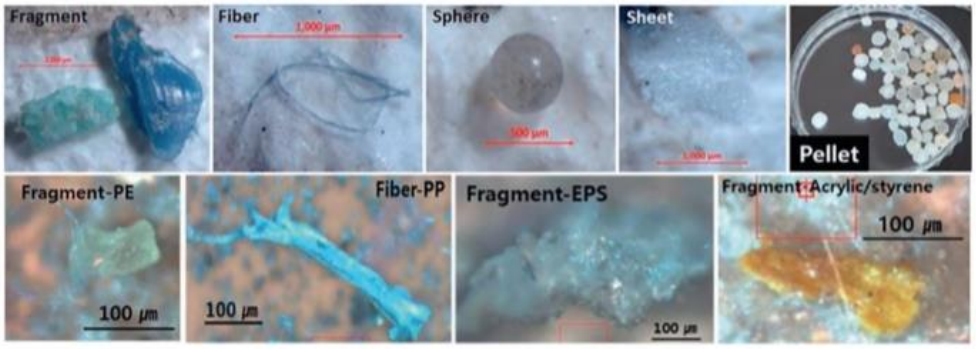

Fig. 4. Examples of different types of plastic debris (Zeng, 2018).

1.3 Micro- and nanoplastics in the environment

1.3.1 Sources

Primary micro- and nanoplastics, such as microbeads or synthetic fibers, are directly released into the environment, through residual industrial effluents or domestic discharges (Oliveira et al., 2019). Even if wastewater treatment plants (WWTPs) were supposed to be one of the major solutions for plastic

pollution, they are now considered as one of the main sources for the aquatic environment, in amounts that depend on treatment facilities and efficiency, temporal factors and sampling methodologies (Zeng, 2018). A recent study comparing the efficiency of different South Korean WWTPs in the removal of microplastics demonstrated how some treatment stages are effective at removing the majority (up to 99.2%) of plastic debris (Hidayaturrahman and Lee, 2019). However, considering the average flow rate of a WWTP, calculated concentrations of discharged plastic can be very high. A study conducted in an important WWTP of Northern Italy, calculated a daily amount of 160,000,000 of particles released by effluent (Magni et al., 2019). These huge amounts could even be underestimated, considering that it has been possible to only quantify particles larger than 0.01 mm, hence underestimating the smaller size classes. Furthermore, the same study reported a significant number of particles retained within the sewage sludge, approximately equal to 3,400,000,000 particles/day, which are highly used in land applications or simply landfilled (Fytili and Zabaniotou, 2008). The agricultural use of sewage sludge is one of the major inputs of smaller plastic debris to terrestrial ecosystems (van den Berg et al., 2020). Indeed, even if the majority of current studies consider terrestrial ecosystems only as a pathway of plastic particle distribution to aquatic environments, they have an important role in the plastic fate. The atmospheric fallout is also responsible for plastic pollution in the terrestrial environment (Chen et al., 2020a). The study of Dris and coll. (2016) is one of the few that investigates the contribution of the atmospheric fallout, reporting a flux of microplastic (synthetic fibers) ranging between 2 and 355 particles/m^2/day in the urban area of Paris. Landfills are also a huge deposit and a potential source of small plastic particles and fibers, since they can be spread to surrounding environments via atmospheric transport (Su et al., 2019).

Furthermore, the environment is being increasingly exposed to secondary micro- and nanoplastics derived from the deterioration of human plastic waste (mostly released by shipping industry and coastal tourism) or from plastic objects that undergo natural erosion and abrasion, such as tires,

mulching film, textiles and paint (GESAMP, 2015). The major sources and distribution pathways of smaller plastic pollution are illustrated in Figure 5.

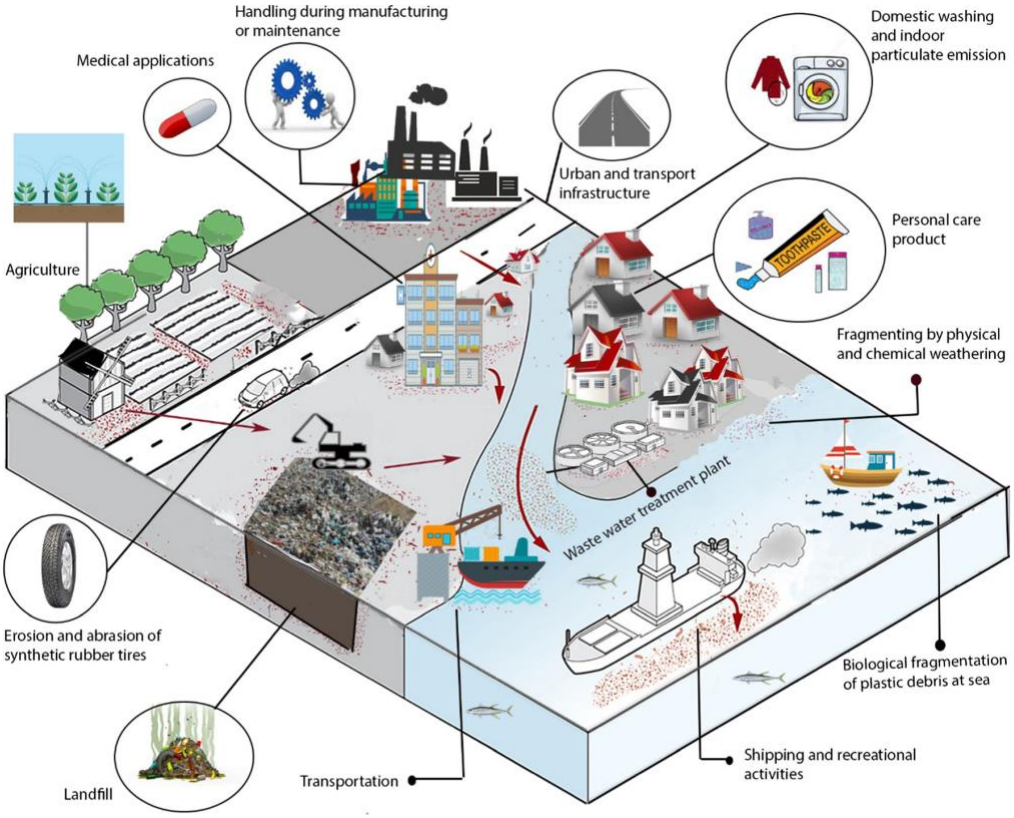

Fig. 5. Sources and pathways of micro- and nanoplastic contamination (Karbalaei et al., 2018).

All these plastic particles are released into the aquatic and terrestrial ecosystems, from which they can be further transported by several pathways such as wind, rainfall and runoff (Kooi et al., 2018), reaching the most remote places from any anthropogenic activities. Accordingly, smaller plastic pollution has been demonstrated even in Antarctic sediments (Munari et al., 2017) and in the Arctic ice (Peeken et al., 2018).

Sampling and analysis of smaller plastics in natural systems is challenging. Thus, reported values of plastic amounts vary widely between studies, and differences in detection methods and their effectiveness make the comparison of data even more difficult. Moreover, the limits of sampling methods (such as mesh sizes and instruments' detection limits) may well underestimate the levels of contamination, excluding particles in the nano-size range (Mattsson et al., 2015). The great difference in plastic abundance depends also on sampling sites. Usually, higher concentrations are reported for

highly populated areas and intense anthropogenic activities (Jambeck et al., 2015). A study conducted in China, one the largest producer of plastic worldwide (PlasticsEurope, 2019), showed that detected microplastic concentrations were significantly negatively correlated with the distance of lakes from the urban area of Wuhan, which accounts for a population >10 million (Wang et al., 2017). Extreme weather conditions may also influence the occurrence of plastics. Wang et al. (2019) showed that the microplastic abundance in the seawaters of Sanggou Bay, an important aquaculture region in China, increased by 40% after the typhoon period. A general overview on microplastic mean range in the main aquatic compartments is shown in Table 1 (Zeng, 2018).

Table 1. Microplastic concentration range in different environmental compartments.

Environmental compartment	**Concentration (n=number of items)**
Sea surface waters	$4.8x10^{-6}$-$1.6x10^{4}$ n/m^3
Lake surface waters	0.01-5 n/m^2
River surface waters	0.02-24.6 n/m^2

Since terrestrial systems have received far less scientific attention than aquatic ones, specific data on their microplastic abundance are scarce. However, an investigation by Horton et al. (2017) estimated a release of plastics into European continental environments between 4 and 23 times higher than oceans, basing its calculation on present data on plastic production and plastic waste management.

1.3.2 Effects on organisms

Due to their ubiquity in the environment, micro- and nanoplastics can easily be ingested by both aquatic and terrestrial organisms. Plastic uptake by organisms can follow several routes, which depend both on particle size and shape and on organism behavior and feeding strategy (Rist and Hartmann, 2018). In aquatic ecosystems, the uptake of smaller plastic particles by organisms can occur by different active and passive pathways, which include engulfment, ingestion of suspended materials, filtration, water intake, and transfer along the food chain (Fig. 6A; Roch et al., 2020). Fish

can actively uptake microplastics by mistaking them for their natural preys, as observed in the Amberstripe scad *Decapterus muroadsi*, whose diet mainly consists of blue-pigmented copepods that can be easily confused with small blue plastic particles (Fig. 6B). Moreover, an interesting study about fish foraging behavior revealed that biofouled plastic fragments (coated with algae) can elicit olfactory search behaviors in the northern anchovy *Engraulis mordax* (Savoca et al. 2017). Generally, marine species eating primary consumers are those who mainly risk confusing plastic for food.

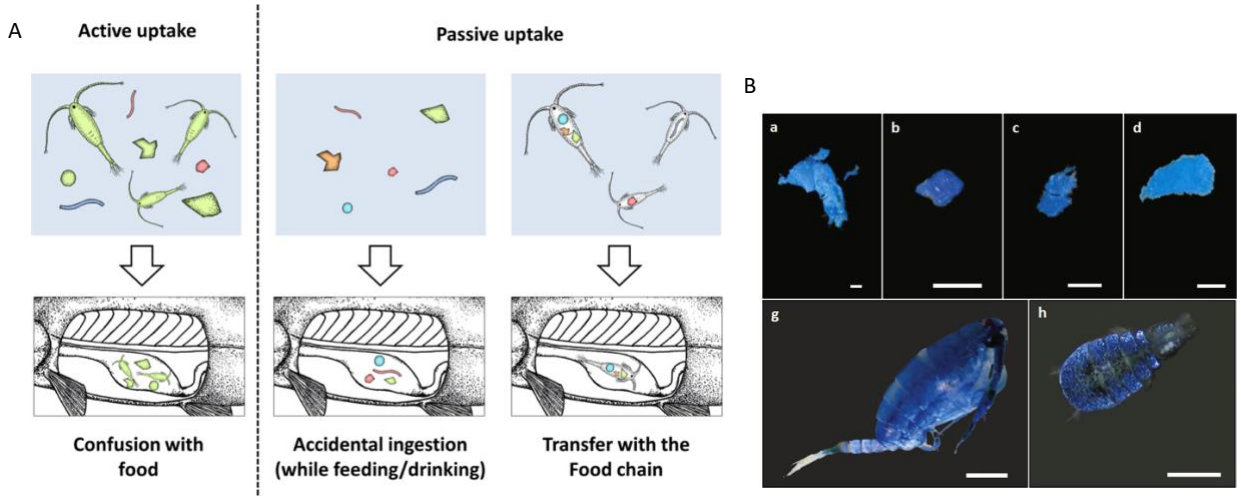

Fig. 6. (A) Three possible uptake routes of microplastics for fish (Roch et al., 2020); (B) Samples of blue microplastics (a-d) found into the gut of D. muroadsi compared with two species of blue copepods (g-h) (Ory et al., 2017).

The ingestion of plastic particles (< 5 mm) was assessed at all levels of the aquatic food web (Fig. 7), from microalgae (Sjollema et al., 2016; Zhang et al., 2017) to small crustaceans and bivalves (Cole et al., 2013; Lee et al., 2013; Rehse et al., 2016; Rochman et al., 2015; Van Cauwenberghe and Janssen, 2014), and fishes (Avio et al., 2015b; Jabeen et al., 2017; Lusher et al., 2013; Rochman et al., 2015; Rummel et al., 2016; Tanaka and Takada, 2016), reaching also the higher level of marine mammals (Besseling et al., 2015; Fossi et al., 2012) and seabirds (Avery-Gomm et al., 2018). The evidence of plastic ingestion was found both in field and performing laboratory exposures, with less data concerning freshwater species (Eerkes-Medrano et al., 2015).

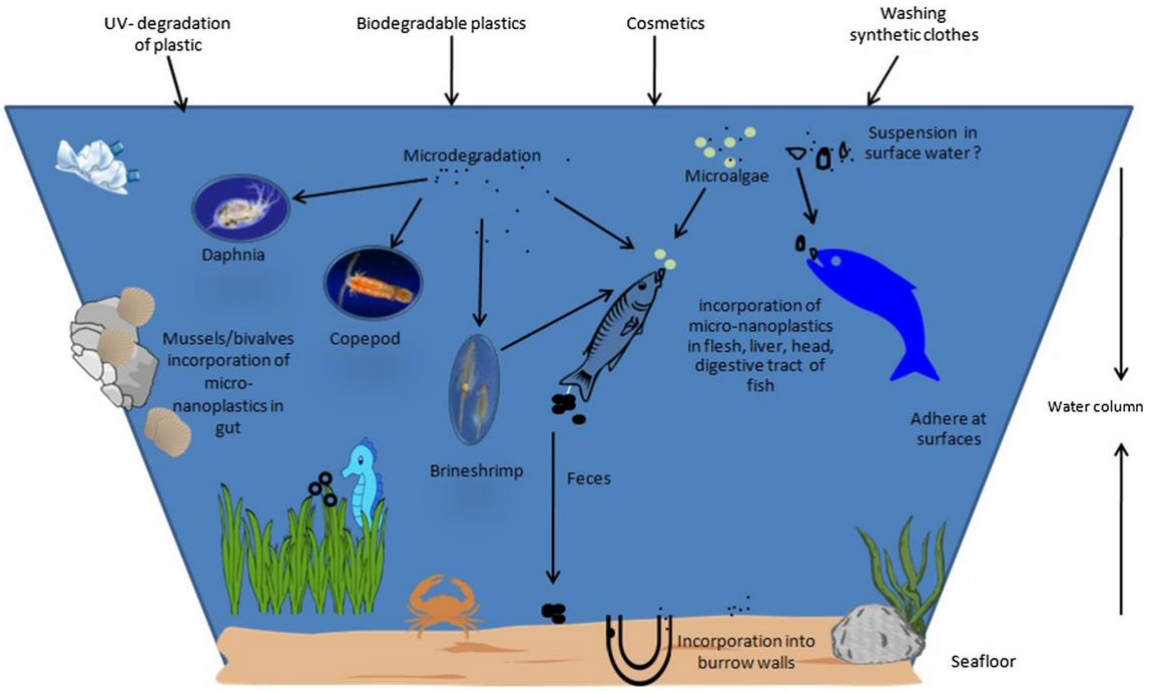

Fig. 7. Micro- and nanoplastics and the aquatic food web (Al-Thawadi, 2020).

Although less studied, the ingestion, accumulation, and trophic transfer of smaller plastics were also observed in terrestrial organisms, such as nematodes (Kiyama et al., 2012), earthworms (Huerta Lwanga et al., 2016; Rodriguez-Seijo et al., 2017), mosquitos (Al-Jaibachi et al., 2018) and birds (Zhao et al., 2016). Earthworms have been predominantly used to investigate the effects of soil plastic pollution on organisms, highlighting important implications for terrestrial ecosystems (Chae and An, 2018). When exposed to PE microparticles (7, 28, 45 and 60% w/w), *Lumbricus terrestris* is able to concentrate them in the cast and also transport them during the formation of the burrows, increasing the presence of plastic particles within the organic matter and affecting waters infiltrations (Huerta Lwanga et al., 2016; 2017a). The ingestion and egestion of plastics by earthworms open the door to the transfer to upper levels of the terrestrial food chain, since the presence of microplastics was observed also in gizzards and faeces of chicken collected in Mexican home gardens (Huerta Lwanga et al., 2017b).

Following ingestion, plastics can be excreted with faeces, retained in the gut or even cross the intestinal epithelium and be transported to other body tissues (Gallo et al., 2018). The fate and

biological effects of plastics debris after being ingested are highly influenced by their size and shape, leading to different uptake rate and retention time in the gut (Zeng, 2018). A laboratory study on the exposure of the grass shrimp *Palaemonetes pugio* to different sizes and shapes of microplastics showed that retention time in the digestive tract was significantly correlated to particle size, with smaller plastics retained longer (Gray and Weinstein, 2017). Similar results were observed in two zooplankton species, the rotifer *Brachionus koreanus* (Jeong et al., 2016) and the cladocera *Daphnia magna* (Rist et al., 2017), where plastic beads in the nano-size range showed prolonged retention times. Retention time in the digestive tract is also affected by particles shape, since smooth and spherical particles are more easily egested than fibers, which may be entangled within intestinal structures. The analysis of the stomach content of the decapod *Nephrops norvegicus* showed how the normal digestive process of crustacean species is not designed to cope with microplastic filaments, which are retained in the gut forming dangerous filament balls potentially causing false sense of satiation and intestinal blockage (Murray and Cowie, 2011).

A serious concern comes from the ability of smaller particles to migrate from the gut to other tissues, where they can be retained for weeks, increasing their potential toxic effects. The first studies investigating the distribution of microplastics following uptake by the blue mussel *Mytilus edulis* showed the presence inside the gills and the epithelial cells of the digestive tubules (von Moos et al., 2012), whereas Browne et al. (2008) demonstrated that microplastics are able to reach the haemolymph from the gut cavity. Other studies showed the bioaccumulation of ingested plastic particles in fish tissues, such as the liver, gills and brain of the red tilapia *Oreochromis niloticus* exposed for 14 days to PS beads (0.1 μm size; Ding et al., 2018), or the liver of the mullet *Mugil cephalus* after a 7-day exposure to different sized PE and PS particles (0.1-1 mm; Avio et al. 2015b). Figure 5 summarizes the existing data on the accumulation of microplastics in bivalves and fish, highlighting their accumulation in different tissues and organs.

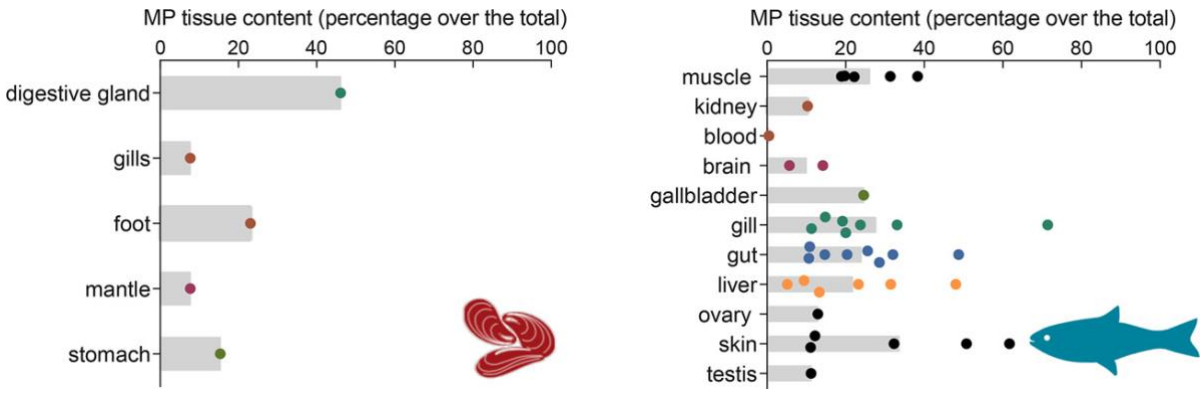

Fig. 5. Percentage of MP distribution in different tissues of bivalves and fishes (Franzellitti et al., 2019).

A still controversial aspect is whether these small particles can be taken up by cells and, if so, the mechanisms of cellular internalization. Chen et al. (2020b) observed that plastic microspheres (1-2 µm) are internalized by phytoplankton cells, suggesting a size-dependent mechanism of phagocytosis or a change or disruption of cell wall permeability occurring during cell division.

The ability of plastic particles to migrate and accumulate into organism tissues and cells facilitates the transfer of these contaminants to upper trophic levels. Different studies documented the presence of plastics in the gut and tissues of predators fed with contaminated preys (Batel et al., 2016; Farrell and Nelson, 2013; Mattsson et al., 2014). Moreover, a dietary exposure of zebrafish to fluorescent PS nanoparticles showed the potential existence of a maternal transfer of plastic debris, being detected in the yolk sac, gastrointestinal tract, liver, pancreas, and gall bladder of parentally exposed embryos and larvae (Pitt et al., 2018b).

All these reports highlight the risks associated with the ingestion of micro- and nanoplastics by biota and raise a global concern on their potential toxic effects (Al-Thawadi, 2020). As monitoring studies, the current scientific literature concerning plastic particle toxicity is mainly focused on marine ecosystems, whereas less is known on their effects on freshwater and terrestrial organisms. Several studies reported a wide range of toxic effects of plastics, that depend on several factors, such as physical properties (size, shape, surface functionalization, etc.), polymer type, exposure time and concentration (Kögel et al., 2020). Adverse effects of microplastics were observed in the majority of

aquatic organisms, both at the molecular, cellular, tissue/organ and individual level (Franzellitti et al., 2019). In the recent study of Botterell et al. (2019), conducted on zooplankton, it has been observed that the consumption of microplastics can alter the eating behavior, thus causing a lower energy consumption, which may result in reduced growth, reproduction and fitness. Moreover, the presence of microplastics within zooplankton faecal pellets may result in an enhanced transfer of plastic throughout the trophic web and, at the same time, it may affect the sinking rates and cause a reduced export of organic matter to deeper waters (Cole et al., 2016). Significant effects at organism level were also observed in bivalves, where microplastic exposure can impair respiration and feeding (Cole and Galloway, 2015; Rist et al., 2016), alteration in development and reproduction (Sussarellu et al., 2016), decreased growth and increased mortality (Rist et al., 2016). Bivalves have also shown a plethora of effects of microplastics at molecular and cellular level, such as DNA damage, differential gene expression, activation of cellular stress responses, oxidative stress, and alterations of metabolism (Avio et al., 2015a; Paul-Pont, et al., 2016; Von Moos et al., 2012). Moreover, microplastics were shown to cause toxic effects at any level of the biological organization in fish, including DNA damage (Pannetier et al., 2020), neurotoxicity (Oliveira et al., 2013), oxidative stress (Lu et al., 2016), endocrine disruption (Rochman et al., 2014), histopathological alterations (Pedà et al., 2016) and behavioural changes (de Sá et al., 2015; Pannetier et al., 2020).

The few studies on the microplastic interaction with soil fauna showed that microplastic exposure can cause the inhibition of growth, histological damage and alteration of gene expression in earthworms (Huerta Lwanga et al., 2016; Rodriguez-Seijo et al., 2017). In addition, shortened survival, impaired reproduction, intestinal damage, oxidative stress and reduction in calcium levels were reported in nematodes (Lei et al., 2018).

Specific data on the interaction between nanoplastics and biota, as well as their impact, are rather limited. Until July 2020, the ISI Web of Science database had listed only 47 articles containing the the combination of words “nanoplastics” and “fish”, of which 33 published in the last two years. As previously mentioned, the small size of these particles could be responsible for the increasingly

negative effects since they can more easily enter the body tissues and cells. An increased toxicity of nanoplastics was observed in the copepod *Tigriopus japonicus*, where 0.05 and 0.5 μm PS beads affected the survival and development, whereas no effects where induced by 6 μm-particles (Lee et al., 2013). The presence of a size-dependent effect of plastics is also evident for benthic invertebrates, where nanoplastics were identified as the most harmful, causing an increased mortality, reduced growth rate, developmental alterations, oxidative stress, and altered feeding behavior (Haegerbaeumer et al., 2019). Among the vertebrates, the zebrafish *D. rerio* is an emerging model for nanoplastic studies because of the transparency of embryo and larvae, that facilitates the imaging of fluorescently labeled nanobead localization (Bhagat et al., 2020). The uptake and the effects of both micro- and nanoplastics were observed at all life stages of *D. rerio*, after exposure to different range of plastic concentrations and polymers. Table 2 reports the most recent scientific literature concerning the effects of PS nanoplastics in zebrafish embryos, larvae and adults.

Table 2. Recent studies reporting the effects of PS nanoparticles on zebrafish.

Zebrafish stage	Diameter	Concentration	Exposure time	Observed effects	Ref.
Adult	70 nm	20 mg L^{-1}	7 days	↑CAT and ↑SOD, local infection and lipid accumulation in the liver, upregulation of fatty acids and downregulations of amino acids	Lu et al., 2016
Adult	50 nm	1 mg L^{-1}	72 h	↓acetylcholinesterase activity and up-regulation of myeline, tubulin protein/gene expression, dopamine content	Chen et al., 2017
Adult	500 nm	1 mg L^{-1}	14 days	microbiota disbiosis	Jin et al., 2018
Larvae	25 nm	0.2, 2, 20 mg L^{-1}	48 h	↓level of glucose, ↑cortisol secretion, hyperactivity	Brun et al., 2019
Embryo, larvae	1 μm	1 mg L^{-1}	120 h	↓distance moved and velocity and up-regulation of expression of genes involved inflammation and oxidative stress	Qiang and Cheng, 2019
Embryo, larvae	51 nm	0.1, 1, 10 ppm	120 h	↓heart rate and altered locomotor behavior	Pitt et al., 2018a

In summary, a wide range of toxic effects of micro- and nanoplastics is reported in published literature, using a great variety of experimental conditions and biological models, which sometimes lead to controversial or even opposite results. The application of integrated and multilevel approaches

is needed to identify the potential common target of plastic contamination in aquatic and terrestrial biota and better quantify the level of danger for the ecosystems.

1.3.3 Carriers of pollutants

The study of the impact of smaller plastic particles on organisms is even further complex if we consider the potential effects due to the contemporary presence of chemical catalyzers or additives during their synthesis (Rochman, 2015). For instance, the presence of additives was detected in leachates from plastic debris collected in the environment worldwide (Franzellitti et al., 2019), including some known endocrine disruptors, such as bisphenol A (BPA) and phthalates, as well as other toxic compounds, such as flame-retardant chemicals (e.g. polybrominated diphenyl ether, PBDE).

When released into the environment, plastic particles can also adsorb and concentrate other contaminants, due to their increased surface area/volume ratio and surface hydrophobicity (Gall and Thompson, 2015). These "chemical cocktails" may enhance the risks associated with plastic ingestion by organisms (Jahnke et al., 2017). As regard to the adsorption of environmental contaminants, the chemical analysis of microplastics collected along different beaches worldwide has shown the presence on their surface of polycyclic aromatic hydrocarbons (PAHs), polychlorinated biphenyls (PCBs) and pesticides (Frias et al., 2010, Pannetier et al., 2019). Under laboratory conditions, the adsorption capability of micro- and nanoplastics was assessed for a huge range of pollutants, such as glyphosate (Zhang et al., 2018) and antimicrobial agents (Ma et al., 2019).

The presence of contaminants adsorbed to plastic particles raises concern on their role as vectors for the transfer of chemicals along the food web, following desorption from particles after ingestion and accumulation within tissues. Accordingly, the ingestion of plastic particles would increase the transport and the bioavailability of contaminants (Rist and Hartmann, 2018), hence acting as a sort of trojan-horse. Chen et al. (2017) found that adult zebrafish exposed to a mixture of BPA (1 μg L^{-1}) and PS nanoplastics (1 mg L^{-1}) showed higher BPA concentrations in head and viscera than fish

exposed to BPA alone (1 μg L^{-1}). Other studies have demonstrated that the presence of small plastic debris enhance the bioavailability of heavy metals in zebrafish tissues: higher accumulation of Cd (Lu et al., 2018) and Cu (Qiao et al., 2019) were reported in liver, gut and gills of adult zebrafish when co-exposed with PS microplastics (10 μg L^{-1} Cd + 20 and 200 μg L^{-1} microbeads and 50 μg L^{-1} Cu + 200 μg L^{-1} microbeads, respectively).

Although the chemical adsorption may be the main cause of acute effects on organisms, when plastics alone are inert (Prinz and Korez, 2020), very few studies have investigated the combined toxicity of micro- and nanoplastics with the adsorbed pollutants on aquatic and terrestrial organisms. The effect of a co-exposure to pyrene (20 μg L^{-1}) and PE microplastics (184 μg L^{-1}) were investigated on juveniles of the common goby *Pomatoschistus microps*, showing an increased accumulation of pyrene metabolites in the bile and an inhibition of isocitrate dehydrogenase (IDH) activity, an enzyme involved in the energy production (Oliveira et al., 2013). Chemical analyses revealed the bioaccumulation of pyrene in the digestive gland and gills of the marine mussel *Mytilus galloprovincialis* after a 7 day-exposure to 1.5 g L^{-1} of contaminated PE and PS microbeads, causing genotoxic and neurotoxic effects (Avio et al., 2015a). Another study performed on *Mytilus spp*. showed as PS microplastics modulate the kinetics and toxicity of fluoranthene, hence inhibiting the activity of the P-glycoprotein, a plasma membrane protein involved in the excretion of xenobiotics, and lowering the metabolic rate (Paul-Pont, et al., 2016). Beside PAHs, micro- and nanoplastics may affect the fate and toxicity of other environmental pollutants. Rainieri et al. (2018) compared the effects of different contaminated feeds on zebrafish organs, revealing that fish fed with microplastics alone (LD-PE) showed no significant effects, while the 60% of fish fed with microplastics, previously contaminated with a mixture of PCBs, PBDE, perfluorinated compounds (PFCs) and methylmercury, showed significant effects in the liver, which appeared with greater level of vacuolization. Combined effects of microplastics and chemical contaminants were also observed at organism level in the European seabass (*Dicentrarchus labrax*) after a short-term exposure to two concentrations of microplastics (0.26 and 0.69 mg L^{-1}) and mercury (0.010 and 0.016 mg L^{-1}), which caused reduced

swimming velocity and resistance time (Barboza et al., 2018). Furthermore, a 14 days exposure to PS nanoplastics (100 μg L^{-1}) combined with the antibiotic roxithromycin (50 μg L^{-1}) induced a significant increase of SOD activity and reduced malondialdehyde (MDA) content in the liver of red tilapia *O. niloticus*, suggesting the activation of the antioxidant defense system (Zhang et al., 2019). Bivalves are also affected by the transfer of contaminants adsorbed on plastic particles, as seen in *Corbicula fluminea* exposed to different mixtures of microplastics and the antimicrobial florfenicol (1.8 and 7.1 mg L^{-1} florfenicol + 0.2 and 0.7 mg L^{-1} microplastics), showing not only a highest florfenicol concentration compared to animals exposed to contaminant only, but also a significant inhibition of feeding and neurotoxic effects, with subsequent reduced fitness (Guilhermino et al. 2018).

In this context, Nor and Koelmans (2019) recently hypothesized the existence of three alternative scenarios: (1) plastics could act as vectors for the transfer of chemicals; (2) plastics do not make any difference or (3) plastics can "clean" the gut contents, hence decreasing the bioavailability of chemicals. The evidence of a potential "cleaning" effect of plastics was also reported in a study investigating whether the exposure to microplastics increases the removal of PCB in *Daphnia magna* specimens previously fed with a PCB-contaminated diet (Gerdes et al., 2019). This experiment showed a higher elimination rate of PCBs in the organisms exposed to microplastics compared to those receiving only algal food, thus showing that microplastics can act as a sink for hydrophobic organic contaminants, even if it also evidenced a decreased carbon content in the animals exposed to microplastics.

All together, these studies highlight the possible existence of a trade-off both for positive and negative effects occurring after plastic ingestion. This complex issue has been investigated very recently and further studies are needed to understand the release processes of contaminants adsorbed to plastics, their potential trophic transfer and the associated adverse effects.

1.3.4 What is still unknown?

Although the mounting scientific attention on plastic pollution, a number of questions still wait answers. Particularly, the existing limits of analytical methods to detect the smallest plastic particles (<1 µm), prevent their proper quantification in the environment and biota (Koelmans et al., 2015). The detection of nanoplastics within biological tissues is hard and challenging without the use of advanced microscopical techniques, and proper control for any fluorescent dye leachate and/or cellular autofluorescence is absolutely needed to exclude any confounding data (Catarino et al., 2019; Schür et al., 2019). Moreover, after being ingested by organisms, the mechanisms by which smaller plastics and their degradation products are accumulated inside the tissues are mostly unknown (Jahnke et al., 2017). In addition, less is known on nanoplastic toxicity, even when it is assumed that they have a high impact on ecosystems. The assessment of the effects of a wider range of plastic polymers in the nano-range is absolutely necessary, as well as more studies addressing the impact of lower dosages and longer exposure, to come closer to reproduce a realistic scenario. Finally, there are few studies available, in particular those relating to the effects of micro and nanoplastics on freshwater and terrestrial organisms.

2. AIMS OF THE PROJECT

The project was aimed at investigating the adverse effects of micro- and nanoplastics on aquatic and terrestrial organisms using multi-tiered approaches. Polystyrene (PS) was the specific type of plastic material chosen to investigate the effects of environmental contamination by smaller plastic debris, due to its large usage in the manufacture of utensils and food packages (Andrady, 2011).

PS micro- and nanoparticles (1-10 µm and 0.5 µm, respectively) were tested both as commercially available to evaluate their ecotoxicity (Par. 3.1 and 3.2), and in association with triclosan (TCS) to assess their adsorption capability for chemicals, and to evaluate the combined effect in comparison with those caused by the single contaminants (Par. 3.3). TCS is an antimicrobial agent included in a wide range of personal care products (PCPs). Despite its documented occurrence in the aquatic environment, information on the adsorption capacity of plastic particles for this emerging contaminant are very scarce, and the adverse effects of TCS on aquatic organisms have been only investigated at not environmentally relevant concentrations.

Two freshwater models and one terrestrial model were chosen to represent the less studied environmental compartments in the field of plastic contamination. Multiple laboratory experiments were performed to investigate and compare the effects of plastic particles on the freshwater zebra mussel *Dreissena polymorpha*, the zebrafish *Danio rerio* and the silkworm *Bombyx mori*. These biological models are easy to maintain at laboratory conditions and their physiological differences have enabled us to obtain a deep insight on the toxicity targets of micro- and nanoplastics.

Plastic uptake was always verified using advanced microscopical techniques, that allowed the detection of single particles within organisms' tissues. Then, a multi-tiered approach was performed to explore the effects of these emerging contaminants, which are still poorly understood and often controversial. The ecotoxicological analyses covered all levels of biological organization, from organism level through the application of behavioural assays to cellular and molecular levels through the application of a wide range of biomarkers (endpoints of cellular stress, oxidative damage and

neuro/genotoxicity), and the evaluation of protein modulation using the high-throughput technology based on functional proteomics.

3. RESULTS AND DISCUSSION (ORIGINAL PAPERS)

3.1 Effects of micro- and nanoplastics on two freshwater models

One of the most discussed issue related to micro- and nanoplastic environmental contamination regards the uptake in the organisms and its correlated effects, with a lack of data particularly concerning freshwater and terrestrial compartments. For this reason, the first part of the project aimed to investigate plastic ingestion, tissue distribution and toxicity on two freshwater models: *D. rerio* and *D. polymorpha*. Zebrafish embryos were exposed from 72 to 120 hours post-fertilization (hpf) to 1 mg L^{-1} of PS nanobeads with a size of 0.5 µm (3.1.1), while zebra mussels were exposed for 6 days to different mixtures of PS microbeads of 10 and 1 µm diameter (3.1.2 and 3.1.3). Plastic uptake and tissue distribution were evaluated through advanced confocal microscopy techniques, while a suite of biomarkers was applied to evaluate the presence of effects on cellular stress, oxidative damage and neuro- genotoxicity. Furthermore, to the best of our knowledge, these are the first studies including also the effects of plastic exposure on protein modulation in zebra mussels and on zebrafish behaviour, which were performed, respectively, applying functional proteomics and video tracking.

PUBLICATION LIST:

3.1.1 Parenti, C.C., Ghilardi, A., Della Torre, C., Magni, S., Del Giacco, L., Binelli, A., 2019. **Evaluation of the infiltration of polystyrene nanobeads in zebrafish embryo tissues after short-term exposure and the related biochemical and behavioural effects**. Environmental Pollution 254, A, 112947.

3.1.2 Magni, S., Gagné, F., André, C., Della Torre, C., Auclair, J., Hanana, H., Parenti, C.C., Bonasoro, F., Binelli, A., 2018. **Evaluation of uptake and chronic toxicity of virgin polystyrene microbeads in freshwater zebra mussel *Dreissena polymorpha* (Mollusca: Bivalvia)**. Science of the Total Environment 631, 778-788.

3.1.3 Magni, S., Della Torre, C., Garrone, G., D'Amato, A., Parenti, C.C., Binelli, A., 2019. **First evidence of protein modulation by polystyrene microplastics in a freshwater biological model**. Environmental Pollution 250, 407-415.

Environmental Pollution 254 (2019) 112947

Contents lists available at ScienceDirect

Environmental Pollution

journal homepage: www.elsevier.com/locate/envpol

Evaluation of the infiltration of polystyrene nanobeads in zebrafish embryo tissues after short-term exposure and the related biochemical and behavioural effects☆

Camilla Carla Parenti, Anna Ghilardi, Camilla Della Torre, Stefano Magni, Luca Del Giacco, Andrea Binelli*

Department of Biosciences, University of Milan, Via Celoria 26, 20133 Milan, Italy

ARTICLE INFO

Article history:
Received 26 March 2019
Received in revised form
1 July 2019
Accepted 22 July 2019
Available online 4 August 2019

ABSTRACT

One of the current main challenges faced by the scientific community is concerning the fate and toxicity of plastics, due to both the well-known threats made by larger plastic items spreading in ecosystems and their fragmentation into micro- and nanoparticles. Since the chemical and physical characteristics of these smaller plastic fragments are markedly different with respect to their bulk product, the potential toxicological effects in the environment need to be deeply investigated. To partially fill this gap of knowledge, the aim of this study was to evaluate the polystyrene nanobead intake in the tissues of zebrafish (*Danio rerio*) embryos and their related toxicity. Embryos at 72 h post fertilization (hpf) were exposed for 48 h to 0.5 μm fluorescent polystyrene nanobeads at a concentration of 1 mg L^{-1}. Confocal microscopy was employed to investigate nanoplastic ingestion and tissue infiltration, while potential sub-lethal effects were evaluated by measuring several endpoints, which covered the adverse effects at the molecular (protein carbonylation), cellular (P-glycoprotein, activity of several antioxidant/detoxifying enzymes) and organism levels by evaluating of possible changes in the embryos' swimming behaviour. Imaging observations clearly highlighted the nanoplastics' uptake, showing nanobeads not only in the digestive tract, but also migrating to other tissues through the gut epithelium. Biomarker analyses revealed a significant decrease in cyclooxygenase activity and an induction of superoxide dismutase. The behavioural test highlighted a significant ($p < 0.05$) variation in the turn angle between the control and exposed embryos. This study points out the capability of nanoplastics to infiltrate zebrafish embryo tissues, even after a short exposure, thus suggesting the need for deeper investigations following longer exposure times, and highlighting the potential of nanoplastics to cause toxicological effects on freshwater organisms, at the organism level.

1. Introduction

Plastic has changed our lifestyle, allowing the low-cost production of many large consumer goods, but the increase in its production leads to an unavoidable glut of plastic waste, of which its disposal is often improper. Furthermore, the increasing number of plastic objects released into the environment is crucial for risk management, due to their fragmentation by mechanical abrasion, photodegradation, oxidation and hydrolytic degradation (Lehner et al., 2019). The consequential plastic debris was recently reclassified by Hartmann et al. (2019) into two size categories: microplastics in the size range of 1 μm to < 1000 μm and nanoplastics between 1 nm and <1000 nm, in accordance with another recent report by Gigault et al. (2018), which defined nanoplastics as particles "within a size ranging from 1 nm to 1000 nm resulting from the degradation of industrial plastic objects that can exhibit a colloidal behaviour". The new suggested definition seems to be easier and more precise than the official EU recommendation for the nanomaterials' definition (EC, 2018) because it respects the international definition of micro- and nanoscale, avoiding many misunderstandings. Nanoplastics exhibit different properties than their original macroplastic items (Murty et al., 2013); therefore, their environmental fate, intake by organisms and toxicological

☆ This paper has been recommended for acceptance by Lian-Jun Bao.

* Corresponding author.
E-mail address: andrea.binelli@unimi.it (A. Binelli).

https://doi.org/10.1016/j.envpol.2019.07.115
0269-7491/

behaviour should be independently investigated (Zhang et al., 2012). Even if studies on the occurrence and adverse effects of plastic debris in the environment are growing rapidly (Barboza and Gimenez, 2015; Andrady, 2017; Bouwman et al., 2018; Lambert and Wagner, 2018), only a few of these studies are addressed to nanoplastics. The reason should be related to the nanoscale range, which makes the nanoplastic particle collection and quali-quantitative analyses very problematic (Nguyen et al., 2019; Peiponen et al., 2019). These discrepancies in knowledge are reflected in the number of studies concerning the uptake of micro- and nanoplastics by organisms. The ingestion and accumulation of microplastics have been assessed at all trophic levels in marine and freshwater environments (Ferreira et al., 2016; Fossi et al., 2016; Rehse et al., 2016; Alomar et al., 2017; Ding et al., 2018; Magni et al., 2018). Indeed, fewer studies have focused on the uptake of nanoplastics by aquatic organisms, including sea urchin, daphnia, mussels, zooplankton, and algae (Della Torre et al., 2014; Besseling et al., 2014; Canesi et al., 2015; Booth et al., 2016). Concerning the ecotoxicological impact, the effects of micro- and nanoplastic exposure depend on their physical-chemical properties, size, shape, colour and the environmental pollutants adsorbed on their surface (Bouwman et al., 2018; Jiang et al., 2018). Recent studies have demonstrated that nanoplastics are able to cause many adverse effects on marine and freshwater species. Lu et al. (2016) observed an increase in inflammation and lipid accumulation in the livers of zebrafish (*Danio rerio*) exposed to 70 nm polystyrene nanoparticles at concentrations ranging from 25 to 200 mg L^{-1}. Zebrafish also showed an alteration in larval behaviour, measured by a decrease in swimming activity, after exposure to 51 nm polystyrene nanoparticles up to 120 h post fertilization (hpf; Pitt et al., 2018). Furthermore, substantial histopathological damage to the intestine of adult zebrafish has been observed upon exposure to different types of virgin plastic particles at the same concentrations of nanoplastics used in the present study (1 mg L^{-1}), indicating the this is likely the major target of plastic exposure. Concerning aquatic invertebrates, exposure to 30 nm polystyrene nanoparticles (100–300 mg L^{-1}) reduced the filtering activity of *Mytilus edulis* (Wegner et al., 2012), while exposure to 75 nm polystyrene beads (10–400 mg L^{-1}) affected the survival and the expression of stress defence genes of *Daphnia pulex* (Liu et al., 2018).

Our study fits into this context, investigating the fate and the toxicological behaviour of nanoplastics on the freshwater model zebrafish (*D. rerio*) exposed for 48 h, from 72 hpf until 120 hpf, to 1 mg L^{-1} polystyrene nanospheres (PNs), which are representative of one of the main polymer classes found in the aquatic environment (Lu et al., 2016). Confocal microscopy observations were performed to allow the identification of single particles within tissues/cells, while a suite of biomarkers was applied to assess the cellular stress response and oxidative damage. In detail, the cellular stress was assessed by monitoring the P-glycoprotein (P-gp) and cyclooxygenase (COX) activities, as well as measuring the reactive oxygen species (ROS) production and the activity of the antioxidant/detoxifying enzymes glutathione-S-transferase (GST), superoxide dismutase (SOD), glutathione peroxidase (GPx) and catalase (CAT). The oxidative damage was assessed by measuring the protein carbonylation content (PCC). Furthermore, given that PNs have been shown to infiltrate multiple embryo tissues, we assessed whether they could alter zebrafish neural pathways, by analysing the embryos' swimming behaviour. To the best of our knowledge, this is one of the first studies to simultaneously investigate the uptake, tissue distribution, behaviour and toxicity of virgin PNs in zebrafish embryos under short-term exposure conditions.

2. Materials and methods

2.1. PNs characterization and concentration selection

Fluorescent PNs (cat. #FSFR003; 1% solids aqueous suspension), with a mean diameter of 500 nm, were purchased from Bangs Laboratories, Inc. (Fishers, IN, USA). We chose the internally dyed beads (Flash Red, ex./em. 660/690 nm) that have been extensively used in imaging applications. The stock solution was characterized by confocal microscopy to assess the shape and fluorescence of the nanospheres (Fig. S1), while the size distribution and zeta potential were measured using a Malvern Zetasizer Nano ZS instrument (Malvern instruments, UK) in exposure medium, confirming the diameter size and showing neutral surface charge (see Supplementary Materials). The stock solution of virgin PNs, with the addition of 0.1% Tween 20 and 0.09% sodium azide to prevent particle aggregation and bacterial growth, respectively, was diluted to obtain a final concentration of 1 mg L^{-1}. The chosen concentration is probably well above than the concentration occurring in freshwater, even if no proper information is available on the levels of nanoplastics in this environmental compartment, due to the lack of a sensitive and robust methodology (Koelmans et al., 2015). The concentration of 1 mg L^{-1} was selected to maximize the intake of PNs by the embryos, as well as their passage through the intestinal barrier and the consequential potential infiltration in tissues, and their capability to trigger adverse effects despite the short exposure time allowed by the 2010/63/EU directive on the animal welfare. On the other hand, 1 mg L^{-1} is a concentration much lower than the ones tested in several studies investigating the adverse effects of nanoplastics in many aquatic biological models (Wegner et al., 2012; Lu et al., 2016; Pitt et al., 2018; Liu et al., 2018).

2.2. Zebrafish husbandry and embryo exposure

Adult zebrafish, reared in the facility of the Department of Biosciences, University of Milan, were maintained at 28 °C on a 14:10 h light/dark cycle. The facility follows Italian laws, rules and regulations (Legislative Decree No. 116/92), as confirmed by the authorization issued by the municipality of Milan (PG 384983/2013).

Different groups of embryos were collected by natural spawning and randomly divided into 2 groups: control (CTRL) and exposed (PN). CTRL embryos were maintained in zebrafish water (Instant Ocean, 0.1% methylene blue), while PN embryos were exposed to a concentration of 1 mg L^{-1} virgin PNs suspended in zebrafish water. To prevent pigmentation, the embryos used for the imaging analyses were treated by adding 0.003% 1-phenyl-2-thiourea (PTU) to the water at 6 hpf. The collected data resulted from different independent experiments, which were carried out at least two times exposing embryos of both the AB strain and the fli1:GFP transgenic line *TG(fli1a:EGFP)* (Lawson and Weinstein, 2002), the latter of which exhibited green fluorescence in the vascular system. The exposure proceeded from 72 to 120 hpf at 28 °C under semi-static conditions, changing the embryo media every day. Mortality, as well as effects on the morphology, developmental delay and behavioural alterations were assessed systematically. The same exposure was performed in parallel exposing embryos to 0.00001% sodium azide to certify that the antimicrobial additive did not affect the investigated endpoints (see Supplementary Materials for details). At the end of the exposures, embryos were immediately processed for advanced microscopy or collected and stored at −80 °C for biochemical analyses.

2.3. Fixation, cryo-sectioning and confocal microscopy analyses

At the end of the exposure, 10 embryos from each experimental group were fixed in a solution of paraformaldehyde (4%) in PBS and maintained at 4 °C. After fixation, embryos designated for whole mount observations were treated with the DNA-binding dye 40-60-diamidino2-phenylindole (DAPI) and mounted on microscope slides (1–2 embryos each slide). The embryos designated for cryo-sectioning were washed in PBS and 15% and 30% sucrose solutions, included in the cryostat-embedding medium (Bio Optica, Milan, Italy) and maintained in dry ice (Magni et al., 2018). Samples were then stored at −80 °C. Cryostat sections (15 μm), both transversal and longitudinal, were cut at −20 °C with a CM1850 cryostat (Leica, Wetzlar, Germany) and mounted directly on slides. Sections were then treated with DAPI. Sample observation was performed by confocal microscopy (Laser Scanning Confocal Microscope Nikon A1) using dedicated software (NIS-Elements) to achieve interactive stack rotations and orthogonal projections to exclude any uncertainty in the particle localization.

2.4. Embryo swimming behaviour

Embryo locomotor activity was measured at the end of the exposure on a total of 72 embryos (120 hpf), using the DanioVision™ observation chamber (Noldus Inc., Wageningen, The Netherlands) with a temperature control unit that maintained the water temperature at 28 °C. Live zebrafish embryos were rinsed to remove the nanoplastics adsorbed on the skin and transferred in a 24-well plate (1 embryo/well; 12 wells/treatment and 12 wells/control). Their locomotor response was assessed over the course of a 70 min alternating dark/light period (Leuthold et al., 2019). We performed a pre-test adaptation (5 min dark and 5 min light), followed by 2 cycles of alternating periods of dark (20 min) and light (10 min). This dark-light transition is an efficient locomotor response test to detect any defective brain functions or nervous system development in zebrafish, caused by several contaminants (Ali et al., 2011). Video data were recorded from three independent experiments ($n = 36$) at a sample rate of 30 frames/second via a high-speed infrared camera. The software EthoVision XT® (Noldus Inc., Wageningen, The Netherlands) was used to analyse embryo locomotor activity in terms of total distance moved and absolute turn angle for each individual embryo during the 60 min dark/light cycle. To remove outliers from the embryo tracks due to an erratic detection of the subject by the camera during the experiment, we applied the Maximum Distance Moved smoothing method, which set sample points to missing if the distance moved was >20 mm, and the Minimal Distance Moved smoothing method, which filtered out small movements caused by random noise.

2.5. Biomarker analyses

2.5.1. Biomarkers of the cellular stress response

The efflux functionality of P-gp was evaluated according to Fischer et al. (2013) using Rhodamine B (RhB) as the fluorescent substrate. A pool of 30 embryos *per* treatment was collected and incubated for 90 min in zebrafish water with 1 μM RhB. After that, the embryos were homogenized using a pestle in 350 μL of lysis buffer (pH 7.4) containing 10 mM KCl, 1.5 mM $MgCl_2$, and 10 mM Tris and then centrifuged at 12,000×*g* for 10 min. An aliquot of 100 μL of the supernatant was transferred to a multi-well plate in triplicate and the RhB fluorescence was measured using the EnSight™ multimode plate reader (PerkinElmer, Milan, Italy) at ex./em. 530/595 nm. The amount of RhB was quantified with a standard curve ranging from 0 to 0.1 μM RhB ($R^2 = 0.99$). COX activity was assessed using the COX Activity Assay Kit (Cayman Chemical, USA). The peroxidase activity was assayed colourimetrically by monitoring the appearance of oxidized N,N,N′,N′-tetramethyl-*p*-phenylenediamine (TMPD). Approximately 70 embryos from each experimental group were homogenized in 600 μL of 0.1 M Tris-HCl with 1 mM EDTA (pH 7.8) and centrifuged at 10,000×*g* for 15 min at 4 °C. The supernatants were collected, and 40 μL of each was added in triplicate into a 96-well plate with 120 μL of assay buffer (100 mM Tris-HCl, pH 8.0), 10 μL of heme, 20 μL of TMPD and 20 μL of arachidonic acid. Since each sample should have a background value, inactive samples were obtained by collecting 150 μL from each sample and placing this aliquot in boiling water for 5 min. After centrifugation, the removed supernatants were used as background values. The absorbance was read at 590 nm using the EnSight™ multimode plate reader (PerkinElmer, Milan, Italy). The calculated total COX activity for each sample was normalized to the total protein content (Bradford, 1976) and expressed in U mg protein^{-1}. The measurement of GST, CAT, GPx and SOD activity, as well as ROS production, followed the methods described by Parenti et al. (2019). Briefly, pools of 60 embryos from each experimental group were collected and homogenized in 800 μL of 100 mM phosphate buffer (pH 7.4), with 100 mM KCl, 1 mM ethylenediamine tetraacetic acid (EDTA), 100 mM dithiothreitol (DTT), and protease inhibitors (1:100 v/v). The homogenates were centrifuged at 12,000 X *g* for 10 min at 4 °C, and the supernatant was removed and used to measure the enzymatic activities in triplicate, as described in detail in the Supplementary Materials, using a 6715 UV/Vis spectrophotometer (Jenway, USA). ROS levels were measured using the dichlorofluorescein-diacetate (DCFH-DA) method. At the end of the exposure, 12 embryos from each experimental group were washed with PBS and homogenized as described above. The homogenates were centrifuged at 15,000×*g* for 20 min at 4 °C and 20 μL of each supernatant was added to a 96-well plate and incubated for 5 min at 37 °C. To each well, we added 100 μL of PBS and 8.3 μL of DCFH-DA (10 mg mL^{-1} in DMSO), and the plate was incubated again for 30 min at 37 °C. ROS concentration, expressed in fluorescence units (FU), was measured using the EnSight™ multimode plate reader (PerkinElmer) at λ_{ex} 485 nm and λ_{em} 530 nm. Both enzymatic activity and ROS production were normalized to the total protein content of each sample (Bradford, 1976).

2.5.2. Biomarkers of oxidative damage

The PCC was measured using 2,4-dinitrophenylhydrazine (DNPH) according to a previous study (Della Torre et al., 2018). Homogenates were obtained from the pools of 80 embryos as described above. After precipitation of the proteins, the pellets were resuspended in 10 mM DNPH, washed with ethanol-ethylacetate (1:1) and dissolved in 6 M guanidine. After centrifugation, the carbonyl content was spectrophotometrically determined at 375 nm and normalized to the protein concentration measured according to the Bradford (1976) method.

2.6. Statistical analysis

Shapiro-Wilk and Levene tests were performed to assess data normality and homoscedasticity. Statistical analyses were carried out using the STATISTICA 7.0 software package. Biomarker data were evaluated by analysis of variance (one-way ANOVA), where the treatment (CTRL and PN) was the predictor factor and each biomarker was a dependent variable. The significant differences between exposure groups were identified using Duncan's multiple range *post-hoc* test (DMRT), using $p < 0.05$ as the significant cut-off. Data resulting from the behaviour test were elaborated and exported using the EthoVision XT® software and Student's *t*-test

was applied to compare means between control and treated embryos (means were considered significantly different as $p < 0.05$).

3. Results and discussion

The need to explore the capability of the PNs to infiltrate and accumulate in an organisms' tissues involves the use of several specific equipments and techniques. To observe the infiltration of PNs through epithelial membranes, the use of fluorescent-labelled particles is mandatory, along with the recourse to advanced microscopy, such as confocal microscopy. Indeed, a recent manuscript by Catarino et al. (2019) reported that fluorescently labelled PNs may release the fluorescent dye that accumulates in the tissues of zebrafish larvae, misinterpreting their fate in the organism. The authors demonstrated that most PN inclusions observed in the tissues by fluorescence microscopy were simply due to the leaching of their fluorophore. Thus, during image analysis, it is necessary to not only evaluate the fluorescence intensity, which may also be caused by zebrafish tissue autofluorescence (e.g., eye, swim bladder, yolk) but also visualize the single particles, checking their size. In our study, imaging observations by confocal microscopy highlighted the large numbers of PNs ingested by zebrafish embryos, despite the short-term exposure. Both whole mount observations (Fig. 1) and tissue sections (Fig. 2) showed a clear accumulation of red nanobeads at the gut level (Figs. 1B and 2B), compared to CTRL embryos (Figs. 1A and 2A). Although micro- and nanoplastic uptake in the gut of freshwater fish has been reported in several previous studies (Eerkes-Medrano et al., 2015; Duis and Coors, 2016; Ding et al., 2018), this is the first report highlighting PN accumulation following a short exposure time (48 h), bearing in mind that zebrafish embryos are still relying exclusively on the yolk contents for feed until 120 hpf (Fraher et al., 2016) and open their mouths as early as 96 hpf (Muto and Kawakami, 2013). Consequently, although the exposure lasted 48 h, the actual PN uptake by the oral route was possible only during the last 24 h of the treatment (96–120 hpf). A more detailed observation of embryo sections underlined that PN accumulation was not restricted to the gastrointestinal tract; indeed, a relevant number of microscopy sections (30%) showed a clear infiltration of PNs in the surrounding tissues, possibly from crossing the intestinal epithelium (Fig. 3). Few studies actually report the presence of polymers in the tissues of aquatic organisms, such as mussels (von Moos et al., 2012; Li et al., 2015; Magni et al., 2018), mullet (*Mugil cephalus*) (Avio et al., 2015), European anchovies (*Engraulis encrasicolus*) (Collard et al., 2017) and adult zebrafish (Lu et al., 2016; Batel et al., 2018), but this is the first evidence of the translocation of nanoplastics from the gastrointestinal tract to other tissues in zebrafish embryos. Although the accumulation of nanoplastics in the digestive tract is certainly a relevant detection, this apparatus is defined as an interface between the external environment and the body. As long as nanoplastics are withheld in the gut without the capability to pass biological barriers, they may negatively affect the organism's gut at the local level, causing inflammation and/or ultrastructure damage by both physical and chemical (through the possible release of adsorbed compounds) insult; but in (eco)toxicological terms, the infiltration of nanoplastics into other tissues, potentially reaching other districts via the circulatory system, deserves more scientific interest. Our imaging analysis showed that the PNs were also localized at the gills level in close proximity to blood vessels (Fig. 4A), confirming that the respiratory system represents one of the main entrance routes for nanoplastics in fish (van Pomeren et al., 2017; Yin et al., 2018). In addition to this already known evidence, we highlighted a new potential uptake pathway, which is observed in Fig. 4B. This image shows the presence of a single nanosphere in the neuromast, a mechanosensory organ belonging to the lateral line system and localized on the surface of embryos. The centre of each neuromast is composed of several sensory hair cells that detect water movements (Chitnis et al., 2012). The ciliary bundles exposed to water might trap some plastic particles, which can easily cross the gelatinous cupula that surrounds the organ and potentially infiltrate into organisms. Deeper analyses are required to elucidate the contribution of this putative PN infiltration route. Overall, the results obtained by confocal microscopy underlined the benefit of this advanced technique in understanding the fate and behaviour of these emerging contaminants.

Furthermore, a suite of biomarkers was employed to evaluate the cellular stress level of treated embryos. The P-gp is one of the best characterized proteins belonging to the multi-xenobiotic resistance system (MXR), which plays a pivotal role in the protective response towards a wide range of environmental stressors (Fischer et al., 2013). An increase of abcb1 gene encoding for P-gp has been observed in embryos of sea urchin *Paracentrotus lividus* exposed to carboxylated-PN (Della Torre et al., 2014). Moreover, a very recent paper suggested that the MXR system could be modulated by polystyrene microplastics as a generalized response toward particles ingestion both in larvae and adult mussels (Franzellitti et al., 2019a,b). Our results (Table 1) showed that P-gp activity was not significantly modified by PN ingestion, suggesting that this membrane protein is not affected by physical contaminants under the tested conditions. No significant effects were observed for GST activity (Table 1). The induction of oxidative stress is one of the most established toxicity mechanism described for

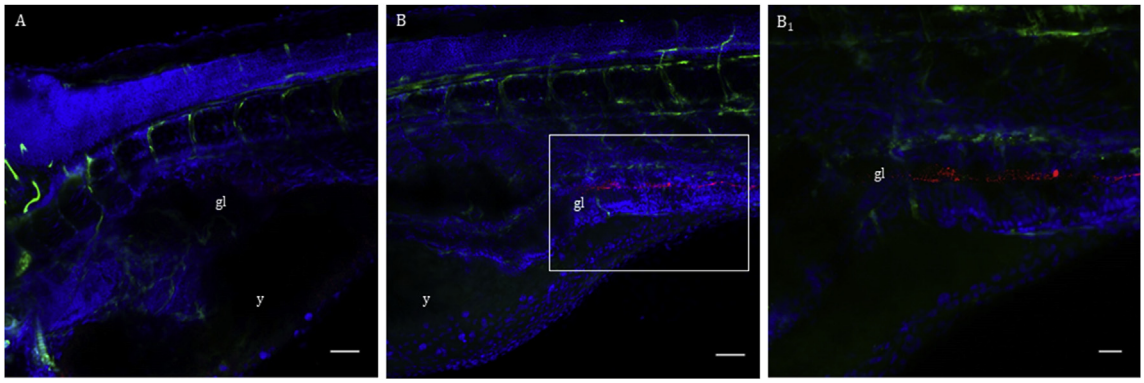

Fig. 1. Confocal microscopy observations of whole mount *TG(fli1a:EGFP)* zebrafish embryos showing the uptake of PNs (in red). (A) Control embryo and (B) exposed embryo [scale bar: 50 μm]. (B_1) corresponds to the rectangular area shown in (B) [scale bar: 20 μm]. Cell nuclei are marked in blue (stained with DAPI). gl = gut lumen, y = yolk. (For interpretation of the references to colour in this figure legend, the reader is referred to the Web version of this article.)

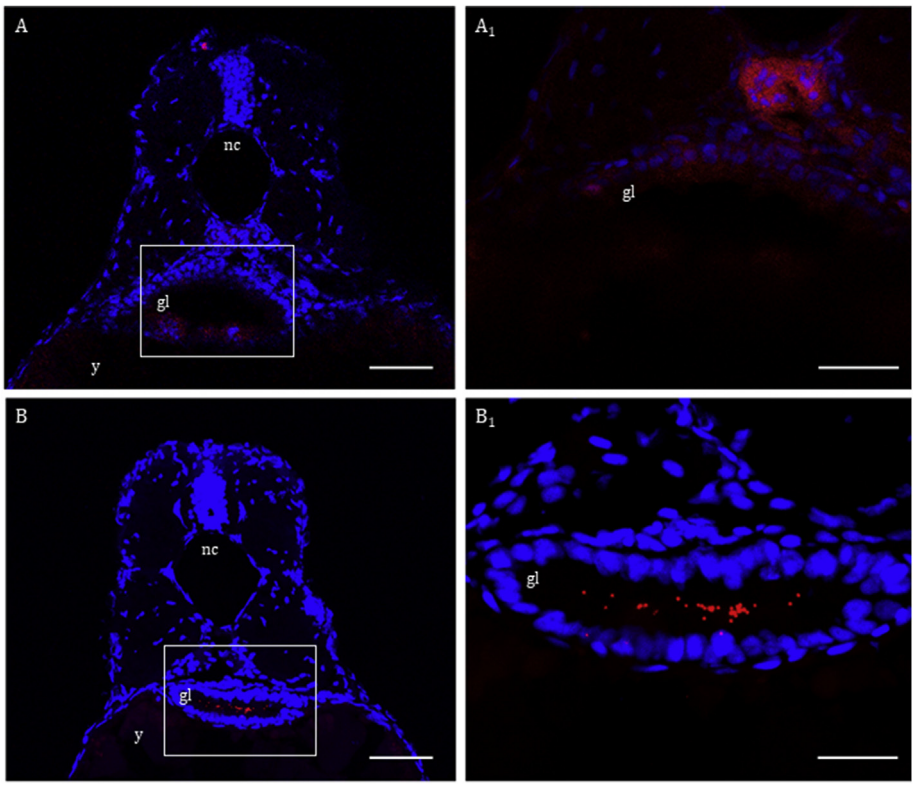

Fig. 2. Transversal cryosections (15 μm) of zebrafish embryos, observed by confocal microscopy, showing the uptake of PNs (in red) in the gastrointestinal tract. (A) Control embryo and (B) exposed embryo [scale bar: 50 μm]. (A_1) and (B_1) correspond to the rectangular area shown in (A) and (B), respectively [scale bar: 20 μm]. Cell nuclei are marked in blue (stained with DAPI). gl = gut lumen, y = yolk, nc = notochord. (For interpretation of the references to colour in this figure legend, the reader is referred to the Web version of this article.)

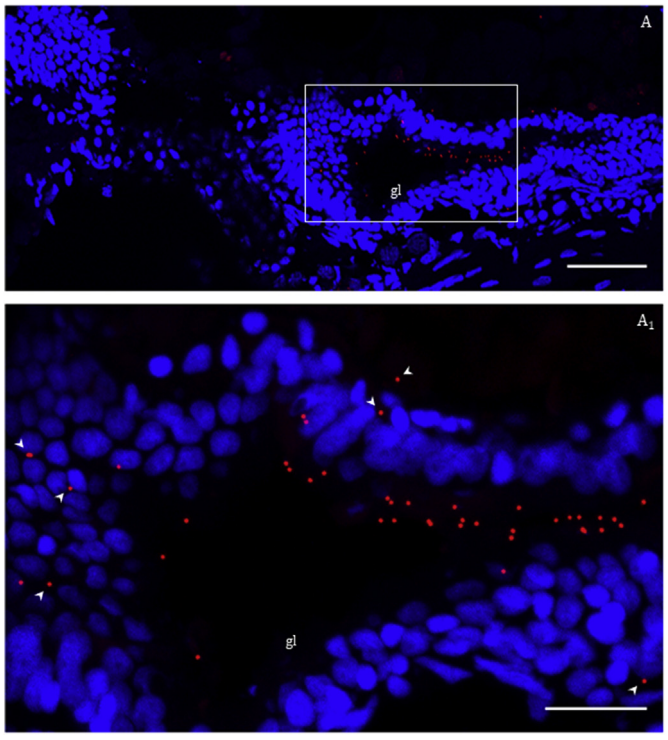

Fig. 3. (A) Longitudinal cryosections of zebrafish embryos, observed by confocal microscopy, showing the uptake of PNs (in red) in the gut [scale bar: 50 μm]. Cell nuclei are marked in blue (stained with DAPI). (A_1) shows that some particles infiltrated into the intestinal epithelium, as indicated by the white arrows [scale bar: 20 μm]. gl = gut lumen. (For interpretation of the references to colour in this figure legend, the reader is referred to the Web version of this article.)

micro- and nanoplastics in aquatic organisms (Franzellitti et al., 2019a,b and citations therein). For example, a significant induction of antioxidant enzymes was determined by Tang et al. (2018), exposing the scleractinian coral to 50 mg L^{-1} of 1 μm polystyrene beads. The same antioxidant response was observed in rotifers and copepods exposed to different sizes of polystyrene particles (Jeong et al., 2017, 2016). Regarding our study, no significant increases were observed in the level of ROS after PN exposure, while we measured a significant ($F_{1,4} = 10.603$; $p < 0.05$) induction of the activity of SOD (Table 1). SOD is classified as an essential antioxidant enzyme involved in the metabolization of superoxide anions (Ighodaro and Akinloye, 2018). An increase in the activity of SOD was observed in another study on zebrafish exposed to larger-sized polystyrene microplastics (5 μm) at three different concentrations (20, 200 and 2,000 μg L^{-1}), which was attributed to a lower food intake caused by the ingestion of microplastics (Lu et al., 2016). A similar antioxidant response to nanoplastic-induced oxidative stress was found also in the red tilapia *Oreochromis niloticus*, which showed the most significant induction of SOD activity after 24 h of exposure to polystyrene beads with a size of 0.1 μm (Ding et al., 2018). Therefore, the activation of SOD seems to suggest the start of the embryos' defence systems against PN exposure, since the enzyme is involved in the first line defence system against ROS, whose overproduction seems to be efficiently counteracted by the embryos. Further studies using fluorescence dyes specific to superoxide anion are warranted to confirm this hypothesis. Nevertheless, we did not observe any marked changes in CAT and GPx activities, suggesting low oxidative stress caused by the PNs. This was consistent with our PCC analysis, which showed no significant oxidative damage.

COX are a family of proteins involved in the synthesis of

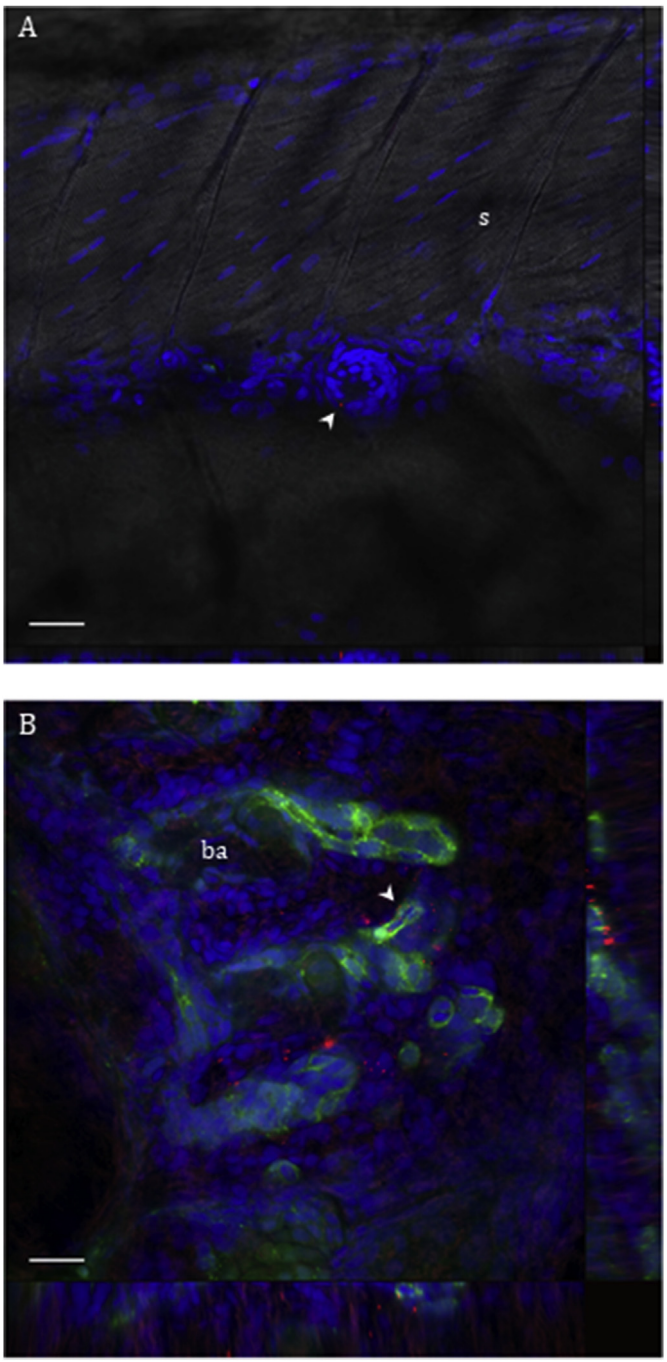

Fig. 4. Orthogonal projections of whole mount of *TG(fli1a:EGFP)* zebrafish embryos showing the uptake of PNs (in red) in the (A) neuromast and (B) gills, as indicated by the white arrows. Cell nuclei are marked in blue (stained with DAPI), while blood vessels are marked in green [scale bar: 20 μm]. s = somites, ba = branchial arches. (For interpretation of the references to colour in this figure legend, the reader is referred to the Web version of this article.)

different prostaglandins that are activated in response to an inflammatory status and have been identified in several fish species, including zebrafish (Grosser et al., 2002). Increased COX-2 gene expression in fish is mainly related to parasitic infections (Lindenstrøm et al., 2004; Sarker et al., 2015), metal exposure (Wang et al., 2016), and intestinal stress (Montero et al., 2015). Until now, the potential interaction of micro- and nanoplastics with COX have never been investigated. Nevertheless, since inflammation is one of the known toxic outcome for zebrafish embryos exposed to polystyrene nanoplastics (5 mg mL^{-1}; Veneman et al., 2017), we expected to obtain an enhancement in the COX activity as a signal of possible inflammation caused by the amount of PNs that accumulated in the gut. On the contrary, our results highlighted a significant decrease in COX activity ($F_{1,4} = 85.062$; $p < 0.001$) that was negatively correlated with the increase in SOD activity (Table S1; $p < 0.05$). We do not know which could be the mechanism through which this inhibition occurs, so this is another crucial point that deserves to be deeper investigated. Biomarker results suggest that PNs, after a short exposure time, induce only slight effects on zebrafish embryos, which is in agreement with a previous study by Jovanović and collaborators (2018), suggesting that virgin plastic particles, due to their smoother surface and spherical shape, caused limited damage to tissues and facilitated particle excretion, as described in other juvenile fish (Ory et al., 2018; Yin et al., 2018). Nanoplastic excretion can also highlight that egested faecal material might act as a vector for plastic particles, facilitating their vertical translocation to the aquatic environment (Cole et al., 2016).

Since the measured biomarkers provided information only at the molecular and cellular levels, we performed a behavioural test to verify any possible negative effects due to the PNs at the organism level. The alteration of swimming performance could affect the prey-predator relationship, as well as the food uptake in wildlife, therefore the evaluation of behavioural effects is a predictive endpoint for potential impacts also at population level. The locomotor response test seemed to confirm the slight toxicity highlighted by the biomarker suite since the PNs did not affect zebrafish locomotor activity, as measured by the total distance moved. Indeed, we found a significant increase ($p < 0.05$) in the absolute turn angle of the treated embryos throughout the first light period compared with the controls (Fig. 5). The measurement of the absolute turn angle reflects changes in zebrafish swimming direction (Girdhar et al., 2015), which may suggest defective brain functions or nervous system development in zebrafish (Ali et al., 2011). Most of the literature available so far showed mostly hypoactivity in aquatic species exposed to micro- and nanoplastics, and this effect was related to the interference on molecular pathways, such as an inhibition of acetylcholinesterase activity (Pitt et al., 2018). Conversely, Kim et al. (2019) demonstrated that the increase in zebrafish turning behaviour under treatment with plastic particles indicates that they may recognize particles as food, exhibiting the same increase in turning behaviour after food or microplastic supply, which seems more in line with our findings. Thus, future studies on the zebrafish behavioural effects after a longer exposure to PNs are needed to investigate the mechanism responsible for this effect in depth.

4. Conclusions

The current state-of-the-art knowledge about pollution from nanoplastics points out that they are surely a ubiquitous environmental problem, being present in every aquatic and terrestrial ecosystem, including remote areas. Nevertheless, the understanding of the toxicological hazards of nanoplastics and their mechanism of action on organisms, including humans, is still far from being reached. To correctly evaluate the environmental risks of nanoplastics, further effort in the comprehension of the fate and behaviour of these physical contaminants, both through laboratory studies and field surveys, is absolutely needed. Therefore, the relevance of this study is to provide an overview of the effects of nanoscale polystyrene bead exposure on one of the most characterized freshwater model organisms. We demonstrated that zebrafish embryos can ingest a large number of PNs, which are

Table 1
Cellular stress response (activity of P-glycoprotein, GST and COX), oxidative stress (level of ROS and activity of antioxidant enzymes SOD, GPx and CAT), and oxidative damage (level of PCC) in zebrafish embryos exposed from 72 to 120 hpf to 0.5 μm PN (mean ± SD). Significant differences between control and exposed groups are reported in bold (one-way ANOVA, Duncan's multiple range *post-hoc* test: *p < 0.05, ***p < 0.001).

SAMPLE	P-glycoprotein (pmol RhB mg prot^{-1})	GST (mmol min^{-1} mg prot^{-1})	SOD (U SOD mg prot^{-1})	GPx (μmol min^{-1} mg prot^{-1})
CTRL	9.23 ± 7.72	373.09 ± 111.75	13.29 ± 1.55	63.78 ± 25.2
PN	3.44 ± 3.46	388.59 ± 95.36	**18.26 ± 2.14***	67.27 ± 32.03
SAMPLE	**CAT** (μmol min^{-1} mg prot^{-1})	**ROS** (FU mg prot^{-1})	**PCC** (PCC nmol mg prot^{-1})	**COX** (U mg prot^{-1})
CTRL	34.54 ± 14.07	79371.85 ± 8455.41	6.11 ± 1.64	1.17 ± 0.09
PN	34.31 ± 17.7	86663.09 ± 33726.39	4.11 ± 2.44	**0.58 ± 0.06*****

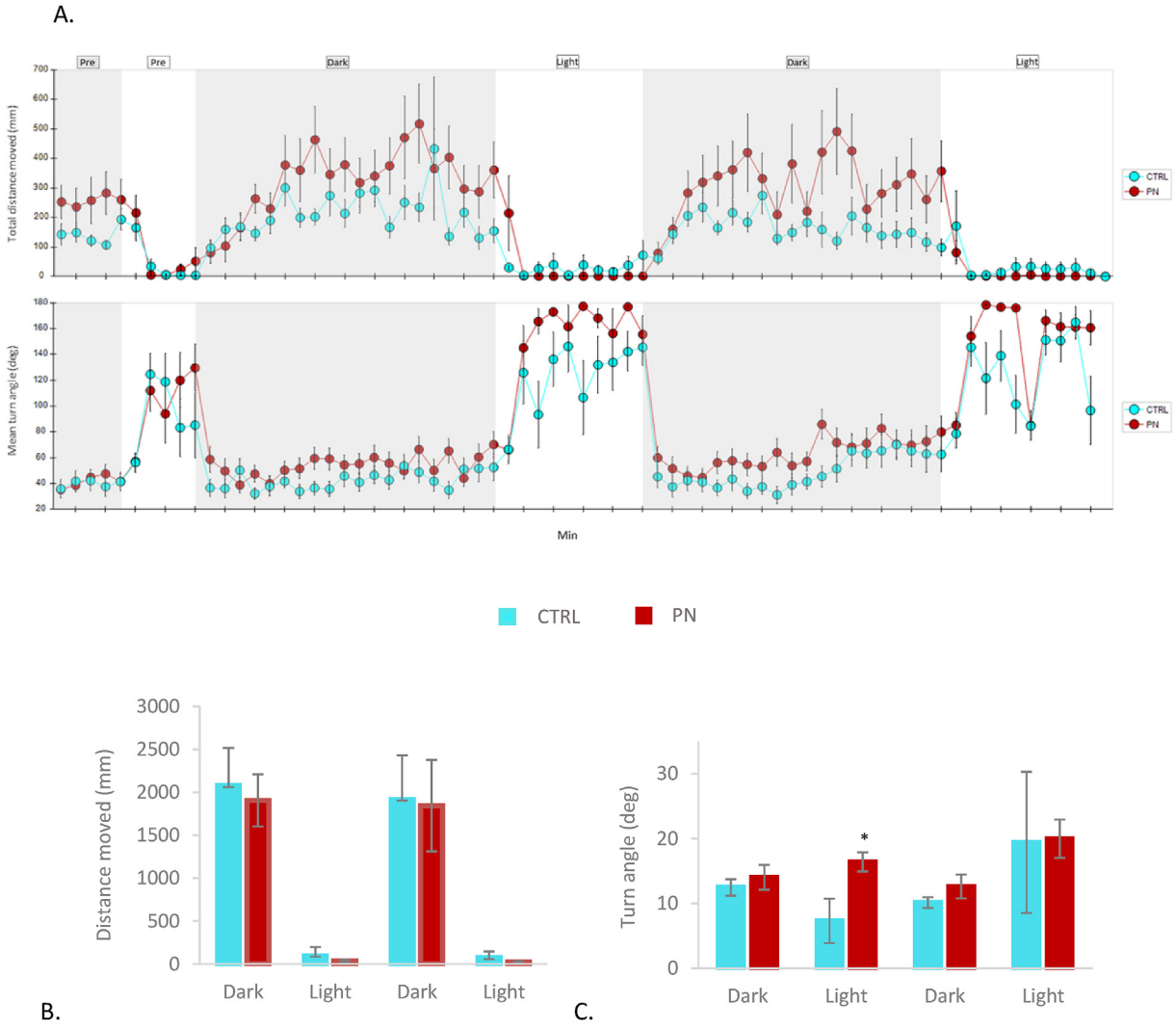

Fig. 5. (A) Behavioural effects of PNs on zebrafish embryos, measured by total distance moved and absolute turn angle during the dark/light transition test. (B) and (C) total distance moved and absolute turn angle presented as the means ± standard dev. * = p < 0.05, according to Student's *t*-test.

distinctly shown in the intestinal tract and through which they are able to infiltrate into other tissues. The PNs then initiated defence mechanisms in the short timeframe of 48 h of exposure, suggesting the activation of the machinery against oxidative stress and a decrease in COX activity. Moreover, PN exposure might affect zebrafish embryos by changing their turning behaviour, which could be coupled with neurotoxic effects. Overall, the results highlighted the need for deeper investigations on PN infiltration in fish tissue and the potential toxicological effects, performing longer exposures at lower concentrations to best mimic the natural aquatic environments.

Declaration of interests

The authors declare that they have no known competing financial interests or personal relationships that could have

appeared to influence the work reported in this paper.

Appendix A. Supplementary data

Supplementary data to this article can be found online at https://doi.org/10.1016/j.envpol.2019.07.115.

References

Andrady, A.L., 2017. The plastic in microplastics: a review. Mar. Pollut. Bull. 119, 12–22.

Ali, S., Champagne, D.L., Alia, A., Richardson, M.K., 2011. Large-scale analysis of acute ethanol exposure in zebrafish development: a critical time window and resilience. PLoS One 6 (5), e20037.

Alomar, C., Sureda, A., Capó, X., Guijarro, B., Tejada, S., Deudero, S., 2017. Microplastic ingestion by *Mullus surmuletus* Linnaeus, 1758 fish and its potential for causing oxidative stress. Environ. Res. 159, 135–142.

Avio, C.G., Gorbi, S., Regoli, F., 2015. Experimental development of a new protocol for extraction and characterization of microplastics in fish tissues: first observations in commercial species from Adriatic Sea. Mar. Environ. Res. 111, 18–26.

Barboza, L.G.A., Gimenez, B.C.G., 2015. Microplastics in the marine environment: current trends and future perspectives. Mar. Pollut. Bull. 97, 5–12.

Besseling, E., Wang, B., Lürling, M., Koelmans, A.A., 2014. Nanoplastic affects growth of *S. obliquus* and reproduction of *D. magna*. Environ. Sci. Technol. 48 (20), 12336–12343.

Batel, A., Borchert, F., Reinwald, H., Erdinger, L., Braunbeck, T., 2018. Microplastic accumulation patterns and transfer of benzo[a]pyrene to adult zebrafish (*Danio rerio*) gills and zebrafish embryos. Environ. Pollut. 235, 918–930.

Booth, A.M., Hansen, B.H., Frenzel, M., Johnsen, H., Altin, D., 2016. Uptake and toxicity of methylmethacrylate-based nanoplastic particles in aquatic organisms. Environ. Toxicol. Chem. 35 (7), 1641–1649.

Bouwman, H., Minnaar, K., Bezuidenhout, C., Verster, C., 2018. Microplastics in Freshwater Environments. WRC Report 2610/1/18.

Bradford, M.M., 1976. A rapid and sensitive method for the quantification of microgram quantities of protein using the principle of protein-dye binding. Anal. Biochem. 72, 248–254.

Canesi, L., Ciacci, C., Bergami, E., Monopoli, M.P., Dawson, K.A., Papa, S., Canonico, B., Corsi, I., 2015. Evidence for immunomodulation and apoptotic processes induced by cationic polystyrene nanoparticles in the hemocytes of the marine bivalve *Mytilus*. Mar. Environ. Res. 111, 34–40.

Catarino, A.I., Frutos, A., Henry, T.B., 2019. Use of fluorescent-labelled nanoplastics (NPs) to demonstrate NP absorption is inconclusive without adequate controls. Sci. Total Environ. 670, 915–920.

Chitnis, A.B., Dalle Nogare, D., Matsuda, M., 2012. Building the posterior lateral line system in zebrafish. Dev. Neurobiol. 72 (3), 234–255.

Cole, M., Lindeque, P.K., Fileman, E., Clark, J., Lewis, C., Halsband, C., Galloway, T.S., 2016. Microplastics alter the properties and sinking rates of zooplankton faecal pellets. Environ. Sci. Technol. 50, 3239–3246.

Collard, F., Gilbert, B., Compère, P., Eppe, G., Das, K., Jauniaux, T., Parmentier, E., 2017. Microplastics in livers of European anchovies (*Engraulis encrasicolus*, L.). Environ. Pollut. 229, 1000–1005.

Della Torre, C., Maggioni, D., Ghilardi, A., Parolini, M., Santo, N., Landi, C., Madaschi, L., Magni, S., Tasselli, S., Ascagni, M., Bini, L., La Porta, C., Del Giacco, L., Binelli, A., 2018. The interactions of fullerene C60 and Benzo(α)pyrene influence their bioavailability and toxicity to zebrafish embryos. Environ. Pollut. 241, 999–1008.

Della Torre, C., Bergami, E., Salvati, A., Faleri, C., Cirino, P., Dawson, A.K., Corsi, I., 2014. Uptake, disposition and toxicity of polystyrene nanoparticles in sea urchin embryos *Paracentrotus lividus*. Environ. Sci. Technol. 48, 12302–12311.

Ding, J., Zhang, S., Razanajatovo, R.M., Zou, H., Zhu, W., 2018. Accumulation, tissue distribution, and biochemical effects of polystyrene microplastics in the freshwater fish red tilapia (*Oreochromis niloticus*). Environ. Pollut. 238, 1–9.

Duis, K., Coors, A., 2016. Microplastics in the aquatic and terrestrial environment: sources (with a specific focus on personal care products), fate and effects. Environ. Sci. Eur. 28, 2.

Eerkes-Medrano, D., Thompson, R.C., Aldridge, D.C., 2015. Microplastics in freshwater systems: a review of the emerging threats, identification of knowledge gaps and prioritisation of research needs. Water Res. 75, 63–82.

European Commission, 2018. Definition of a Nanomaterial. http://ec.europa.eu/environment/chemicals/nanotech/faq/definition_en.htm.

Ferreira, P., Fonte, E., Soares, M.E., Carvalho, F., Guilhermino, L., 2016. Effects of multi-stressors on juveniles of the marine fish *Pomatoschistus microps*: gold nanoparticles, microplastics and temperature. Aquat. Toxicol. 170, 89–103.

Fischer, S., Klüver, N., Burkhardt-Medicke, K., Pietsch, M., Schmidt, A., Wellner, P., Schirmer, K., Luckenbach, T., 2013. Abcb4 acts as multixenobiotic transporter and active barrier against chemical uptake in zebrafish (*Danio rerio*) embryos. BMC Biol. 11, 69.

Fossi, M.C., Marsili, L., Baini, M., Giannetti, M., Coppola, D., Guerranti, C., Caliani, I., Minutoli, R., Lauriano, G., Finoia, M.G., Rubegni, F., Panigada, S., Bérubé, M., Ramírez, J.U., Panti, C., 2016. Fin whales and microplastics: the Mediterranean sea and the sea of Cortez scenarios. Environ. Pollut. 209, 68–78.

Fraher, D., Sanigorski, A., Mellett, N.A., Meikle, P.J., Sinclair, A.J., Gibert, Y., 2016. Zebrafish embryonic lipidomic analysis reveals that the yolk cell is metabolically active in processing lipid. Cell Rep. 14, 1317–1329.

Franzellitti, S., Canesi, L., Auguste, M., Wathsala, R.H.G.R., Fabbri, E., 2019a. Microplastic exposure and effects in aquatic organisms: a physiological perspective. Environ. Toxicol. Pharmacol. 68, 37–51.

Franzellitti, S., Capolupo, M., Wathsala, R.H.G.R., Valbonesi, P., Fabbri, E., 2019b. The Multixenobiotic resistance system as a possible protective response triggered by microplastic ingestion in Mediterranean mussels (*Mytilus galloprovincialis*): larvae and adult stages. Comp. Biochem. Physiol., C 219, 50–58.

Gigault, J., Halle, A.T., Baudrimont, M., Pascal, P.Y., Gauffre, F., Phi, T.L., El Hadri, H., Grassl, B., Reynaud, S., 2018. Current opinion: what is a nanoplastic? Environ. Pollut. 235, 1030–1034.

Girdhar, K., Gruebele, M., Chemla, Y.R., 2015. The behavioral space of zebrafish locomotion and its neural network analog. PLoS One 10 (7), e0128668.

Grosser, T., Yusuff, S., Cheskis, E., Pack, M.A., FitzGerald, G.A., 2002. Developmental expression of functional cyclooxygenases in zebrafish. PNAS 99 (12), 8418–8423.

Hartmann, N.B., Hüffer, T., Thompson, R.C., Hassellöv, M., Verschoor, A., Daugaard, A.E., Rist, S., Karlsson, T., Brennholt, N., Cole, M., Herrling, M.P., Hess, M.C., Ivleva, N.P., Lusher, A.L., Wagner, M., 2019. Are we speaking the same language? Recommendations for a definition and categorization framework for plastic debris. Environ. Sci. Technol. 53 (3), 1039–1047.

Ighodaro, O.M., Akinloye, O.A., 2018. First line defence antioxidants-superoxide dismutase (SOD), catalase (CAT) and glutathione peroxidase (GPX): their fundamental role in the entire antioxidant defence grid. Alexandria Med. J. 54, 287–293.

Jeong, C.B., Won, E.J., Kang, H.M., Lee, M.C., Hwang, D.S., Hwang, U.K., Zhou, B., Souissi, S., Lee, S.J., Lee, J.S., 2016. Microplastic size-dependent toxicity, oxidative stress induction, and p-JNK and p-p38 activation in the monogonont rotifer (*Brachionus koreanus*). Environ. Sci. Technol. 50 (16), 8849–8857.

Jeong, C.B., Kang, H.M., Lee, M.C., Kim, D.H., Han, J., Hwang, D.S., Souissi, S., Lee, S.J., Shin, K.H., Park, H.G., Lee, J.S., 2017. Adverse effects of microplastics and oxidative stress- induced MAPK/Nrf2 pathway-mediated defense mechanisms in the marine copepod *Paracyclopina nana*. Sci. Rep. 7, 41323.

Jiang, R., Lin, W., Wu, J., Xiong, Y., Zhu, F., Bao, L.J., You, J., Ouyang, G., Zeng, E.Y., 2018. Quantifying nanoplastic-bound chemicals accumulated in *Daphnia magna* with a passive dosing method. Environ. Sci. Nano 5 (3), 776–781.

Jovanović, B., Gökdağ, K., Güven, O., Emre, Y., Whitley, E.M., Kideys, A.E., 2018. Virgin microplastics are not causing imminent harm to fish after dietary exposure. Mar. Pollut. Bull. 130, 123–131.

Kim, S.W., Chae, Y., Kim, D., An, Y.J., 2019. Zebrafish can recognize microplastics as inedible materials: quantitative evidence of ingestion behaviour. Sci. Total Environ. 649, 156–162.

Koelmans, A.A., Besseling, E., Shim, W.J., 2015. Nanoplastics in the aquatic environment. Critical Review. In: Bergmann, M., Gutow, L., Klages, M. (Eds.), Marine Anthropogenic Litter. Springer, Cham.

Lambert, S., Wagner, M., 2018. Microplastics are contaminants of emerging concern in Freshwater environments: an overview. In: Freshwater Microplastics. Hdb Env. Chem., vol. 58.

Lawson, N.D., Weinstein, B.M., 2002. *In vivo* imaging of embryonic vascular development using transgenic zebrafish. Dev. Biol. 248, 307–318.

Lehner, R., Weder, C., Petri-Fink, A., Rothen-Rutishauser, B., 2019. Emergence of nanoplastic in the environment and possible impact on human health. Environ. Sci. Technol. 53, 1748–1765.

Leuthold, D., Klüver, N., Altenburger, R., Busch, W., 2019. Can environmentally relevant neuroactive chemicals specifically be detected with the locomotor response test in zebrafish embryos? Environ. Sci. Technol. 53, 482–493.

Li, J., Yang, D., Li, L., Jabeen, K., Shi, H., 2015. Microplastics in commercial bivalves from China. Environ. Pollut. 207, 190–195.

Lindenstrøm, T., Secombes, C.J., Buchmann, K., 2004. Expression of immune response genes in rainbow trout skin induced by *Gyrodactylus derjavini* infections. Vet. Immunol. Immunopathol. 97, 137–148.

Liu, Z., Cai, M., Yu, P., Chen, M., Wu, D., Zhang, M., Zhao, Y., 2018. Age-dependent survival, stress defense, and AMPK in *Daphnia pulex* after short-term exposure to a polystyrene nanoplastic. Aquat. Toxicol. 204, 1–8.

Lu, Y., Zhang, Y., Deng, Y., Jiang, W., Zhao, Y., Geng, J., Ding, L., Ren, H., 2016. Uptake and accumulation of polystyrene microplastics in zebrafish (*Danio rerio*) and toxic effects in liver. Environ. Sci. Technol. 50, 4054–4060.

Magni, S., Gagné, F., André, C., Della Torre, C., Auclair, J., Hanana, H., Parenti, C.C., Bonasoro, F., Binelli, A., 2018. Evaluation of uptake and chronic toxicity of virgin polystyrene microbeads in freshwater zebra mussel *Dreissena polymorpha* (Mollusca: Bivalvia). Sci. Total Environ. 631–632, 778–788.

Montero, D., Benitez-Dorta, V., Caballero, M.J., Ponce, M., Torrecillas, S., Izquierdo, M., Zamorano, M.J., Manchado, M., 2015. Dietary vegetable oils: effects on the expression of immune-related genes in Senegalese sole (Solea senegalensis) intestine. Fish Shellfish Immunol. 44, 100–108.

Murty, B.S., Shankar, P., Raj, B., Rath, B.B., Murday, J., 2013. Unique properties of nanomaterials. In: Textbook of Nanoscience and Nanotechnology. Springer, Berlin, Heidelberg.

Muto, A., Kawakami, K., 2013. Prey capture in zebrafish larvae serves as a model to study cognitive functions. Front. Neural Circuits 7, 110.

Nguyen, B., Claveau-Mallet, D., Herandez, L.M., Xu, E.G., Farner, J.M., Tufenkji, N., 2019. Separation and analysis of microplastics and nanoplastics in complex environmental samples. Acc. Chem. Res. 52, 858–866.

Ory, N.C., Gallardo, C., Lenz, M., Thiel, M., 2018. Capture, swallowing, and egestion of

microplastics by a planktivorous juvenile fish. Environ. Pollut. 240, 566–573.
Parenti, C.C., Ghilardi, A., Della Torre, C., Mandelli, M., Magni, S., Del Giacco, L., Binelli, A., 2019. Environmental concentrations of triclosan activate cellular defence mechanism and generate cytotoxicity on zebrafish (*Danio rerio*) embryos. Sci. Total Environ. 650, 1752–1758.
Peiponen, K.E., Räty, J., Ishaq, U., Pélisset, S., Ali, R., 2019. Outlook on optical identification of micro- and nanoplastics in aquatic environments. Chemosphere 214, 424–429.
Pitt, J.A., Kozal, J.S., Jayasundara, N., Massarsky, A., Trevisan, R., Geitner, N., Wiesner, M., Levin, E.D., Di Giulio, R.T., 2018. Uptake, tissue distribution, and toxicity of polystyrene nanoparticles in developing zebrafish (*Danio rerio*). Aquat. Toxicol. 194, 185–194.
Rehse, S., Kloas, W., Zarfl, C., 2016. Short-term exposure with high concentrations of pristine microplastic particles leads to immobilisation of *Daphnia magna*. Chemosphere 153, 91–99.
Sarker, S., Kumar, G., Saleh, M., El-Matbouli, M., 2015. Protease-activated receptor-2 and innate immune response genes differentially express in the salmonid central nervous system in whirling disease. SM J Clin. Med. 1 (1), 1001.
Tang, J., Ni, X., Zhou, Z., Wang, L., Lin, S., 2018. Acute microplastic exposure raises stress response and suppresses detoxification and immune capacities in the scleractinian coral *Pocillopora damicornis*. Environ. Pollut. 243, 66–74.
van Pomeren, M., Brun, N.R., Peijnenburg, W.J.G.M., Vijver, M.G., 2017. Exploring uptake and biodistribution of polystyrene (nano)particles in zebrafish embryos at different developmental stages. Aquat. Toxicol. 190, 40–45.
Veneman, W.J., Spaink, H.P., Brun, N.R., Bosker, T., Vijver, M.G., 2017. Pathway analysis of systemic transcriptome responses to injected polystyrene particles in zebrafish larvae. Aquat. Toxicol. 190, 112–120.
von Moos, N., Burkhardt-Holm, P., Köhler, A., 2012. Uptake and effects of microplastics on cells and tissue of the blue mussel *Mytilus edulis* L. after an experimental exposure. Environ. Sci. Technol. 46, 11327–11335.
Wang, T., Mai, K., Ai, Q., 2016. A review of cyclooxygenase-2 role in fish. Austin J. Nutr. Metab. 3 (1), 1037.
Wegner, A., Besseling, E., Foekema, E.M., Kamermans, P., Koelmans, A.A., 2012. Effects of nanopolystyrene on the feeding behavior of the blue mussel (*Mytilus edulis* L.). Environ. Toxicol. Chem. 31 (11), 2490–2497.
Yin, L., Chen, B., Xia, B., Shi, X., Qu, K., 2018. Polystyrene microplastics alter the behaviour, energy reserve and nutritional composition of marine jacopever (*Sebastes schlegelii*). J. Hazard. Mater. 360, 97–105.
Zhang, X.Q., Xu, X., Bertrand, N., Pridgen, E., Swami, A., Farokhzad, O.C., 2012. Interactions of nanomaterials and biological systems: implications to personalized nanomedicine. Adv. Drug Deliv. Rev. 64 (13), 1363–1384.

Supporting Information

1. Materials and methods

1.1 PNs characterization

PN properties were assessed by confocal microscopy (Fig. S1) and Malvern Zetasizer Nano ZS instrument (Malvern instruments, UK) (Table S1). Furthermore, to eliminate any doubt on the relevance of obtained results, zebrafish embryos were treated with the equivalent concentration of SDS contained in 1 mg L^{-1} PN (0.00001%) using the same exposure condition described in the manuscript (Section 2.2). The results demonstrated that SDS did not affect the detoxifying and antioxidant enzymes activity and COX activity (Table S2). No significant effects were also observed for embryo locomotor activity response (Fig. S2).

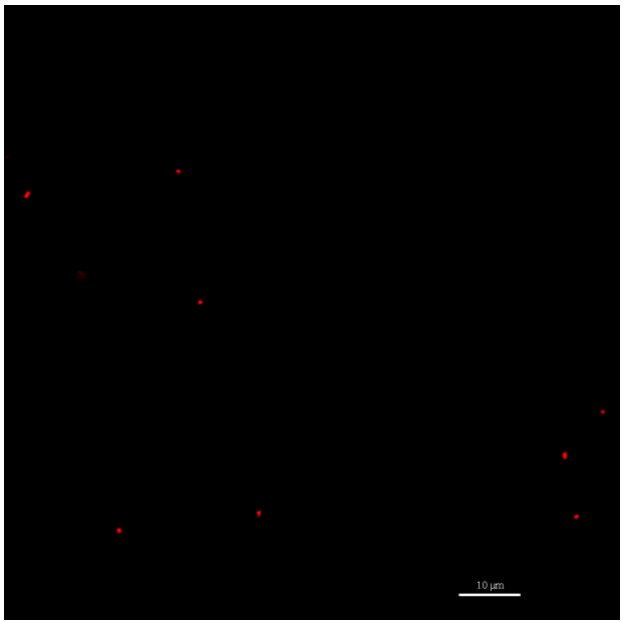

Fig. S1. Confocal fluorescence microscopy image of PN stock solution.

Table S1. Chemical parameters of PNs in exposure medium, referred to a concentration of 1 mg L^{-1}. Size distribution is reported as average ± standard deviation of 3 measurements.

0.5 µm PN	Zeta potential	Size distribution by DLS
	0.13 mV	533.17 ± 17.8 nm

1.2 The activity of antioxidant/detoxifying enzymes

The GST activity was measured by adding reduced glutathione (1 mM) in 100 mM phosphate buffer (pH 7.4) and using 1-chloro-2,4-dinitrobenzene (CDNB; 1 mM) as substrate. The reaction was

monitored for 1 min at 340 nm. The CAT activity was determined by measuring the consumption of H_2O_2 (50 mM) in 100 mM potassium phosphate buffer (pH 7) at 240 nm. The SOD activity was calculated measuring the degree of inhibition of cytochrome C (10 μM) reduction by the superoxide anion generated by xanthine oxidase (1.87 mU/mL)/hypoxanthine (50 μM) reaction at 550 nm. The activity is given as SOD units (1 SOD unit = 50% inhibition of the xanthine oxidase reaction). The GPx activity was assessed by measuring the consumption of nicotinamide adenine dinucleotide phosphate (NADPH) at 340 nm using H_2O_2 (0.2 mM) in 50 mM potassium phosphate buffer (pH 7) as substrate, including glutathione (2 mM), sodium azide (NaN_3; 1mM), glutathione reductase (2 U/mL) and NADPH (120 μm).

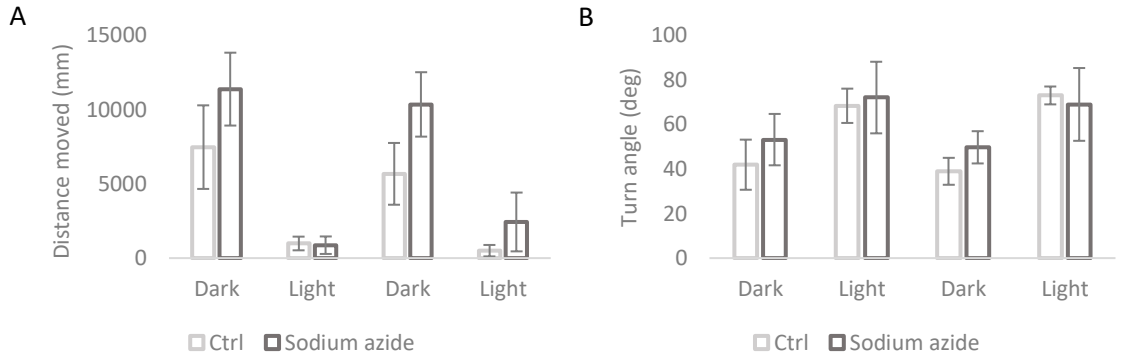

Fig. S2. Behavioural effects in zebrafish embryos exposed to SDS (0.00001%), measured by (A) total distance moved and (B) absolute turn angle. Data are from three experiments (n = 36) and are presented as the means ± standard dev. No significant ($p < 0.05$) effects were observed, according to Student's *t*-test.

Table S2. Cellular stress response (GST, SOD, GPx, CAT and COX) in zebrafish embryos exposed from 72 to 120 hpf to 0.00001% SDS (mean ± SD). No significant differences were observed.

SAMPLE	**GST** (mmol min^{-1} mg $prot^{-1}$)	**SOD** (U SOD mg $prot^{-1}$)	**GPx** (μmol min^{-1} mg $prot^{-1}$)	**CAT** (μmol min^{-1} mg $prot^{-1}$)	**COX** (U mg $prot^{-1}$)
CTRL	213.39 ± 3.96	13.24 ± 3.37	104.67 ± 10.1	10.37 ± 1.16	3.19 ± 0.06
SODIUM AZIDE	210.7 ± 5.03	12.62 ± 2.52	110 ± 10.4	10.82 ± 1.67	3.24 ± 0.14

Table S3. Matrix of Pearson's correlation, showing r and p-level, for enzymes and COX activities examined in zebrafish exposed to PNs. Significant correlations ($p < 0.05$) are reported in bold.

	GST	CAT	GPx	SOD	COX
GST	1.0000	**0.8157**	-0.4573	-0.1069	-0.1496
		p=0.048	p=0.362	p=0.840	p=0.777
CAT		1.0000	0.1121	-0.0618	0.0642
			p=0.833	p=0.907	p=0.904
GPx			1.0000	0.3037	0.0827
				p=0.559	p=0.876
SOD				1.0000	**-0.8396**
					p=0.037
COX					1.0000

Science of the Total Environment 631–632 (2018) 778–788

Contents lists available at ScienceDirect

Science of the Total Environment

journal homepage: www.elsevier.com/locate/scitotenv

Evaluation of uptake and chronic toxicity of virgin polystyrene microbeads in freshwater zebra mussel *Dreissena polymorpha* (Mollusca: Bivalvia)

Stefano Magni [a,*], François Gagné [b], Chantale André [b], Camilla Della Torre [a], Joëlle Auclair [b], Houda Hanana [b], Camilla Carla Parenti [a], Francesco Bonasoro [c], Andrea Binelli [a,*]

[a] Department of Biosciences, University of Milan, Via Celoria 26, 20133 Milan, Italy
[b] Aquatic Contaminants Research Division, Environment and Climate Change Canada, 105 McGill, H2Y 2E7 Montréal, Québec, Canada
[c] Department of Environmental Science and Policy, University of Milan, Via Celoria 2, 20133 Milan, Italy

HIGHLIGHTS

- Few information about microplastic toxicity in freshwaters were available.
- Uptake/toxicity of virgin polystyrene microbeads (PMs) were evaluated in zebra mussel.
- PMs are concentrated in the gut lumen, tissues and hemolymph of zebra mussel.
- PMs induce a low alteration of oxidative status and dopamine level in zebra mussel.
- A considerable uptake and low toxicity summarize the effects of PMs in zebra mussel.

GRAPHICAL ABSTRACT

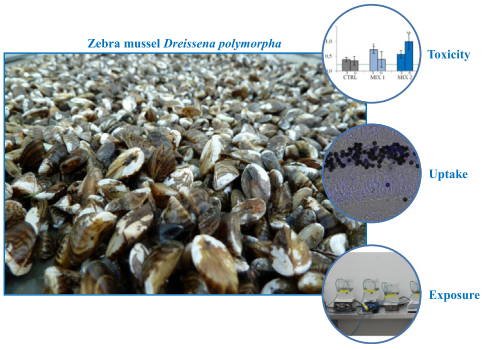

ARTICLE INFO

Article history:
Received 2 February 2018
Received in revised form 7 March 2018
Accepted 7 March 2018
Available online xxxx

Editor: D. Barcelo

Keywords:
Microplastics
Zebra mussel *Dreissena polymorpha*
Uptake
Confocal microscopy
Chronic toxicity
Biomarkers

ABSTRACT

Microplastics (MPs), plastic debris smaller than 5 mm, are widely found in both marine and freshwater ecosystems. However, few studies regarding their hazardous effects on inland water organisms, have been conducted. For this reason, the aim of our research was the evaluation of uptake and chronic toxicity of two mixtures (MIXs) of virgin polystyrene microbeads (PMs) of 10 μm and 1 μm in size (MIX 1, with 5×10^5 of 1 μm size PMs/L and 5×10^5 of 10 μm size PMs/L, and MIX 2 with 2×10^6 of 1 μm size PMs/L and 2×10^6 of 10 μm size PMs/L) on freshwater zebra mussel *Dreissena polymorpha* (Mollusca: Bivalvia) during 6 exposure days. The PM uptake in the mussel body and hemolymph was assessed using confocal microscopy, while the chronic toxicity of PMs was evaluated on exposed mussels using a comprehensive battery of biomarkers of cellular stress, oxidative damage and neuro- genotoxicity. Confocal microscopy analyses showed that MPs concentrated in the gut lumen of exposed mussels, absorbed and transferred firstly in the tissues and then in the hemolymph. The results revealed that PMs do not produce oxidative stress and genetic damage, with the exception of a significant modulation of catalase and glutathione peroxidase activities in mussels exposed to MIX 1. Regarding neurotoxicity, we observed only a significant increase of dopamine concentration in mussels exposed to both MIXs, suggesting a possible implication of this neurotransmitter in an elimination process of accumulated PMs. This research represents a first study about the evaluation of virgin MP toxicity in zebra mussel and more research is warranted concerning the long term neurological effects of virgin MPs.

* Corresponding authors.
E-mail addresses: stefano.magni@unimi.it (S. Magni), andrea.binelli@unimi.it (A. Binelli).

https://doi.org/10.1016/j.scitotenv.2018.03.075
0048-9697/

1. Introduction

The problem of plastics as emerging environmental pollutants is a growing concern because the global plastic production has risen exponentially since the 1950's, reaching >320 millions of tons in 2014 (PlasticsEurope, 2016). China is the largest producer of plastic materials (26%), followed by Europe (20%) and NAFTA (North American Free Trade Agreement) countries (19%). It is interesting that two third of plastic demand in Europe is concentrated in only five countries: Germany (24.8%), Italy (14.3%), France (9.6%), UK (7.7%) and Spain (7.4%; PlasticsEurope, 2016). Therefore, the so-called "plastic age" carries negative consequences for aquatic and terrestrial ecosystems, biota and human health. Sutherland et al. (2010) suggested that the problem due to plastic debris must be considered, along with the climate change, as the issue which could affect the conservation of biological diversity in the short to medium-term.

Microplastics (MPs) are operationally defined as plastic fragments <5 mm in diameter down to the μm range (Thompson et al., 2009). The release of fragments down to the nanometer range is also considered given that nanomaterials could be become more reactive owing to their increased surface area/volume ratio and readily available towards cells. They are produced by primary and secondary sources: the first one includes manufactured plastic products, such as scrubbers in cleaning and cosmetic products or pellets used in feedstock or plastic production (Fendall and Sewell, 2009; Cole et al., 2011), while the secondary origin of MPs results from the breakdown of larger plastic items, such as fishing nets, line fibers, films, industrial raw materials, consumer products and pellets and polymer fragments from degradable plastic (Hidalgo-Ruz et al., 2012; Free et al., 2014). Although there is little information about degradation rates of plastic items and their fragmentation in the environment, the spread and abundance of MPs is raising worldwide (Browne et al., 2011; Law and Thompson, 2014).

The studies regarding the impact of MPs on aquatic environments have been focused mainly on marine ecosystems, while a more limited amount of studies have been conducted on freshwater habitats (Wagner et al., 2014; Horton et al., 2017). For instance, MPs have been recently found in Europe in surface waters or sediments of Lake Geneva (Switzerland; Faure et al., 2012), Lake Garda (Italy, Imhof et al., 2013, 2018), Danube River (Austria; Lechner et al., 2014), Tamar estuary (UK; Sadri and Thompson, 2014) and in the Elbe, Mosel, Neckar and Rhine rivers (Germany; Wagner et al., 2014). Other surveys were carried out on freshwater ecosystems of North America, Asia and Africa (Free et al., 2014; Su et al., 2016; Wang et al., 2016, 2017; Anderson et al., 2017; Di and Wang, 2018; Nel et al., 2018). The gap in the knowledge of MPs' distribution between marine and freshwater ecosystems is also reflected in the knowledge of their potential toxic effects on biota.

Indeed, while several studies were carried out in field and under laboratory conditions to evaluate the ingestion and effects of MPs in marine organisms, studies regarding the impact of MPs on freshwater species are wanting (e.g. Wagner et al., 2014; Guilhermino et al., 2018; Lei et al., 2018). While the available results showed the ingestion capability of MPs in all the examined freshwater taxa (fish, crustaceans, ostracods, gastropods and chironomids; Imhof et al., 2013; Nel et al., 2018), their ecotoxicological effects remain largely unknown. However, the few available studies seemed to suggest physical impacts similar to those observed for marine organisms (Eerkes-Medrano et al., 2015).

Another problem of MPs is related to their composition and large surface area, which make them prone to adsorb waterborne organic contaminants (Cole et al., 2011) that can be then transported in the aquatic organism trough a "Trojan-horse mechanism" as with products from nanotechnology. Moreover, also the leaching of the plasticizers (e.g., phthalates and bisphenol A) can increase the toxicity of MPs when in the organism. A review by Wagner et al. (2014) underlined several gaps of knowledge about monitoring, source, fate, exposure and effects of MPs, that need to be addressed by the near future studies on freshwater ecosystems and biota.

Therefore, in the present study, we investigated the gaps related to the evaluation of the MP exposure and effects in freshwater organisms. In particular, we choose as biological model the freshwater zebra mussel *Dreissena polymorpha* (Mollusca: Bivalvia), considering its physiological characteristics, as the high filtration rate (Binelli et al., 2014, 2015; Magni et al., 2015), its easiness in stabulation, and its key role in the European and American freshwater ecosystems, being a species that links the littoral and benthic habitats. We exposed for 6 days in static conditions zebra mussel specimens to two different mixtures (MIXs), at different concentration, of virgin polystyrene microbeads (PMs), one of the main MP class detected in the environment, with size of 10 μm and 1 μm, respectively. After the exposures, we investigated the MP ingestion and their eventual uptake and infiltration in the mussel tissues through the use of cryostat and confocal microscopy, while a wide battery of biomarkers was used to assess the potential chronic toxicity of selected contaminants. In particular, on the basis of other evidences of MP effects on oxidative status and neuro-enzyme activity on aquatic organisms (Oliveira et al., 2013; Avio et al., 2015; Ribeiro et al., 2017; Barboza et al., 2018), in the present work we choose to investigate more profoundly these aspects evaluating end-points of cellular stress, oxidative damage and neuro- genotoxicity. To the best of our knowledge, the present study represents an innovative attempt to simultaneously investigate both the fate of MPs and their toxicological impact on freshwater mussels by a multiple biomarker approach.

2. Materials and methods

2.1. Mussel collection

We collected zebra mussel specimens from Lake Iseo (Lovere, North Italy) in January 2017. Mussels were collected from the rocks and transported in containers filled with lake water to the laboratory. Before the exposure, mussels were acclimated for a period of two weeks in 15 L tanks with tap and deionized water (50:50 v/v) and maintained at 20 ± 1 °C in oxygen saturation conditions, with natural photoperiod. Mussels were fed three times *per* week with phytoplankton (*Spirulina* sp.), as reported in our previous work (Magni et al., 2016, 2017).

2.2. Concentration selection and mussel exposure to polystyrene microbeads

The two standard aqueous suspensions (5%) of virgin PMs with a size of 10 μm and 1 μm were purchased from Sigma-Aldrich (Italy). Selected standards were diluted in ultrapure water to obtain the 2 PM working suspensions of 50 mg/L. Since we decided to perform the exposures by considering the real number of beads (and not a simple mass/volume ratio), we quantified the number of 10 μm and 1 μm PMs in the 50 mg/L working suspensions using the Bürker chambers (neutral beads were not subjected to aggregation phenomena), obtaining the following bead numbers (mean ± SD): $116 \times 10^6 \pm 33 \times 10^6$ of 10 μm PMs/L and $23 \times 10^9 \pm 530 \times 10^6$ of 1 μm PMs/L. Because of the great release of MPs in the freshwater environment from Wastewater Treatment Plants (WWTPs) of about 65 millions of MPs/day (Murphy et al., 2016), we chose to test the toxicity of these two different PM MIXs: MIX 1, with 5×10^5 of 1 μm size PMs/L and 5×10^5 of 10 μm size PMs/L, and MIX 2 with 2×10^6 of 1 μm size PMs/L and 2×10^6 of 10 μm size PMs/L. The PM exposures were conducted in triplicate (three tanks for control, three tanks both for MIX 1 and MIX 2), placing in each tank (4 L) 70 mussels under static conditions for 6 days (from $t = 0$ to $t = 6$ days), feeding the animals two times with phytoplankton (*Spirulina* sp.), and maintaining a low stirring to avoid PM sedimentation. Considering the high number of animals required to carry out both microscopy analyses and biomarker measurements, we conducted three different PM exposures in the same conditions. Before the treatment we assessed the baseline levels ($t = 0$) of biomarkers on mussels collected from the acclimation tanks, as reported by Magni

et al. (2017). Every three days ($t = 3$ and $t = 6$ days) we collected mussels from each tank to measure the selected end-points. To evaluate the genotoxicity on mussel hemocytes, we collected the hemolymph from 3 mussels *per* tank (9 mussel *per* treatment), measuring the viability of hemocytes using the Trypan blue exclusion method. The soft tissues of these mussels were then stored at −80 °C to evaluate the oxidative damage. We also collected the soft tissues of other 9 mussels *per* treatment, then stored at −80 °C, to perform the measurement of antioxidant/detoxifying enzyme activity. Lastly, the visceral masses (containing three nerve ganglia: one in foot, one near the digestive gland and one near the gonads) without gills of other 3 mussels *per* tank (9 mussel *per* treatment) were stored at −80 °C for the neurotoxicity assessment (Gagné and Blaise, 2003; Gagné et al., 2010). Lastly, we collected 12 mussels *per* treatment (4 mussels *per* tank) at the end of exposure ($t = 6$) for the confocal microscopy observations.

2.3. Evaluation of polystyrene microbead uptake: confocal microscopy analyses

To establish the uptake of PMs on zebra mussel tissues, we prepared 6 mussels *per* treatment ($n = 6$) for cryostat analyses, considering that traditional preparation for paraffin inclusion, with xylene, causes a plastic dissolution (Callebaut and Meeussen, 1989). Therefore, to fix the mussel tissues, we firstly injected 4% paraformaldehyde in phosphate buffer saline solution (PBS) 0.1 M at pH = 7.2 into the mussel adductor muscle, then we gently opened the valves with a scalpel to make easier the preservative absorbance. The whole mussel body (shell included) was inserted in tubes with 4% paraformaldehyde, then preserved at 4 °C. After fixation, we opened the shell, cutting the muscles and ligaments, and placed the soft body mass (without *byssus*) in PBS for 45 min. We repeated this wash for three times. After that, we placed the soft tissues in 15% sucrose solution, for 2 h at room temperature and subsequently transferred the samples in a 30% sucrose solution overnight at 4 °C under agitation (150 rpm). We gently removed the cryoprotectant solution, using filter paper, and included the samples in the cryostat embedding medium (Bio Optica), maintaining the samples on dry ice. The samples were then stored at −80 °C. We obtained 30 μm cryostat transversal section of mussels, using the CM1850 cryostat (Leica, Wetzlar, Germany) and cutting the samples at −23 °C. We collected the sections on the Superfrost® Plus microscope slide (Thermo Scientific), then stained with ProLong® Gold antifade reagent with DAPI (Invitrogen). To investigate the eventual presence of PMs into the thickness of the sections, along the Z axis, we observed the samples using the Leica SP2 laser scanning confocal microscope (Leica Microsystems) exploiting the intrinsic reflection of PMs. To facilitate the detection of 10 μm and 1 μm PMs we characterized the PM standards in the aqueous matrix at confocal microscopy. To avoid the overestimation of 1 μm PM beads, we eliminated any interference of other materials in the mussel tissues by investigating the section thickness with serial scan of 1 μm. In addition, to exclude the possibility that observed PMs in the cryostat sections were originally on the surface of the sections, we performed the orthogonal projections of selected PMs using the software of confocal microscopy. To observe the uptake of PMs in the hemolymph, we collected 6 mussels *per* treatment. Before the sampling of the hemolymph, to exclude the eventual contamination by PMs present in the mantle cavity, we washed the shell with ultrapure water and drained the pallial water on filter paper. To collect hemolymph from the mussel abductor muscle we used a hypodermic syringe contained 100 μL of 10 mM EDTA/PBS to avoid hemocyte agglutination. To conserve the hemolymph samples at −80 °C, we added 10% DMSO and fetal calf serum (FBS) in PBS medium (90%) as cryoprotectant agent. To observe PMs in the hemolymph exploiting their intrinsic reflection, we added 500 μL of hemolymph-EDTA-FBS complex on the microscope glasses previously covered with poly-lysine, to facilitate the cell attachment. In addition, considering that coccus bacteria present in the mussel hemolymph have the same size, shape and reflection of 1 μm PMs, we stained the hemolymph with 1 μg/mL Hoechst to exclude bacteria from PM detection.

2.4. Evaluation of polystyrene microbead chronic toxicity: biomarker analyses

Since the procedure for cellular stress, oxidative damage and genotoxicity biomarkers is highlighted in previous studies (Magni et al., 2016, 2017), in this paper we reported only a brief description of these methods.

2.4.1. Biomarkers of cellular stress

The kinetics of antioxidant enzymes superoxide dismutase (SOD), catalase (CAT) and glutathione peroxidase (GPx) and the activity of detoxifying enzyme glutathione-S-transferase (GST) were evaluated in triplicate on the homogenate of 3 mussels collected from each tank ($n = 3$ pools of three mussels *per* treatment; 9 mussels *per* treatment). The soft tissues of mussels were homogenized in 100 mM phosphate buffer (pH = 7.4), 1:10 W/V ratio, with 100 mM KCl, 1 mM EDTA, 1 mM dithiothreitol (DTT) and protease inhibitors (1:100 v/v). The homogenates were centrifuged at 15,000*g* (S15 fraction) for 30 min at 4 °C. Subsequently, after S15 protein quantification (Bradford, 1976), to normalize the enzyme kinetics, we processed the homogenates for the absorbance measurement of the enzymatic activity, using the 6715 UV/Vis spectrophotometer (Jenway), as reported by Orbea et al. (2002). The results were expressed as SOD units (U) mg prot^{-1} (1 SOD unit = 50% inhibition of the xanthine oxidase reaction), nM of hydrogen peroxide (H_2O_2) consumption min^{-1} mg prot^{-1} for CAT activity, μM of H_2O_2 consumption min^{-1} mg prot^{-1} for GPx activity and mM of gluthatione and 1-chloro-2,4-dinitrobenzene (GSH-CDNB) conjugated min^{-1} mg prot^{-1} for GST activity.

2.4.2. Biomarkers of oxidative damage

The level of lipid peroxidation (LPO) and protein carbonyl content (PCC) were determined in triplicate on the homogenate of 3 mussels collected from each tank ($n = 3$ pools of three mussels *per* treatment; 9 mussels *per* treatment). The homogenates were obtained by homogenizing the soft tissues of mussels in 100 mM phosphate buffer (pH = 7.4), 1:10 W/V ratio, with 100 mM KCl, 1 mM EDTA, 1 mM DTT and protease inhibitors (1:100 v/v). Subsequently, after homogenate protein quantification (Bradford, 1976) to normalize the PCC, we processed the samples for LPO and PCC assays (Ohkawa et al., 1979; Mecocci et al., 1999), measuring spectrophotometrically the absorbance. The results for LPO were expressed as nM of thiobarbituric acid (TBA) reactants/g wet weight (ww), while the results for PCC were expressed as nM of carbonyls mg prot^{-1}.

2.4.3. Biomarkers of neuro-genotoxicity

We evaluated the neurotoxicity on the homogenate of 3 mussels took from each tank ($n = 3$ pools of three mussels *per* treatment; 9 mussels *per* treatment), as described by Gagné (2014). The homogenates were obtained pottering the mussel soft tissues in 25 mM HEPES-NaOH buffer (pH = 7.4), 1:5 W/V ratio, with 100 mM NaCl, 0.1 mM DTT and aprotinin as protease inhibitor. Subsequently, we centrifuged a first aliquot of the homogenates at 15,000*g* (S15) for 20 min at 4 °C and a second aliquot of the homogenates at 1000*g* (S1) for 20 min at 4 °C, and performed in each sample the protein quantification (Bradford, 1976) to normalize all the biomarkers. Analyses were performed using the multi-plate readers BioTek-Synergy 4 and BioTek-EON. For the evaluation of the levels of neurotransmitters dopamine (DOP) and serotonin (SER) in mussel tissues, we used a competitive enzyme-linked immunosorbent assay (ELISA). We quantified DOP in S15 fraction; we coated the wells with 100 μL of 10 μg/mL conjugated BSA-DOP and incubated the plate at 4 °C overnight. We emptied and washed the wells for three times with PBS; subsequently we added in each well 250 μL of blocking buffer (1% fat dry milk in PBS) and

incubated the plate for 90 min at room temperature under agitation (150 rpm) and the wells were washed once with PBS and added 50 μL of samples, or DOP standards for the calibration curve, to the wells and 50 μL of primary antibody (rabbit IgG polyclonal to DOP glutaraldehyde BSA; Abcam) and incubated the plate for 90 min at room temperature under agitation (150 rpm). The wells were emptied and washed three times with PBS, 100 μL of secondary antibody (anti-rabbit IgG, polyclonal antibody, conjugated with horseradish peroxidase; Enzo) was added and incubated for 60 min at room temperature under agitation (150 rpm). The wells were washed three times with PBS and added 100 μL of peroxidase substrate (BM Chemiluminescence ELISA Substrate POD; Sigma-Aldrich) to the wells and incubated the plate for 3 min at room temperature in dark condition. Luminescence was measured using a microplate luminescence reader (Synergy microplate reader, USA). The results were expressed as μmol DOP mg prot^{-1}. For the quantification of SER in the S1 fraction we used the Serotonin ELISA Kit (Enzo), reading the absorbance at 405 nm at room temperature. The results were expressed as ng SER mg prot^{-1}. For the quantification of the neurotransmitter glutamate (GLU) in the S1 fraction, we used the Amplex® Red Glutamic Acid/Glutamate Oxidase Assay Kit (Invitrogen), reading the fluorescence at 37 °C with excitation at 540 nm and emission at 600 nm. The results were expressed as nmol GLU mg prot^{-1}. We measured the activity of acetylcholinesterase (AChE) in the S15 fraction using the Ellman reagent (Ellman et al., 1961), which contains 1 mM 5,5′-dithiobis-2-nitrobenzoic acid (DTNB) in 100 mM Tris-acetate pH = 7.4, and 1 mM acetylthiocholine in 50 mM Tris-HCl as substrate. We assessed the absorbance at 30 °C for 28 min (read interval of 1 min) at 412 nm. The results were expressed as μmol of thiocholine formed min^{-1} mg prot^{-1}. The kinetics of monoamine oxidase (MAO) was measured in S1 fraction using 1 mM tyramine as substrate, 10 μM dichlorofluorescein diacetate in a 140 mM NaCl, 10 mM HEPES-NaOH buffer, pH = 7.4, 1 mg/mL peroxidase and 10 mM of 3-amino-1,2,4-triazole (catalase inhibitor). We measured the fluorescence for 3 min (read interval of 42 s) with excitation at 485 nm and emission at 528 nm. The results were expressed as fluorescein produced min^{-1} mg prot^{-1}. Regarding genotoxicity, we measured the frequency of micronuclei (MN) in 9 mussels *per* treatment. The MN test was conducted as reported by Pavlica et al. (2000). In particular, 400 hemocytes for each slide were counted (9 slides *per* each treatment; 1 slide per specimens) and micronuclei were checked using the criteria suggested by Kirsch-Volders et al. (2000). The results were expressed as frequency of micronuclei (‰).

2.4.4. Statistical analyses

To perform the statistical analyses, we used STATISTICA 7.0 software package. We verified the data normality and homoscedasticity using the Shapiro-Wilk and Levene tests respectively and identified the differences between treated and control performing a two-way analysis of variance (two-way ANOVA), where treatment (control, MIX 1 and MIX 2), time ($t = 3$ and $t = 6$) and their interaction (treatment *per* time) were predictor factors, and each biomarker was a dependent variable. To evaluate the differences ($^{*}p < 0.05$; $^{**}p < 0.01$) between treated and control, time *versus* time, we used the Fisher LSD post-hoc test. Lastly, to observe the eventual covariation between tested biomarkers, we performed the Pearson's correlation considering all end-points.

3. Results

3.1. Microscopy observations

Fig. 1 illustrates how both 10 μm (A) and 1 μm (B) PMs can be view in bright field and in reflection mode, without aggregation phenomena.

Confocal observations of cryostat sections stained with DAPI highlighted the ingestion of the two types of PMs (Fig. 2A, B, C) and their concentration in the gut lumen, completely saturated mainly by the larger PMs. Although the identification of the smaller MPs was much more complicated in the mussel tissues than standards, considering the different matrices, their co-presence with 10 μm PMs in the gut lumen was observed (Fig. 2C). The merging of fluorescence, reflection and bright field acquisition at confocal microscope showed the capability at least of the 10 μm PMs to pass through the biological barriers, moving to the basal lamina of the gut epithelium (Figs. 2B, 3A) and to reach the tissues of the digestive gland (Fig. 3B). Lastly, it was observed the presence of 10 μm and 1 μm PMs (Fig. 4A, B, C) in the mussel hemolymph, close to the hemocytes, demonstrating the translocation of these beads inside the organism. The PM uptake and their infiltration in mussel tissues was confirmed by the orthogonal projections (Fig. 3) conducted both at gut level and in digestive gland tissues.

3.2. Biomarker responses

During the exposures, the percentage of hemocyte viability was 93 ± 6% for control group, 89 ± 7% for MIX 1 and 91 ± 1% for MIX 2, values much higher than the required 70% for genotoxicity tests (Kirkland et al., 2007).

The two PM MIXs did not modulate the activity of the detoxifying enzyme GST since only a marginally non-significant ($p = 0.087$, with $n = 3$ pools) increase of about 28% was noticed after the MIX 1 exposure in comparison with the relative control (Fig. 5A). Regarding the antioxidant enzymes, for SOD we obtained only a significant effect of treatment ($F_{2,12} = 6.46$; $p < 0.05$), and no significant ($p > 0.05$) variations in the SOD activity during the exposure was observed (Fig. 5B), while a significant ($p < 0.01$) increase of CAT was measured in mussels at the end of the MIX 1 exposure (Fig. 5C). For CAT activity we obtained indeed a significant effect of treatment ($F_{2,12} = 5.59$; $p < 0.05$) and of the interaction between time and treatment ($F_{2,12} = 4.22$; $p < 0.05$). MIX 1 caused a significant decrease ($p < 0.01$) of the GPx activity in mussels at $t = 3$ days with a recovery to the control activity at the end of exposure, while MIX 2 did not influence GPx (Fig. 5D). We obtained for GPx activity a significant effect of time ($F_{1,12} = 16.01$; $p < 0.01$) and of interaction time to treatment ($F_{2,12} = 11.66$; $p < 0.01$). The low effects observed for the antioxidant activities were also reflected by the lack of significant ($p > 0.05$) oxidative damage measured by LPO (Fig. 5E) and PCC (Fig. 5F). For LPO we obtained indeed only a marginally non-significant effect of the interaction time to treatment ($F_{2,12} = 3.70$; $p = 0.056$) and only a significant effect of time ($F_{1,12} = 7.79$; $p < 0.01$) and treatment ($F_{2,12} = 6.56$; $p < 0.01$), but a marginally non-significant effect of their interaction ($F_{2,12} = 3.66$; $p = 0.057$), for PCC. Regarding the neurotoxicity biomarkers, DOP amount was increased by both PM MIXs (Fig. 6A), with a significant interaction time and treatment ($F_{2,12} = 6.57$; $p < 0.05$). In detail, we measured a significant ($p < 0.05$) increase of DOP after 3 days (+47% than relative control) when mussels were exposed to MIX 1, while the highest significant ($p < 0.01$) increase was obtained at the end of MIX 2 exposure (+65% than relative control). By contrast, the other measured neurotransmitters (SER and GLU) did not shown any significant ($p > 0.05$) variation (Fig. 6B, C); only for SER we observed a marginally non-significant effect of interaction time to treatment ($F_{2,12} = 3.59$; $p = 0.060$). Even the activities of the two-selected neuro-enzymes (AChE and MAO) were not changed by MIX 1 and MIX 2 exposures (Fig. 6D, E); indeed, we obtained only a marginally non-significant effect of interaction time to treatment ($F_{2,12} = 3.70$; $p = 0.056$) for AChE. The measurement of micronucleus frequency showed the lack of irreversible effects on the genetic material (Fig. 6F).

Lastly, we observed correlations (Table 1) between: GST and CAT ($r = 0.7074$; $p = 0.001$), GST and GPx ($r = 0.5805$; $p = 0.012$), GST and SER ($r = 0.4929$; $p = 0.038$), CAT and SER ($r = 0.4703$; $p = 0.049$), CAT and MAO ($r = 0.5377$; $p = 0.021$), DOP and GLU ($r = 0.5961$; $p = 0.009$), MAO and SER ($r = 0.7145$; $p = 0.001$), MAO and AChE ($r = 0.5126$; $p = 0.030$).

4. Discussion

The present study firstly highlights the capability of PMs to enter in the gastrointestinal tract of zebra mussel and to be transferred in the

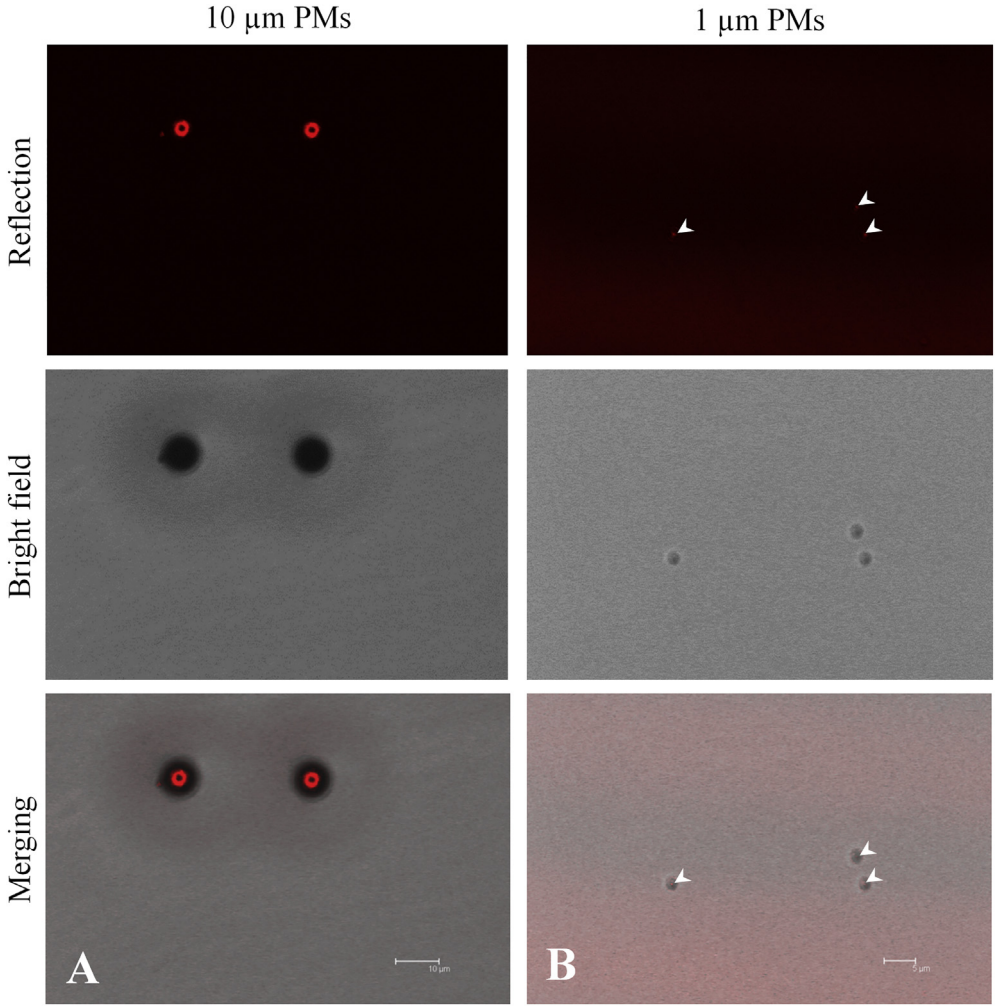

Fig. 1. Characterization of standard aqueous suspensions of 10 μm (A) and 1 μm (B; see the white arrows) PMs at confocal microscopy in reflection mode (red reflection). (For interpretation of the references to colour in this figure legend, the reader is referred to the web version of this article.)

mussel tissues and hemolymph. The characterization of standard aqueous suspensions (Fig. 1A, B) facilitated the detection of PMs in the tissues of mussels, exploiting the intrinsic reflection of beads. However, Fig. 2 shows that within the mussel tissues the PM reflection is much lower compared to standards. This aspect is probably due to the different matrix where beads are suspended, which may interfere with their reflection; in this context, the merging of collected images (Fig. 2B, C) can facilitate the localization of beads in the mussel tissues. Indeed, we observed a great concentration of MPs in the gut lumen of mussels exposed to both MIXs (Fig. 2B), as previously observed also for other animals, such as vertebrates (Derraik, 2002) and invertebrates (Murphy and Quinn, 2018). A large amount of 10 μm PMs found in the gut lumen (Fig. 2B) in comparison to the low presence of 1 μm PMs (Fig. 2C), could be only associated to the difficulties in the detection of 1 μm beads in mussels, as previously described. Nevertheless, the presence of MPs in the gut lumen have only a limited relevance in the light of toxicity since the gastrointestinal tract is considered outer to the body and the fast elimination of MPs can cause only mechanical effects on the gut structures. The study highlighted that even the 10 μm PMs are able to penetrate the epithelium (Fig. 3A) but also the digestive gland tissues (Fig. 3B), close to the mantle cavity. This observation clearly demonstrates that at least the 10 μm PMs are able to pass the biological membranes and move into the mussel tissues, while this phenomenon needs to be further investigated for 1 μm PMs due to the limited instrumental resolution.

Our results regarding the PM uptake in the gut lumen and in the tissues of zebra mussel are in accordance with other observations in *Mytilus* spp. and *Crassostrea gigas* exposed to polystyrene and polyethylene beads with a variable range < 100 μm (von Moos et al., 2012; Avio et al., 2015; Paul-Pont et al., 2016; Sussarellu et al., 2016). Therefore, the capability of MPs to penetrate bivalves' tissues suggests that zebra mussel can be a useful bio-indicator of MP pollution in freshwater. Probably the size of MPs, with similar dimension of plankton and suspended matter, and the high filtration rate of zebra mussel (200 mL/bivalve/h; Ackerman, 1999), are the main factors involved in the considerable MP uptake of this filter-feeding organism.

Another important finding is the detection of both 10 μm and 1 μm PMs in the mussel's hemolymph (Fig. 4B, C). Indeed, the PM presence in the circulatory system confirms that these MPs are able to pass-through the gut epithelium interface, translocate in the soft tissues (Fig. 2B, C) and then in hemolymph (Fig. 4B, C). Our observations are supported by Browne et al. (2008) who reported the presence of 3 μm and 9.6 μm PMs in the hemolymph of *Mytilus edulis*. Moreover, MPs with a dimension <100 μm were also found in the hemolymph of *Mytilus galloprovincialis* by Avio et al. (2015). Recently, Farrell and Nelson (2013) highlighted the transfer of MPs from *Mytilus edulis* to the hemolymph of its predator *Carcinus maenas*, showing the capability of MPs to pass through the food chain and this poses a serious threat to human food safety especially with edible marine mussels (Van Cauwenberghe and Janssen, 2014). Indeed, microparticulates with a

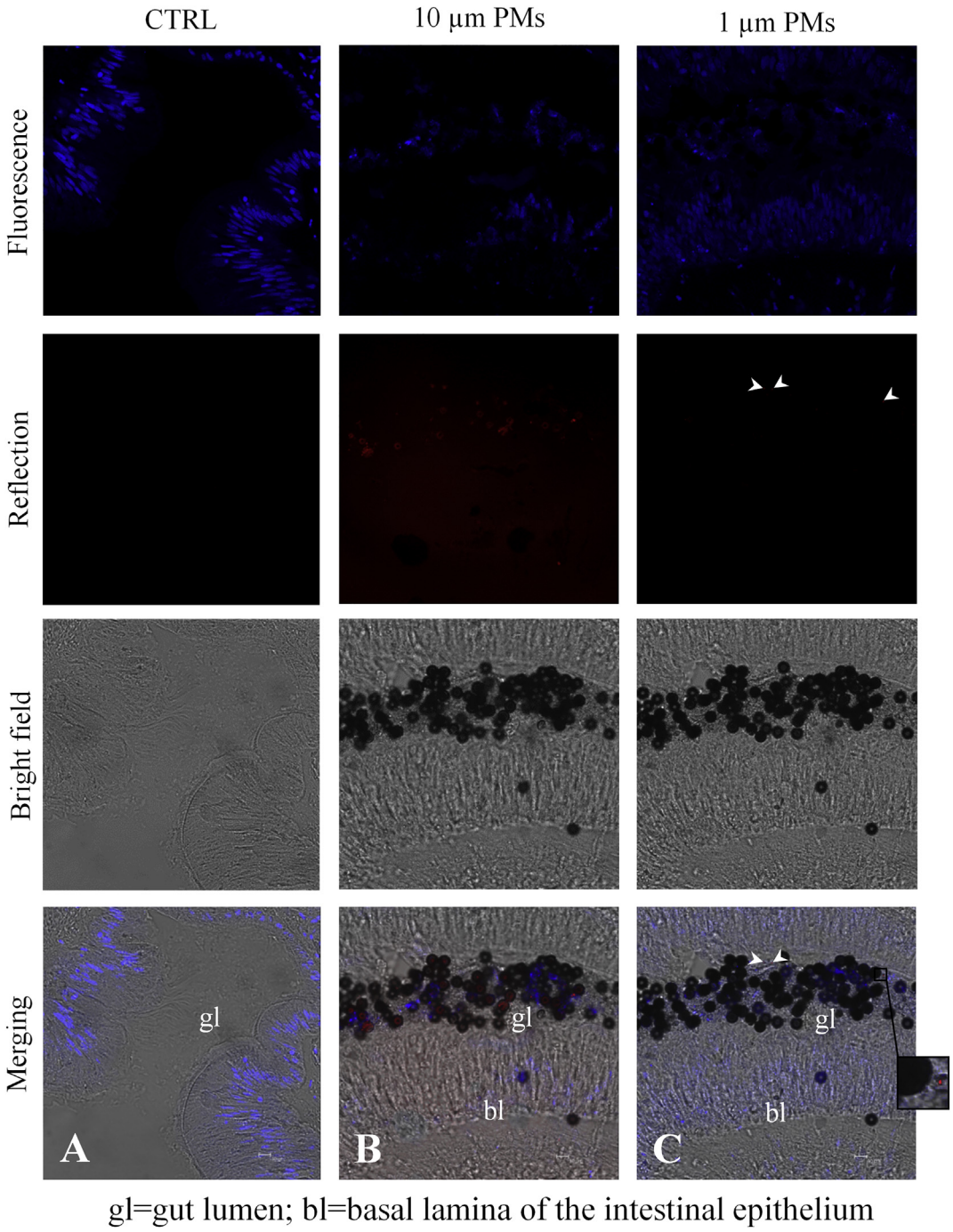

Fig. 2. 30 μm cryostat transversal sections of zebra mussel specimens ($n = 6$ mussels *per* treatment) observed at confocal microscopy at the end of exposure ($t = 6$). In blue are shown the cell nuclei stained with DAPI and in red the PM reflection. It is possible to observe the control (A) and the uptake of both 10 μm (B) and 1 μm (C; see the white arrows and zoom) PMs in the gut lumen and tissues of exposed mussels. (For interpretation of the references to colour in this figure legend, the reader is referred to the web version of this article.)

range from 0.03 to 150 μm have been demonstrated to be transferred in humans, dogs and rodents across the gut lumen towards other tissues, as lymphatic system (Hussain et al., 2001), due to the microfold cells (M cells) in the Peyer's patches of gut epithelium (Van Cauwenberghe and Janssen, 2014).

Apparently, the important concentration of PMs in the gut lumen of zebra mussel and the following infiltration in tissues and hemolymph do not cause neither particular biological responses nor affect the cellular functionality at least within the duration of the experiment. We observed significant ($p < 0.01$) alterations only for CAT and GPx activity (Fig. 5C, D), as well as for DOP levels (Fig. 6A). The DOP is a catecholamine mainly found in nerve ganglia and gonads that acts as neurohormone in mollusks, regulating gametogenesis and spawning (Fong et al., 1993), with the indolamine SER which is more involved in the final maturation stage and spawning. More specifically, DOP regulates oogenesis (Khotimchenko, 1991) but also the inhibition of the cilia movement in bivalves (Stefano and Aiello, 1975; Smith, 1982), especially in gills (Fong et al., 1993). Therefore, the significant increase of DOP, which is observed in mussels exposed to both MIX 1 ($p < 0.05$ at $t = 3$) and MIX 2 ($p < 0.01$ at $t = 6$), could be explained as a defense mechanism of zebra mussel due to the reduction of the entrance of PMs across the inhalant siphon. Perhaps, the presence of PMs in the gut lumen (Fig. 2B, C), and probably in the gills (several 10 μm PMs were observed in fresh gills by optical microscope, data not shown),

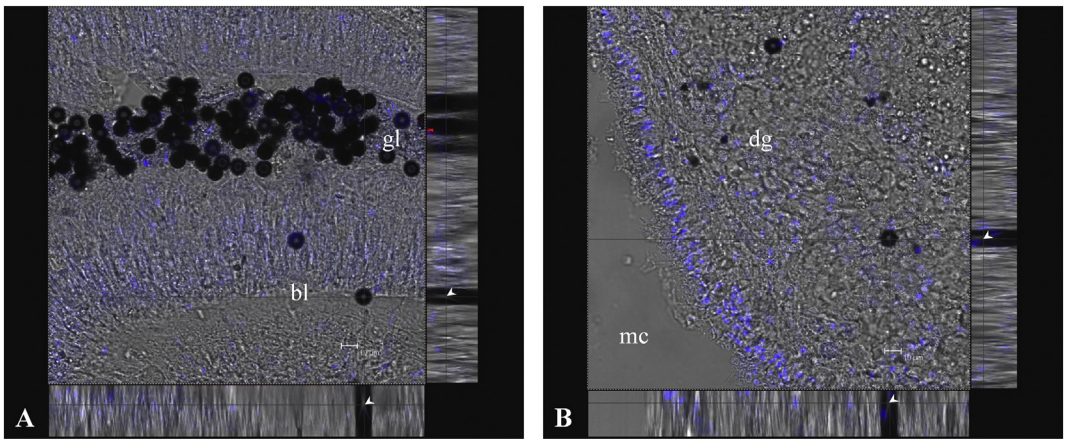

gl=gut lumen; mc=mantle cavity; bl=basal lamina of the intestinal epithelium; dg=digestive gland

Fig. 3. Orthogonal projection of 10 μm PMs in the 30 μm cryostat transversal sections of zebra mussel. In blue are shown the cell nuclei stained with DAPI. It is possible to observe that 10 μm PM at the level of the basal lamina epithelium (A) and in the digestive gland tissue (B) are into the section thickness, as highlighted by the white arrows in the orthogonal projection line intersection. (For interpretation of the references to colour in this figure legend, the reader is referred to the web version of this article.)

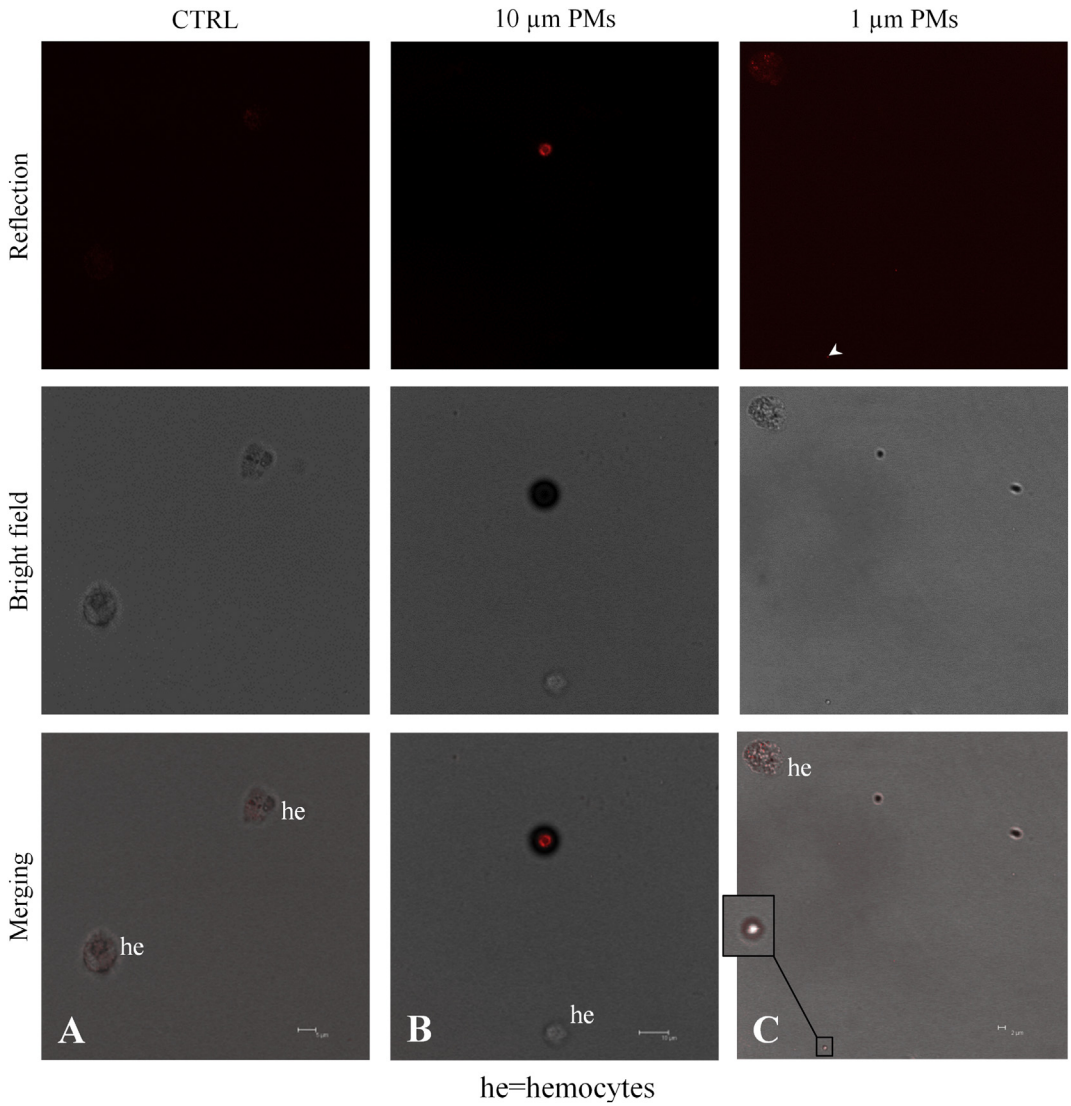

he=hemocytes

Fig. 4. Zebra mussel hemolymph ($n = 6$ mussels *per* treatment) observed at confocal microscopy in reflection mode (red reflection) at the end of exposure ($t = 6$). It is possible to observe the control (A) and the uptake of 10 μm (B) and 1 μm (C; see the white arrow and zoom) PMs in the mussel hemolymph close to the hemocytes. (For interpretation of the references to colour in this figure legend, the reader is referred to the web version of this article.)

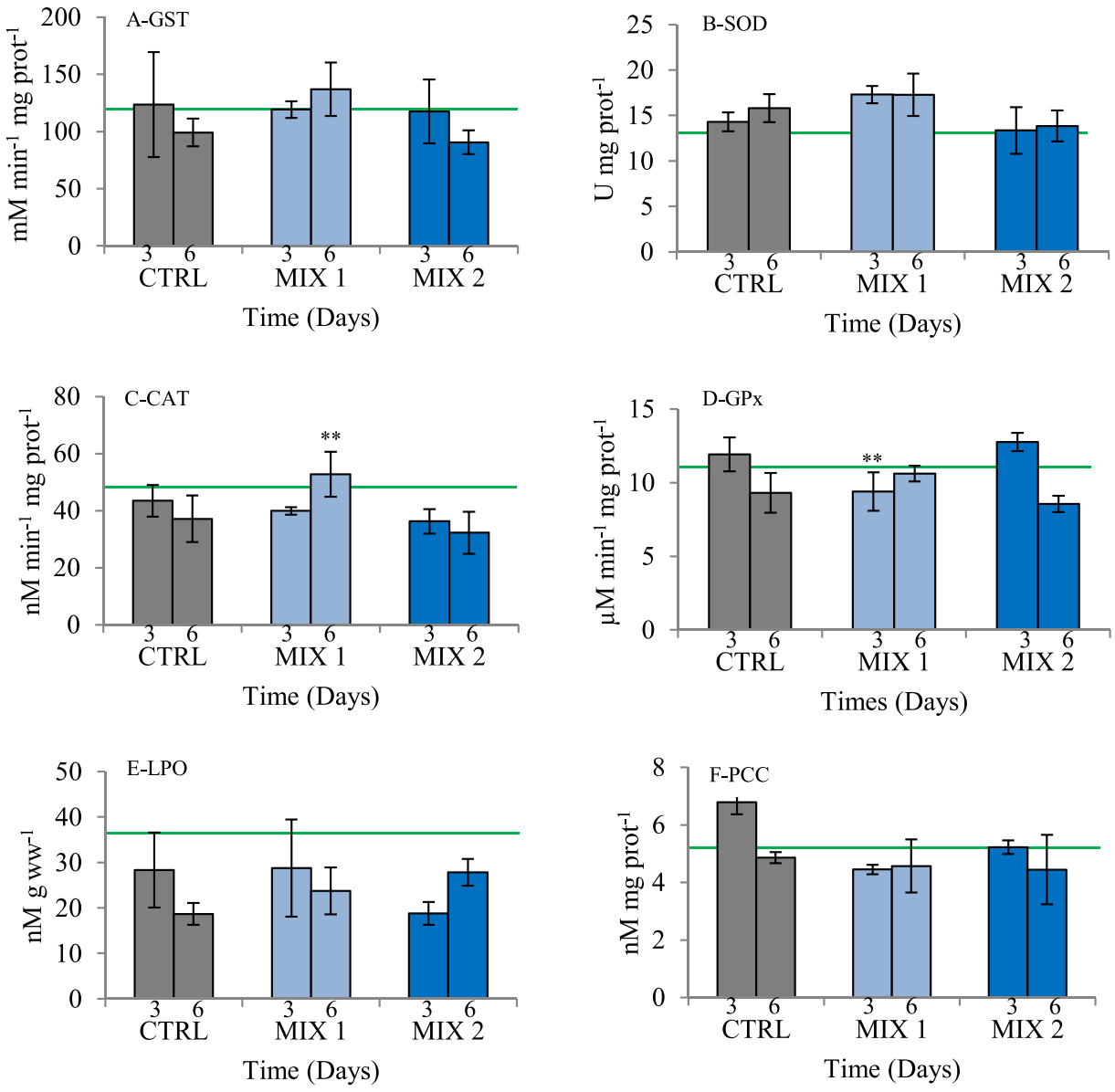

Fig. 5. Cellular stress (activity of detoxifying/antioxidant enzymes A-GST, B-SOD, C-CAT and D-GPx) and oxidative damage (levels of LPO and PCC) in zebra mussel soft tissues ($n = 3$ pools of three mussels *per* treatment; 9 mussels *per* treatment) during 6 days of exposure (from $t = 0$ to $t = 6$ days) at 10 µm and 1 µm PM MIXs (mean ± SD). Asterisks indicate the significant differences, time *versus* time, between MIXs and control (two-way ANOVA, Fisher LSD post-hoc test: $^{*}p < 0.05$, $^{**}p < 0.01$). The green line indicates the baseline level ($t = 0$) of considered end-point. (For interpretation of the references to colour in this figure legend, the reader is referred to the web version of this article.)

can induce mussels to reduce the filtration rate. Indeed, the recent study of Murphy and Quinn (2018) reported that polyethylene flakes fill the gastric cavity of *Hydra attenuata*, reducing its feeding rate. This is further corroborated by the observation of increasing DOP concentrations increasingly inhibited food uptake in *Mytilus edulis* veliger larvae while SER and norepinephrine increased food uptake (Beiras et al., 1995). Hence, the increase of DOP levels could have been involved in feeding activity as part of defense mechanisms in mussels.

On the contrary, Gardiner et al. (1991) reported that DOP increases the cilia activity in unionids. Therefore, another hypothesis might be that the significant increase of DOP could be associated to an enhancement of cilia movement in the gut epithelium and gills to eliminate the PMs, in a manner similar to pseudofaeces. In this context, the eventual increase of filtration/respiration rate could be associated to a major energy consumption (Van Cauwenberghe et al., 2015) and, perhaps, to the decrease of energy storage, as observed in lugworms exposed to MPs (Wright et al., 2013). More experiments would be required to examine more closely ciliary activity in mussels exposed to small MPs.

Since the autoxidation or enzyme degradation processes of DOP produce reactive oxygen species (ROS; Luo and Roth, 2000), it is possible that the significant increase ($p < 0.01$ at $t = 6$) of CAT and the significant decrease ($p < 0.01$ at $t = 3$) of GPx (substrate inhibition) activities in mussels exposed to MIX 1 is due to the formation of the H_2O_2 during the DOP deamination reaction catalyzed by MAO, as suggested by Spina and Cohen (1989). Indeed, the specimens exposed to the lowest concentration of PMs (MIX 1) could adapt themselves during the exposure, and the significant increase of DOP at t = 3 days is consequently reduced by MAO at the end of exposure (t = 6; Fig. 6A), causing the alteration of the oxidative balance. On the other hand, we did not obtain an oscillatory trend for DOP in the mussels exposed to MIX 2 since the higher amount of PMs could produce a high generic stress in exposed specimens, showing that the high levels of DOP are fundamental in

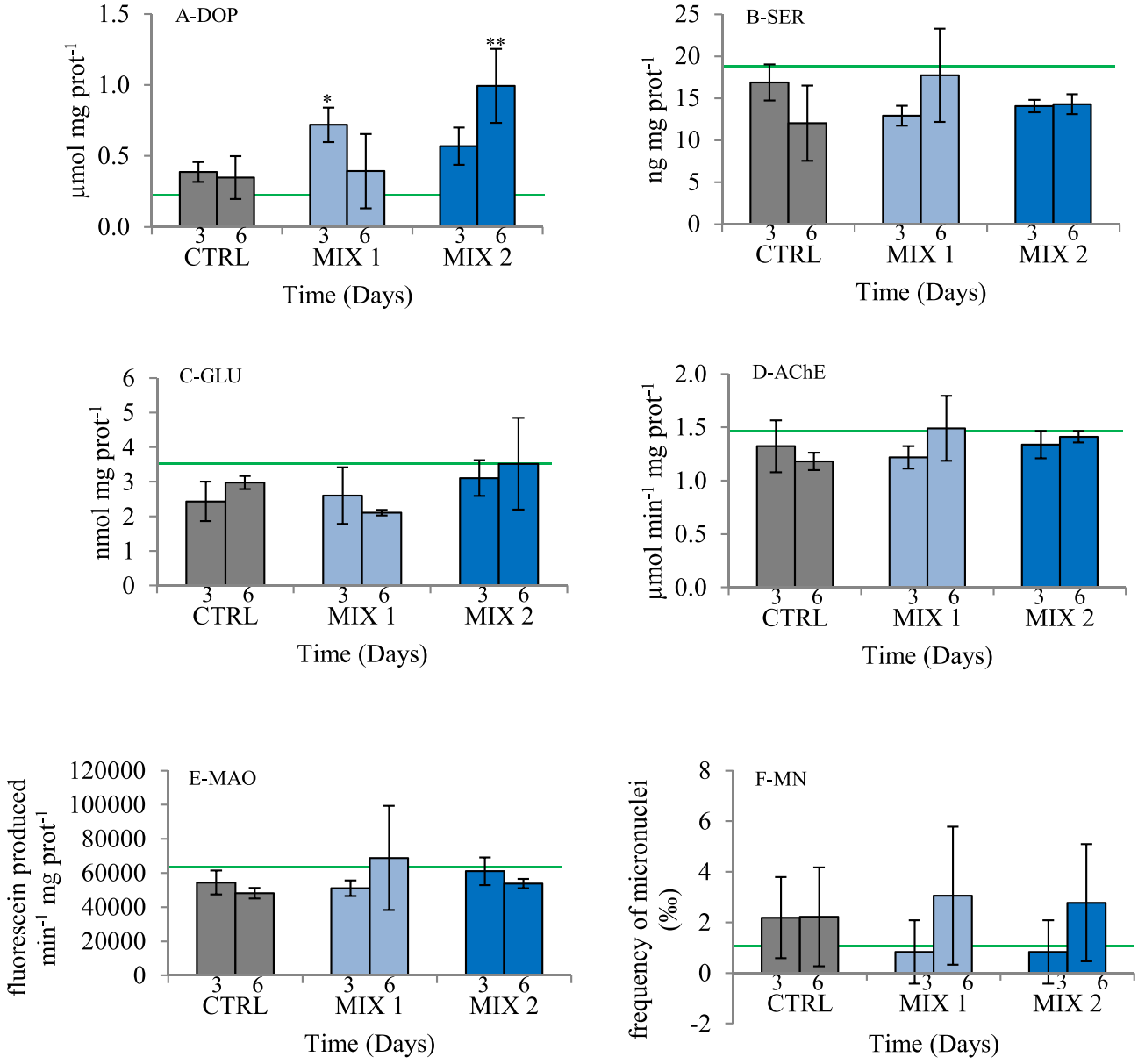

Fig. 6. Neurotoxicity (levels of neurotransmitters A-DOP, B-SER and C-GLU and activity of neuro-enzymes D-AChE and E-MAO) in zebra mussel soft tissues without gills ($n = 3$ pools of three mussels *per* treatment; 9 mussels *per* treatment) and genotoxicity (frequency of F-MN) in zebra mussel hemocytes ($n = 9$ mussels *per* treatment) during 6 days of exposure (from $t = 0$ to $t = 6$ days) at 10 µm and 1 µm PM MIXs (mean ± SD). Asterisks indicate the significant differences, time *versus* time, between MIXs and control (two-way ANOVA, Fisher LSD post-hoc test: $^{*}p < 0.05$, $^{**}p < 0.01$). The green line indicates the baseline level ($t = 0$) of considered end-point. (For interpretation of the references to colour in this figure legend, the reader is referred to the web version of this article.)

the reduction of PM uptake in zebra mussels, as described above. In this context, as suggested by Rist et al. (2016) in a study on *Perna viridis* exposed for 91 days to polyvinylchloride MPs, the stress exerted by MPs leads to valve closure and a reduction of respiration rate with no immediate consequence given the relatively short exposure times in the present study. At the same time, it is important to consider that we did not obtain a significant increase of MAO activity during the exposure and the level of DOP was not correlated with MAO activity ($p = 0.648$), even if the activities of CAT and MAO show similar trends and significant positive correlation ($p = 0.021$), as reported in Table 1. According to our results, low levels of oxidative stress/damage were obtained also by Avio et al. (2015) on *Mytilus galloprovincialis* exposed to MPs for 7 days.

Since we debated two contrary hypotheses regarding the phenomenon associated with DOP increase, in future studies will be necessary the evaluation of other physiological end-points, as the filtration rate, to validate one of these suggestions. Given that SER levels were not affected, it appears that former hypothesis is more likely i.e., DOP increase decrease feeding rate activity since an increase of SER would have followed feeding activity. The lack of significant alteration of AChE activity in treated mussels, in contrast with other studies on fish (Oliveira et al., 2013; Barboza et al., 2018) and bivalves (Avio et al., 2015; Ribeiro et al., 2017), could be associated to the difference in the selected tissues for the analyses. Indeed, while Avio et al. (2015) and Ribeiro et al. (2017) evaluated AChE activity in gills of *Mytilus galloprovincialis* and *Scrobicularia plana* respectively, we assessed all neurotoxicity end-points in the whole visceral mass (without gills), which could have decreased the responses to PMs. The lack of increased AChE activity and SER with increased DOP is consistent with the cilio-inhibitory action of DOP (Aiello et al., 1986) as explained above. However, DOP levels were significantly correlated ($p = 0.009$) with GLU levels in the visceral mass which suggests a neuro-excitatory state induced by MPs concentration in the gut lumen. This suggests that mussels are actively

Table 1
Matrix of Pearson's correlation for all considered end-points: activity of antioxidant enzymes superoxide dismutase (SOD), catalase (CAT) and glutathione peroxidase (GPx), activity of detoxifying enzyme glutathione-S-transferase (GST), level of lipid peroxidation (LPO) and protein carbonyl content (PCC), frequency of micronuclei (MN), levels of neurotransmitters dopamine (DOP), serotonin (SER) and glutamate (GLU), activity of neuro-enzymes acetylcholinesterase (AChE) and monoamine oxidase (MAO). Significant correlations ($p < 0.05$) are reported in bold.

	SOD	CAT	GPx	GST	LPO	PCC	MN	DOP	SER	GLUT	MAO	AChE
SOD	1.0000	0.3547	−0.1874	0.2195	0.3203	−0.4129	−0.1728	−0.2021	0.1187	−0.3256	0.3013	0.1954
	$p = -$	$p = 0.149$	$p = 0.457$	$p = 0.382$	$p = 0.195$	$p = 0.089$	$p = 0.493$	$p = 0.421$	$p = 0.639$	$p = 0.187$	$p = 0.224$	$p = 0.437$
CAT		1.0000	0.2525	**0.7074**	0.0232	−0.0651	0.1664	−0.3048	**0.4703**	−0.2499	**0.5377**	0.2682
		$p = -$	$p = 0.312$	$\mathbf{p = 0.001}$	$p = 0.927$	$p = 0.797$	$p = 0.509$	$p = 0.219$	$\mathbf{p = 0.049}$	$p = 0.317$	$\mathbf{p = 0.021}$	$p = 0.282$
GPx			1.0000	**0.5805**	−0.0793	0.4360	−0.2585	−0.3730	0.3479	−0.1364	0.3148	0.0355
			$p = -$	$\mathbf{p = 0.012}$	$p = 0.755$	$p = 0.070$	$p = 0.300$	$p = 0.127$	$p = 0.157$	$p = 0.589$	$p = 0.203$	$p = 0.889$
GST				1.0000	−0.0567	0.0492	−0.2023	−0.1951	**0.4929**	−0.1749	0.4436	0.0010
				$p = -$	$p = 0.823$	$p = 0.846$	$p = 0.421$	$p = 0.438$	$\mathbf{p = 0.038}$	$p = 0.488$	$p = 0.065$	$p = 0.997$
LPO					1.0000	0.0593	−0.0526	0.2917	0.2441	−0.1574	0.2158	−0.0332
					$p = -$	$p = 0.815$	$p = 0.836$	$p = 0.240$	$p = 0.329$	$p = 0.533$	$p = 0.390$	$p = 0.896$
PCC						1.0000	0.2327	−0.3776	0.0596	−0.2529	−0.2592	−0.2517
						$p = -$	$p = 0.353$	$p = 0.122$	$p = 0.814$	$p = 0.311$	$p = 0.299$	$p = 0.314$
MN							1.0000	0.0398	−0.0784	−0.0834	−0.0841	0.2812
							$p = -$	$p = 0.875$	$p = 0.757$	$p = 0.742$	$p = 0.740$	$p = 0.258$
DOP								1.0000	−0.1676	**0.5961**	−0.1154	−0.1291
								$p = -$	$p = 0.506$	$\mathbf{p = 0.009}$	$p = 0.648$	$p = 0.610$
SER									1.0000	−0.2377	**0.7145**	0.3162
									$p = -$	$p = 0.342$	$\mathbf{p = 0.001}$	$p = 0.201$
GLUT										1.0000	−0.1090	−0.1747
										$p = -$	$p = 0.667$	$p = 0.488$
MAO											1.0000	**0.5126**
											$p = -$	$\mathbf{p = 0.030}$
AChE												1.0000
												$p = -$

involved in the "digestion/assimilation" process when exposed to MPs at first which is followed by decreased GLU levels as the concentrations in MPs increase.

Lastly, considering that the significant increase of DOP can be a defense mechanism towards PMs through reduced intake and elimination phenomena, we can assert that PMs, contextually to our experimental design, do not have direct adverse effects on the nervous system of zebra mussel. Probably the bivalves, being a suspension feeder, are adapted to fight more abrasive items than plastic beads, such as sands and diatom frustules. As suggested by Rist et al. (2016), MPs should be currently considered as a new component of seston and their effects on bivalves could be comparable to natural suspended matter. Therefore, in future studies it will be pivotal to investigate better these factors, prolonging the exposure to observe eventual adverse effects on longer times, as well as to deepen the knowledge regarding possible oscillatory behavior (wave trend) of assessed end-points, which represents an interesting aspect about the biomarker interpretation in ecotoxicology (Gagné, 2016; André and Gagné, 2017).

5. Conclusions

Our results confirm the uptake of 10 μm and 1 μm PMs in the gut lumen, tissues and circulatory system of zebra mussel after only 6 days of exposure. However, despite the accumulation of PMs in the exposed mussels, our results highlight that PMs did not induce great alteration of both oxidative balance and neuro- genotoxicity in zebra mussel, for the selected end-points and exposure time. Significant increase of DOP level can be considered only an indirect neurotoxic effect of PMs, to either promote their elimination or reduce intake of MPs in exposed organisms. However, considering the important uptake of PMs in the tissues and gut lumen of bivalves, it will be interesting to evaluate the inflammation and the modulation of the energy storage in the exposed mussels. At the same time, it will be important to investigate also the carrier role of MPs towards chemical pollutants, as well as the effect of plastic debris using the "omics" techniques, to completely characterize the MP toxic action on freshwater species. Lastly, this is a first study about the evaluation of oxidative stress/damage and neurogenotoxicity of virgin MP in zebra mussel where the presence findings will stimulate further investigation on the influence of MPs on feeding behavior and energy reserves.

Acknowledgements

We thank the Brusarosco Association and the Italian Ecological Society (S.It.E.) who funded the staying of Dr. Stefano Magni in the laboratory coordinated by Dr. François Gagné at Environment and Climate Change Canada (Government of Canada, Montréal, Québec, Canada) to perform the neurotoxicity biomarkers reported in this study.

References

Ackerman, J.D., 1999. Effect of velocity on the filter feeding of dreissenid mussels (*Dreissena polymorpha* and *Dreissena bugensis*): implications for trophic dynamics. Can. J. Fish. Aquat. Sci. 56, 1551–1561.

Aiello, E., Hager, E., Akiwumi, C., Stefano, G.B., 1986. An opioid mechanism modulates central and not peripheral dopaminergic control of ciliary activity in the marine mussel *Mytilus edulis*. Cell. Mol. Neurobiol. 6, 17–30.

Anderson, P.J., Warrack, S., Langen, V., Challis, J.K., Hanson, M.L., Rennie, M.D., 2017. Microplastic contamination in Lake Winnipeg, Canada. Environ. Pollut. 225, 223–231.

André, C., Gagné, F., 2017. Effect of the periodic properties of toxic stress on the oscillatory behaviour of glycolysis in yeast-evidence of a toxic effect frequency. Comp. Biochem. Physiol. C 196, 36–43.

Avio, C.G., Gorbi, S., Milan, M., Benedetti, M., Fattorini, D., d'Errico, G., Pauletto, M., Bargelloni, L., Regoli, F., 2015. Pollutants biovailability and toxicological risk from microplastics to marine mussels. Environ. Pollut. 198, 211–222.

Barboza, L.G.A., Vieira, L.R., Branco, V., Figueiredo, N., Carvalho, F., Carvalho, C., Guilhermino, L., 2018. Microplastics cause neurotoxicity, oxidative damage and energy-related changes and interact with the bioaccumulation of mercury in the European seabass, *Dicentrarchus labrax* (Linnaeus, 1758). Aquat. Toxicol. 195, 49–57.

Beiras, R., Widdows, J., Beiras, R., Widdows, J., 1995. Effect of the neurotransmitters dopamine, serotonin and norepinephrine on the ciliary activity of mussel (*Mytilus edulis*) larvae. Mar. Biol. 122, 597–603.

Binelli, A., Magni, S., Soave, C., Marazzi, F., Zuccato, E., Castiglioni, S., Parolini, M., Mezzanotte, V., 2014. The biofiltration process by the bivalve *D. Polymorpha* for the removal of some pharmaceuticals and drugs of abuse from civil wastewaters. Ecol. Eng. 71, 710–721.

Binelli, A., Della Torre, C., Magni, S., Parolini, M., 2015. Does zebra mussel (*Dreissena polymorpha*) represent the freshwater counterpart of *Mytilus* in ecotoxicological studies? A critical review. Environ. Pollut. 196, 386–403.

Bradford, M.M., 1976. A rapid and sensitive method for the quantification of microgram quantities of protein using the principle of protein-dye binding. Anal. Biochem. 72, 248–254.

Browne, M.A., Dissanayake, A., Galloway, T.S., Lowe, D.M., Thompson, R.C., 2008. Ingested microscopic plastic translocates to the circulatory system of the mussel, *Mytilus edulis* (L.). Environ. Sci. Technol. 42, 5026–5031.
Browne, M.A., Crump, P., Niven, S.J., Teuten, E., Tonkin, A., Galloway, T., Thompson, R., 2011. Accumulation of microplastic on shorelines worldwide: sources and sinks. Environ. Sci. Technol. 45, 9175–9179.
Callebaut, M., Meeussen, C., 1989. Method for the preservation of polystyrene latex beads in tissue sections. Stain. Technol. 64, 100–102.
Cole, M., Lindeque, P., Halsband, C., Galloway, T.S., 2011. Microplastics as contaminants in the marine environment: a review. Mar. Pollut. Bull. 62, 2588–2597.
Derraik, J.G.B., 2002. The pollution of the marine environment by plastic debris: a review. Mar. Pollut. Bull. 44, 842–852.
Di, M., Wang, J., 2018. Microplastics in surface waters and sediments of the Three Gorges Reservoir, China. Sci. Total Environ. 616, 1620–1627.
Eerkes-Medrano, D., Thompson, R.C., Aldridge, D.C., 2015. Microplastics in freshwater systems: a review of the emerging threats, identification of knowledge gaps and prioritisation of research needs. Water Res. 75, 63–82.
Ellman, G.L., Courtney, K.D., Andres Jr., R., Featherstone, R.M., 1961. A new and rapid colorimetric determination of acetylcholinesterase activity. Biochem. Pharmacol. 7, 88–90.
Farrell, P., Nelson, K., 2013. Trophic level transfer of microplastic: *Mytilus edulis* (L.) to *Carcinus maenas* (L.). Environ. Pollut. 177, 1–3.
Faure, F., Corbaz, M., Baecher, H., de Alencastro, L., 2012. Pollution due to plastics and microplastics in Lake Geneva and in the Mediterranean Sea. Arch. Des. Sci. 65, 157–164.
Fendall, L.S., Sewell, M.A., 2009. Contributing to marine pollution by washing your face: microplastics in facial cleansers. Mar. Pollut. Bull. 58, 1225–1228.
Fong, P., Noordhuis, R., Ram, J.L., 1993. Dopamine reduces intensity of serotonin-induced spawning in the zebra mussel *Dreissena polymorpha* (Pallas). J. Exp. Zool. 266, 79–83.
Free, C.M., Jensen, O.P., Mason, S.A., Eriksen, M., Williamson, N.J., Boldgiv, B., 2014. High-levels of microplastic pollution in a large, remote, mountain lake. Mar. Pollut. Bull. 85, 156–163.
Gagné, F., 2014. Biochemical Ecotoxicology: Principles and Methods. 1st Edition. Elsevier, London.
Gagné, F., 2016. The wave nature of molecular responses in ecotoxicology. Curr. Top. Toxicol. 12, 12–24.
Gagné, F., Blaise, C., 2003. Effects of municipal effluents on serotonin and dopamine levels in the freshwater mussel *Elliptio complanata*. Comp. Biochem. Physiol. C 136, 117–125.
Gagné, F., André, C., Gélinas, M., 2010. Neurochemical effects of benzodiazepine and morphine on freshwater mussels. Comp. Biochem. Physiol. C 152, 207–214.
Gardiner, D.B., Silverman, H., Dietz, T.H., 1991. Musculature associated with the water canals in freshwater mussels and response to monoamines *in vitro*. Biol. Bull. 180, 453–465.
Guilhermino, L., Vieira, L.R., Ribeiro, D., Tavares, A.S., Cardoso, V., Alves, A., Almeida, J.M., 2018. Uptake and effects of the antimicrobial florfenicol, microplastics and their mixtures on freshwater exotic invasive bivalve *Corbicula fluminea*. Sci. Total Environ. 622, 1131–1142.
Hidalgo-Ruz, V., Gutow, L., Thompson, R.C., Thiel, M., 2012. Microplastics in the marine environment: a review of the methods used for identification and quantification. Environ. Sci. Technol. 46, 3060–3075.
Horton, A.A., Walton, A., Spurgeon, D.J., Lahive, E., Svendsen, C., 2017. Microplastics in freshwater and terrestrial environments: evaluating the current understanding to identify the knowledge gaps and future research priorities. Sci. Total Environ. 586, 127–141.
Hussain, N., Jaitley, V., Florence, A.T., 2001. Recent advances in the understanding of uptake of microparticulates across the gastrointestinal lymphatics. Adv. Drug Deliv. Rev. 50, 107–142.
Imhof, H.K., Ivleva, N.P., Schmid, J., Niessner, R., Laforsch, C., 2013. Contamination of beach sediments of a subalpine lake with microplastic particles. Curr. Biol. 23, R867–R868.
Imhof, H.K., Wiesheu, A.C., Anger, P.M., Niessner, R., Ivleva, N.P., Laforsch, C., 2018. Variation in plastic abundance at different lake beach zones - a case study. Sci. Total Environ. 613-614, 530–537.
Khotimchenko, Y.S., 1991. Biogenic monoamines in oocytes of echinoderms and bivalve mollusks: a formation of intracellular regulatory systems in oogenesis. Comp. Biochem. Physiol. C 100, 671–675.
Kirkland, D.J., Hayashi, M., Jacobson-Kram, D., Kasper, P., MacGregor, J.T., Müller, L., 2007. Summary of major conclusions from the 4th IWGT, San Francisco, 9–10 September, 2005. Mutat. Res. 627, 5–9.
Kirsch-Volders, M., Sofuni, T., Aaderma, M., Albertini, S., Eastmond, D., Fenech, M., Ishidate Jr., M., Kirchner, S., Lorge, E., Morita, T., Norppa, H., Surrallés, J., Vanhauwaet, A., Wakata, A., 2000. Report from the *in vitro* micronucleus assay working group. Environ. Mol. Mutagen. 35, 167–172.
Law, K.L., Thompson, R.C., 2014. Microplastics in the seas. Science 345, 144–145.
Lechner, A., Keckeis, H., Lamesberger-Loisl, F., Zens, B., Krusch, R., Tritthart, M., Glas, M., Schludermann, E., 2014. The Danube so colourful: a potpourii of plastic litter outnumbers fish larvae in Europe's second largest river. Environ. Pollut. 188, 177–181.
Lei, L., Wu, S., Lu, S., Liu, M., Song, Y., Fu, Z., Shi, H., Raley-Susman, K.M., He, D., 2018. Microplastic particles cause intestinal damage and other adverse effects in zebrafish *Danio rerio* and nematode *Caenorhabditis elegans*. Sci. Total Environ. 619, 1–8.
Luo, Y., Roth, G.S., 2000. The roles of dopamine oxidative stress and dopamine receptor signaling in aging and age-related neurodegeneration. Antioxid. Redox Signal. 2, 449–460.
Magni, S., Parolini, M., Soave, C., Marazzi, F., Mezzanotte, V., Binelli, A., 2015. Removal of metallic elements from real wastewater using zebra mussel bio-filtration process. J. Environ. Chem. Eng. 915-921.
Magni, S., Parolini, M., Binelli, A., 2016. Sublethal effects induced by morphine to the freshwater biological model *Dreissena polymorpha*. Environ. Toxicol. 31, 58–67.
Magni, S., Parolini, M., Della Torre, C., Fernandes de Oliveira, L., Catani, M., Guzzinati, R., Cavazzini, A., Binelli, A., 2017. Multi-biomarker investigation to assess toxicity induced by two antidepressants on *Dreissena polymorpha*. Sci. Total Environ. 578, 452–459.
Mecocci, P., Fano, G., Fulle, S., MacGarvey, U., Shinobu, L., Polidori, M.C., Cherubini, A., Vecchiet, J., Senin, U., Flint Beal, M., 1999. Age-dependent increases in oxidative damage to DNA, lipids, and proteins in human skeletal muscle. Free Radic. Biol. Med. 26, 303–308.
von Moos, N., Burkhardt-Holm, P., Köhler, A., 2012. Uptake and effects of microplastics on cells and tissue of the blue mussel *Mytilus edulis* L. after an experimental exposure. Environ. Sci. Technol. 46, 11327–11335.
Murphy, F., Quinn, B., 2018. The effects of microplastic on freshwater *Hydra attenuata* feeding, morphology & reproduction. Environ. Pollut. 234, 487–494.
Murphy, F., Ewins, C., Carbonnier, F., Quinn, B., 2016. Wastewater treatment works (WwTW) as a source of microplastics in the aquatic environment. Environ. Sci. Technol. 50, 5800–5808.
Nel, H.A., Dalu, T., Wasserman, R.J., 2018. Sinks and sources: assessing microplastic abundance in river sediment and deposit feeders in an Austral temperate urban river system. Sci. Total Environ. 612, 950–956.
Ohkawa, H., Ohisi, N., Yagi, K., 1979. Assay for lipid peroxides in animal tissues by thiobarbituric acid reaction. Anal. Biochem. 95, 351–358.
Oliveira, M., Ribeiro, A., Hylland, K., Guilhermino, L., 2013. Single and combined effects of microplastics and pyrene on juveniles (0+ group) of the common goby *Pomatoschistus microps* (Teleostei, Gobiidae). Ecol. Indic. 34, 641–647.
Orbea, A., Ortiz-Zarragoitia, M., Solé, M., Porte, C., Cajaraville, M.P., 2002. Antioxidant enzymes and peroxisome proliferation in relation to contaminant body burdens of PAHs and PCBs in bivalve molluscs, crabs and fish from the Urdaibai and Plentzia estuaries (Bay of Biscay). Aquat. Toxicol. 58, 75–98.
Paul-Pont, I., Lacroix, C., González Fernández, C., Hégaret, H., Lambert, C., Le Goïc, N., Frère, L., Cassone, A.L., Sussarellu, R., Fabioux, C., Guyomarch, J., Albentosa, M., Huvet, A., Soudant, P., 2016. Exposure of marine mussels *Mytilus* spp. to polystyrene microplastics: toxicity and influence on fluoranthene bioaccumulation. Environ. Pollut. 216, 724–737.
Pavlica, M., Klobucar, G.I.V., Vetma, N., Erben, R., Papes, D., 2000. Detection of micronuclei in haemocytes of zebra mussel and ramshorn snail exposed to pentachlorophenol. Mutat. Res. 465, 145–150.
PlasticsEurope, 2016. An analysis of European plastics production, demand and waste data. http://www.plasticseurope.org.
Ribeiro, F., Garcia, A.R., Pereira, B.P., Fonseca, M., Mestre, N.C., Fonseca, T.G., Ilharco, L.M., Bebianno, M.J., 2017. Microplastics effects in *Scrobicularia plana*. Mar. Pollut. Bull. 122, 379–391.
Rist, S.E., Assidqi, K., Zamani, N.P., Appel, D., Perschke, M., Huhn, M., Lenz, M., 2016. Suspended micro-sized PVC particles impair the performance and decrease survival in the Asian green mussel *Perna viridis*. Mar. Pollut. Bull. 111, 213–220.
Sadri, S.S., Thompson, R.C., 2014. On the quantity and composition of floating plastic debris entering and leaving the Tamar Estuary, Southwest England. Mar. Pollut. Bull. 81, 55–60.
Smith, J.R., 1982. A survey of endogenous dopamine and serotonin in ciliated and nervous tissue of five species of marine bivalves, with evidence for specific, high-affinity dopamine receptors in ciliated tissue of *Mytilus californianus*. Comp. Biochem. Physiol. 71, 57–61.
Spina, M.B., Cohen, G., 1989. Dopamine turnover and glutathione oxidation: implications for Parkinson disease. Proc. Natl. Acad. Sci. U. S. A. 86, 1398–1400.
Stefano, G.B., Aiello, E., 1975. Histofluorescent localization of serotonin and dopamine in the nervous system and gill of *Mytilus edulis* (Bivalvia). Biol. Bull. 148, 141–156.
Su, L., Xue, Y., Li, L., Yang, D., Kolandhasamy, P., Li, D., Shi, H., 2016. Microplastics in Taihu Lake, China. Environ. Pollut. 216, 711–719.
Sussarellu, R., Suquet, M., Thomas, Y., Lambert, C., Fabioux, C., Pernet, M.E.J., Le Goïc, N., Quillien, V., Mingant, C., Epelboin, Y., Corporeau, C., Guyomarch, J., Robbens, J., Paul-Pont, I., Soudant, P., Huvet, A., 2016. Oyster reproduction is affected by exposure to polystyrene microplastics. Proc. Natl. Acad. Sci. 113, 2430–2435.
Sutherland, W., Clout, M., Cote, I., Daszak, P., Depledge, M., Fellman, L., Fleishman, E., Garthwaite, R., Gibbons, D., De Lurio, J., Impey, A., Lickorish, F., Lindenmayer, D., Madgwick, J., Margerison, C., Maynard, T., Peck, L., Pretty, J., Prior, S., Redford, K., Scharlemann, J., Spalding, M., Watkinson, A., 2010. A horizon scan of global conservation issues for 2010. Trends Ecol. Evol. 25, 1–7.
Thompson, R.C., Moore, C.J., vom Saal, F.S., Swan, S.H., 2009. Plastics, the environment and human health: current consensus and future trends. Philos. Trans. R. Soc. B 364, 2153–2166.
Van Cauwenberghe, L., Janssen, C.R., 2014. Microplastics in bivalves cultured for human consumption. Environ. Pollut. 193, 65–70.
Van Cauwenberghe, L., Claessens, M., Vandegehuchte, M.B., Janssen, C.R., 2015. Microplastics are taken up by mussels (*Mytilus edulis*) and lugworms (*Arenicola marina*) living in natural habitats. Environ. Pollut. 199, 10–17.
Wagner, M., Scherer, C., Alvarez-Munõz, D., Brennholt, N., Bourrain, X., Buchinger, S., Fries, E., Grosbois, C., Klasmeier, J., Marti, T., Rodriguez-Mozaz, S., Urbatzka, R., Vethaak, A., Winther-Nielsen, M., Reifferscheid, G., 2014. Microplastics in freshwater ecosystems: what we know and what we need to know. Environ. Sci. Eur. 26, 12.
Wang, J., Peng, J., Tan, Z., Gao, Y., Zhan, Z., Chen, Q., Cai, L., 2016. Microplastics in the surface sediments from the Beijiang River littoral zone: composition, abundance, surface textures and interaction with heavy metals. Chemosphere 171, 248–258.
Wang, W., Ndungu, A.W., Li, Z., Wang, J., 2017. Microplastics pollution in inland freshwaters of China: a case study in urban surface waters of Wuhan. China. Sci. Total Environ. 575, 1369–1374.
Wright, S.L., Rowe, D., Thompson, R.C., Galloway, T.S., 2013. Microplastic ingestion decreases energy reserves in marine worms. Curr. Biol. 23, R1031–R1033.

Environmental Pollution 250 (2019) 407–415

Contents lists available at ScienceDirect

Environmental Pollution

journal homepage: www.elsevier.com/locate/envpol

First evidence of protein modulation by polystyrene microplastics in a freshwater biological model

S. Magni [a], C. Della Torre [a], G. Garrone [b], A. D'Amato [c], C.C. Parenti [a], A. Binelli [a, *]

[a] Department of Biosciences, University of Milan, Via Celoria 26, 20133, Milan, Italy
[b] UNITECH OMICS Platform, University of Milan, Viale Ortles 22/4, 20139, Milan, Italy
[c] Department of Pharmaceutical Sciences (DISFARM), University of Milan, Via Mangiagalli 25, 20133, Milan, Italy

ARTICLE INFO

Article history:
Received 19 February 2019
Received in revised form
15 April 2019
Accepted 17 April 2019
Available online 17 April 2019

ABSTRACT

Microplastics (MPs) are now one of the major environmental problems due to the large amount released in aquatic and terrestrial ecosystems, as well as their diffuse sources and potential impacts on organisms and human health. Still the molecular and cellular targets of microplastics' toxicity have not yet been identified and their mechanism of actions in aquatic organisms are largely unknown. In order to partially fill this gap, we used a mass spectrometry based functional proteomics to evaluate the modulation of protein profiling in zebra mussel (*Dreissena polymorpha*), one of the most useful freshwater biological model. Mussels were exposed for 6 days in static conditions to two different microplastic mixtures, composed by two types of virgin polystyrene microbeads (size = 1 and 10 μm) each one. The mixture at the lowest concentration contained 5 × 105 MP/L of 1 μm and 5 × 105 MP/L of 10 μm, while the higher one was arranged with 2 × 106 MP/L of 1 μm and 2 × 106 MP/L of 10 μm.

Proteomics' analyses of gills showed the complete lack of proteins' modulation after the exposure to the low-concentrated mixture, while even 78 proteins were differentially modulated after the exposure to the high-concentrated one, suggesting the presence of an effect-threshold. The modulated proteins belong to 5 different classes mainly involved in the structure and function of ribosomes, energy metabolism, cellular trafficking, RNA-binding and cytoskeleton, all related to the response against the oxidative stress.

1. Introduction

The increasing production and use of plastic goods and mainly their improper disposal, as well as the poor management of plastic wastes, have led to a great and continuous release of plastics in terrestrial and water ecosystems. Plastics are now one of the main challenges in the environmental management since the solution or more probably the mitigation of this problem affects the lifestyle, habits and behavior of each of us. In the last years, the scientific community focused the attention to microplastics (MPs), which are recently re-defined as synthetic polymers from 1 to <1000 μm in the largest dimension (Hartmann et al., 2019). They derive from two different sources: the primary MPs originate from some plastic products, such as toothpastes, scrubs, cosmetics or pellets used in plastic production (Hidalgo-Ruz et al., 2012; Carr et al., 2016), while secondary MPs are small debris degraded through physical, chemical and biological processes from large plastics, such as shopping bags, fishing nets, resin pellets and household items (Browne et al., 2007). Although the MPs from terrestrial sources contribute to 80% of the total plastic debris that reach marine ecosystems (Cole et al., 2011), only few studies were conducted in freshwaters, as recently highlighted by Lambert and Wagner (2018) who indicated that less than 4% of studies related to MPs can be associated to inland waters. The MPs in freshwaters are characterized by an outstanding heterogeneity depending on sampling location, weather conditions, human activities and also sampling approaches (Eerkes-Medrano et al., 2015). The mean density of MPs in freshwaters changes dramatically, varying from almost none to many million MPs/m^3 (Li et al., 2018). The environmental impact of MPs can be categorized to physical, chemical and toxicological effects, each of them were identified mainly in marine organisms.

While the physical impacts of macroplastics include entanglement and ingestion which cause drowning, suffocation, strangulation and starving (Allsopp et al., 2006), MPs' ingestion can

* Corresponding author.
E-mail address: andrea.binelli@unimi.it (A. Binelli).

https://doi.org/10.1016/j.envpol.2019.04.088
0269-7491/

damage the gastrointestinal tract by mechanical rubbing and physical blockage of digestive organs (Jovanovic, 2017). The chemical and toxicological impacts are linked both to the intrinsic toxicity of MPs, but especially to the effects of additives, such as phthalates and bisphenol A used as plasticizers (Hammer et al., 2012), or to the plethora of environmental pollutants adsorbed on their surface that can be firstly ingested with MPs and then released in the organism even faster than that in the environment (Bakir et al., 2014). Up to now, only few studies were carried out in freshwater organisms: a very recent research showed an inhibition of cholinesterase activity on the bivalve *Corbicula fluminea* due to a mixture of the antimicrobial florfenicol and MPs (Guilhermino et al., 2018), while several studies conducted on larval and adult zebrafish (*Danio rerio*) demonstrated as MPs caused locomotion alteration, intestinal damage and metabolic changes (Lu et al., 2016; Chen et al., 2017; Sleight et al., 2017; Lei et al., 2018). Ding et al., 2018 found an activation of EROD (7-ethoxyresorufin O-deethylase), BFCOD (7-benzyloxy-4-trifluoromethyl-coumarin O-dibenzyloxylase) and SOD (superoxide dismutase) in the liver, as well as an inhibition of AChE (acetylcholinesterase) in the brain of the fish red Tilapia (*Oreochromis niloticus*) exposed for 14 days to 0.1 mm polystyrene MPs administered at different concentrations. Instead, Weber et al. (2018) have not monitored any significant effects on survival, development, metabolism and feeding activity in the freshwater crustacean *Gammarus pulex* exposed to irregular fragments of polyethylene terephthalate (PET; 10–150 μm) for 48 h. Our previous results obtained on the same freshwater zebra mussel (*Dreissena polymorpha*) used in this proteomic study showed a significant ($p < 0.05$) increase of catalase and dopamine and a significant ($p < 0.05$) decrease of glutathione peroxidase (Magni et al., 2018).

Therefore, in order to partially fill this gap of knowledge on the impact of MPs in freshwater organisms, we investigated the possible proteins' modulation in zebra mussels (*Dreissena polymorpha*) exposed to two different concentrations of a mixture of two types of virgin polystyrene microbeads (size = 1 and 10 μm). We carried out static exposures for 6 days, performing proteomics analyses on mussels' gills, considering that this organ can represent a route of entrance for these emerging contaminants and that gills could be a target for MPs, being the first barrier that they encounter when enter through the inhalant siphon of mussels. The selection of zebra mussel as biological model is due to its specific characteristics, such as high filtration rate, easiness in laboratory maintenance, size suitable to expose a significant number of specimens and its ecological position that links littoral and benthic ecosystems (Binelli et al., 2015). Mass spectrometry-based proteomics is one of the most sensitive methodology available in ecotoxicology (Monsinjor and Knigge, 2007) and allowed us to study the potential toxicity of the virgin MPs. To our knowledge, this represents the first attempt to investigate the possible role played by MPs to modulate the proteins' expression of a freshwater organism.

2. Materials and methods

2.1. Selection of concentrations and exposure to polystyrene MPs

We collected hundreds of zebra mussels in Lake Iseo (Northern Italy) at 2–3 m of depth, then transported in lake water to the laboratory. Before the exposure tests, mussels were acclimated for 2 weeks in 15 L tanks (50:50 v/v of tap and deionized water), at 20 ± 1 °C under oxygen saturation and natural photoperiod, and fed with *Spirulina* sp., as described in other previous studies (Binelli et al., 2015; Magni et al., 2016, 2017, 2018).

We purchased the standard suspension (5%) of polystyrene MPs (1 and 10 μm) from Sigma Aldrich (Milan, Italy), which were subsequently diluted in ultrapure water to reach 50 mg/L of suspensions. Then, we quantified the number of the two types of MPs by a Bürker chamber, achieving $116 \times 10^6 \pm 33 \times 10^6$ of 10 μm MP/L and $23 \times 10^9 \pm 530 \times 10^6$ of 1 μm MP/L, respectively. We did not notice any MPs' aggregation in the working suspensions observed by confocal microscopy (Magni et al., 2018). We measured the number of MPs only in the working suspensions, because it was impossible their measurement in the exposure beakers. We tried by coulter counter, but the lack of any surface charge prevents any possible realistic measure. Then, we tried by the Bürker chamber, by which we measured the MPs in the working suspensions. However, after the dilutions to reach the selected concentration in the exposure beakers, the average number of 10 μm microparticles in M2 (the highest suspension) was only 1.8 particles in the Bürker chamber: 2.000.000 particles/L = 2 particles/μL (mm^3). Then, (2 particles/mm^3) x 9 mm^2 (chamber area) = 18 particles/mm x 0.1 mm (thickness of chamber) = 1.8 average total particles in the Bürker chamber. This low value made not possible a plausible evaluation of the final suspensions' concentration. Furthermore, MPs of 1 μm were impossible to check in the exposure beakers due to their small size and the presence of the microalgae used as food that interfere on the microscopy observations.

Since the aim of this study was the preliminary investigation of the possible role of this kind of MPs to modulate the proteome of a non-target freshwater organism, we selected two MPs' concentrations higher than those now found in the inland waters in order to evaluate the mechanism of action (MoA) of these physical environmental contaminants. The reason is exactly the same even for the choice to use two mixtures of MPs with two different sizes (1 and 10 μm): the first one (M1) with 5×10^5 MP/L of 1 μm and 5×10^5 MP/L of 10 μm (total amount: 1×10^6 MP/L), while the second one (M2) with 2×10^6 MP/L of 1 μm and 2×10^6 MP/L of 10 μm (total concentration: 4×10^6 MP/L).

Exposures were carried out in triplicate (3 tanks for controls, M1 and M2, respectively), placing 70 mussels on suspended nets in each 4 L glass beakers (n = 9) for each of the two mixtures (Ms) and related control for 6 days in static conditions in the same maintenance conditions above mentioned and under slow stirring to prevent the MPs' sedimentation. Thus, the sample size for each treatment and controls was 210 each one (70 mussels/tank x 3 tanks) which were then used both for biomarker analyses and proteomics. The short exposure time is related to the onset of deleterious effects caused by the bivalve metabolism and the food degradation after 6 days due to the lack of water change.

We added food only two times during the exposure to avoid a possible effect simply due to the under-nutrition, but at the same time to eliminate any possible interference of algae to the MPs' bioavailability, bearing in mind that the aim of the study was the investigation of the potential toxicity of the only MPs. On the other hand, the primary effect of toxicants should appear early, since it affects the molecular level at first. Indeed, we previously evaluated that this exposure time is sufficient to produce some cyto- and genotoxic effects, as well as proteins' modulation on this biological model (Binelli et al., 2015; Magni et al., 2018).

At the end of exposure, we dissected one gill from 5 mussels *per* treatment, randomly selected from the three beakers, then stored at −80 °C, while the other mussels were used for biomarkers measurements (Magni et al., 2018). Contemporarily, the other fresh dissected gill was quickly observed with an optical microscope without any preliminary treatment to confirm the presence of MPs in this tissue.

2.2. Mass spectrometry based proteomic analysis

2.2.1. Sample preparation

We homogenized a pool of 5 gills *per* treatment (1 gill for each mussel randomly selected from the three tanks) in 500 μL of lysis buffer containing 20 mM 4-(2-hydroxyethyl)-1-piperazineethanesulfonic acid pH = 7.5 (HEPES), 320 mM sucrose, 1 mM ethylenediaminetetraacetic acid pH = 8.5 (EDTA), 5 mM ethylene glycol-bis(β-aminoethyl ether)-N,N,N′,N′-tetraacetic acid pH = 8.1 (EGTA), 1 mM sodium ortho-vanadate (Na_3VO_4), 10 mM β-glycerophosphate, 10 mM sodium fluoride (NaF), 10 mM sodium pyrophosphate (NaPPi), 1 mM phenylmethylsulfonyl fluoride (PMSF) in ethanol, 5 mM dithiothreitol (DTT) and protease inhibitors (Roche) in Milli Q® water (Binelli et al., 2017). We centrifuged the homogenates at 15,000 g (S15 fraction) for 10 min at 4 °C and quantified the proteins with Bradford method (Bradford, 1976); 300 μg of proteins were then precipitated with methanol/chloroform/Milli Q water (4:1:3 ratio v/v). Obtained pellets were re-suspended in 8 M urea in 50 mM tris hydrochloride (Tris-HCl), 30 mM sodium chloride (NaCl) pH = 8.5 and protease inhibitors (Roche) and centrifuged at 14,000 g for 30 min at 4 °C. We re-quantified the proteins in the supernatant with Bradford method (Bradford, 1976). Then, 10 μg of proteins were incubated with 50 mM DTT in 50 mM ammonium bicarbonate (AMBIC) for 30 min at 52 °C under stirring (600 rpm) to perform the reduction of disulfide bonds; subsequently, we added in each sample 100 mM iodoacetamide ($IANH_2$) and incubated for 20 min at room temperature (RT) to alkylate the sulfhydryl groups. To obtain peptide mixture, proteins were digested by Trypsin Sequencing Grade (Roche, Monza, Italy) in 50 mM AMBIC overnight at 37 °C under stirring (400 rpm). Peptides were purified by reverse phase chromatography, using Zip Tips (μ-C18; Millipore, Milan, Italy).

2.2.2. High resolution mass spectrometry analysis (nLC-MSMS)

Tryptic peptides were analyzed at UNITECH OMICs (University of Milano, Italy) using a Dionex Ultimate 3000 nano-LC system (Sunnyvale CA, USA) connected to an Orbitrap Fusion™ Tribrid™ Mass Spectrometer (Thermo Scientific, Bremen, Germany) equipped with a nano-electrospray ion source. Peptide mixtures were pre-concentrated onto an Acclaim PepMap 100 - 100 μm × 2 cm C18 and separated on EASY-Spray column, 15 cm × 75 μm ID packed with Thermo Scientific Acclaim PepMap RSLC C18, 3 μm, 100 Å. The temperature was set to 35 °C and the flow rate was 300 nL min^{-1}. Mobile phases were the following: 0.1% Formic acid (FA) in water (solvent A); 0.1% FA in water/acetonitrile (solvent B) with 2/8 ratio. Peptides were eluted from the column with the following gradient: 4%–28% of B for 90 min and then 28%–40% of B in 10 min, and to 95% within the following 6 min to rinse the column. Column was re-equilibrated for 20 min. Total run time was 130 min. One blank was run between triplicates to prevent sample carryover. MS spectra were collected over an m/z range of 375–1500 Da at 120,000 resolutions, operating in the data dependent mode, cycle time 3 s between master scans. HCD was performed with collision energy set at 35 eV. Each sample was analyzed in three technical triplicates.

LTQ raw data was searched against a protein database using SEQUEST algorithm in Proteome Discoverer software version 2.2 (Thermo Scientific) for peptide/protein identification. The searches were performed against Uniprot KnowledgeBase (KB) (taxonomy Bivalvia, 83922 entries). The minimum peptide length was set to six amino acids and enzymatic digestion with trypsin was selected, with maximum 2 missed cleavages. A precursor mass tolerance of 8 ppm and fragment mass tolerance of 0.02 Da were used; acetylation (N-term), oxidation (M) were used as dynamic modifications and carbamidomethylation (C) as static modification. The false discovery rates (FDRs) at the protein and peptide level were set to 0.01 for highly confident peptide-spectrum matches and 0.05 for peptide-spectrum matches with moderate confidence.

We considered only proteins with a score of coverage >2% with at least two identified peptides. Differences in abundance ratio (AR) of proteins between M1 and M2 against control were considered only with at least a 2-fold change and with a standard deviation between replicates less than 20%. We identified 425 different proteins, but the cut-offs made and the necessity of the homology search, based on the "Bivalvia" taxonomy entry only, decreased the proteins to 152.

3. Results and discussion

Although we had previous evidences of the intake of this kind of MPs both in other soft tissues and hemolymph of *D. polymorpha*, as reported in our recent work (Magni et al., 2018), we wanted the certainty of the MPs' presence in the gills to be sure that the potential effects observed on the proteome were effectively due to these contaminants. Thus, we used the optical microscopy (20×) directly on one of the fresh gills extracted from the mussels collected for the analyses. The microscopy observations pointed out the presence of many MPs of 10 μm interposed among the gill lamellae (Fig. 1 B, C, D) for the two Ms, confirming the uptake capability of zebra mussels also for this physical contaminant. The intake of 1 μm MP, not visible by optical microscopy, was already observed in this biological model by confocal observations in our previous study (Magni et al., 2018).

Moving to the proteomics' results, no proteins' modulation was obtained at the end of the exposure to M1 in comparison to controls, while M2 was able to modulate 78 different proteins (Fig. 2), but one of the most relevant results concerned the fact that 18 proteins were completely not expressed in zebra mussels exposed to M2 compared to controls (Table 1).

The two Ms showed a very different impact on zebra mussels' gill proteome considering the lack of changes observed for the exposure to M1 compared to the heavy effect made by M2, which contain an MPs' concentration only four times greater. This seems to suggest a kind of threshold whose reasons can be simply related to the higher intake of MPs in the mussels that reached the level-threshold to be toxic, but maybe also to the overrun of homeostatic responses that are no longer able to fight the injuries made by MPs. This result, which is the first evidence of this kind of effect due to MPs on the proteome of freshwater organisms, surely opens new questions on the toxicological behavior due to these physical contaminants and maybe can represent the first step to identify hypothetic limits to the environmental concentrations of MPs to be used in a future risk management. Other additional experiments will certainly be needed to confirm the threshold we found, bearing in mind the inability to measure the MPs' concentrations directly in the exposure beakers, as well explained in the paragraph 2.1.

Moving to the modulation of gill protein, we did not observe a specific metabolic pathway as target, but rather a diffuse effect on many protein classes. Fig. 3 shows that the catalytic activity (27%) and nucleotide binding were the major classes of proteins modified by the M2 exposure, followed by proteins involved in the structural molecule activity (12%) and protein binding (11%). Proteins related to RNA (5%) and metal ion (4%) bindings close the list of modulated protein classes. More in detail, the changed proteins are mainly involved in the structure and function of ribosomes, energy metabolism, cellular trafficking, RNA-binding and cytoskeleton (Table 1), which are directly or indirectly involved in the oxidative stress homeostasis. Indeed, several recent studies highlighted that the increase of oxidative stress and the consequent imbalance of the antioxidant defense mechanism are one of the major effects

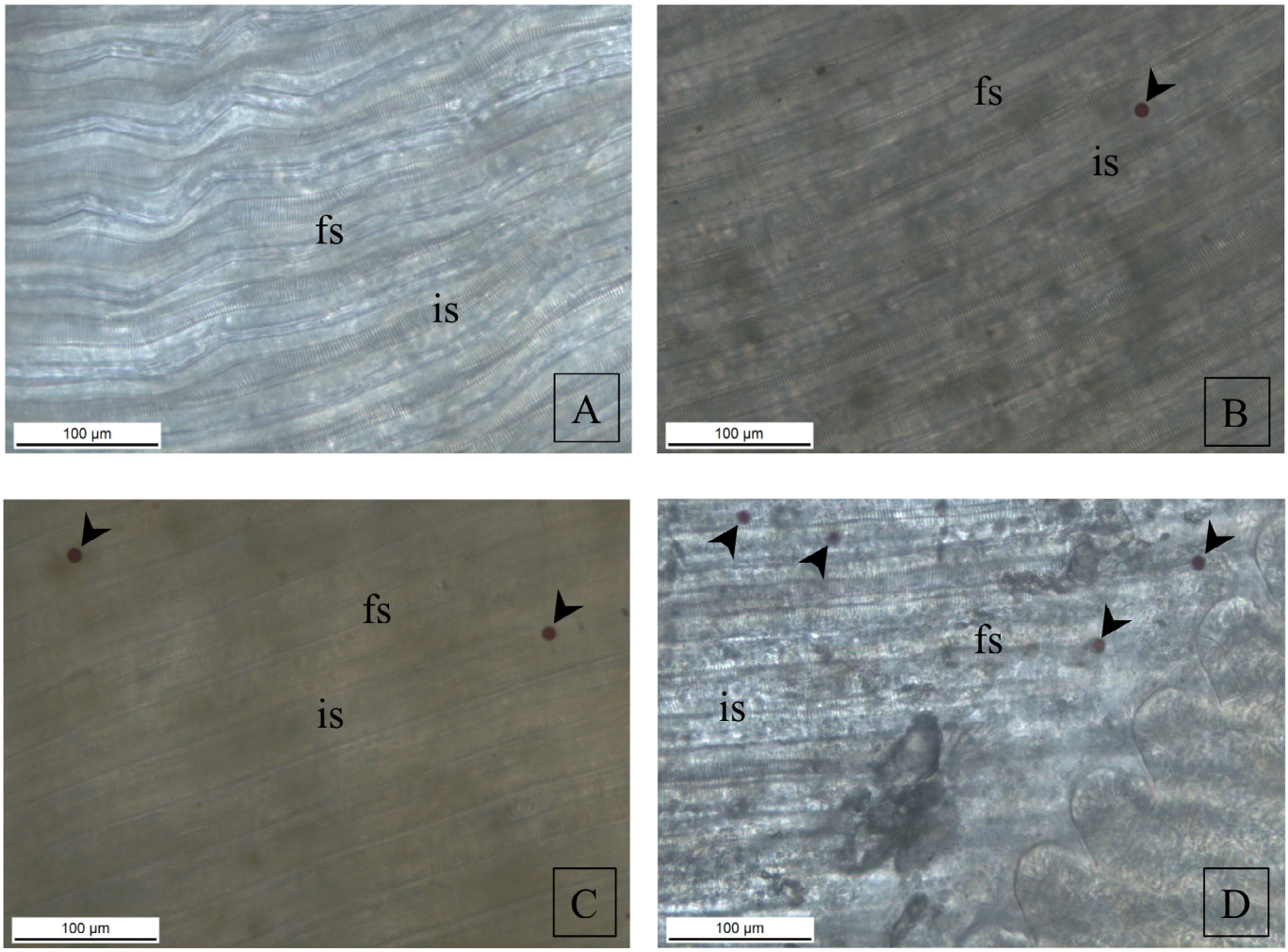

Fig. 1. Intake of MPs: microplastics of 10 μm (indicated by arrows) inserted in the gills' lamellae of zebra mussels (B, C, D) in comparison to controls (A). fs = frontal surface of a filament; is = interfilament space.

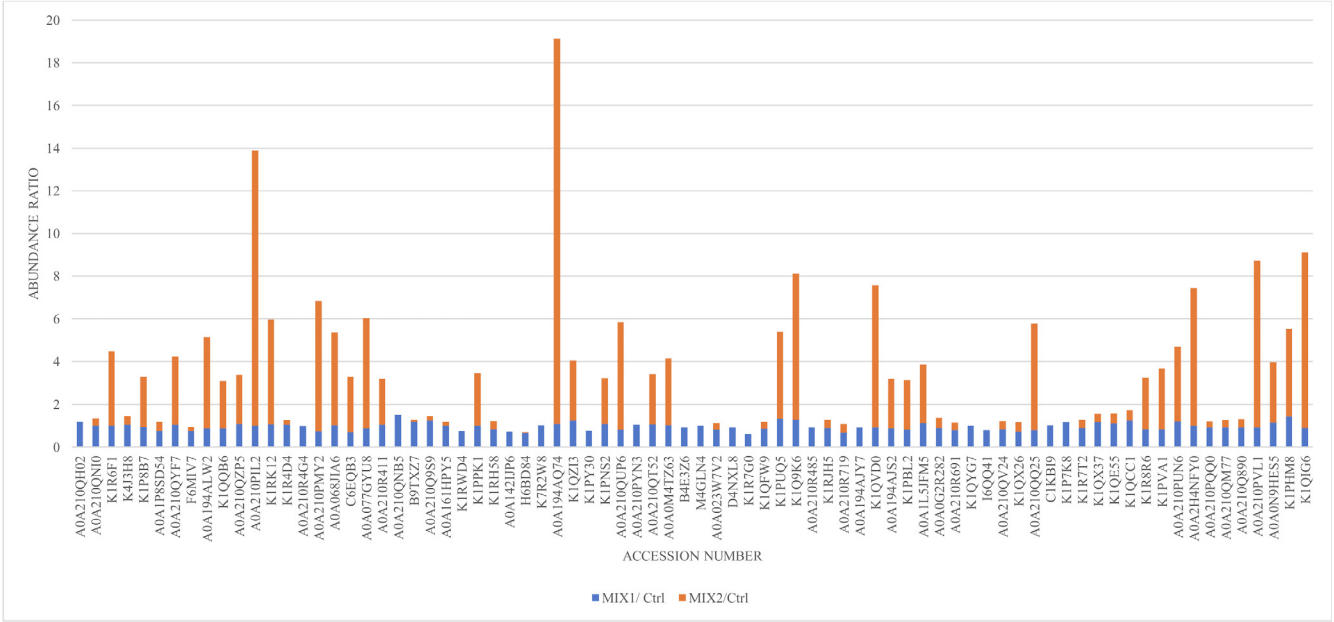

Fig. 2. Protein profiling modulation: differentially modulated proteins due to M1 and M2 related to controls.

Table 1
Description of the proteins modulated in the zebra mussel gills by M1 and M2.

Main Function	UniProt Accession	Description	Coverage [%]	Peptides	Unique Peptides	MW [kDa]	pI	AR: (M1)/(Ctrl)	AR: (M2)/(Ctrl)
Protein degradation									
	A0A210QH02	26S proteasome non-ATPase regulatory subunit 7 (Mizuhopecten yessoensis)	9	2	2	38.1	6.62	1.180	NOT FOUND
	A0A210QNI0	26S proteasome non-ATPase regulatory subunit 14 (*Mizuhopecten yessoensis*)	6	2	2	34.6	6.58	0.998	0.349
	K1R6F1	Proteasome subunit alpha type (*Crassostrea gigas*)	31	6	6	28.0	7.47	0.995	3.466
	K4J3H8	Activated protein kinase C receptor (Fragment) (*Solen grandis*)	23	6	5	26.5	8.63	1.040	0.403
	K1P8B7	Ubiquitin-conjugating enzyme E2-17 kDa (Fragment) (*Crassostrea gigas*)	40	3	3	14.7	5.41	0.930	2.344
	A0A1P8SD54	Ubiquitin (*Ruditapes philippinarum*)	86	8	8	8.7	7.25	0.743	0.443
	A0A210QYF7	cAMP-dependent protein kinase regulatory subunit (*Mizuhopecten yessoensis*)	6	2	2	42.2	5.43	1.030	3.187
	F6MIV7	Cathepsin B (*Cristaria plicata*)	4	2	2	38.5	6.10	0.758	0.176
Ribosome structure									
	A0A194ALW2	40S ribosomal protein S6 (*Pinctada fucata*)	12	4	2	27.9	10.83	0.879	4.252
	K1QQB6	40S ribosomal protein S14 (*Crassostrea gigas*)	25	6	6	16.3	10.36	0.866	2.217
	A0A210QZP5	40S ribosomal protein S17 (*Mizuhopecten yessoensis*)	21	3	3	16.9	9.70	1.071	2.286
	A0A210PIL2	40S ribosomal protein S20 (*Mizuhopecten yessoensis*)	24	2	2	13.7	10.32	1.000	12.887
	K1RK12	40S ribosomal protein S23 (*Crassostrea gigas*)	3	2	2	79.5	7.12	1.054	4.891
	K1R4D4	40S ribosomal protein SA (*Crassostrea gigas*)	38	9	2	33.3	4.92	1.041	0.212
	A0A210R4G4	60S ribosomal protein L18a (*Mizuhopecten yessoensis*)	9	2	2	20.9	10.90	0.979	NOT FOUND
	A0A210PMY2	60S ribosomal protein L36 (*Mizuhopecten yessoensis*)	10	2	2	12.7	11.80	0.725	6.096
	A0A068JIA6	60S ribosomal protein L6 (Fragment) (*Azumapecten farreri*)	9	3	3	24.7	10.54	1.022	4.331
	C6EQB3	Ribosomal protein L8 (Fragment) (*Modiolus modiolus*)	8	2	2	24.4	10.36	0.692	2.586
	A0A077GYU8	Ribosomal protein L19 (Fragment) (*Mytilus trossulus*)	22	6	6	23.8	11.43	0.874	5.134
	A0A194AJY7	Putative eukaryotic translation initiation factor 1-like protein (*Pinctada fucata*)	14	2	2	12.9	8.02	0.924	NOT FOUND
Protein synthesis									
	A0A210R411	Serine–tRNA ligase, cytoplasmic (*Mizuhopecten yessoensis*)	5	2	2	58.6	6.44	1.046	2.138
	A0A210QNB5	Small nuclear ribonucleoprotein E (*Mizuhopecten yessoensis*)	16	2	2	10.5	9.38	1.515	NOT FOUND
Protein Folding									
	B9TXZ7	Peptidyl-prolyl cis-trans isomerase (Fragment) (*Dreissena polymorpha*)	63	4	4	8.4	8.51	1.180	0.103
	A0A210Q9S9	Peptidyl-prolyl cis-trans isomerase (*Mizuhopecten yessoensis*)	23	4	4	18.1	8.07	1.251	0.198
Cytoskeleton structure									
	A0A161HPY5	Actin (*Crassostrea brasiliana*)	94	43	10	41.7	5.48	1.005	0.182
	K1RWD4	Actin, cytoplasmic (*Crassostrea gigas*)	79	40	4	41.9	5.39	0.744	NOT FOUND
	K1PPK1	Actin-related protein 2/3 complex subunit 4 (*Crassostrea gigas*)	13	3	3	19.6	8.92	1.003	2.441
	K1RH58	Alpha-actinin, sarcomeric (*Crassostrea gigas*)	23	19	9	102.1	5.45	0.825	0.402
	A0A142IJP6	Beta-actin (*Sinanodonta woodiana*)	76	36	2	41.8	5.48	0.711	NOT FOUND
	H6BD84	Tropomyosin 1 (Fragment) (*Ostrea edulis*)	13	2	2	16.3	4.88	0.645	0.051
	K7R2W8	Tubulin alpha chain (Fragment) (*Scrobicularia plana*)	43	22	2	50.3	5.20	1.015	NOT FOUND
	A0A194AQ74	Tubulin beta chain (*Pinctada fucata*)	74	32	4	43.3	4.86	1.073	18.064
	K1QZI3	Myosin-le (*Crassostrea gigas*)	3	2	2	127.9	9.16	1.233	2.803
	K1PY30	Septin-2 (*Crassostrea gigas*)	4	2	2	72.3	8.81	0.771	NOT FOUND
	K1PNS2	33 kDa inner dynein arm light chain, axonemal (*Crassostrea gigas*)	10	2	2	27.0	9.11	1.074	2.133
	A0A210QUP6	Dynein light chain roadblock (*Mizuhopecten yessoensis*)	18	3	3	11.3	9.41	0.819	5.007
Transport									
	A0A210PYN3	AP complex subunit beta (*Mizuhopecten yessoensis*)	4	2	2	103.7	5.03	1.043	NOT FOUND
	A0A210QT52	Pleckstrin homology domain-containing family F member 2 (*Mizuhopecten yessoensis*)	9	2	2	26.7	8.00	1.065	2.347
Heat shock proteins									
	A0A0M4TZ63	Heat shock cognate 70 (*Septifer virgatus*)	28	18	3	71.2	5.43	1.019	3.114
	B4E3Z6	Heat shock cognate 70 kDa protein (Fragment) (*Laternula elliptica*)	33	4	2	12.3	8.38	0.912	NOT FOUND

(*continued on next page*)

Table 1 (*continued*)

Main Function	UniProt Accession	Description	Coverage [%]	Peptides	Unique Peptides	MW [kDa]	pI	AR: (M1)/(Ctrl)	AR: (M2)/(Ctrl)
	M4GLN4	Heat shock protein 70 (*Sinonovacula constricta*)	28	20	3	70.9	5.41	0.995	NOT FOUND
	A0A023W7V2	HSP90 protein (*Ruditapes philippinarum*)	19	13	4	83.6	4.93	0.807	0.302
	D4NXL8	Putative heat shock protein 90 (Fragment) (*Dreissena polymorpha*)	56	6	3	11.5	5.19	0.919	NOT FOUND
Binding proteins									
	K1R7G0	Chromobox-like protein 5 (*Crassostrea gigas*)	13	2	2	22.4	4.91	0.616	NOT FOUND
	K1QFW9	Uncharacterized protein (*Crassostrea gigas*)	5	3	3	94.8	7.06	0.846	0.337
DNA-binding proteins									
	K1PUQ5	Histone H2B (*Crassostrea gigas*)	35	5	5	13.7	10.59	1.331	4.047
	K1Q9K6	Histone H3 (*Crassostrea gigas*)	13	3	3	28.9	10.62	1.276	6.833
RNA-binding proteins									
	A0A210R485	RNA-binding protein Nova-1 (*Mizuhopecten yessoensis*)	4	2	2	66.6	6.80	0.909	NOT FOUND
	K1RJH5	Polyadenylate-binding protein (*Crassostrea gigas*)	9	5	5	71.6	9.41	0.904	0.373
	A0A210R719	Small nuclear ribonucleoprotein Sm D2 (*Mizuhopecten yessoensis*)	33	2	2	13.7	9.95	0.670	0.406
	K1QVD0	Small nuclear ribonucleoprotein Sm D3 (*Crassostrea gigas*)	11	3	3	14.2	10.54	0.923	6.645
	A0A194AJS2	Putative eukaryotic initiation factor 4A-II (*Pinctada fucata*)	24	4	4	28.5	5.83	0.865	2.317
	K1PBL2	Eukaryotic initiation factor 4A-III (*Crassostrea gigas*)	3	3	3	137.7	7.18	0.809	2.319
	A0A1L5JFM5	GTP-binding nuclear protein (*Paphia undulata*)	28	7	7	24.8	6.92	1.121	2.73
Calcium-binding proteins									
	A0A0G2R282	Calmodulin (Fragment) (*Isognomon nucleus*)	61	4	3	12.4	4.23	0.894	0.475
	A0A210R691	Calmodulin (*Mizuhopecten yessoensis*)	21	2	2	16.8	4.34	0.785	0.362
Biosynthesis									
	K1QYG7	Glucosamine–fructose-6-phosphate aminotransferase [isomerizing] 1 (*Crassostrea gigas*)	5	2	2	81.9	6.80	0.996	NOT FOUND
Chaperones									
	I6QQ41	Protein disulfide-isomerase (*Mytilus galloprovincialis*)	7	3	3	55.1	4.65	0.797	NOT FOUND
	A0A210QV24	78 kDa glucose-regulated protein (*Mizuhopecten yessoensis*)	22	9	2	72.7	5.05	0.836	0.392
	K1QX26	Endoplasmin (*Crassostrea gigas*)	3	4	2	125.3	4.97	0.712	0.456
	A0A210QQ25	T-complex protein 1 subunit eta (*Mizuhopecten yessoensis*)	11	4	4	59.4	6.21	0.801	4.968
Trafficking									
	C1KBI9	Rab7-like protein (*Pinctada martensii*)	12	2	2	23.1	5.48	1.024	NOT FOUND
Energy source/production									
	K1P7K8	Vesicle-fusing ATPase 1 (*Crassostrea gigas*)	3	2	2	82.7	6.77	1.154	NOT FOUND
	K1R7T2	Isocitrate dehydrogenase [NADP] (*Crassostrea gigas*)	6	2	2	46.3	6.55	0.900	0.374
	K1QX37	Enolase (*Crassostrea gigas*)	5	4	4	127.3	7.34	1.164	0.388
	K1QE55	Methylmalonyl-CoA mutase, mitochondrial (*Crassostrea gigas*)	4	2	2	81.7	5.90	1.106	0.455
	K1QCC1	Phosphoglycerate kinase (*Crassostrea gigas*)	7	2	2	43.0	7.72	1.246	0.490
	K1R8R6	Fructose-bisphosphate aldolase (*Crassostrea gigas*)	11	4	4	43.5	6.20	0.834	2.385
	K1PVA1	Transitional endoplasmic reticulum ATPase (*Crassostrea gigas*)	24	16	5	88.6	5.30	0.832	2.827
	A0A210PUN6	V-type proton ATPase subunit E (*Mizuhopecten yessoensis*)	5	2	2	26.1	7.03	1.199	3.480
	A0A2H4NFY0	GAPDH (Fragment) (*Ruditapes philippinarum*)	12	3	3	20.0	8.35	0.998	6.448
Signaling									
	A0A210PQQ0	Serine/threonine-protein phosphatase (*Mizuhopecten yessoensis*)	12	3	3	41.1	5.17	0.916	0.282
	A0A210QM77	Glutamate dehydrogenase (*Mizuhopecten yessoensis*)	6	3	3	59.5	7.93	0.907	0.357
	A0A210Q890	Major vault protein (*Mizuhopecten yessoensis*)	11	8	8	96.4	5.94	0.915	0.387
Antioxidant activity									
	A0A210PVL1	Glutathione reductase (*Mizuhopecten yessoensis*)	3	2	2	49.1	6.87	0.921	7.806
Multifunction									
	A0A0N9HES5	Ras-related C3 botulinum toxin substrate 1 (*Mizuhopecten yessoensis*)	17	3	2	21.4	8.32	1.133	2.817
	K1PHM8	14-3-3 protein zeta (*Crassostrea gigas*)	6	3	2	28.6	4.93	1.432	4.084
	K1QIG6	ADP-ribosylation factor-like protein 3 (*Crassostrea gigas*)	10	3	3	28.2	9.20	0.885	8.223

MW = molecular weight; pI = isoelectric point; AR = abundance ratio.

made by MPs (Jeong et al., 2017; Magara et al., 2018; Yu et al., 2018) probably due to both their intrinsic toxicological effects and the mechanic injuries made by these physical pollutants that increase the inflammatory status (Jin et al., 2018). The only comparison with other proteomic data is possible with results recently made by Green et al. (2019) which however evaluate the effects of other MPs

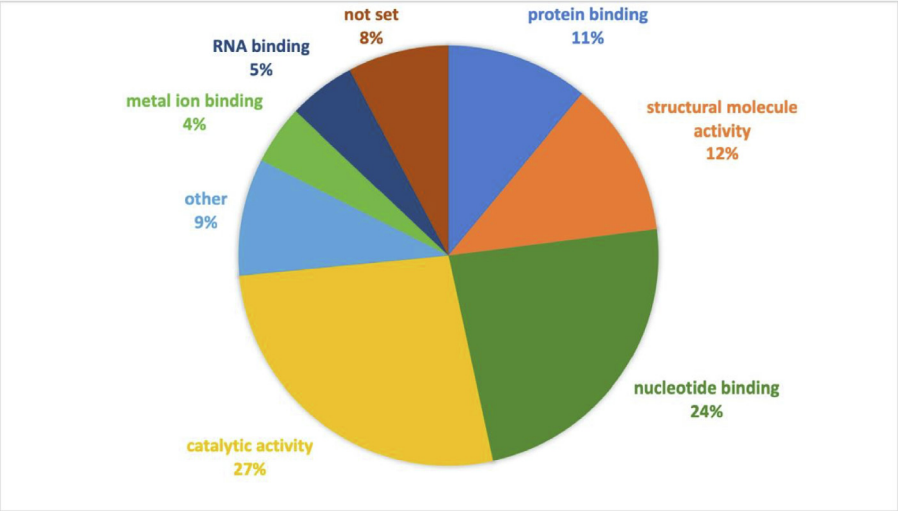

Fig. 3. Molecular function of modulated proteins: gene ontology analyses of identified proteins in M1 and M2. The showed enriched categories are related to the molecular functions of gills' proteins.

(polylactic acid and polyethylene) in the marine *Mytilus edulis*. Furthermore, comparisons among MPs' impact are more difficult than those made by chemicals since uptake and toxicological effects can be influenced by other physical variables, mainly size and shape. Anyway, the authors found some of the same protein classes modulated by M2, such as proteins involved in the cellular structure, DNA binding, detoxification (e.g. metal ion binding) and metabolism, but also another specific class not modulated by M2 linked to immune response (Green et al., 2019).

In detail, we found an up-regulation of the glutathione reductase (7.8-fold increase; Table 1) which suggests the activation of the antioxidant defense chain in the mussel gills. Glutathione reductase (*Gsr*) is a highly-conserved protein involved in the regulation, modulation and maintenance of cellular redox homeostasis by the transformation of oxidized glutathione into its reduced form (Couto et al., 2016). The up-regulation of *Gsr* suggests the attempt of zebra mussels to increase the production of reduced glutathione that is a direct scavenger of OH° and other cell radicals and one of the substrates involved in the glutathione machinery to counteract the oxidative stress.

Another indication of this mechanism of action can be seen through the modulation of the cytoskeleton proteins (Table 1) which were always found as one of the major targets of some xenobiotics in different model organisms (Miura et al., 2005; Hanisch et al., 2010; Riva et al., 2012; Binelli et al., 2013). This kind of proteins, which are involved in the maintenance of cell shape, locomotion, intracellular organization and transport, have been indicated as one of the first targets of the oxidative stress (Riva et al., 2012; Wilson and Gonzalez-Billault, 2015; Belcastro et al., 2017). The M2 modulated 11 different proteins directly ascribable to cytoskeleton functions (Table 1). In detail, 5 of them were up-regulated: actin-related protein 2/3 complex subunit 2, K1PPK1; myosin-Ie, K1QZI3; tubulin β chain, A0A194AQ74; 33 kDa inner dynein arm light chain, K1PNS2; dynein light chain roadblock, A0A210QUP6; 2 proteins were down-regulated (tropomyosin 1, H6BD84; α-actinin, K1RH58) and 4 of them were not expressed (actin, A0A161HPY5; β-actin, A0A142IJP6; tubulin α chain, K1QII6; septin-2, K1PY30), in the exposed bivalves (Fig. 2 and Table 1). It is well known that oxidative stress induces the breakage of F-actin, impairing the microtubule polymerization (Wilson and Gonzalez-Billault, 2015) and that tubulins α and β chain contain many cysteine residues that can be oxidized by endogenous and exogenous oxidizing agents (Landino et al., 2004). The tubulins α chain (*Tuba*) and β chain (*Tubb*) were modulated by the exposure to M2 in different way: the former was completely not expressed (Table 1), while the latter was the protein most up-regulated (Table 1; Fig. 2). The block of expression for *Tuba* is a dramatic event because it normally binds the other dimer β to form the microtubules. M2 seems not only to interfere on the microtubules' assemblage, modifying the cellular stability and organization, but could alter also the mechanical defense of the digestive tract of zebra mussel. Indeed, *Tuba* and *Tubb* are also the main components of cilia, which in mussels are present mainly in the syphons with the task to reject dangerous particles, such as diatom frustules and large particulate matter, and facilitate respiration (Magi et al., 2008).

Another effect noticed after the exposure to M2 was the impact on many proteins directly and indirectly involved in the RNA translation and protein synthesis. We found 7 RNA-binding proteins modulated (Table 1), 4 of them up-regulated (putative eukaryotic initiation factor 4A-II, A0A194AJS2; eukaryotic initiation factor 4A-III, K1BPL2; GTP-binding nuclear protein, A0A1L5JFM5; small nuclear ribonucleoprotein Sm D3, K1QVD0), 2 proteins down-regulated (polyadenylate-binding protein, K1RJH5; small nuclear ribonucleoprotein Sm D2, A0A210R719) and the RNA-binding protein Nova-1 (A0A210R485) not expressed (Fig. 2 and Table 1).

The RNA-binding proteins (RBPs) play a crucial role in the regulation of gene expression, mainly based on splicing regulation, mRNA transport, modulation of mRNA translation and also in decay. Furthermore, RBPs are strictly involved in response to stress (Alves and Goldenberg, 2016) since it is crucial for the cell to control and arrest mRNA translation during stressful situations, as shown by Holcik and Sonenberg (2005) who indicated as 50% of cell energy is consumed during translation. In particular, the RBPs are one of the main constituents of the so-called stress granules (SGs), which are formed in cytoplasm of cells exposed to many environmental stressors, such as hypoxia, UV, heat and oxidative stress (Anderson and Kedersha, 2006). The role played by SGs was confirmed by the observation of their rapid induction, estimated in 15–30 min, in the cell cytoplasm of different model-organisms exposed to different stressors (Mangiardi et al., 2004; Moeller et al., 2004; Kayali et al., 2005). During stress, most mRNAs are directed to either the degradation machinery or SGs, where they

remain untranslated until homeostatic conditions are reactivated (Alves and Goldenberg, 2016). SGs are composed by an assemblage of different proteins, that include also the eukaryotic initiation factors (*EiFs*), some ribosomal subunits, scaffold proteins, RNA-stability proteins and many others (Wheeler et al., 2017). It is interesting to note that some proteins included in the classes forming SGs were effectively modulated by M2. Specifically, 2 *EiFs* were up-regulated (*EiF 4A-II* A0A194AJS2 and *EiF 4A-III*, K1PBL2) and one of them was not expressed (putative *EiF 1-like*, A0A194AJY7), as shown in Table 1.

Very interestingly, almost all the ribosomal proteins were up-regulated (Table 1), confirming the over-production of these proteins' class necessary for the SG formation and considered markers of these cytoplasmic structures (Kedersha and Anderson, 2002). Another evidence of this possible defense mechanism can be highlighted in the lack of expression of many proteins. Table 1 shows that three heat shock proteins (*Hsps*) were below the detection limit (Heat shock cognate 70 kDa protein, B4E3Z6; Heat shock protein 70, M4GLN4; Putative heat shock protein 90) compared to controls and one was down-regulated (HSP90 protein, A0A023W7V2), while only one was up-regulated (Heat shock cognate 70, A0A0M4TZ63). The *Hsps* are involved in many cell activities, such as folding/unfolding of proteins, cell-cycle control and signaling, protein transport and protection against stress and apoptosis (Li and Srivastava, 2004). Although several studies highlighted an activation of the *Hsps* related to the increasing oxidative stress (Oksala et al., 2014; Liu et al., 2015; Wang et al., 2018; Ikwegbue et al., 2018), our proteomics results seem to show a more complicated situation. Indeed, if the "silver thread" among the modulation of the different protein classes made by M2 is effectively the activation of the response machinery against the oxidative stress, the inactivation or down-regulation of *Hsps* seems to be inconsistent. Actually, the modulation of *Hsps* noticed could be simply related to one of the numerous other functions above described, but the most intriguing explanation concerns the physical nature of the administered contaminant that can trigger a different cascade of events than that produced by chemical pollutants. Since a background level of these *Hsps* was evaluated in the controls, the complete blockage of their expression could point out that cells consider them as housekeeping proteins, whose mRNA must be untranslated for cellular energy-saving, instead of possible barrier against the injuries made by M2 exposure. Another evidence on the response based on the energy pathways was the modulation of some proteins related to energy source and production, whose 4 of them were down-regulated, 4 up-regulated and one not expressed (Table 1). More specifically, 5 proteins (isocitrate dehydrogenase, K1R7T2; enolase, K1QX37; phosphoglycerate kinase, K1QCC1; fructose-bisphosphate aldolase, K1R8R6 and GAPDH, A0A2H4NFY0) were directly involved in the glycolysis and one in the Krebs cycle (methylmalonyl-CoA mutase, K1QE55), showing as M2 was able to interfere also on the cellular energetic balance. Indeed, similar results were obtained in a previous study (Sussarellu et al., 2016) in which polystyrene microparticles were administered to Pacific oysters, interfering with energy uptake and allocation. This negative effect shifted the energy flows toward organism maintenance and structural growth at the expense of reproduction.

Lastly, the last big protein class modulated by M2 was related to protein degradation with 3 proteins up-regulated, 3 down-regulated and one not expressed (Table 1). In detail, 3 of them (26S proteasome non-ATPase regulatory subunit 7, A0A210QH02; 26S proteasome non-ATPase regulatory subunit 14, A0A210QNI0; proteasome subunit α type, K1R6F1) are components of the proteasome, a multiprotein complex mainly involved in the ATP-dependent degradation of ubiquitinated proteins.

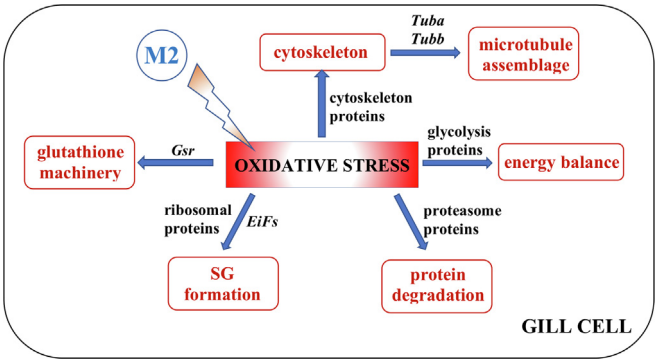

Fig. 4. Proteins' classes affected by M2: Summarizing scheme of the suggested mechanism of action with the main proteins' classes modulated by the M2 exposure. *Gsr* = glutathione reductase; *Tuba* = tubulin α chain; *Tubb* = tubulin β chain; *EiFs* = eukaryotic initiation factors.

In summary, even if some evidences must be confirmed, for instance through microscopy observations for the probable formation of SGs, our results confirmed the sensitivity of the proteomic approach in ecotoxicology and its capability to highlight the adverse effects made also by these physical contaminants. In particular, this methodology suggested that M2 was able to create an imbalance in the oxidative status of gill cells which was reflected in the modulation of many proteins involved in some different cellular pathways, as summarized in Fig. 4.

4. Conclusions

This study adds another brick in the knowledge of the risk assessment associated to virgin MPs. One of the pivotal results is the discovery of a "quantal effect" demonstrated by a clear threshold between M1 and M2, situation absolutely not predictable before the exposures and never described in the previous studies on MPs. Proteomics performed this task very well, proving its sensitivity and the capability to investigate the deepest effects due to M2 that modulate especially proteins belonging to 5 different classes involved in crucial cellular pathways. The ultimate effect which connects the modulation of these protein classes seemed to be the increase of oxidative stress and the related activation of the antioxidant machinery.

Our data drive to other in-depth studies, based on different techniques, to evaluate if the biochemical effects noticed could determine negative consequences also at the higher levels of the biological scale. Moreover, other experiments should be conducted considering also the possible adsorption of phytoplankton and/or environmental pollutants to MPs that can modify both their aggregation and bioavailability.

References

Allsopp, M., Walters, A., Santillo, D., Johnsto, P., 2006. Plastic Debris in the World's Oceans. Greenpeace International, Amsterdam, Netherlands.
Alves, L.R., Goldenberg, S., 2016. RNA-binding proteins related to stress response and differentiation in protozoa. World J. Biol. Chem. 26, 78–87.
Anderson, P., Kedersha, N., 2006. RNA granules. JCB (J. Cell Biol.) 172, 803–808.
Bakir, A., Rowland, S.J., Thompson, R.C., 2014. Enhanced desorption of persistent organic pollutants from microplastics under simulated physiological conditions. Environ. Pollut. 185, 16–23.
Belcastro, E., Wu, W., Fries-Raeth, I., Corti, A., Pompella, A., Leroy, P., Larteaud, I., Gaucher, C., 2017. Oxidative stress enhances and modulates protein S-nitrosation in smooth muscle cells exposed to S-nitrosoglutathione. Nitric Oxide 69, 10–21.
Binelli, A., Del Giacco, L., Santo, N., Bini, L., Magni, S., Parolini, M., Madaschi, L., Ghilardi, A., Maggioni, D., Ascagni, M., Armini, A., Prosperi, L., Landi, L., La Porta, C., Della Torre, C., 2017. Carbon nanopowder acts as a Trojan-horse for benzo(α)pyrene in *Danio rerio* embryos. Nanotoxicology 11, 371–381.

Binelli, A., Della Torre, C., Magni, S., Parolini, M., 2015. Does zebra mussel (*Dreissena polymorpha*) represent the freshwater counterpart of *Mytilus* in ecotoxicological studies? A critical review. Environ. Pollut. 196, 386–403.
Binelli, A., Marisa, I., Fedorova, M., Hoffmann, R., Riva, C., 2013. First evidence of protein profile alteration due to the main cocaine metabolite (benzoylecgonine) in a freshwater biological model. Aquat. Toxicol. 140–141, 268–278.
Bradford, M.M., 1976. A rapid and sensitive method for the quantification of microgram quantities of protein using the principle of protein-dye binding. Anal. Biochem. 72, 248–254.
Browne, M.A., Galloway, T., Thompson, R.C., 2007. Microplastic-an emerging contaminant of potential concern? Integr. Environ. Assess. Manag. 3, 559–566.
Carr, S.A., Liu, J., Tesoro, A.G., 2016. Transport and fate of microplastic particles in wastewater treatment plants. Water Res. 91, 174–182.
Chen, Q., Gundlach, M., Yang, S., Jiang, J., Velki, M., Yin, D., Hollert, H., 2017. Quantitative investigation of the mechanisms of microplastics and nanoplastics toward zebrafish larvae locomotor activity. Sci. Total Environ. 584–585, 1022–1031.
Cole, M., Lindeque, P., Halsband, C., Galloway, T.S., 2011. Microplastics as contaminants in the marine environment: a review. Mar. Pollut. Bull. 62, 2588–2597.
Couto, N., Wood, J., Barber, J., 2016. The role of glutathione reductase and related enzymes on cellular redox homoeostasis network. Free Radical Biol. Med. 95, 27–42.
Ding, J., Zhang, S., Razanajatovo, R.M., Zou, H., 2018. Accumulation, tissue distribution, and biochemical effects of polystyrene microplastics in the freshwater fish red tilapia (*Oreochromis niloticus*). Environ. Pollut. 238, 1–9.
Eerkes-Medrano, D., Thompson, R.C., Aldridge, D.C., 2015. Microplastics in freshwater systems: a review of the emerging threats, identification of knowledge gaps and prioritization of research needs. Water Res. 75, 63–82.
Green, D.S., Colgan, T.J., Thompson, R.C., Carolan, J.C., 2019. Exposure to microplastics reduces attachment strength and alters the haemolymph proteome of blue mussels (*Mytilus edulis*). Environ. Pollut. 246, 423–434.
Guilhermino, L., Vieira, L.R., Ribeiro, D., Tavares, A.S., Cardoso, V., Alves, A., Almeida, J.M., 2018. Uptake and effects of the antimicrobial florfenicol, microplastics and their mixtures on freshwater exotic invasive bivalve *Corbicula fluminea*. Sci. Total Environ. 622–623, 1131–1142.
Hammer, J., Kraak, M.H.S., Parsons, J.R., 2012. Plastics in the marine environment: the dark side of a modern gift. In: Whitacre, D.M. (Ed.), Reviews of Environmental Contamination and Toxicology. Springer, New York, pp. 1–44.
Hanisch, K., Küster, E., Altenburger, R., Gündel, U., 2010. Proteomic signatures of the Zebrafish (*Danio rerio*) embryo: sensitivity and specificity in toxicity assessment of chemicals. Int. J. Proteomics, 2010 Article ID 630134.
Hartmann, N.B., Huffer, T., Thompson, R.C., Hasselov, M., Verschoor, A., Daugaard, A.E., Rist, S., Karlsson, T., Brennholt, N., Cole, M., Herrling, M.P., Hess, M.C., Ivleva, N.P., Lusher, A.L., Wagner, M., 2019. Are we speaking the same language? Recommendations for a definition and categorization framework for plastic debris. Environ. Sci. Technol. 53, 1039–1047.
Hidalgo-Ruz, V., Gutow, L., Thompson, R.C., Thiel, M., 2012. Microplastics in the marine environment: a review of the methods used for identification and quantification. Environ. Sci. Technol. 46, 3060–3075.
Holcik, M., Sonenberg, N., 2005. Translational control in stress and apoptosis. Nat. Rev. Mol. Cell Biol. 6, 318–327.
Ikwegbue, P.C., Masamba, P., Oyinloye, B.E., Kappo, A.P., 2018. Roles of heat shock proteins in apoptosis, oxidative Stress, human inflammatory diseases, and cancer. Pharmaceuticals 11, 2.
Jeong, C.B., Kang, H.M., Lee, M.C., Kim, D.H., Han, J., Hwang, D.S., Souissi, S., Lee, S.J., Shin, K.H., Park, H.G., Lee, J.S., 2017. Adverse effects of microplastics and oxidative stress-induced MAPK/Nrf2 pathway-mediated defense mechanisms in the marine copepod *Paracyclopina nana*. Sci. Rep. 41323.
Jin, Y.X., Xia, J.Z., Pan, Zh, Jang, J.J., Wang, W.C., 2018. Polystyrene microplastics induce microbiota dysbiosis and inflammation in the gut of adult zebrafish. Environ. Pollut. 235, 322–329.
Jovanovic, B., 2017. Ingestion of microplastics by fish and its potential consequences from a physical perspective. Integr. Environ. Assess. Manag. 13 (3), 510–515.
Kayali, F., Montie, H.L., Rafols, J.A., De Gracia, D.J., 2005. Prolonged translation arrest in reperfused hippocampal cornu Ammonis 1 is mediated by stress granules. Neuroscience 134, 1223–1245.
Kedersha, N., Anderson, P., 2002. Stress granules: sites of mRNA triage that regulate mRNA stability and translatability. Biochem. Soc. Trans. 30, 963–969.
Lambert, S., Wagner, M., 2018. Freshwater Microplastics. Springer International Publishing, Cham, Switzerland.
Landino, L.M., Moynihan, K.L., Todd, J.V., Kennett, K.L., 2004. Modulation of the redox state of tubulin by the glutathione/glutaredoxin reductase system. Biochem. Biophys. Res. Commun. 314, 555–560.
Lei, L., Wu, S., Lu, S., Liu, M., Song, Y., Fu, Z., Shi, H., Raley-Susman, K.M., He, D., 2018. Microplastic particles cause intestinal damage and other adverse effects in zebrafish *Danio rerio* and nematode *Caenorhabditis elegans*. Sci. Total Environ. 619–620, 1–8.
Li, J., Liu, H., Chen, J.P., 2018. Microplastics in freshwater systems: a review on occurrence, environmental effects, and methods for microplastics detection. Water Res. 137, 362–374.
Li, Z., Srivastava, P., 2004. Heat-shock proteins. Curr. Protoc. Im. 58. A.1T.1-A.1T.6.
Liu, C.P., Fu, J., Xu, F.P., Wang, X.S., Li, S., 2015. The role of heat shock proteins in oxidative stress damage induced by Se deficiency in chicken livers. Biometals 28, 163–173.
Lu, Y., Zhang, Y., Deng, Y., Jiang, W., Zhao, Y., Geng, J., Ding, L., Ren, H., 2016. Uptake and accumulation of polystyrene microplastics in zebrafish (*Danio rerio*) and toxic effects in liver. Environ. Sci. Technol. 50, 4054–4060.
Magara, G., Elia, A.C., Syberg, K., Khan, F.R., 2018. Single contaminant and combined exposures of polyethylene microplastics and fluoranthene: accumulation and oxidative stress response in the blue mussel, *Mytilus edulis*. J. Toxicol. Environ. Health Part A 81, 761-733.
Magi, E., Liscio, C., Pistarino, E., Santamaria, B., Di Carro, M., Tiso, M., Scaloni, M., Renzone, G., Cosulich, M.E., 2008. Interdisciplinary study for the evaluation of biochemical alterations on mussel *Mytilus galloprovincialis* exposed to a tributyltin-polluted area. Anal. Bioanal. Chem. 391, 671–678.
Magni, S., Gagné, F., André, C., Della Torre, C., Auclair, J., Hanana, H., Parenti, C.C., Bonasoro, F., Binelli, A., 2018. Evaluation of uptake and chronic toxicity of virgin polystyrene microbeads in freshwater zebra mussel *Dreissena polymorpha* (Mollusca: Bivalvia). Sci. Total Environ. 631–632, 778–788.
Magni, S., Parolini, M., Binelli, A., 2016. Sublethal effects induced by morphine to the freshwater biological model *Dreissena polymorpha*. Environ. Toxicol. 31, 58–67.
Magni, S., Parolini, M., Della Torre, C., de Oliveira, L.F., Catani, M., Guzzinati, R., Cavazzini, A., Binelli, A., 2017. Multi-biomarker investigation to assess toxicity induced by two antidepressants on *Dreissena polymorpha*. Sci. Total Environ. 578, 452–459.
Mangiardi, D.A., McLaughlin-Williamson, K., May, K.E., Messana, E.P., Mountain, D.C., Cotanche, D.A., 2004. Progression of hair cell ejection and molecular markers of apoptosis in the avian cochlea following gentamicin treatment. J. Comp. Neurol. 475, 1–18.
Miura, Y., Kano, M., Abe, K., Urano, S., Suzuki, S., Toda, T., 2005. Age-dependent variations of cell response to oxidative stress: proteomic approach to protein expression and phosphorylation. Electrophoresis 26, 2786–2796.
Moeller, B.J., Cao, Y., Li, C.Y., Dewhirst, M.W., 2004. Radiation activates HIF-1 to regulate vascular radiosensitivity in tumors: role of reoxygenation, free radicals, and stress granules. Cancer Cell 5, 429–441.
Monsinjor, T., Knigge, T., 2007. Proteomic applications in ecotoxicology. Proteomics 7, 2997–3009.
Oksala, N.K.J., Ekmekci, F.G., Ozsoy, E., Kirankaya, S., Kokkola, T., Emecen, G., Lappalainen, J., Kaarniranta, K., Atalay, M., 2014. Natural thermal adaptation increases heat shock protein levels and decreases oxidative stress. Redox Biol. 3, 25–28.
Riva, C., Cristoni, S., Binelli, A., 2012. Effects of Triclosan in the freshwater *Dreissena polymorpha*: a proteomic investigation. Aquat. Toxicol. 118–119, 62–71.
Sleight, V.A., Bakir, A., Thompson, R.C., Henry, T.B., 2017. Assessment of microplastic-sorbed contaminant bioavailability through analysis of biomarker gene expression in larval zebrafish. Mar. Pollut. Bull. 116, 291–297.
Sussarellu, R., Suquet, M., Thomas, Y., Lambert, C., Fabioux, C., Pernet, M.E.J., Le Goïc, N., Quillien, V., Mingant, C., Epelboin, Y., Corporeau, C., Guyomarch, J., Robbens, J., Paul-Pont, I., Soudant, P., Huvet, A., 2016. Oyster Reproduction Is Affected by Exposure to Polystyrene Microplastics.
Wang, Y., Zhao, H., Liu, J., Shao, Y., Li, J., Luo, L., Xing, M., 2018. Copper and arsenic-induced oxidative stress and immune imbalance are associated with activation of heat shock proteins in chicken intestines. Int. Immunopharmacol. 60, 64–75.
Weber, A., Scherer, C., Brennholt, N., Reifferscheid, G., Wagner, M., 2018. PET microplastics do not negatively affect the survival, development, metabolism and feeding activity of the freshwater invertebrate *Gammarus pulex*. Environ. Pollut. 234, 181–189.
Wheeler, J.R., Jain, S., Khong, A., Parker, R., 2017. Isolation of yeast and mammalian stress granule cores. Methods 126, 12–17.
Wilson, C., Gonzalez-Billault, C., 2015. Regulation of cytoskeletal dynamics by redox signaling and oxidative stress: implications for neuronal development and trafficking. Front. Cell. Neurosci. 9, 381.
Yu, P., Liu, Z.Q., Wu, D.L., Chen, M.H., Lv, W.W., Zhao, Y.L., 2018. Accumulation of polystyrene microplastics in juvenile *Eriocheir sinensis* and oxidative stress effects in the liver. Aquat. Toxicol. 200, 28–36.

3.2 Effects of polystyrene nanoparticles in a terrestrial model

The majority of studies on micro- and nanoplastics report effects on marine organisms, while their potential impacts on terrestrial species is widely unexplored. In this context, the aim of this study was to evaluate the uptake and detrimental effects of nanoplastics on silkworm (*B. mori*) larvae, a well-studied Lepidopteran model system (3.2.1). Newly hatched *B. mori* larvae were reared ad libitum on artificial diet overlaid with 0.5 µm PS nanobeads. Plastic uptake and tissue distribution were investigated in larval transversal sections by confocal microscopy, while the effects of the exposure were investigated at different levels of biological organizations, focusing on development, biochemical endpoints associated with oxidative status and locomotor behaviour. Moreover, to confirm the ability of cells to internalize nanoplastics, haemolymph samples were both collected from treated larvae and exposed in vitro to the same nanobeads and then observed under confocal microscope.

PUBLICATION LIST:

3.2.1 Parenti, C.C., Binelli, A., Caccia, S., Della Torre, C., Magni, S., Pirovano, G., Casartelli, M., 2020. **Ingestion and effects of polystyrene nanoparticles in the silkworm *Bombyx mori***. Chemosphere, 257, 127203.

Chemosphere 257 (2020) 127203

Contents lists available at ScienceDirect

Chemosphere

journal homepage: www.elsevier.com/locate/chemosphere

Ingestion and effects of polystyrene nanoparticles in the silkworm *Bombyx mori*

C.C. Parenti [a], A. Binelli [a, *], S. Caccia [b], C. Della Torre [a], S. Magni [a], G. Pirovano [a], M. Casartelli [a]

[a] Department of Biosciences, University of Milan, Via Celoria 26, 20133, Milan, Italy
[b] Department of Agricultural Sciences, University of Naples "Federico II", Via Università 100, 80055, Portici, Naples, Italy

HIGHLIGHTS

- First study on nanoplastic uptake and effects in the silkworm *Bombyx mori*.
- Presence of nanoplastics in tissues and haemolymph.
- Nanoplastic ingestion alters larval locomotor behaviour.

GRAPHICAL ABSTRACT

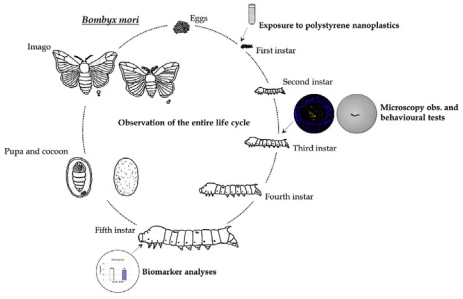

ARTICLE INFO

Article history:
Received 24 February 2020
Received in revised form
15 May 2020
Accepted 22 May 2020
Available online 26 May 2020

Handling Editor: Tamara S. Galloway

Keywords:
Nanoplastics
Terrestrial environments
Biomarker
Behaviour
Emerging contaminants

ABSTRACT

Information on the occurrence and effects of nanoplastics in ecosystems worldwide currently represent one of the main challenges from the ecotoxicological point of view. This is particularly true for terrestrial environments, in which nanoplastics are released directly by human activities or derive from the fragmentation of larger plastic items incorrectly disposed. Since insects can represent a target for these emerging contaminants in land-based community, the aim of this study was the evaluation of ingestion of 0.5 μm polystyrene nanoplastics and their effects in silkworm (*Bombyx mori*) larvae, a useful and well-studied insect model. The ingestion of nanoplastics, the possible infiltration in the tissues and organ accumulation were checked by confocal microscopy, while we evaluated the effects due to the administered nanoplastics through a multi-tier approach based on insect development and behaviour assessment, as endpoints at organism level, and the measurements of some biochemical responses associated with the imbalance of the redox status (superoxide dismutase, catalase, glutathione s-transferase, reactive oxygen species evaluation, lipid peroxidation) to investigate the cellular and molecular effects. We observed the presence of microplastics in the intestinal lumen, but also inside the larvae, specifically into the midgut epithelium, the Malpighian tubules and in the haemocytes. The behavioural observations revealed a significant ($p < 0.05$) increase of erratic movements and chemotaxis defects, potentially reflecting negative indirect effects on *B. mori* survival and fitness, while neither effect on insect development nor redox status imbalance were measured, with the exception of the significant ($p < 0.05$) inhibition of superoxide dismutase activity.

* Corresponding author.
E-mail address: andrea.binelli@unimi.it (A. Binelli).

https://doi.org/10.1016/j.chemosphere.2020.127203
0045-6535/

1. Introduction

Almost 50 years have passed since plastic waste has been assessed as one of the emerging environmental problems (Kramm and Vö lker, 2018). Since then, the perceived impact of plastic has been linked to their widespread and growing use (Heidbreder et al., 2019) and their high persistence in ecosystems due to the extreme resistance to degradation (Horton et al., 2017).

Plastics reach the environment from several sources, mostly related to human activities, such as littering and inadequate disposal. Once in the environment, the larger plastic items are fragmented into microplastics (MPs) and nanoplastics (NPs) by sunlight, mechanical abrasion, salinity and temperature fluctuations, increasing their potential to be incorporated by organisms (Oliveira et al., 2019a). Although oceans have always been considered the major sink of plastics (Cózar et al., 2014), recent studies estimated that the contamination of terrestrial ecosystems might be up to 20-fold larger (Oliveira et al., 2019b). One of the major concerns related to plastic deposition in inland areas is the atmosphere circulation, which is responsible for the transport of plastic debris also to remote terrestrial areas, such as high-altitude glaciers (Zhang et al., 2019). Another source of plastics is the sewage sludge used as fertilizer in agricultural practises, since it represents the major fate of plastic debris removed from wastewaters (Nizzetto et al., 2016).

Nevertheless, terrestrial environments have been less studied than aquatic ecosystems with limited and variable monitoring data on plastic particle abundance, as demonstrated by the recent study by Wang et al. (2020) that reported a very wide range in plastic distribution from 1 to 40,000 items/kg in soils. As well as for monitoring, also studies concerning the uptake and the effects of plastic particles on terrestrial organisms are scarce. Among them, earthworms are the predominant model species used to investigate the potential negative effects in soil biota (Wang et al., 2020). For instance, growth rate, survival and reproduction of *Lumbricus terrestris* exposed to polyethylene MPs (<150 μm) were significantly reduced (Huerta Lwanga et al., 2016), while histopathological analyses on the gut of *Eisenia andrei* demonstrated that the ingestion of polyethylene microbeads (250–1000 μm) caused tissue damage and immune reactions (Rodriguez-Seijo et al., 2017).

Regarding terrestrial ecosystems, there is few evidences also for the impact of NPs, which are recently redefined as debris in the range of 1 to <1000 nm (Hartmann et al., 2019). The main reason is due to the extreme difficulty in their detection and characterization because of their smaller size, factor that may underestimate the existing concentrations both in aquatic and terrestrial environments. Another problem is related to the bioavailability of NPs, since their capability to enter organisms and induce negative effects have to be surely assessed yet (Stapleton, 2019), especially because the nano-scale particles may cross the intestinal barrier more easily than larger plastic debris (Shen et al., 2019). NP effects were studied only on a few species of soil invertebrates: polystyrene NPs (50–200 nm particle size) were shown to reduce body weight and changed the gut microbiome of the soil oligochaete *Enchytraeus crypticus*, while they affected the energy metabolism in the soil nematode *Caenorhabditis elegans*, causing decreased locomotion and reproduction (Zhu et al., 2018; Kim et al., 2019). On the contrary, no data are available about ingestion and effects of NPs on insects that are the most varied and adapted group of organisms on earth. This is surprising in the light of their distribution worldwide that, combined with the ubiquitous nature of plastic contamination, make the contact between these arthropods and plastic particles unavoidable (Oliveira et al., 2019b). Furthermore, an interesting study by Al-Jaibachi et al. (2018) focused the attention on those insect groups, such as mayflies, dragonflies, midges and mosquitos, who become an important pathway for plastic particles dispersal, being their life cycle both aquatic and terrestrial. In detail, they demonstrated that polystyrene microplastics (2 and 15 μm) ingested by mosquito larvae were found in adults, exposing terrestrial predators to the risk of plastic ingestion.

Among insects, Lepidoptera is the second largest order (Powell, 2009) and their fundamental ecological role is not only related to their biomass and biodiversity, but also to their role as herbivores, pollinators and food for insectivores. In ecotoxicological studies, adult stage of Lepidoptera is often used to test the impact of insecticides on non-target organisms, which is a major reason for pollinators decline (Mulé et al., 2017). Among lepidopteran species, the domesticated silkworm (*Bombyx mori*) is considered a useful model system to evaluate toxicity and mode of action of various substances such as drugs, pesticides and metallic nanomaterials (Meng et al., 2017a). Therefore, it can be used in health safety and environmental pollution assessment (Abdelli et al., 2018) since *B. mori* larvae own considerable advantages in comparison to other invertebrate and vertebrate models. They are easy to handle and have a relatively short life cycle, they can be easily maintained under laboratory conditions and are ideal to screen fast the toxicity of many substances at low cost (Abdelli et al., 2018). Moreover, the genome of *B. mori* was completely sequenced in 2008 (The International Silkworm Genome Consortium, 2008), giving a major boost in molecular and functional genomic studies. The efficacy of *B. mori* larvae as model organism in toxicological studies has been evaluated in a number of studies: Hamamoto et al. (2004) used silkworm to test the efficacy of several antibiotics, demonstrating that 50% of the effective dose (ED_{50}) is consistent with those reported for mice, and different studies established that it can be used as infection model for the identification of bacterial virulence factors and as human disease model (Kaito, 2016; Ishii et al., 2015; Meng et al., 2017a). This species has also been applied for environmental monitoring, since it has been found to be highly sensitive to pesticides, heavy metals and other harmful chemicals (Meng et al., 2017a). Silkworms were also employed to assess nanomaterial hazard, such as Ag nanoparticles, which can affect growth and survival in a dose dependent manner, causing a variation in gene expression pattern of the fat body (Meng et al., 2017b).

To the best of our knowledge, *B. mori* has never been used as a model species to unravel the effects of NPs in insects. This study reports, for the first time, the fate of spherical polystyrene nanoplastics (PNPs) administered by ingestion on *B. mori* larvae and their effects by a multi-tier approach based on development and behaviour assessment, as endpoints at organism level, and a biomarker suite associated with the oxidative balance to measure the potential effects at molecular and cellular levels. In detail, we measured the reactive oxygen species (ROS) and the detoxifying enzyme of Phase II glutathione s-transferase (GST), as well as the activity of the main three anti-oxidant enzymes, namely superoxide dismutase (SOD) and catalase (CAT), while the lipid peroxidation (LPO) was measured as a typical endpoint of oxidative damage. Moreover, we evaluated the capability of *B. mori* larvae to ingest PNPs through the observations of cryo-sections at confocal microscopy, as well as the possible crossing of PNPs through the intestinal barrier, the transport by the circulatory system and the potential accumulation in the internal organs.

2. Materials and methods

2.1. Characteristics of PNPs

We used fluorescent-labelled PNPs (Flash Red, excitation

wavelength 660 nm, emission wavelength 690 nm) with a mean diameter of 0.513 μm (Bangs Laboratories, Inc., Fishers, IN, USA) for the microscopy observations, while non fluorescent PNPs with comparable size (diameter range = 0.4–0.6 μm; Spherotech, Inc., Lake Forest, IL, USA) for the exposure assays. Before the exposures, size distribution and zeta potential of PNPs were certified by a Malvern Zetasizer Nano ZS instrument (Malvern Panalytical Ltd, Malvern, UK; see Supplementary Materials). The nanoparticles' characterization showed some differences in terms of size (Table S1), which were not relevant to the purposes of our study (both PNPs did not exceed the nanosize range).

2.2. Insect rearing and bioassays with PNPs

Eggs of *Bombyx mori* and the artificial diet for larvae rearing (Cappellozza et al., 2005) were provided by the Research Centre for Agriculture and Environment (CREA-AA, Padova, Italy). Larvae were reared on artificial diet based on mulberry leaves, under controlled conditions (25 ± 1 °C, 65–70% relative humidity, 12:12 h light/dark period).

PNP exposures were performed by feeding larvae on artificial diet in multi-well plastic trays (Bio-Rt-32, Frontier Agricultural Sciences) covered with perforated plastic lids (Bio-Cv-4, Frontier Agricultural Sciences), maintaining the same rearing conditions reported above. We fed larvae *ad libitum* with artificial diet overlaid with an aqueous suspension of PNPs (pieces of diet of 0.5 g were overlaid with 50 μl of an aqueous suspension of PNPs at different concentration depending on the experiment). Control larvae were fed with diet overlaid with distilled water (50 μl/0.5 g diet) containing a proper dilution of the preservative of the PNP stock solution (Tween 20 or sodium azide). The diet was replaced every day.

Two different feeding bioassays on *B. mori* were carried out, depending on the analysis to be performed. To assess the presence of PNPs within tissues and organs by confocal microscopy, *B. mori* larvae were exposed to fluorescent PNPs (0.25 mg/0.5 g diet) for 10 days (from hatching to the second day of the 3rd instar). Subsequently, to evaluate the effect of PNP ingestion on larval behaviour, development and biochemical parameters, three independent experiments were performed exposing the larvae to 0.25 μg of PNPs per 0.5 g of diet. In detail, the exposure lasted for 10 days for behaviour analysis (from hatching to the second day of the third instar), for 21 days for biochemical analyses (from hatching to the third day of the last fifth instar) or from hatching until the end of the last instar to monitor insect development.

2.3. Sample preparation for microscopy and image analysis

Larvae were first anaesthetized with CO_2 and dissected immediately at the end of exposures. Then, the anterior and posterior ends of the larvae were discarded by cutting between the first and the second pair of legs and the fourth and fifth pseudolegs. The central portions of the body were individually fixed for 3 h at 4 °C in 4% (w/v) paraformaldehyde in phosphate buffered saline (PBS, 137 mM NaCl, 2.7 mM KCl, 8.1 mM Na_2HPO_4, 1.76 mM KH_2PO_4, pH 7.4). Samples were washed 3 times in PBS (rinses of 30 min each) and placed in 15% and 30% sucrose solutions (w/v in PBS) for 30 min and overnight, respectively, prior to inclusion in the cryostat-embedding medium (Bio Optica, Milan, Italy). Samples were then frozen in liquid nitrogen and stored at −80 °C. A CM1850 cryostat (Leica, Wetzlar, Germany) was used to cut transversal sections of 15 μm at −20 °C. Sections were mounted on glass microscope slides using the ProLong™ Gold mounting medium containing 0.2 μg ml^{-1} DAPI (4',6-diamidin-2- phenylindole) (Invitrogen, Carlesbad, CA). Controls were processed similarly.

To observe the PNP internalization in haemocytes, third instar larvae were anaesthetized with CO_2 immediately after the bioassays and haemolymph was collected from a cut of an abdominal pseudoleg. After isolation, a 40 μl aliquot of haemolymph was placed on a glass microscope slide to allow the haemocytes to settle and attach to the glass. After 15 min, the plasma was carefully removed and adhered haemocytes rinsed three times with PBS, fixed for 10 min in 4% (w/v) paraformaldehyde in PBS and rinsed again. Haemocytes were thus stained with Hoechst 33342 solution (10 μg ml^{-1}), rinsed three times with PBS and mounted for confocal microscopy with PBS:glycerol 2:1 (v:v).

For the *in vitro* exposure to fluorescent PNPs, haemocytes were isolated from untreated fifth instar larvae as described above and incubated for 1 h to a 10 mg L^{-1} solution of fluorescent PNPs in 5 mM Tris-HCl, 280 mM sucrose, 4.8 mM $MgSO_4$ and 1 mM $CaCl_2$. Fixation and mounting were carried out as described above.

Sections and haemocytes samples (prepared from at least three larvae) were observed by confocal microscopy (Laser Scanning Confocal Microscope Nikon A1, NITAL S.P.A., Moncalieri, Italy) and acquisition details of different channels are included in Supplementary Materials (Table S2). Imaging analyses were performed using the dedicated software (NIS-Elements) to exclude any uncertainty on particle localization. Images were acquired merging different channels (bright field and fluorescence), assuring that the fluorescent signal of beads was unequivocally distinguished from autofluorescence.

2.4. Growth and development analysis

To monitor insect growth and development different parameters were recorded: larval mortality (reported as percentage of the initial number of larvae), length of the larval stage (from hatching to the occurrence of wandering behaviour), maximum larval weight (recorded just before the wandering phase), weight of the pupae and cocoon (registered on the sixth day of the pupal stage) and adult emergence (reported as percentage of the total number of pupae). Developmental stages of *B. mori* were defined according to Franzetti et al. (2012). Three groups of 25 larvae were treated with PNPs and the same number of larvae was kept as control.

2.5. Biomarkers of oxidative stress

We exposed 9 *B. mori* larvae to PNPs for 21 days and an equal number were reared as controls. Larvae were then dissected for homogenate preparation. Briefly, the anterior and the posterior ends of the larvae were discarded by cutting between the first and the second pair of legs and the fourth and the fifth pseudolegs. The central part of the body was opened lengthwise and midgut along with Malpighian tubules isolated and deprived of the midgut content. The carcass was scraped to recover internal tissues (fat body with adhered haemocytes, tracheae, nerves, muscles). Midguts, Malpighian tubules and tissues recovered from the carcass of three larvae were pooled and homogenized in 100 mM phosphate buffer (pH 7.4), with 100 mM KCl, 1 mM ethylenediamine tetraacetic acid (EDTA), 100 mM dithiothreitol (DTT), and protease inhibitors (Roche, 1:100 v/v in deionized water). The homogenates were centrifuged at 15,000×*g* for 15 min at 4 °C and supernatants were recovered and stored at −80 °C.

The measurement of GST, SOD and CAT, as well as the ROS production followed the methods described by Parenti et al. (2019), with minor modifications. The day of the analyses, homogenates were thawed, and protein concentration was measured by the Coomassie Brilliant Blue G-250 (Pierce) protein assay, with bovine serum albumin as standard.

The levels of enzymatic activity were assessed using the 6715 UV/Vis spectrophotometer (Jenway, USA). GST activity, expressed in

mmol min^{-1} mg $protein^{-1}$, was measured at 340 nm. The activity was quantified adding the reduced glutathione (20 mM) in 100 mM phosphate buffer (pH 7.4) and the substrate 1-Chloro-2,4-dinitrobenzene (CDNB) (20 mM). SOD activity, expressed in SOD units mg $protein^{-1}$ (1 SOD unit = 50% inhibition of the xanthine oxidase reaction), was measured at 550 nm. The activity was quantified measuring the degree of inhibition of cytochrome C (0.3 mM) in 50 mM phosphate buffer + EDTA (0.1 mM), generated by the reaction mix of 1.5 mM hypoxanthine and xanthine oxidase 56.1 mU mL^{-1}. CAT activity, expressed in μmol min^{-1} mg $protein^{-1}$, was analysed at 240 nm. The activity was determined by measuring the consumption of H_2O_2 (150 mM) in 100 mM phosphate buffer (pH 7). ROS level was assessed using the dichlorofluorescein-diacetate (DCFH-DA) method. Larval homogenates were added in triplicate to a 96-well plate and incubated for 5 min at room temperature. In each well, 100 μL of PBS and 8.3 μL of DCFH-DA (10 mg mL^{-1} in DMSO) were also added and the plate was then incubated for 30 min at 37 °C. ROS concentration, expressed in fluorescence units (FU), was measured using the EnSight™ multimode plate reader (PerkinElmer) at λ_{ex} 485 nm and λ_{em} 530 nm. Enzymatic activities and ROS production were normalized on the total protein content of each sample.

The oxidative damage was evaluated measuring the LPO, following the method of Ohkawa et al. (1979). In brief, 100 μl of each homogenate were placed in glass tubes with 500 μl of 12% (v/v) trichloroacetic acid (TCA) in deionized water, 400 μl of 0.6 M Tris-HCl and 500 μl of 0.37% (v/v) thiobarbituric acid (TBA) in deionized water, and incubated 1 h in boiling water. The suspension was then refreshed in ice and centrifuged at 15,000×*g* for 10 min at 20 °C. The level of TBA-reactive substances, expressed in nmol g^{-1} $w.w.^{-1}$ (wet weight), was estimated in the supernatants, reading the absorbance at 535 nm.

2.6. Behavioural tests

To evaluate the potential effects of ingested PNPs on behaviour, *B. mori* larvae were exposed to PNPs for 10 days and an equal number of larvae were reared as controls.

Control and PNP-exposed larvae were subjected to an alternating dark/light test (8 min) and a chemotaxis test (5 min) and filmed by an infrared camera (sample rate of 6 frames/second) using the DanioVision™ observation chamber (Noldus Inc., Wageningen, The Netherlands). The evaluation of chemotaxis defects was performed by a single odour assay by using 20 μL of mulberry leaves extract as olfactory stimulus that was produced by mixing the artificial diet powder with distilled water (4 ml of water each g of powder) followed by centrifugation at 10,000×*g* for 5 min and supernatant recovery. The motion of single larvae exposed to the odour source was recorded during the entire duration of the trial (5 min with light on). The EthoVision XT® software (Noldus Inc., Wageningen, The Netherlands) was used to elaborate several parameters for behavioural quantification (total mobility, time course of distance to odour source). Measurements have been performed on groups of at least 6 larvae.

2.7. Statistics

The effect of PNP exposure on larval growth was investigated by means of a generalized linear model (GLM) with mean weight as depended variable and day and treatment (control and PNPs) as response variables. Since mean weight variable distribution was right-skewed, we assumed a Poisson distribution of the variable. In a former model, we included the two-way interaction between treatment and day to assess the potential effect of the treatment, considering the day. However, since the two-way interaction did not significantly affect the mean weight ($p > 0.9$), we removed this interaction in the final model. Only the variable day had a significant and positive effect on larval mean weight (estimate Standard Error: 0.33(0.05), $z = 6.15$, $p < 0.001$, $n = 96$), while no effects of treatment have been observed ($p > 0.8$). A generalized linear model (GLM) was performed using R v.3.6.1. To identify any significant effects of PNPs on larval stress and behaviour, we analysed data using the STATISTICA 7.0 package. After having certified the normality of the data and homoscedasticity using the Shapiro-Wilk and Levene tests, the significant differences between the two independent groups (control and PNP) were analysed by one-way ANOVA followed by the Fisher LSD *post-hoc* test, taking $p < 0.05$ as significant cut-off.

3. Results and discussion

3.1. General considerations

One of the most critical aspects in the study of NP toxicity is to clearly demonstrate their internalization in the organism by different intake routes (e.g. gills, gut and skin), as well as the infiltration of plastic particles in the tissues and/or internalization in the cells and the eventual clearance. To do this, it is crucial the selection of reliable methods which make conclusive evidence of plastics intake. Indeed, if the use of fluorescent-labelled particles solves many interpretation problems by the elimination of some interferences, the lack of adequate controls can give inconclusive evidence of plastic accumulation in the tissues of the selected biological model. Catarino et al. (2019) showed that commercial fluorescent NPs can leach the fluorophores that accumulate in the same internal tissues of zebrafish larvae where NP accumulation was observed. Thus, we performed a double-check method based on the use of labelled-PNPs coupled with the identification of single nanospheres by the observation of cryo-sections, able to preserve the sample avoiding too much aggressive treatments. This guaranteed, together with the orthogonal projections (see Fig. 1B_2), a conclusive evidence about their accumulation in the larvae tissues and the lack of accidental transport of the administered PNPs during the cryo-section preparation. The need to check the capability of plastic particles to enter the organisms forced the use of PNP concentrations much higher than environmental ones, decreasing the ecological realism. On the other hand, this is the only possible approach in a preliminary study whose purpose was the evaluation of the uptake, transport and accumulation of PNPs and their ecotoxicological potential, without any claim to reach an environmental risk assessment (ERA).

3.2. Detection of PNPs in B. mori larvae

The observation of sections of third instar *B. mori* larvae by confocal microscopy showed the presence of fluorescent PNPs inside the intestinal lumen (Fig. 1B_2), demonstrating the ingestion of the food along with the plastic particles.

Furthermore, PNPs were observed not only inside the intestinal lumen, but also into Malpighian tubules (Mts; Fig. 1B_2), which are excretory and osmoregulatory organs of insects (Xia et al., 2007). Mts are considered analogous to the nephridia in annelids or kidneys in vertebrates (Wigglesworth, 2003), but they are also involved in other essential functions, such as the immunological defence, regulation and secretion of calcium and also in chemical detoxification processes (Beyenbach et al., 2010). Mts transport solutes and water from haemolymph forming the primary urine which is collected in Mt lumen and poured into the intestine between the midgut and the hindgut. In the latter the primary urine is modified and discarded with the feces (Nocelli et al., 2016). The

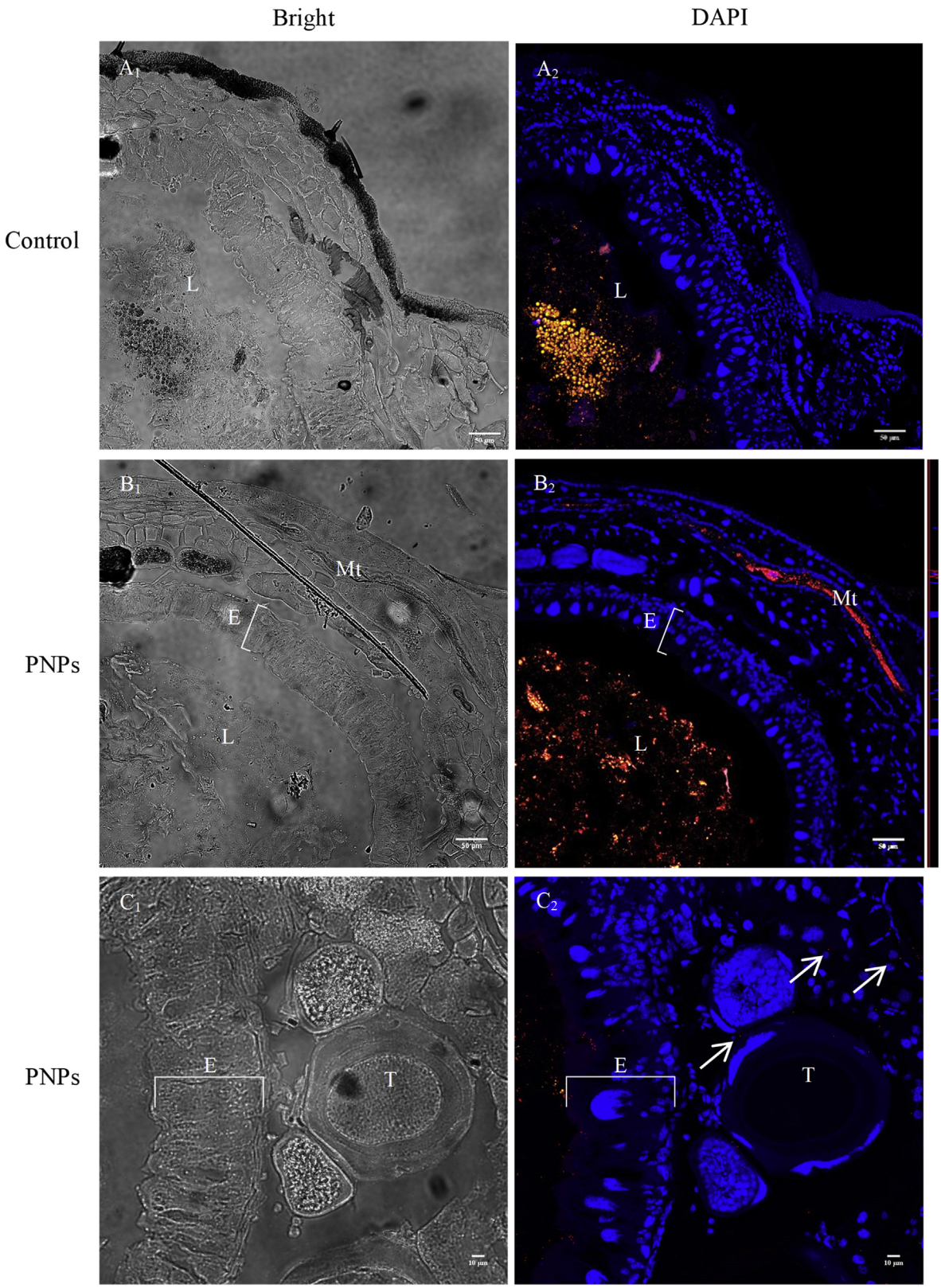

Fig. 1. Confocal microscopy observations of 15 µm transversal cryo-sections of third instar *B. mori* larvae. Fluorescent beads are shown in red, while yellow fluorescence resulted from the merge of PNPs and administered diet. Cell nuclei were stained with DAPI. (A_1)(A_2) Transversal section of a control larva [L: intestinal lumen; scale bar 50 µm] (B_1)(B_2) Transversal section of a larva exposed to PNPs with orthogonal projections of Z-stacks evidencing the nanobeads at cellular level [L: intestinal lumen, E: gut epithelium, Mt: Malpighian tubule; scale bar 50 µm] (C_1)(C_2) Detail of a transversal section of a larva exposed to PNPs [E: gut epithelium, T: trachea; scale bar 10 µm]. (For interpretation of the references to colour in this figure legend, the reader is referred to the Web version of this article.)

observed presence of PNPs in these organs can be due to the possible movement of PNPs from the gut to the Mt lumen, but it might also suggest the involvement of an unidentified process that leads to the movement of PNPs from the haemolymph to the Mt lumen in the attempt to eliminate these potential hazardous materials. Our results are also similar to those revealed in a recent study that showed the presence of 2 μm MP in the Mts of adult *Culex* mosquitoes (Al-Jaibachi et al., 2018). The authors fed aquatic larvae with MPs and detected their presence in the abdomen and Mts of adults, indicating the transfer of ingested microparticles from larval to the adult stage, although no effects on body weight and mortality were recorded (Al-Jaibachi et al., 2019). This accumulation of plastics in terrestrial organisms at low trophic level may support further transfer and accumulation along food chains, posing a threat to insect-eating species.

Microscopy observations of *B. mori* sections showed also the presence of PNPs into the midgut epithelium (Fig. 1C_2), pointing out the capability of these physical contaminants to pass through the gut barrier and infiltrate in the near larval tissues.

The most intriguing result obtained by microscopy was probably the observation of PNPs in the cytoplasm of haemocytes sampled from larvae after the treatments (Fig. 2A). Given that this evidence is crucial to demonstrate the transport of these physical pollutants by the circulatory system and their potential accumulation in all the organism tissues, we carried out *in vitro* experiments by incubating haemocytes isolated from untreated larvae with PNPs which confirmed the capability of haemocytes to internalize them (Fig. 2B). The presence of plastic particles in the haemolymph was already demonstrated in different bivalves (Browne et al., 2008; Ribeiro et al., 2017; Magni et al., 2018), indicating that plastic debris may be retained in the organisms and potentially transported in all the tissues.

3.3. Effects of PNPs on insect development

After demonstrating the presence of PNPs in many larval tissues, we investigated their possible negative effects at different level of biological organization. Moving to results obtained at organism level, PNP exposure caused neither larval mortality nor alteration in the duration of the larval cycle (Table 1). Moreover, no significant difference in body weight was observed in respect to controls over the entire larval stage (Fig. 3, Table 1). To clarify whether the exposure may affect metamorphosis, the pupal and cocoon weight, as well as adult emergence, were also recorded, showing no detrimental effects (Table 1). Emerged adults were monitored and no differences in mortality was observed between exposed and untreated larvae, as all the adults survived and females oviposited (data not shown). The overall data indicated that PNP exposure did not alter the individual and population fitness of *B. mori*, at least in our experimental conditions.

3.4. Behavioural tests

To further assess the potential effects of PNPs at organism level, we performed also several assays based on larval behaviour, whose endpoints link molecular and physiological effects with ecological processes, providing information at various levels of biological organization (Scott and Sloman, 2004). Indeed, any behavioural variation caused by the exposure to environmental contaminants may compromise directly or indirectly the organism survival and fitness. Behavioural effects caused by MPs and NPs, in terms of changes in locomotor activity and feeding behaviour, were already observed in several aquatic organisms, such as *Daphnia magna* (De Felice et al., 2019), *Carcinus maenas* (Watts et al., 2014) and *Danio rerio* embryos and adults (Parenti et al., 2019; Qiang and Cheng, 2019; Mak et al., 2019).

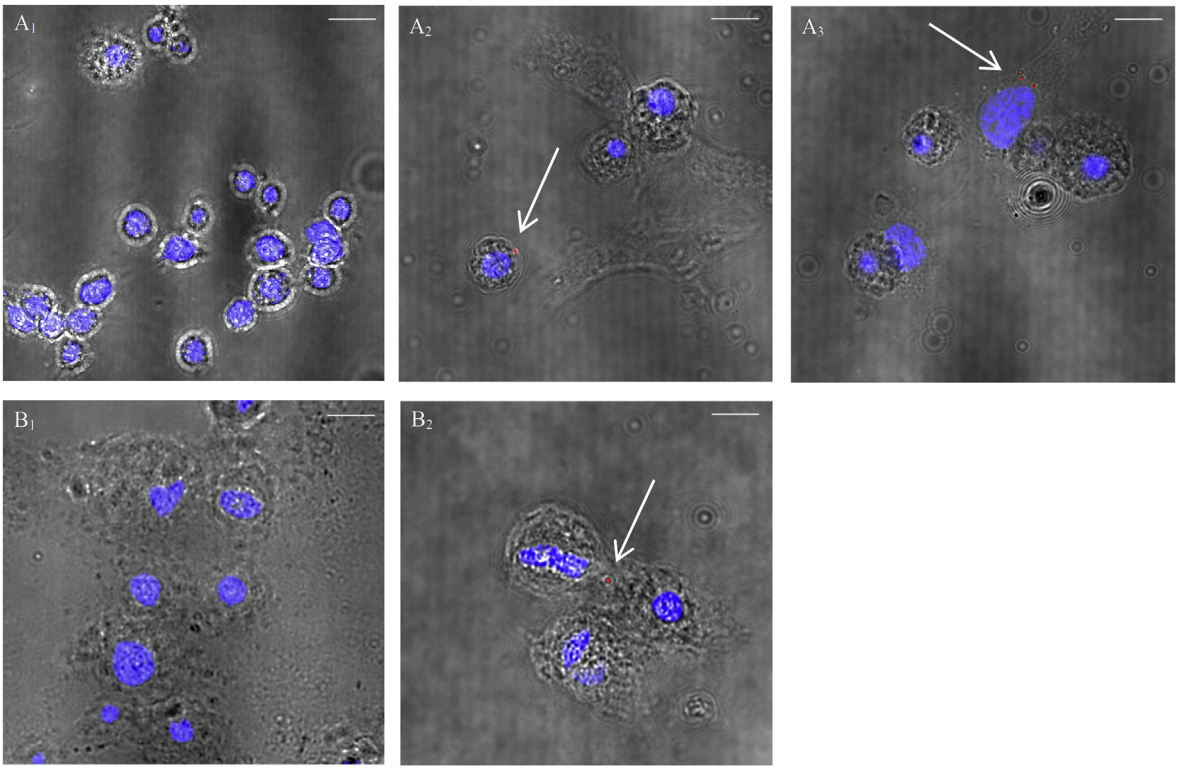

Fig. 2. Haemocytes collected from control (A_1) and treated larvae (A_2 and A_3) [scale bar 10 μm]. Isolated haemocytes of *B. mori* larva incubated *in vitro* for 60 min: (B_1) control and (B_2) exposed to PNPs [scale bar 10 μm]. White arrows indicate the nanobeads, nuclei are stained with Hoechst 33342.

Table 1
Growth parameters of *B. mori* larvae exposed to PNPs. The maximum larval weight refers to the maximal weight reached by last instar larvae. The experiment was performed in triplicate with groups of 25 larvae. The values are reported as mean ± standard error.

Treatment	Mortality	Larval cycle (days)	Maximum larval weight (g)	Pupal weight (g)	Cocoon weight (g)	Adult emergence (%)
Control	0	24.58 ± 0.92	4.48 ± 0.26	1.92 ± 0.47	0.28 ± 0.01	100
PNP	0	24.78 ± 0.94	4.50 ± 0.07	1.61 ± 0.08	0.28 ± 0.04	100

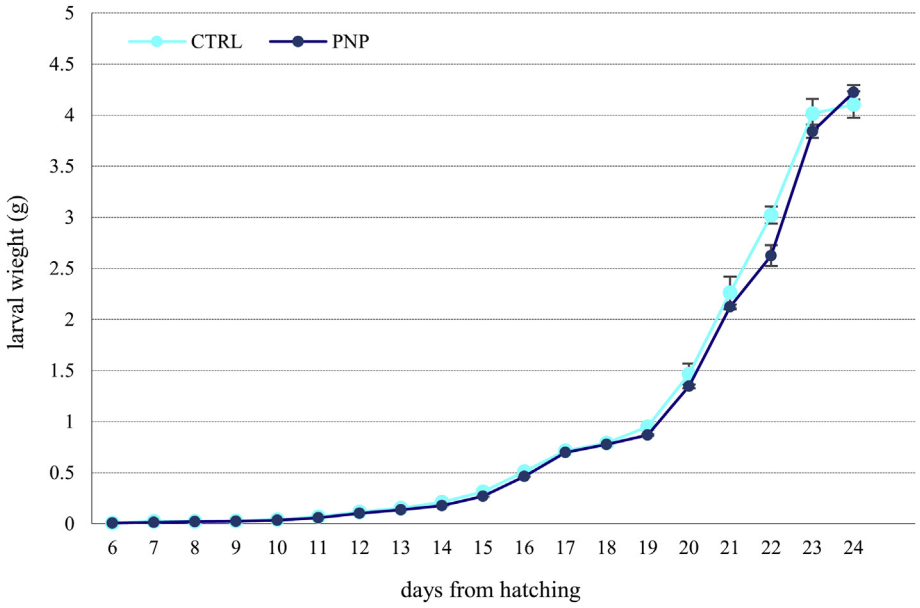

Fig. 3. Growth curve of *B. mori* larvae exposed to PNPs and controls. The weight was recorded from 6th day to 24th day (mean body weight of larvae from each experimental group), when larvae started to enter the wandering phase.

In this study, DanioVision™ was used to record the mobility state of larvae in two different tests, measuring the percentage of the movement time and the larval response to a chemical stimulus, respectively. In the first assay, we measured a mobility parameter able to detect the movement independently by the spatial displacement of the organism. This allowed to evaluate the whole movement of the larva, even in the absence of a real movement within the test arena. The mobility test showed a significant hyperactivity of treated larvae (Fig. 4A), both during the light phase ($p < 0.05$) and especially the dark phase ($p < 0.001$), suggesting that the stress condition represented by darkness may further increase the effect. The higher mobility of larvae exposed to PNPs was not related to an increase in the distance moved, but rather to erratic movements that can have crucial ecological consequences because lepidopteran larvae may be, for example, particularly vulnerable to detection by predators. An excitatory effect of NPs on locomotor behaviour was also observed in *Caenorhabditis elegans* (Lei et al., 2018), explained as a potential interaction of NPs with neurons.

Olfaction is one of the most important ways through which insects interact with their surroundings (Gadenne et al., 2016). Since, among its many functions, insects rely on chemoreception to locate food sources, we performed another behavioural test using an olfactive stimulus to investigate if the PNP exposure could alter silkworm feeding behaviour. Very interestingly, collected data reported a significant increase of mobility during the first 2 min of the test for exposed larvae (Fig. 4B, $p < 0.05$), while the cumulative duration of time spent in the area surrounding the olfactive stimulus was not significantly different (Fig. 4C). Thus, the PNP effect seemed to interfere mainly on the feeding initiation (meal-start), which is driven by a complex co-action of physical and chemical factors (Audsley and Weaver, 2009).

3.5. Biomarkers of oxidative stress

We applied a biomarker suite for the evaluation of possible impacts due to PNPs at cellular and molecular level, focusing mainly on their possible role in the imbalance of redox homeostasis through the antioxidant response. Oxidative stress is included in the fourth main category (physiological stress) of effects reported for plastic particles <10 μm on aquatic and shoreline biota (Kögel et al., 2020). A recent review by Prokić et al. (2019) reported a huge and sometimes controversial variety of oxidative stress responses for organisms exposed to plastic beads (ranging from 0.05 to 100 μm), depending on several factors, such as tissue chosen for the analysis or composition, size, shape and concentration of plastics. For instance, the effect of the particle size was highlighted by Jeong et al. (2016, 2017) who observed that lower-sized polystyrene particles (50 nm) were able to induce a higher oxidative stress in the rotifer *Brachionus koreanus* and in the copepod *Paracyclopina nana* while, in contrast, Lu et al. (2016) showed as the greatest antioxidant response was observed in *Danio rerio* as a response to larger plastic particles (5 μm). The same study found that the induction of two antioxidant enzymes (SOD and CAT) increased with higher concentration of MPs. Furthermore, biomarkers of oxidative stress often showed a tissue-specific response to MPs (20 μm), as observed in gills and digestive gland of the clam *Scrobicularia plana* (Ribeiro et al., 2017). In our study, the exposure to PNPs did not induce any variation in ROS level (Fig. 5A) or CAT (Fig. 5B) and GST (Fig. 5D) activities. On the contrary, a significant ($p < 0.01$) inhibition of SOD (Fig. 5C) emerged after the exposure to PNPs. A study by Liu et al. (2019) of NP effects on *Daphnia pulex* showed that NPs (75 nm) lead to changes in the relative expression of some oxidative stress-mediated genes (*SOD*, *GST*, *GPx* and *CAT*),

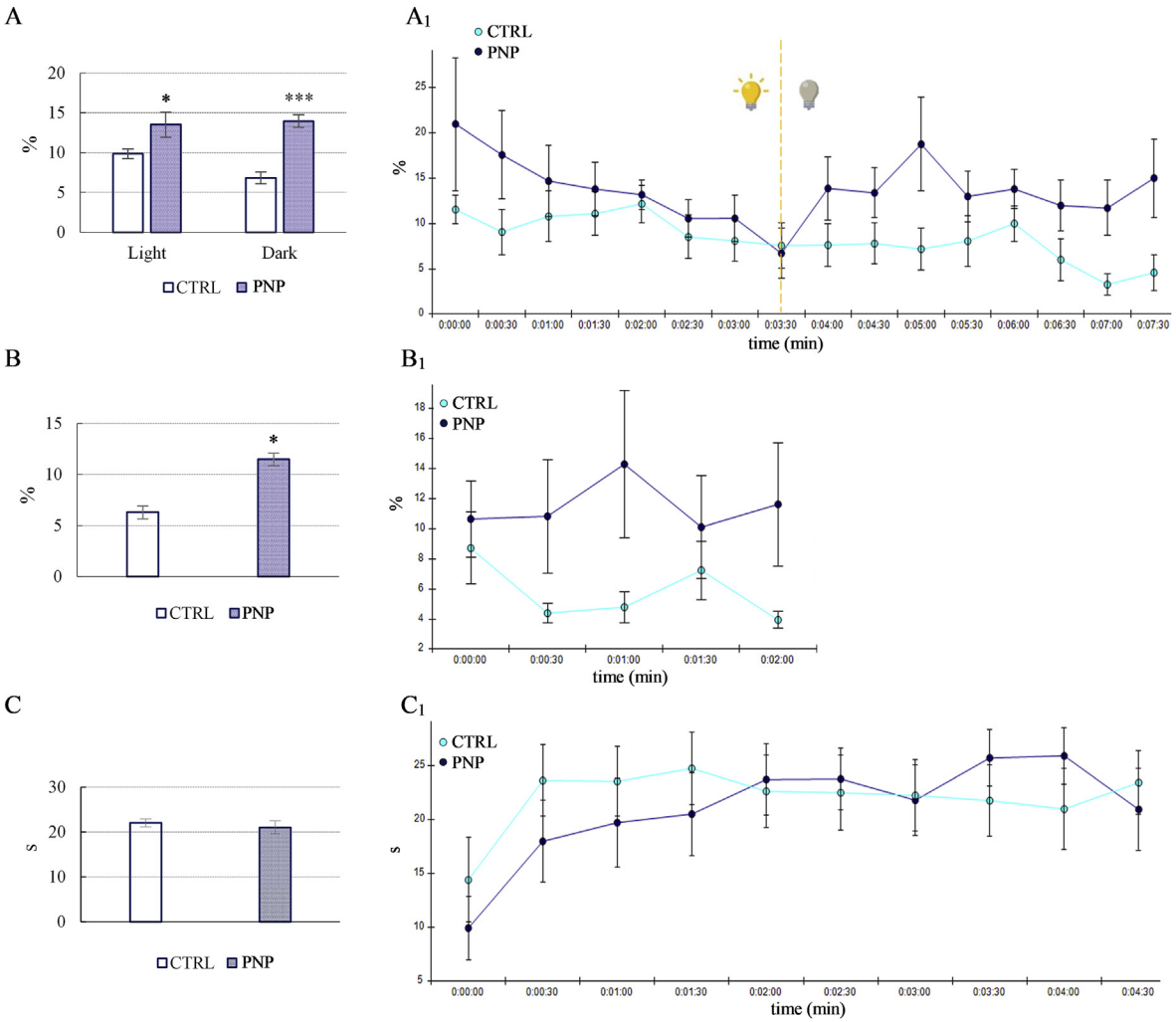

Fig. 4. Behavioural effects of PNP ingestion on third instar larvae, respect to controls. (A) Mean percentage of maximum mobility during the 8 min of the alternating light-dark test. (A1) Percentage of maximum mobility during the alternating light-dark test, calculated every 30 s. (B) Mean percentage of maximum mobility during the first 2 min of the chemotaxis test. (B1) Percentage of maximum mobility during the first 2 min of the chemotaxis test, calculated every 30 s. (C) Cumulative duration of the stay in the stimulus zone during the 5 min of the chemotaxis test. (C1) Cumulative duration of the stay in the stimulus zone during the 5 min of the chemotaxis test, calculated every 30 s. Data are from three experiments and are presented as mean ± standard error. (one-way ANOVA followed by Fisher LSD post-hoc test, *** = $p < 0.001$, * = $p < 0.05$).

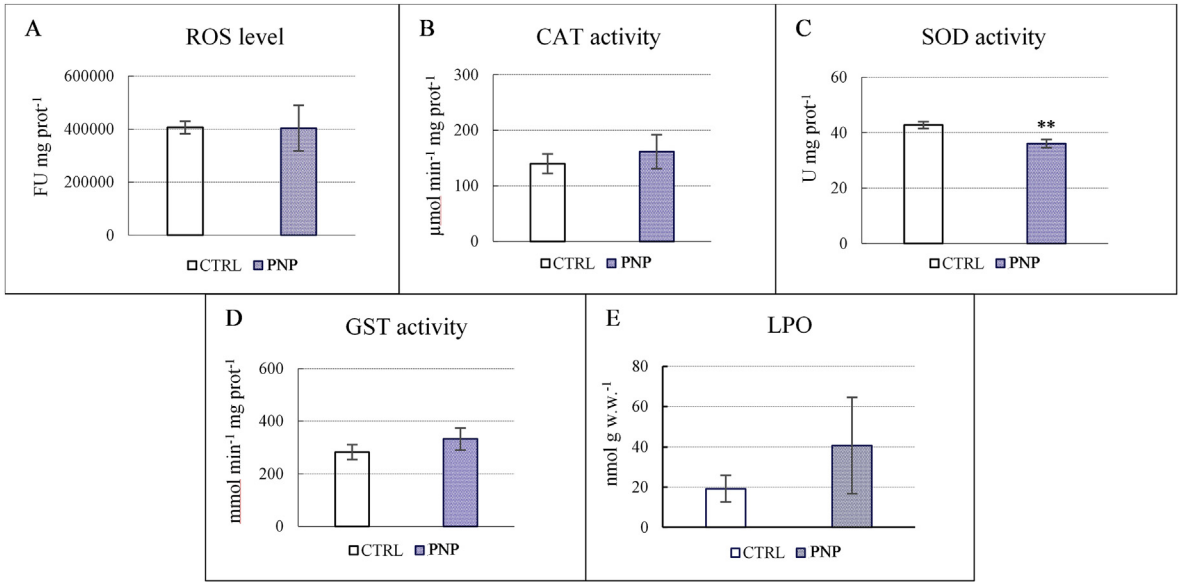

Fig. 5. Sub-individual effects of PNP ingestion on fifth instar larvae, respect to controls. (A) Quantity of ROS. (B) Activity of CAT. (C) Activity of SOD. (D) Activity of GST. (E) Level of LPO. Data are from three experiments and are presented as mean ± standard error. (one-way ANOVA followed by Fisher LSD post-hoc test, ** = $p < 0.01$).

which increased or decreased depending on the concentration of the particles (from 0.1 to 2 mg L^{-1}), showing a downward trend with the higher concentrations. In the same way, the SOD inhibition observed in treated larvae might suggest the onset of oxidative stress imbalance caused by the high PNP concentration used in the study. Nevertheless, no oxidative damage was observed, concerning the level of lipid peroxidation (Fig. 5E), which is considered an indicator of the adaptive response to oxidative stress. This result is consistent with the level of ROS (Fig. 5A), which did not present any difference between controls and exposed groups.

4. Conclusions

This study represents the first investigation on the uptake and effects of PNP exposure in the Lepidoptera model organism *B. mori*. The overall dataset demonstrated the capability of silkworm larvae to ingest PNPs, which were then able to pass the intestinal barrier and reach the internal tissues and organs and the circulatory system, as clearly shown by the presence of PNPs in the haemocytes. Another crucial result of this study was the application of a multi-tier approach to investigate the potential toxicity of these physical contaminants. The non-exhaustive results obtained by the measured endpoints at different levels of the biological organization confirmed the need to use several approaches that allow the comparison and integration of the entire dataset. Indeed, neither biochemical analyses nor endpoints of development revealed significant impact at cellular and molecular levels or an alteration of larval life cycle, while the most relevant outcome emerged from the behaviour observations, since PNPs affected locomotor activity, with potential negative indirect effects on *B. mori* survival and fitness from the ecological point of view.

Declaration of competing interest

The authors declare that they have no known competing financial interests or personal relationships that could have appeared to influence the work reported in this paper.

CRediT authorship contribution statement

C.C. Parenti: Conceptualization, Methodology, Validation, Formal analysis, Investigation, Writing - original draft. **A. Binelli:** Conceptualization, Resources, Supervision, Writing - review & editing, Project administration, Funding acquisition. **S. Caccia:** Investigation, Methodology, Writing - review & editing. **C. Della Torre:** Methodology, Writing - review & editing. **S. Magni:** Investigation, Writing - review & editing. **G. Pirovano:** Investigation. **M. Casartelli:** Conceptualization, Project administration, Conceptualization, Resources, Supervision, Writing - review & editing.

Acknowledgements

We thank Dr. Silvia Cappellozza from the Council for Agricultural Research (CREA-AA, Padua, Italy) for providing *B. mori* eggs and the artificial diet used in this work.

Appendix A. Supplementary data

Supplementary data to this article can be found online at https://doi.org/10.1016/j.chemosphere.2020.127203.

References

Abdelli, N., Peng, L., Chen, K., 2018. Silkworm, *Bombyx mori*, as an alternative model organism in toxicological research. Environ. Sci. Pollut. Res. 25, 35048–35054.

Al-Jaibachi, R., Cuthbert, R.N., Callaghan, A., 2018. Up and away: ontogenic transference as a pathway for aerial dispersal of microplastics. Biol. Lett. 14, 20180479.

Al-Jaibachi, R., Cuthbert, R.N., Callaghan, A., 2019. Examining effects of ontogenic microplastic transference on *Culex* mosquito mortality and adult weight. Sci. Total Environ. 651 (1), 871–876.

Audsley, N., Weaver, R.J., 2009. Neuropeptides associated with the regulation of feeding in insects. Gen. Comp. Endocrinol. 162 (1), 93–104.

Beyenbach, K.W., Skaer, H., Dow, J.A.T., 2010. The developmental, molecular, and transport biology of Malpighian tubules. Annu. Rev. Entomol. 55, 351–374.

Browne, M.A., Dissanayake, A., Galloway, T.S., Lowe, D.M., Thompson, R.C., 2008. Ingested microscopic plastic translocates to the circulatory system of the mussel, *Mytilus edulis* (L.). Environ. Sci. Technol. 42 (13), 5026–5031.

Cappellozza, L., Cappellozza, S., Saviane, A., Sbrenna, G., 2005. Artificial diet rearing system for the silkworm *Bombyx mori* (Lepidoptera:Bombycidae): effect of vitamin C deprivation on larval growth and cocoon production. Appl. Entomol. Zool. 40 (3), 405–412.

Catarino, A.I., Frutos, A., Henry, T.B., 2019. Use of fluorescent-labelled nanoplastics (NPs) to demonstrate NP absorption is inconclusive without adequate controls. Sci. Total Environ. 670, 915–920.

Cózar, A., Echevarría, F., González-Gordillo, J.I., Irigoien, X., Úbeda, B., Hernández-León, S., Palma, Á.T., Navarro, S., García-de-Lomas, J., Ruiz, A., Fernández-de-Puelles, M.L., Duarte, C.M., 2014. Plastic debris in the open ocean. PNAS 111 (28), 10239–10244.

De Felice, B., Sabatini, V., Antenucci, S., Gattoni, G., Santo, N., Bacchetta, R., Ortenzi, M.A., Parolini, M., 2019. Polystyrene microplastics ingestion induced behavioral effects to the cladoceran *Daphnia magna*. Chemosphere 231, 423–431.

Franzetti, E., Huang, Z.J., Shi, Y.X., Xie, K., Deng, X.J., Li, J.P., Li, Q.R., Yang, W.Y., Zeng, W.N., Casartelli, M., Deng, H.M., Cappellozza, S., Grimaldi, A., Xia, Q., Feng, Q., Cao, Y., Tettamanti, G., 2012. Autophagy precedes apoptosis during the remodeling of silkworm larval midgut. Apoptosis 17, 305–324.

Gadenne, C., Barrozo, R.B., Anton, S., 2016. Plasticity in insect olfaction: to smell or not to smell?.

Hamamoto, H., Kurokawa, K., Kaito, C., Kamura, K., Razanajatovo, I.M., Kusuhara, H., Santa, T., Sekimizu, K., 2004. Quantitative evaluation of the therapeutic effects of antibiotics using silkworms infected with human pathogenic microorganisms. Antimicrob. Agents Chemother. 48, 774–779.

Hartmann, N.B., Hüffer, T., Thompson, R.C., Hassellöv, M., Verschoor, A., Daugaard, A.E., Rist, S., Karlsson, T., Brennholt, N., Cole, M., Herrling, M.P., Hess, M.C., Ivleva, N.P., Lusher, A.L., Wagner, M., 2019. Are we speaking the same language? Recommendations for a definition and categorization framework for plastic debris. Environ. Sci. Technol. 53 (3), 1039–1047.

Heidbreder, L.M., Bablok, I., Drews, S., Menzel, C., 2019. Tackling the plastic problem: a review on perceptions, behaviors, and interventions. Sci. Total Environ. 668, 1077–1093.

Horton, A.A., Walton, A., Spurgeon, D.J., Lahive, E., Svendsen, C., 2017. Microplastics in freshwater and terrestrial environments: evaluating the current understanding to identify the knowledge gaps and future research priorities. Sci. Total Environ. 586, 127–141.

Huerta Lwanga, E., Gertsen, H., Gooren, H., Peters, P., Salánki, T., van der Ploeg, M., Besseling, E., Koelmans, A.A., Geissen, V., 2016. Microplastics in the terrestrial ecosystem: implications for *Lumbricus terrestris* (Oligochaeta, Lumbricidae). Environ. Sci. Technol. 50, 2685–2691.

Ishii, M., Matsumoto, Y., Sekimizu, K., 2015. Drug Discov. & Ther. 9 (4), 234–237.

Jeong, C.B., Won, E.J., Kang, H.M., Lee, M.C., Hwang, D.S., Hwang, U.K., Zhou, B., Souissi, S., Lee, J.S., 2016. Microplastic size-dependent toxicity, oxidative stress induction, and p-JNK and p-p38 activation in the monogonont rotifer (*Brachionus koreanus*). Environ. Sci. Technol. 50, 8849–8857.

Jeong, C.B., Kang, H.M., Lee, M.C., Kim, D.H., Han, J., Hwang, D.S., Souissi, S., Lee, S.J., Shin, K.H., Park, H.G., Lee, J.S., 2017. Adverse effects of microplastics and oxidative stress-induced MAPK/Nrf2 pathway-mediated defense mechanisms in the marine copepod *Paracyclopina nana*. Sci. Rep. 7, 41323.

Kaito, C., 2016. Understanding of bacterial virulence using the silkworm infection model. Drug Discov. & Ther. 10 (1), 30–33.

Kim, H.M., Lee, D.K., Long, N.P., Kwon, S.W., Park, J.H., 2019. Uptake of nano-polystyrene particles induces distinct metabolic profiles and toxic effects in *Caenorhabditis elegans*. Environ. Pollut. 246, 578–586.

Kögel, T., Bjorøy, Ø., Benuarda, T., Bienfait, A.M., Sanden, M., 2020. Micro- and nanoplastic toxicity on aquatic life: determining factors. Sci. Total Environ. 709, 136050.

Kramm, J., Völker, C., 2018. Understanding the risks of microplastics: a social-ecological risk perspective. In: Wagner, M., Lambert, S. (Eds.), Freshwater Microplastics. The Handbook of Environmental Chemistry, vol. 58. Springer, Cham, pp. 223–237.

Lei, L., Liu, M., Song, Y., Lu, S., Hu, J., Cao, C., Xie, B., Shi, H., He, D., 2018. Polystyrene (nano)microplastics cause size-dependent neurotoxicity, oxidative damage and other adverse effects in *Caenorhabditis elegans*. Environ. Sci. Nano 5 (8), 2009–2020.

Liu, Z., Yu, P., Cai, M., Wu, D., Zhang, M., Huang, Y., Zhao, Y., 2019. Polystyrene nanoplastic exposure induces immobilization, reproduction, and stress defence in the freshwater cladoceran *Daphnia pulex*. Chemosphere 215, 74–81.

Lu, Y., Zhang, Y., Deng, Y., Jiang, W., Zhao, Y., Geng, J., Ding, L., Ren, H., 2016. Uptake and accumulation of polystyrene microplastics in zebrafish (*Danio rerio*) and toxic effects in liver. Environ. Sci. Technol. 50, 4054–4060.

Magni, S., Gagné, F., André, C., Della Torre, C., Auclair, J., Hanana, H., Parenti, C.C., Bonasoro, F., Binelli, A., 2018. Evaluation of uptake and chronic toxicity of virgin polystyrene microbeads in freshwater zebra mussel *Dreissena polymorpha* (Mollusca:Bivalvia). Sci. Total Environ. 631–632, 778–788.

Mak, C.W., Ching-Fong Yeung, K., Chan, K.M., 2019. Acute toxic effects of polyethylene microplastic on adult zebrafish. Ecotox. Environ. Safe. 182, 1–10.

Meng, X., Zhu, F., Chen, K., 2017a. Silkworm: a promising model organism in life science. J. Insect Sci. 17 (5), 1–6, 97.

Meng, X., Abdlli, N., Wang, N., Lü, P., Nie, Z., Dong, X., Lu, S., Chen, K., 2017b. Effects of Ag nanoparticles on growth and fat body proteins in silkworm (*Bombyx mori*). Biol. Trace Elem. Res. 180, 327–337.

Mulé, R., Sabella, G., Robba, L., Manachini, B., 2017. Systematic review of the effects of chemical insecticides on four common butterfly families. Front. Environ. Sci. 5, 32.

Nizzetto, L., Futter, M., Langaas, S., 2016. Are agricultural soils umps for microplastics of urban origin? Environ. Sci. Technol. 50, 10777–10779.

Nocelli, R.C.F., Cintra-Socolowsky, P., Roat, T.C., Silva-Zacarin, E.C.M., Malaspina, O., 2016. Comparative physiology of Malpighian tubules: form and function. Open Access Insect Physiol 6, 13–23.

Ohkawa, H., Ohisi, N., Yagi, K., 1979. Assay for lipid peroxides in animal tissues by thiobarbituric acid reaction. Anal. Biochem. 95, 351–358.

Oliveira, M., Almeida, M., Miguel, I., 2019a. A micro(nano)plastic boomerang tale: a never ending story? Trends Anal. Chem. 112, 196–200.

Oliveira, M., Ameixa, O.M.C.C., Soares, A.M.V.M., 2019b. Are ecosystem services provided by insects "bugged" by micro(nano)plastics? Trends Anal. Chem. 113, 317–320.

Parenti, C.C., Ghilardi, A., Della Torre, C., Magni, S., Del Giacco, L., Binelli, A., 2019. Evaluation of the infiltration of polystyrene nanobeads in zebrafish embryo tissues after short-term exposure and the related biochemical and behavioural effects. Environ. Pollut. 254 (A), 112947.

Powell, J.A., 2009. Chapter 151: Lepidoptera: moths, butterflies. Encyclopedia of Insects, second ed., pp. 559–587

Prokić, M.D., Radovanović, T.B., Gavrić, J.P., Faggio, C., 2019. Ecotoxicological effects of microplastics: examination of biomarkers, current state and future perspectives. Trends Anal. Chem. 111, 37–46.

Qiang, L., Cheng, J., 2019. Exposure to microplastics decreases swimming competence in larval zebrafish (*Danio rerio*). Ecotox. Environ. Safe. 176, 226–233.

Ribeiro, F., Garcia, A.R., Pereira, B.P., Fonseca, M., Mestre, N.C., Fonseca, T.G., Ilharco, L.M., Bebianno, M.J., 2017. Microplastics effects in *Scrobicularia plana*. Mar. Pollut. Bull. 122 (1–2), 379–391.

Rodriguez-Seijo, A., Lourenço, J., Rocha-Santos, T.A.P., da Costa, J., Duarte, A.C., Vala, H., Pereira, R., 2017. Histopathological and molecular effects of microplastics in *Eisenia andrei* Bouché. Environ. Pollut. 220 (A), 495–503.

Scott, G.R., Sloman, K.A., 2004. The effects of environmental pollutants on complex fish behaviour: integrating behavioural and physiological indicators of toxicity. Aquat. Toxicol. 68 (4), 369–392.

Shen, M., Zhang, Y., Zhu, Y., Song, B., Zeng, G., Hu, D., Wen, X., Ren, X., 2019. Recent advances in toxicological research of nanoplastics in the environment: a review. Environ. Pollut. 252, 511–521.

Stapleton, P.A., 2019. Toxicological considerations of nano-sized plastics. AIMS Environ. Sci. 6 (5), 367–378.

The International Silkworm Genome Consortium, 2008. The genome of a lepidopteran model insect, the silkworm Bombyx mori. Insect Biochemistry and Molecular Biology 38 (12), 1036–1045.

Wang, W., Ge, J., Yu, X., Li, H., 2020. Environmental fate and impacts of microplastics in soil ecosystems: progress and perspective. Sci. Total Environ. 134841.

Watts, A.J.R., Lewis, C., Goodhead, R.M., Beckett, S.J., Moger, J., Tyler, C.R., Galloway, T.S., 2014. Uptake and retention of microplastics by the shore crab *Carcinus maenas*. Environ. Sci. Technol. 48 (15), 8823–8830.

Wigglesworth, V.B., 2003. The Principles of Insect Physiology. John Wiley Sons, New York.

Xia, Q., Cheng, D., Duan, J., Wang, G., Cheng, T., Zha, X., Liu, C., Zhao, P., Dai, F., Zhang, Z., He, N., Zhang, L., Xiang, Z., 2007. Microarray-based gene expression profiles in multiple tissues of the domesticated silkworm, *Bombyx mori*. Genome Biol 8, R162.

Zhang, Y., Gao, T., Kang, S., Sillanpää, M., 2019. Importance of atmospheric transport for microplastics deposited in remote areas. Environ. Pollut. 254 https://doi.org/10.1016/j.envpol.2019.07.121, 113953.

Zhu, B.K., Fang, Y.M., Zhu, D., Christie, P., Ke, X., Zhu, Y.G., 2018. Exposure to nanoplastics disturbs the gut microbiome in the soil oligochaete *Enchytraeus crypticus*. Environ. Pollut. 239, 408–415.

Supporting Information

1. Materials and methods

Table S1. Chemical parameters of PNPs were assessed with the Malvern Zetasizer Nano ZS instrument (Malvern instruments, UK) in the exposure medium. Data referred to a concentration of 1 mg L^{-1}. Size distribution is reported as average ± standard deviation of 3 measurements.

PNPs	Zeta potential	Size distribution by DLS
Non fluo	*-36.27 ± 0.67 mV*	*716.14 ± 23.14 nm*
Fluo	*0.13 mV*	*533.17 ± 17.81 nm*

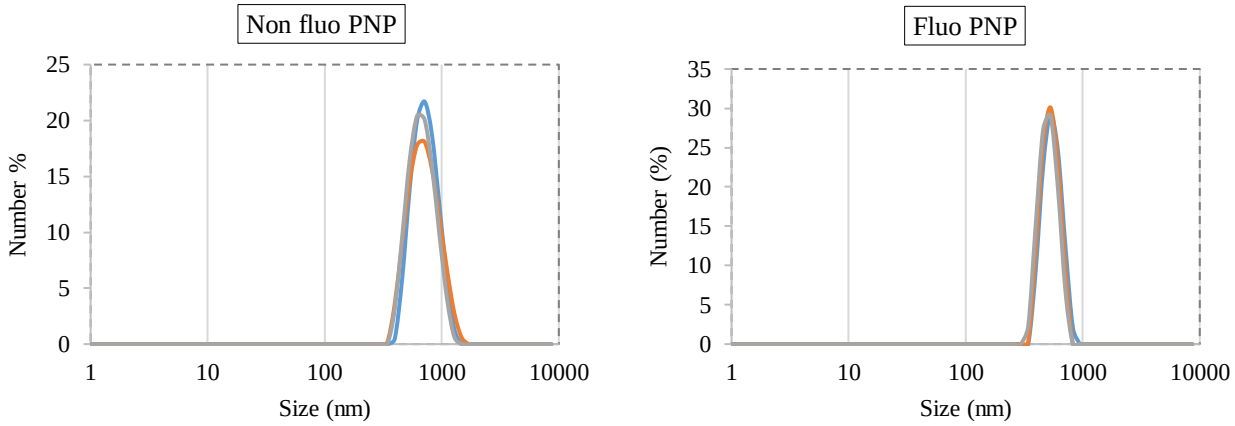

Fig. S1. DLS profile of PNP, non-fluorescent and fluorescent. Size distribution of 3 measurements.

Table S2. Acquisition details of confocal microscopy images.

Nikon A1plus	Emission wavelenght	Excitation wavelenght	Pinhole radius	Channel Modality
DAPI (blue)	*420-460 nm*	*409.1 nm*	*16.6*	*Laser Scan Confocal*
FITC (green)	*680-720 nm*	*487.5 nm*	*16.6*	*Laser Scan Confocal*
Cy5.5 (red)	*691-710 nm*	*635.5 nm*	*16.6*	*Laser Scan Confocal*
TD (bright field)	*N/A*	*N/A*	*16.6*	*Laser Scan Confocal*

3.3 The role of plastic particles as carrier for chemicals

The last and most important step of the project was focused on the evaluation of the risk associated to the role of plastic particles as carrier of environmental pollutants. The possible transfer of hazardous chemicals by plastic ingestion was evaluated by the quantification of the adsorbed concentration of TCS, a commonly used antibacterial agent, whose toxicity was preliminary tested on zebrafish embryos (3.3.1). Therefore, we contaminated a commercial PS powder with TCS and we performed a long-term exposure to TCS, virgin and TCS-contaminated nanobeads using larvae of *D. rerio* as vertebrate experimental model (3.3.2). After 7 days, the uptake of plastic was assessed with advanced microscopy techniques, and sub-individual and individual effects were investigated in treated groups, respect to control. Moreover, to investigate if different treatments play a different role in the modulation of zebrafish protein expression, we applied a functional proteomics analysis.

PUBLICATION LIST:

3.3.1 Parenti, C.C., Ghilardi, A., Della Torre, C., Mandelli, M., Magni, S., Del Giacco, L., Binelli, A., 2019. **Environmental concentrations of triclosan activate cellular defence mechanism and generate cytotoxicity on zebrafish (*Danio rerio*) embryos**. Science of the Total Environment 650, 1752-1758.

3.3.2 Parenti, C.C., Magni, S., Ghilardi, A., Caorsi, G., Della Torre, C., Del Giacco, L., Binelli, A., 2020. **Does triclosan adsorption on polystyrene nanoplastics modify the toxicity of single contaminants?**. Environmental Science: Nano, DOI: 10.1039/d0en00961j.

Science of the Total Environment 650 (2019) 1752–1758

Contents lists available at ScienceDirect

Science of the Total Environment

journal homepage: www.elsevier.com/locate/scitotenv

Environmental concentrations of triclosan activate cellular defence mechanism and generate cytotoxicity on zebrafish (*Danio rerio*) embryos

Camilla Carla Parenti *, Anna Ghilardi, Camilla Della Torre, Matteo Mandelli, Stefano Magni, Luca Del Giacco, Andrea Binelli *

Department of Biosciences, University of Milan, Via Celoria 26, 20133 Milan, Italy

HIGHLIGHTS

- TCS exposure induces P-gp efflux functionality and oxidative stress enzymes.
- Embryos cellular defence system prevents the occurrence of oxidative damage by TCS.
- High levels of cell necrosis underline TCS cytotoxicity potential.
- TCS occurrence in the aquatic environment poses an actual risk for wildlife.

GRAPHICAL ABSTRACT

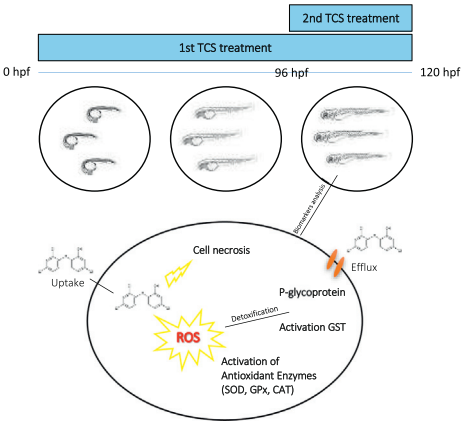

ARTICLE INFO

Article history:
Received 8 June 2018
Received in revised form 20 September 2018
Accepted 21 September 2018
Available online 26 September 2018

Editor: Damia Barcelo

Keywords:
Triclosan
Danio rerio
Oxidative stress
Biomarkers
Genotoxicity
Cytotoxicity

ABSTRACT

Triclosan (TCS, 5 chloro 2 (2,4 dichlorophenoxy) phenol) is becoming a major surface waters pollutant worldwide at concentrations ranging from ng L^{-1} to μg L^{-1}. Up to now, the adverse effects on aquatic organisms have been investigated at concentrations higher than the environmental ones, and the pathways underlying the observed toxicity are still not completely understood. Therefore, the aim of this study was to investigate the toxic effects of TCS at environmental concentrations on zebrafish embryos up to 120 hours post fertilization (hpf). The experimental design was planned considering both the quantity and the exposure time for the effects on the embryos, exposing them to two different concentrations (0.1 μg L^{-1}, 1 μg L^{-1}) of TCS, for 24 h (from 96 to 120 hpf) and for 120 h (from 0 to 120 hpf). A suite of biomarkers was applied to measure the induction of embryos defence system, the possible increase of oxidative stress and the DNA damage. We measured the activity of glutathione *S* transferase (GST), P glycoprotein efflux and ethoxyresorufin *o* deethylase (EROD), the level of ROS, the oxidative damage through the Protein Carbonyl Content (PCC) and the activity of antioxidant enzymes. The genetic damage was evaluated through DNA Diffusion Assay, Micronucleus test (MN test), and Comet test. The results showed a clear response of embryos defence mechanism, through the induction of P-gp efflux functionality and the activity of detoxifying/antioxidant enzymes, preventing the onset of oxidative damage. Moreover, the significant increase of cell necrosis highlighted a strong cytotoxic potential for TCS. The overall results obtained with environmental concentrations and both exposure time, underline the critical risk associated to the presence of TCS in the aquatic environment.

* Corresponding authors.
E-mail addresses: camilla.parenti@unimi.it (C.C. Parenti), andrea.binelli@unimi.it (A. Binelli).

https://doi.org/10.1016/j.scitotenv.2018.09.283
0048-9697/

1. Introduction

Triclosan (TCS, 5 chloro 2 (2,4 dichlorophenoxy) phenol) is an emerging contaminant included as antimicrobial agent in several personal care products (PCPs), such as soaps, deodorants, toothpastes, cosmetics and laundry detergents (Dann and Hontela, 2011), with a typical range of 0.1–0.3% of products weight (Montaseri and Forbes, 2016). The ubiquitous use of these products has drawn the attention of the research community, due to the well documented TCS toxicity in mammalians models, including irritation of eyes and skin, allergies, detrimental effects on development and reproduction, weakening of the immune system, inhibition of muscle function and genotoxicity (Barbaud et al., 2005; Binelli et al., 2009; Dann and Hontela, 2011; Cherednichenko et al., 2012; Savage et al., 2012; Halden, 2014). High levels of TCS were recently found in human urine, blood sample, liver, adipose tissue, brain and breast milk (Ruszkiewicz et al., 2017) and its structure is similar to the polychlorinated phenoxyphenols that, under oxidizing conditions, cyclize to other toxic byproducts, which present very harmful effects on human health (Solá-Gutiérrez et al., 2018). Furthermore, a recent proteomic study (Li et al., 2018) revealed a distinct evidence of the potential impact of TCS on human metabolic pathways.

Nowadays, there is growing awareness for TCS environmental implications so that the marketing of over-the-counter antibacterial soaps and body washes containing TCS was banned in the United States since 2016 (FDA, 2016), while the European Union (EU, 2016) has disapproved the use of TCS in human hygiene biocidal products (product-type 1). Nevertheless, the occurrence of TCS in the aquatic ecosystems is a worldwide issue, being commonly detected in surface waters (lake/river/streams with known input of raw wastewaters) with concentrations ranging from 1.4 to 40,000 ng L^{-1}, and in sea water from <0.001 to 100 ng L^{-1} (Dhillon et al., 2015). There is a scientific evidence of TCS emission from Wastewater Treatment Plants (WWTPs) into the aquatic environment, due to their partial inability to remove it, with detected concentrations ranging from 10 to 2,210 ng L^{-1} in European WWTP effluents (Bedoux et al., 2012). TCS and mostly its methylated degradation product (methyl triclosan) are lipophilic and volatile (Wang and Kelly, 2017), causing a high tendency for bioaccumulation in aquatic organisms, which uptake them directly from food or water with bioconcentration factor (BCF) of 2.7–90 (Dhillon et al., 2015). Detected concentrations of TCS are reported in different wild organisms, such as algae and invertebrates, with concentrations up to 400 μg/kg (Coogan and La Point, 2008), and fish, with values up to 300 ng/g wet weight (ww) in muscle tissue (Yao et al., 2018).

The chronic and acute toxicity of TCS has been demonstrated in several aquatic models, which include green and blue algae (Orvos et al., 2002) and benthic invertebrates (Dussault et al., 2008), showing effects on biomass and growth rate, and generating oxidative stress and genotoxicity (Binelli et al., 2009; Riva et al., 2012; Martínez-Paz, 2018). In fish, TCS impacts equilibrium, swimming, spinal curvature and quiescence (Orvos et al., 2002; Ishibashi et al., 2004), as well as several studies showed the endocrine disruption effect of TCS, as demonstrated for the Japanese medaka *Oryzias latipes* (Ishibashi et al., 2004; Horie et al., 2018). Some recent studies performed on zebrafish *Danio rerio* embryos highlighted that TCS caused heart edema and slow heartbeat (Zhu et al., 2018), delayed hatching and increased mortality (Falisse et al., 2017), impaired lipid metabolism (Ho et al., 2016), and induced hepatotoxicity (Haggard et al., 2016) at concentrations up to 1.25 mg L^{-1}. Furthermore, Muth-Köhne et al. (2012) demonstrated that exposure to 3 μM TCS (870 μg L^{-1}) may have neurotoxic effects, delaying the development of zebrafish embryos motor neurons. Such results underline the TCS toxic potential for aquatic species, but do not represent a realistic scenario, since exposure concentrations are higher than those detected in aquatic ecosystems.

This study aimed to evaluate the environmental impact of TCS on aquatic ecosystem, assessing its toxic effects at environmentally relevant concentrations, and contribute to a better understanding of the response of the organism detoxification systems to TCS exposure, using zebrafish embryos as experimental model. Embryos were exposed to two environmental concentrations (0.1 and 1 μg L^{-1}) of TCS for two different exposure time, from 0 to 120 hpf and from 96 to 120 hpf, to improve the understanding on cellular detoxification mechanisms and to investigate the temporal variation of chronic toxicity in terms of oxidative stress and cyto-genotoxicity. Actually, we used a biomarker suite based on the measure of reactive oxygen species (ROS) production and the antioxidant enzymes' activity, namely catalase (CAT), superoxide dismutase (SOD) and glutathione peroxidase (GP_x). We also measured the induction of detoxification activities by the glutathione *S* transferase (GST), P glycoprotein and ethoxyresorufin *o* deethylase (EROD), as well as the potential oxidative damage through the Protein Carbonyl Content (PCC) and cyto-genotoxic effects through the DNA Diffusion Assay, Micronucleus test (MN test) and Comet test.

2. Materials and methods

2.1. Preparation of TCS solutions

Triclosan (TCS, CAS 3380-34-5, purity 97%) was purchased from Sigma-Aldrich (Milan, Italy). Firstly, a stock solution of TCS, 1 g L^{-1} in dimethyl sulfoxide (DMSO), was prepared and stored at 4 °C, while two TCS working solutions were prepared successively diluting the stock solution in ultrapure water at 0.1 mg L^{-1} and 1 mg L^{-1}, respectively. The maximum percentage of DMSO was lower than 0.0001%, and not produces any changes on hemocyte viability, DNA damage or enzyme activity (Parolini et al., 2011). These working solutions were then properly diluted to reach the selected exposure concentrations of 0.1 μg L^{-1} and 1 μg L^{-1}, which fall in the range of the current environmental freshwater levels of TCS (Ho et al., 2016; Zhou et al., 2017). These concentrations also fall within the Predicted No Effect Concentration (PNEC) range (70 ng L^{-1} to 1,550 ng L^{-1}) reported by Capdevielle et al. (2007), which made a Species Sensitivity Distribution (SSD) analysis based on pre-existing chronic toxicity data of TCS for 14 different aquatic species.

2.2. Zebrafish maintenance and embryos exposure

Adult zebrafish of the AB strain are raised in the facility of the Department of Biosciences, University of Milan, where they are maintained in tanks into a thermostatic chamber (28 °C) with 14-h light/10-h dark cycle. The facility follows Italian laws, rules and regulations (Legislative Decree No. 116/92), as confirmed by the authorization issued by the municipality of Milan (PG 384983/2013).

Different groups of embryos were collected by means of natural spawning, following the procedure for maximal embryo production described by Westerfield (2007). Control embryos were maintained in zebrafish water (Instant Ocean, 0.1% methylene blue), while others were exposed to TCS (0.1 μg L^{-1} and 1 μg L^{-1}) dissolved in zebrafish water.

We planned two different exposures in order to evaluate the potential temporal variations, one from 0 hpf to 120 hpf (120 h of exposure) and the other one from 96 hpf to 120 hpf (24 h of exposure). Biochemical analysis exposures were performed in 90 × 15 mm petri dish with a maximum of 70 embryos per petri and two replicates per experimental group, adding 25 mL of the appropriate TCS working solution to each treatment group and 25 mL of zebrafish water to control groups (Fig. S1a). ROS level and cyto-genotoxic biomarkers were performed in multi-well plates with 12 and 5 embryos per well, respectively, and three replicates per experimental group, adding 2 mL of the appropriate TCS working solution to each treatment group and 2 mL of zebrafish water to control groups (Fig. S1b). Both exposures (120 h and 24 h) proceeded at 28 °C under semi-static conditions, replacing the exposure

medium every 24 h at the longer exposure. Embryo mortality and effects on morphology, developmental delay and behavioural alterations (occurrence of edema, weak or no pigmentation, malformed or underdeveloped embryos, deformed spine and no or malformed fins) were systematically assessed during the experiment, and no significant effects were observed at chosen TCS concentrations. At the end of both exposures, embryos were processed immediately for the cyto-genotoxicity endpoints or collected and stored at −80 °C until further analysis.

2.3. Biochemical analysis

Pools of 60 embryos from each exposure was collected and homogenized, using a motorized pestle mixer, in 800 μL of 100 mM phosphate buffer (pH = 7.4), with 100 mM KCl, 1 mM EDTA, 100 mM dithiothreitol (DTT), and protease inhibitors (1:100 v/v). The homogenates were centrifuged at 12,000 r.p.m. for 10 min at 4 °C. The supernatants were collected, pooled together and immediately used for the measure of glutathione *S* transferase (GST), catalase (CAT), glutathione peroxidase (GPx) and superoxide dismutase (SOD) activities in triplicate, using a 6715 UV/Vis spectrophotometer (Jenway, USA), following the protocol described by Della Torre et al. (2017). ROS production was assessed following the method described by Parolini et al. (2017), using dichlorofluorescein-diacetate (DCFH-DA). Briefly, 12 embryos from each experimental group were washed with PBS and homogenized as described above. The homogenates were centrifuged at 15,000 r.p.m. for 20 min at 4 °C and then twenty microliters of the homogenate were added to a 96-well plate and incubated for 5 min at 37 °C. We added 100 μL of PBS and 8.3 μL of DCFH-DA (10 mg/mL in DMSO) in each well before incubated the plate 30 min at 37 °C. At the end, we measured the fluorescence intensity by the EnSight™ multimode plate reader (PerkinElmer) at λ_{ex} 485 nm and λ_{em} 530 nm. The ROS concentration was expressed in fluorescence units (FU) mg protein^{-1}. Protein carbonyl content (PCC) was measured forming protein hydrazone derivatives with 2,4 dinitrophenylhydrazine (DNPH) (10 mM in 2 M HCl). Proteins were then precipitated and the pellet was washed and resuspended in guanidine hydrochloride (6 M). The absorbance of protein-hydrazone was measured spectrophotometrically at 375 nm (Della Torre et al., 2018). A pool of about 30 embryos from each exposure was used for the ethoxyresorufin *o* deethylase (EROD) activity measure, which followed the same procedure described above. The EROD assay was performed using the EnSight™ multimode plate reader (PerkinElmer) at λ_{ex} 535 nm and λ_{em} 590 nm and temperature of 37 °C. The incubation mixture contained zebrafish embryo homogenates (4 replicates) in 50 mM Tris buffer pH 7.4 with BSA (5.32 mg/mL in 50 mM Tris) and NADPH (6.7 mM in 50 mM Tris), and the reaction substrate ethoxyresorufin (100 μM in 15% MeOH). Standard concentrations of resorufin, ranging from 0 to 0.1 μM, were made by diluting the stock solution in 15% MeOH. EROD activity was calculated from the relative fluorescence units as the product of resorufin, quantified with the resorufin standard curve ($R^2 = 0.99$), in pmol min^{-1} mg prot^{-1}. All analyses were normalized on the total protein content of each sample (Table S1) measured according to Bradford method using bovine serum albumin as standard (Bradford, 1976).

2.4. Quantification of P glycoprotein activity

The efflux functionality of the P glycoprotein (P-gp) was measured according to the procedure described by Fischer et al. (2013), using Rhodamine B (RhB) as fluorescent substrate. A pool of 30 embryos per treatment was collected from two independent exposures and incubated for 90 min in zebrafish water with 1 μM RhB. For quantification of RhB uptake, embryos were homogenized in 350 μL lysis buffer (pH = 7.4) containing 10 mM KCl, 1.5 mM $MgCl_2$, 10 mM Tris, and centrifuged for 10 min at 12000 × *g*. One hundred microliters of the supernatant (3 replicates for each treatment) were transferred to a multi-well plate and the RhB fluorescence was measured using the EnSight™ multimode plate reader (PerkinElmer) at λ_{ex} 530 nm and λ_{em} 595 nm. The amount of RhB was quantified with a RhB standard curve, ranging from 0 to 0.1 μM ($R^2 = 0.99$).

2.5. Cyto-genotoxicity

Biomarkers of cyto-genotoxicity were assessed on cells obtained by mechanical dissociation as described in Parolini et al. (2017), from a pool of five embryos collected from three independent exposures (three pool per treatment). Cells viability was evaluated by Trypan Blue dye exclusion method. The Comet assay (SCGE assay) was performed following the protocol of Kosmehl et al. (2008). One hundred cells per slide (6 slides per each exposure) were analysed with the Comet Score® image analysis software. DNA damage was determined by the percentage of DNA observed in the comet tail and the ratio between the migration length and diameter of the comet head (LDR). The same diffusion assay was used to evaluate the percentage of apoptotic/necrotic cells. Slides were labelled with DAPI in order to observe DNA with a fluorescence microscope (Leica DM2000). One hundred cells per slide (6 slides per each exposure) were counted, among which apoptotic cells were recognized as a dense central zone surrounded by a large DNA halo, while necrotic cells were visualized just as an appearance of a light DNA halo. The frequency of micronuclei (MN) was evaluated on 400 cells per slide (n = 9; 3 slides per pool), as reported in our previous studies (Magni et al., 2016, 2017).

2.6. Statistical analysis

Data normality and homoscedasticity were verified using Shapiro-Wilk and Levene tests, respectively. The differences between treatments and control were identified performing a one-way analysis of variance (one-way ANOVA), where treatment (control, TCS 0.1 μg L^{-1} and TCS 1 μg L^{-1}) was the predictor factor, and each biomarker was a dependent variable. For both exposure times, separately, the differences between treated and control were evaluated using Duncan's Multiple Range *post-hoc* Test (DMRT), taking $p < 0.05$ as significant cut-off. To observe the eventual covariation between tested biomarkers, we performed the Pearson's correlation considering all end-points. Statistical analyses were carried out using STATISTICA 7.0 software package.

3. Results and discussion

Cellular response to TCS uptake was primarily evaluated through the quantification of P-gp activity, which is an efflux transporter protein identified in fish and involved in detoxification mechanisms, preventing the entrance of xenobiotics or eliminating them from cells (Jackson and Kennedy, 2017). We observed a significantly ($F_{2,9} = 75.05$ for 24 h and $F_{2,9} = 93.39$ for 120 h; $p < 0.01$) lower RhB accumulation in all treatment groups compared to the level of RhB measured in controls (Fig. 1a), indicating an induction of P-gp efflux functionality, probably related to active elimination of TCS or its by-products from cells. Another important role in the detoxifying mechanism is due to some isoforms of the cytochrome P450 superfamily, such as EROD, which catalyse the transformation of several planar compounds upon the aryl hydrocarbon receptor mediated regulation (Van Der Oost et al., 2003). Our results showed that TCS was not able to induce significant EROD activity for both tested concentrations at the development stages analysed (Fig. 1b). On the other hand, the involvement of EROD activity in TCS detoxification in aquatic species is still controversial, as recently described by Zhou et al. (2017), who showed the inhibition of EROD upon exposure to levels of TCS up to 0.7 mg L^{-1}. Another hypothesis to explain the lack of EROD modulation is related to the low inducibility of cytochrome P4501A (CYP1A) in developing embryos. Indeed, a recent study in which embryos (96 hpf) were exposed to different concentrations of the CYP1A inducer benzo(α)pyrene (B(α)P) showed only a low

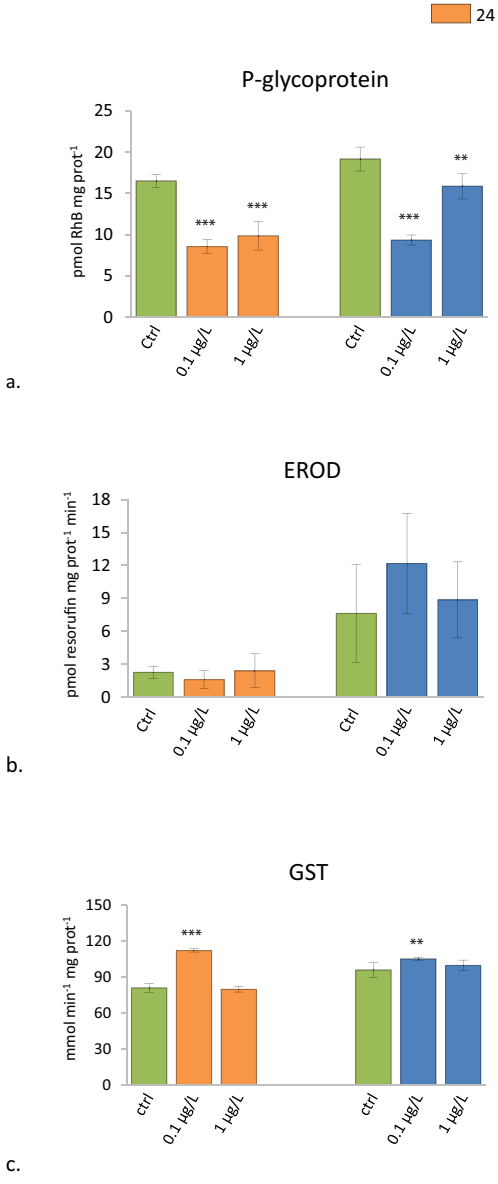

Fig. 1. Activity of P-glycoprotein (a), EROD (b) and GST (c) in zebrafish embryos exposed for 24 h and 120 h to TCS at 0.1 μg L^{-1} and 1 μg L^{-1}, compared to relative control (mean ± SD). One-way ANOVA, Duncan's Multiple Range post-hoc test, **p < 0.01, ***p < 0.001.

increase of *cyp1a* gene transcription at the concentration of 20 μg L^{-1} (Della Torre et al., 2017). Moreover, a previous study by Saad et al. (2016), which aimed to determine the biotransformation potential of zebrafish embryos during their critical window for teratogens, observed a very low CYP1A activity during organogenesis. Our results seem to suggest that other enzymes (for instance CYP3A) could be involved in the first phase of TCS metabolism/detoxification. The assessment of detoxification activity was also evaluated through the analysis of phase II detoxifying enzyme GST, which showed the same trend at the two different exposure times (Fig. 1c). The induction of GST activity resulted significantly higher at the low TCS concentration ($F_{2,9} = 91.49$ and $p < 0.001$ at 24 h; $F_{2,9} = 6.55$ and $p < 0.01$ at 120 h). Our results are in line with findings of Oliveira et al. (2009), who reported an increase of GST activity in zebrafish embryos exposed to TCS (0.25–0.35 mg L^{-1}), underlying the key role of GST in the detoxification response to TCS. The trend observed for GST was also obtained for the activities of other antioxidant enzymes (Fig. 2a–c), suggesting the induction of embryos antioxidant protective response upon TCS exposure.

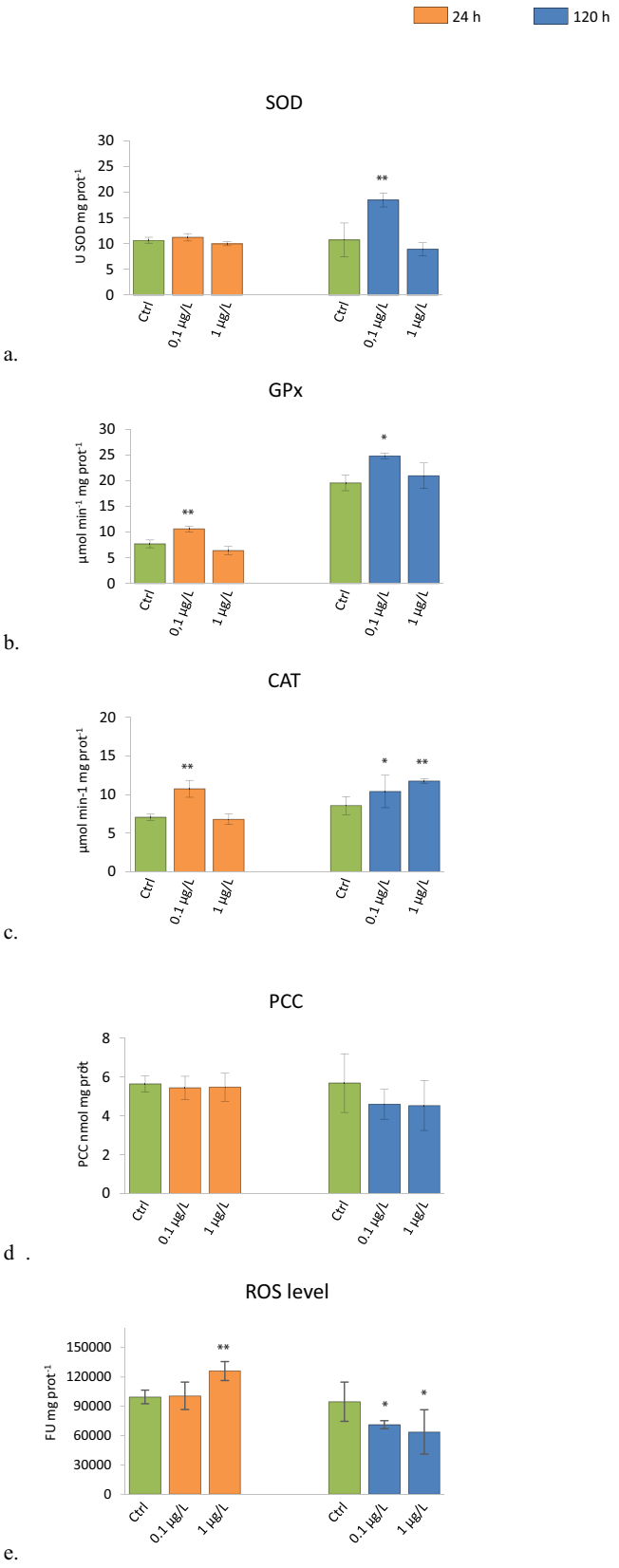

Fig. 2. Activity levels of antioxidant enzymes (SOD, GPx and CAT) in zebrafish embryos exposed for 24 h and 120 h to TCS at 0.1 μg L^{-1} and 1 μg L^{-1}, compared to relative controls (mean ± SD). One-way ANOVA, Duncan's Multiple Range post-hoc test, *p < 0.05, **p < 0.01.

Table 1
Biomarkers of cyto-genotoxicity in zebrafish exposed for 24 h and 120 h to TCS at 0.1 μg L^{-1} and 1 μg L^{-1} (mean ± SD).

Treatment	Cell viability (%)	DNA tail (%)	LDR (%)	Necrosis (%)	Micronuclei (‰)
24 h					
ctrl	96.94 ± 0.52	1.92 ± 0.49	1.03 ± 0.01	2.37 ± 0.93	3.61 ± 1.16
0.1 μg L^{-1}	97.18 ± 1.27	1.87 ± 0.39	1.03 ± 0.00	1.91 ± 0.71	4.45 ± 0.73
1 μg L^{-1}	95.19 ± 3.77	1.55 ± 0.49	1.03 ± 0.01	5.76 ± 1.22***	5.40 ± 2.49
120 h					
ctrl	98.70 ± 1.33	2.07 ± 0.20	1.03 ± 0.00	0.90 ± 0.74	5.03 ± 2.78
0.1 μg L^{-1}	97.16 ± 2.66	1.43 ± 0.39*	1.02 ± 0.01	3.61 ± 1.22*	7.25 ± 2.04
1 μg L^{-1}	94.69 ± 2.36*	2.80 ± 0.34**	1.04 ± 0.00	12.83 ± 2.28***	9.51 ± 7.39

One-way ANOVA, Duncan's Multiple Range post-hoc test.
* $p < 0.05$.
** $p < 0.01$.
*** $p < 0.001$.

Specifically, during the 120 h exposure, SOD was significantly induced at 0.1 μg L^{-1} TCS ($F_{2,9} = 10.895$; $p < 0.01$), while no changes in enzymatic activity were noticed for the shorter exposure time (Fig. 2a). GPx activity was again significantly induced at lower TCS concentration during both exposure times ($p < 0.01$ and $p < 0.05$, respectively; Fig. 2b). Concerning CAT, this enzyme showed a significantly higher activity at lower TCS dose during the 24 h exposure ($F_{2,9} = 16.21$; $p < 0.01$; Fig. 2c), while after the 120 h at both tested concentrations ($F_{2,9} = 7.8609$; $p < 0.05$ and $p < 0.01$, respectively; Fig. 2c). The absence of a significant modulation of detoxifying/antioxidant enzymes activity after 24 h of exposure can explain the significant higher level of ROS measured at the higher TCS concentration, respect to control ($F_{2,9} = 12.07$; $p < 0.01$; Fig. 2e). In the short exposure time, the first cellular defence mechanism (P-gp efflux functionality) is significant activated, while the second line of defence against ROS did not have enough time to be activated. On the contrary, after the longer exposure time, the antioxidant enzyme activities are induced to counteract the formation of ROS and restore the cellular homeostatic condition, as shown in Fig. 2e, where ROS levels are even below the control (120 h exposure). In summary, our results pointed out the ability of embryos cellular defence system to prevent the occurrence of oxidative damage caused by TCS exposure, as it is confirmed by PCC analysis, that did not show any significant oxidative damage at all exposure conditions (Fig. 2d).

Concerning cyto-genotoxic end-points, we verified that all treatment conditions showed a cells viability higher than 90% (Table 1), a percentage well above the minimum required to perform genotoxicity tests, according to the IV International Workshop on Genotoxicity Test Procedures (Kirkland et al., 2007). Nevertheless, a significant decrease of cells viability was recorded in TCS 1 μg L^{-1} treatment after 120 h exposure ($F_{2,9} = 5.11$; $p < 0.05$). This result can be correlated to the observed percentage of necrotic cells, which was significantly different from controls at the higher concentration (Table 1) at both exposure times ($F_{2,9} = 21.733$ for 24 h and $F_{2,9} = 92.238$ for 120 h; $p < 0.001$). Moreover, we also noticed a remarkable increase of necrosis at 0.1 μg L^{-1} TCS ($F_{2,9} = 92.24$; $p < 0.05$) after 120 h. The induction of cytotoxic effects by TCS was expected, since it has antiseptic properties causing cell lysis by lipid, RNA and protein synthesis inhibition, and membrane perturbations (Schweizer, 2001). The biomarkers of genotoxicity (SCGE assay and MN test) revealed that exposures to environmental concentrations of TCS induced only low genotoxic effects in zebrafish embryos. The primary genetic damage measured by the SCGE assay was evaluated both through the percentage of DNA tail and the LDR. Although both of them mostly remained within the physiological range, the percentage of DNA tail showed a significant ($F_{2,9} = 29.32$; $p < 0.01$) frequency of DNA damage at the end of the 120 h exposure, revealing a slight primary genotoxic effect caused by the higher TCS concentration (Table 1). The mild level of genotoxicity

Table 2
Matrix of Pearson's correlation, showing r and p-level, for all biomarkers examined in zebrafish exposed for 24 h and 120 h to TCS at 0.1 μg L^{-1} and 1 μg L^{-1}.

	GST	CAT	GPx	SOD	P-gp	EROD	MN	VIAB	NECRO	COMET	PCC	ROS
GST	1.0000	**0.8028**	**0.6000**	**0.4428**	−0.3059	0.4078	0.2069	0.1975	0.0093	0.1135	0.3700	**−0.5425**
		p = 0.000	**p = 0.003**	**p = 0.039**	p = 0.166	p = 0.060	p = 0.355	p = 0.378	p = 0.967	p = 0.615	p = 0.090	**p = 0.009**
CAT		1.0000	**0.5988**	0.2084	−0.2091	0.3875	0.3761	0.0223	0.3072	0.2782	−0.1322	**−0.4991**
			p = 0.003	p = 0.352	p = 0.350	p = 0.075	p = 0.085	p = 0.921	p = 0.164	p = 0.21	p = 0.557	**p = 0.018**
GPx			1.0000	**0.5134**	0.1423	**0.8040**	0.4211	0.1339	0.2523	0.2642	−0.4003	**−0.7595**
				p = 0.015	p = 0.528	**p = 0.000**	p = 0.051	p = 0.552	p = 0.257	p = 0.235	p = 0.065	**p = 0.000**
SOD				1.0000	**−0.4429**	**0.4839**	0.1515	0.1527	−0.1501	−0.3685	**−0.6590**	−0.3667
					p = 0.039	**p = 0.023**	p = 0.501	p = 0.498	p = 0.505	p = 0.092	**p = 0.001**	p = 0.093
P-gp					1.0000	0.0218	−0.2057	0.2084	−0.0226	**0.4904**	0.2748	−0.1732
						p = 0.923	p = 0.358	p = 0.352	p = 0.920	**p = 0.02**	p = 0.216	p = 0.441
EROD						1.0000	**0.4904**	−0.0211	0.1501	0.1516	−0.3429	**−0.6262**
							p = 0.020	p = 0.926	p = 0.505	p = 0.501	p = 0.118	**p = 0.002**
MN							1.0000	0.0694	0.0736	−0.2301	0.1678	−0.2041
								p = 0.759	p = 0.745	p = 0.303	p = 0.455	p = 0.362
VIAB								1.0000	**−0.6239**	−0.0537	0.2747	0.0962
									p = 0.002	p = 0.812	p = 0.216	p = 0.0670
NECRO									1.0000	**0.6020**	−0.3295	−0.3709
										p = 0.003	p = 0.134	p = 0.089
COMET										1.0000	−0.0553	−0.3663
											p = 0.807	p = 0.094
PCC											1.0000	**0.5256**
												p = 0.012

Significant correlations ($p < 0.05$) are reported in bold.

was confirmed by the lack of chromosomal damage, highlighted by the MN test, that showed no significant differences between treatments and control during both exposure tests (Table 1). This result seems to be in contrast with the high MN frequency observed in zebra mussel specimens exposed to TCS (Binelli et al., 2009), although the previous studies tested concentrations were at least three times higher than those used in this study. The low genetic damage observed might be correlated to embryos high resistance to the genotoxic injury, as well to the short time of exposure, in agreement with a previous study (Della Torre et al., 2017) in which zebrafish embryos exposed to the carcinogen B(α)P up to 96 hpf did not show any significant induction of primary DNA damage and occurrence of MN. The overall results obtained by both biochemical and cyto-genotoxicity analyses suggest that the observed cyto-genotoxic effects were produced directly by TCS and not indirectly related to an increase of oxidative stress.

Finally, all the investigated endpoints were combined together to evaluate their relationship through the Pearson's correlation statistic test (Table 2). The positive significant correlation between GST and antioxidant enzymes suggests that also this enzyme is actively involved in preventing oxidative stress, as also supported by the negative significant correlation with ROS level. These results are similar to those reported for the catfish *Pelteobagrus fulvidraco* (Ku et al., 2014), in which TCS exposure induced a significant increase of CAT activity, and for zebra mussel that showed a rise of GST and CAT activities in response to TCS (Binelli et al., 2011). The positive correlation highlighted between SOD and GPx (Table 2; Fig. S2), but not with CAT, confirmed the slight oxidative stress generated by environmental concentrations of TCS. Indeed, GPx is more sensitive to low H_2O_2 concentrations generated by SOD, while CAT is induced only by high levels of this oxidative by-product (Powers and Lennon, 1999). Lastly, the cell viability was negatively correlated ($p < 0.01$) with necrosis suggesting the independent cytotoxic effect of environmental levels of TCS on zebrafish embryos.

4. Conclusions

This study is the first attempt to investigate the potential toxicity of TCS administered at environmental concentrations on zebrafish embryos. TCS exposure elicited the induction of oxidative stress response in embryos, preventing the occurrence of oxidative damage. Though, the pollutant generated a significant cytotoxicity, which subsequently drives to an increase of cellular necrosis.

Overall results highlight the concern related to the presence of TCS in the aquatic environment, suggesting the need to assess the effective exposure of aquatic wildlife to this pollutant. Further studies focusing on understanding the toxicity mechanisms of TCS on other aquatic models and including the investigation of other endpoints (i.e. transcription levels of stress related genes, proteomics) at environmental concentrations are also recommended.

Appendix A. Supplementary data

Supplementary data to this article can be found online at https://doi.org/10.1016/j.scitotenv.2018.09.283.

References

Barbaud, A., Vigan, M., Delrous, J.L., Assier, H., Avenel-Audran, M., Collet, E., Dehlemmes, A., Dutartre, H., Geraut, C., Girardin, P., Le Coz, C., Milpied-Homsi, B., Nassif, A., Pons-Guiraud, A., Raison-Peyron, N., Membres du Groupe du, R, 2005. Contact allergy to antiseptics: 75 cases analyzed by the dermato-allergovigilance network (Revidal). Ann. Dermatol. Venereol. 132 (12 Pt. 1), 962–965.

Bedoux, G., Roig, B., Thomas, O., Dupont, V., Le Bot, B., 2012. Occurrence and toxicity of antimicrobial triclosan and by-products in the environment. Environ. Sci. Pollut. Res. 19, 1044–1065.

Binelli, A., Cogni, D., Parolini, M., Riva, C., Provini, A., 2009. In vivo experiments for the evaluation of genotoxic and cytotoxic effects of triclosan in zebra mussel hemocytes. Aquat. Toxicol. 91, 238–244.

Binelli, A., Parolini, M., Pedriali, A., Provini, A., 2011. Antioxidant activity in the zebra mussel (*Dreissena polymorpha*) in response to triclosan exposure. Water Air Soil Pollut. 217, 421–430.

Bradford, M.M., 1976. A rapid and sensitive method for the quantification of microgram quantities of protein using the principle of protein-dye binding. Anal. Biochem. 72, 248–254.

Capdevielle, M., Van Egmond, R., Whelan, M., Versteeg, D., Hofmann-Kamensky, M., Inauen, J., Cunningham, V., Woltering, D., 2007. Consideration of exposure and species sensitivity of Triclosan in the freshwater environment. Integr. Environ. Assess. Manag. 4 (1), 15–23.

Cherednichenko, G., Zhang, R., Bannister, R.A., Timofeyev, V., Li, N., Fritsch, E.B., Feng, W., Barrientos, G.C., Schebb, N.H., Hammock, B.D., Beam, K.G., Chiamvimonvat, N., Pessah, I.N., 2012. Triclosan impairs excitation-contraction coupling and Ca^{2+} dynamics in striated muscle. Proc. Natl. Acad. Sci. U. S. A. 109 (35), 14158–14163.

Coogan, M.A., La Point, T.W., 2008. Snail bioaccumulation of triclocarban, triclosan and methyltriclosan in a North Texas, USA, stream affected by wastewater treatment plant runoff. Environ. Toxicol. Chem. 27 (8), 1788–1793.

Dann, A.B., Hontela, A., 2011. Triclosan: environmental exposure, toxicity and mechanisms of action. J. Appl. Toxicol. 31, 285–311.

Della Torre, C., Parolini, M., Del Giacco, L., Ghilardi, A., Ascagni, M., Santo, N., Maggioni, D., Magni, S., Madaschi, L., Prosperi, L., La Porta, C., Binelli, A., 2017. Adsorption of B(α)P on carbon nanopowder affects accumulation and toxicity in zebrafish (*Danio rerio*) embryos. Environ. Sci. Nano 4, 1132–1146.

Della Torre, C., Maggioni, D., Ghilardi, A., Parolini, M., Santo, N., Landi, C., Madaschi, L., Magni, S., Tasselli, S., Ascagni, M., Bini, L., La Porta, C., Del Giacco, L., Binelli, A., 2018. The interactions of fullerene C_{60} and benzo(α)pyrene influence their bioavailability and toxicity to zebrafish embryos. Environ. Pollut. 241, 999–1008.

Dhillon, G.S., Kaur, S., Pulicharla, R., Brar, S.K., Cledón, M., Verma, M., Surampalli, R.Y., 2015. Triclosan: current status, occurrence, environmental risks and bioaccumulation potential. Int. J. Environ. Res. Public Health 12, 5657–5684.

Dussault, È.B., Balakrishnan, V.K., Sverko, E., Solomon, K.R., Sibley, P.K., 2008. Toxicity of human pharmaceutical and personal care products to benthic invertebrates. Environ. Toxicol. Chem. 27 (2), 435–442.

EU, 2016. Commission implementing decision (EU) 2016/110: not approving triclosan as an existing active substance for use in biocidal products for product type1. http://www.eufram.com/documents/EUFRAM%20WP5%20draft%20report%202005.pdf, Accessed date: 11 August 2016.

Falisse, E., Voisin, A., Silvestre, F., 2017. Impacts of triclosan exposure on zebrafish early-life stage: toxicity and acclimation mechanisms. Aquat. Toxicol. 189, 97–107.

FDA, 2016. FDA issues final rule on safety and effectiveness of antibacterial soaps. https://www.fda.gov/NewsEvents/Newsroom/PressAnnouncements/ucm517478.htm, Accessed date: 2 October 2016.

Fischer, S., Klüver, N., Burkhardt-Medicke, K., Pietsch, M., Schmidt, A., Wellner, P., Schirmer, K., Luckenbach, T., 2013. Abcb4 acts as multixenobiotic transporter and active barrier against chemical uptake in zebrafish (*Danio rerio*) embryos. BMC Biol. 11, 69.

Haggard, D.E., Noyes, P.D., Waters, K.M., Tanguay, R.L., 2016. Phenotypically anchored transcriptome profiling of developmental exposure to the antimicrobial agent, triclosan, reveals hepatotoxicity in embryonic zebrafish. Toxicol. Appl. Pharmacol. 308, 32–45.

Halden, R.U., 2014. On the need and speed of regulating triclosan and triclocarban in the United States. Environ. Sci. Technol. 48 (7), 3603–3611.

Ho, J.C.H., Hsiao, C.D., Kawakami, K., Tse, W.K.F., 2016. Triclosan (TCS) exposure impairs lipid metabolism in zebrafish embryos. Aquat. Toxicol. 173, 29–35.

Horie, Y., Yamagishi, T., Takahashi, H., Iguchi, T., Tatarazako, N., 2018. Effects of triclosan on Japanese medaka (*Oryzias latipes*) during embryo development, early life stage and reproduction. J. Appl. Toxicol. 38, 544–551.

Ishibashi, H., Matsumura, N., Hirano, M., Matsuoka, M., Shiratsuchi, H., Ishibashi, Y., Takao, Y., Arizono, K., 2004. Effects of triclosan on the early life stages and reproduction of medaka *Oryzias latipes* and induction of hepatic vitellogenin. Aquat. Toxicol. 67, 167–179.

Jackson, J.S., Kennedy, C.J., 2017. Regulation of hepatic *abcb4* and *cyp3a65* gene expression and multidrug/multixenobiotic resistance (MDR/MXR) functional activity in the model teleost, *Danio rerio* (zebrafish). Comp. Biochem. Physiol. C 200, 34–41.

Kirkland, D., Pfuhler, S., Tweats, D., Aardema, M., Corvi, R., Darroudi, F., Elhajouji, A., Glatt, H., Hastwell, P., Hayashi, M., Kasper, P., Kirchner, S., Lynch, A., Marziu, D., Maurice, D., Meunier, J.R., Muller, L., Nohynek, G., Parry, E., Thybaud, V., Tice, R., Van Benthem, J., Vanparys, P., White, P., 2007. How to reduce false positive results when undertaking in vitro genotoxicity testing and thus avoid unnecessary follow-up animal tests. Report of an ECVAM Workshop. Mutat. Res. 628, 31–55.

Kosmehl, T., Hallare, A.V., Braunbeck, T., Hollert, H., 2008. DNA damage induced by genotoxicants in zebrafish (*Danio rerio*) embryos after contact exposure to freeze-dried sediment and sediment extracts from Laguna lake (The Philippines) as measured by the comet assay. Mutat. Res. 650, 1–14.

Ku, P., Wu, X., Nie, X., Ou, R., Wang, L., Su, T., Li, Y., 2014. Effects of triclosan on the detoxification system in the yellow catfish (*Pelteobagrus fulvidraco*): expression of *CYP* and *GST* genes and corresponding enzyme activity in phase I, II and antioxidant system. Comp. Biochem. Physiol. C 166, 105–114.

Li, Y., Li, C., Qin, H., Yang, M., Ye, J., Long, Y., Ou, H., 2018. Proteome and phospholipid alteration reveal metabolic network of *Bacillus thuringiensis* under triclosan stress. Sci. Total Environ. 615, 508–516.

Magni, S., Parolini, M., Binelli, A., 2016. Sublethal effects induced by morphine to the freshwater biological model *Dreissena polymorpha*. Environ. Toxicol. 31, 58–67.

Magni, S., Parolini, M., Della Torre, C., Fernandes de Oliveira, L., Catani, M., Guzzinati, R., Cavazzini, A., Binelli, A., 2017. Multi-biomarker investigation to assess toxicity induced by two antidepressants on *Dreissena polymorpha*. Sci. Total Environ. 578, 452–459.

Martínez-Paz, P., 2018. Response of detoxification system genes on *Chironomus riparius* aquatic larvae after antibacterial agent triclosan exposures. Sci. Total Environ. 624, 1–8.
Montaseri, H., Forbes, P.B.C., 2016. A review of monitoring methods for triclosan and its occurrence in aquatic environments. Trends Anal. Chem. 85, 221–231.
Muth-Köhne, E., Wichmann, A., Delov, V., Fenske, M., 2012. The classification of motor neuron defects in the zebrafish embryo toxicity test (ZFET) as an animal alternative approach to assess developmental neurotoxicity. Neurotoxicol. Teratol. 34, 413–424.
Oliveira, R., Domingues, I., Grisolia, C.K., Soares, A.M.V.M., 2009. Effects of triclosan on zebrafish early-life stages and adults. Environ. Sci. Pollut. Res. 16, 679–688.
Orvos, D.R., Versteeg, D.J., Inauen, J., Capdevielle, M., Rothenstein, A., Cunningham, V., 2002. Aquatic toxicity of triclosan. Environ. Toxicol. Chem. 21 (7), 1338–1349.
Parolini, M., Binelli, A., Provini, A., 2011. Assessment of the potential cyto-genotoxicity of the nonsteroidal anti-inflammatory drug (NSAID) diclofenac on the zebra mussel (*Dreissena polymorpha*). Water Air Soil Pollut. 217, 589–601.
Parolini, M., Ghilardi, A., Della Torre, C., Magni, S., Prosperi, L., Calvagno, M., Del Giacco, L., Binelli, A., 2017. Environmental concentrations of cocaine and its main metabolites modulated antioxidant response and caused cyto-genotoxic effects in zebrafish embryo cells. Environ. Pollut. 226, 504–514.
Powers, S.K., Lennon, S.L., 1999. Analysis of cellular responses to free radicals: focus on exercise and skeletal muscle. Proc. Nutr. Soc. 58, 1025–1033.
Riva, C., Cristoni, S., Binelli, A., 2012. Effects of triclosan in the freshwater mussel *Dreissena polymorpha*: a proteomic investigation. Aquat. Toxicol. 118-119, 62–71.
Ruszkiewicz, J.A., Shaojun, L., Rodriguez, M.B., Aschner, M., 2017. Is triclosan a neurotoxic agent? J. Toxicol. Environ. Health Part B 20 (2), 104–117.
Saad, M., Verbueken, E., Pype, C., Casteleyn, C., Van Ginneken, C., Maes, L., Cos, P., Van Cruchten, S., 2016. In vitro CYP1A activity in the zebrafish: temporal but low metabolite levels during organogenesis and lack of gender differences in the adult stage. Reprod. Toxicol. 64, 50–56.
Savage, J.H., Matsui, E.C., Wood, R.A., Keet, C.A., 2012. Urinary levels of triclosan and parabens are associated with aeroallergen and food sensitization. J. Allergy Clin. Immunol. 130 (2), 453–460 (e7).
Schweizer, H.P., 2001. Triclosan: a widely used biocide and its link to antibiotics. FEMS Microbiol. Lett. 202, 1–7.
Solá-Gutiérrez, C., San Román, M.F., Ortiz, I., 2018. Fate and hazard of the electrochemical oxidation of triclosan. Evaluation of polychlorodibenzo p dioxins and polychlorodibenzofurans (PCDD/Fs) formation. Sci. Total Environ. 626, 126–133.
Van der Oost, R., Beyer, J., Vermeulen, N.P.E., 2003. Fish bioaccumulation and biomarkers in environmental risk assessment: a review. Environ. Toxicol. Pharmacol. 13, 57–149.
Wang, Q., Kelly, B.C., 2017. Occurrence and distribution of synthetic musks, triclosan and methyl triclosan in a tropical urban catchment: influence of land-use proximity, rainfall and physicochemical properties. Sci. Total Environ. 574, 1439–1447.
Westerfield, M., 2007. A guide for the laboratory use of zebrafish (*Danio rerio*). The Zebrafish Book, 5th ed. University of Oregon Press, Eugene (Paperback).
Yao, L., Zhao, J., Liu, Y., Zhang, Q., Jiang, Y., Liu, S., Liu, W., Yang, Y., Ying, G., 2018. Personal care products in wild fish in two main Chinese rivers: bioaccumulation potential and human health risks. Sci. Total Environ. 621, 1093–1102.
Zhou, Z., Yang, J., Chan, K.M., 2017. Toxic effects of triclosan on a zebrafish (*Danio rerio*) liver cell line, ZFL. Aquat. Toxicol. 191, 175–188.
Zhu, L., Shao, Y., Xiao, H., Santiago-Schübel, B., Meyer-Alert, H., Schiwy, S., Yin, D., Hollert, H., Küppers, S., 2018. Electrochemical simulation of triclosan metabolism and toxicological evaluation. Sci. Total Environ. 622, 1193–1201.

Supporting Information

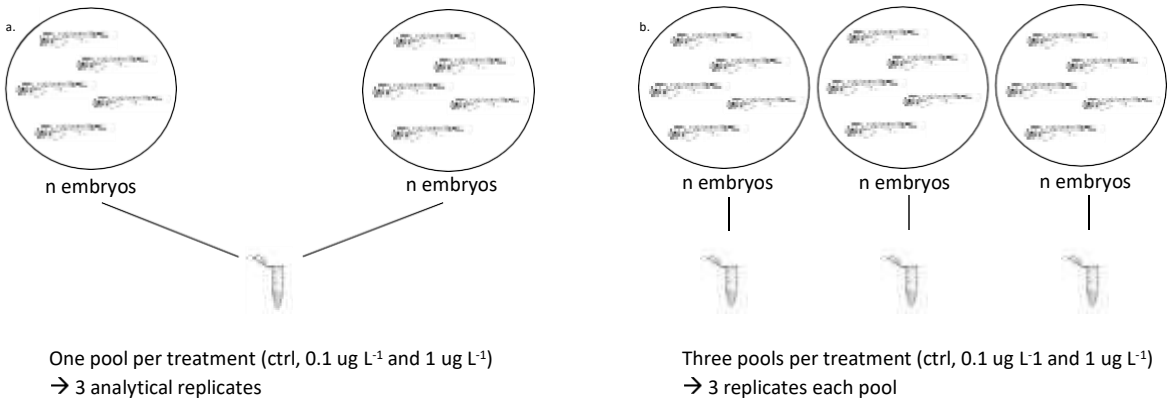

Fig. S1. Set-up of the exposure experiments and the following biomarkers analysis: a. antioxidant and detoxifying enzymes (n = 60), P-gp and EROD (n = 30), PCC (n = 70); b. ROS level (n = 12) and cyto- genotoxicity endpoints (n = 5).

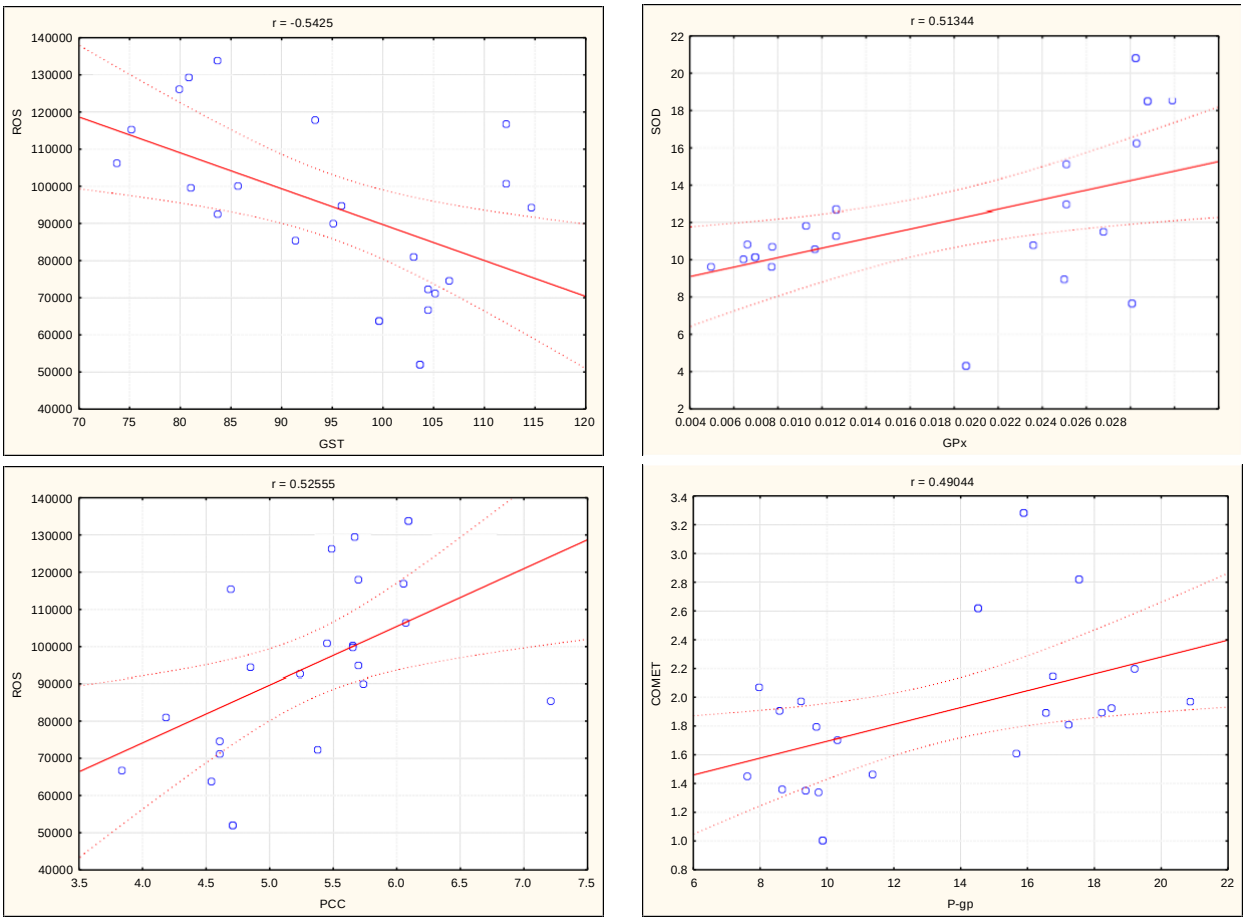

Fig. S2. Scatterplots of significant correlations (GST and ROS, GPx and SOD, PCC and ROS, P-gp and COMET) with correlation coefficient (r) close to ± 0.5.

TREATMENT	ENZYMES	P-gp	EROD	PCC	ROS level
24 h					
ctrl	2.616139	0.560021	6.458732	2.023827	2.174515-1.992151-1.881348
0.1 µg L^{-1}	2.091244	0.943525	8.200638	1.58619	1.816713-1.941367-2.174515
1 µg L^{-1}	3.675742	1.043341	7.211126	2.753222	2.06602-1.844414-1.93675
120 h					
ctrl	1.340692	1.085369	1.340692	1.848772	1.752078-2.05217-1.60434
0.1 µg L^{-1}	1.247486	0.980299	1.247486	1.328471	2.107572-2.001385-1.784395
1 µg L^{-1}	1.507481	0.764907	1.507481	1.736932	1.756694-1.969067-1.70591

Table S1. Total protein content of each sample expressed in mg mL^{-1} measured according to Bradford (1976) method.

Environmental Science Nano

ROYAL SOCIETY OF CHEMISTRY

PAPER

View Article Online
View Journal

Cite this: DOI: 10.1039/d0en00961j

Does triclosan adsorption on polystyrene nanoplastics modify the toxicity of single contaminants?†

C. C. Parenti, S. Magni, A. Ghilardi, G. Caorsi, C. Della Torre, L. Del Giacco and A. Binelli *

The physical and chemical properties of nanoplastics make them potential carriers for some environmental contaminants, modifying their biological effects. Nevertheless, the change in toxicity caused by pollutant adsorption on nanoplastics is still controversial, depending on the interactions between chemical and physical pollutants, the consequent change in bioavailability, the modification of intake, transport and accumulation in the organisms and also on the characteristics of contaminants. In this context, the aim of the present study was the evaluation of combined effects made by 0.5 μm nanobeads of polystyrene and triclosan adsorbed on their surface in comparison with those caused by single contaminants. The systemic effects of 7 day exposure to nanoplastics, triclosan alone and to the nanoplastic–triclosan complex have been analyzed by employing zebrafish larvae and using a multi-tier approach from the evaluation of cellular and molecular effects to the impact at organism level. Results highlighted by confocal microscopy evidenced nanobead ingestion and translocation in several tissues and organs to guarantee the goodness of the exposure results. Behavioral assays were then conducted to highlight larval swimming defects as a 'real-time' readout of the potential effects on the whole organism, while a suite of several biomarkers and functional proteomics was applied to investigate the effects at both cellular and molecular levels. The whole data set pointed out a clear modification in the toxicological effects of the nanoplastic–triclosan complex in comparison with single contaminants, proved by opposite behaviours in the larval swimming activity and modulation of diverse protein classes as well as by different effects on several biochemical endpoints. This means that the interaction between chemical and physical pollutants leads to more complicated responses than additive, synergistic or antagonist models, resulting in a modification of toxicity instead of its increase or decrease.

Received 18th September 2020,
Accepted 1st December 2020

DOI: 10.1039/d0en00961j

rsc.li/es-nano

Environmental significance

The physicochemical properties of nanoplastics (NPs) make them very suitable for the transfer of chemical contaminants, potentially enhancing their risk to aquatic organisms. Nevertheless, a few controversial pieces of evidence that exist relied on the toxic effects caused by NP adsorption of environmental pollutants. To the best of our knowledge, this is the first study assessing the capability of polystyrene nanoparticles to adsorb triclosan (TCS), a known toxic chemical compound, and investigating the effect of the NP–TCS complex and each individual contaminant on a freshwater model. The results pointed out a clear shift in the toxicity when chemical and physical pollutants are bound together, rather than a simple additive, synergistic or competitive effect, suggesting the need to employ more complex interpretative models.

1. Introduction

The invention of plastic surely represented one of the major technological innovations that changed our lifestyle and improved our wellness. Their versatile and unique characteristics (*e.g.* light weight, durability) allowed the application of plastic materials in several sectors, from the construction and transport industries to electrical and electronic applications as well as food conservation and healthcare. The incorrect disposal of plastic products is causing their increasing release in terrestrial and aquatic environments, since 79% of the plastic waste ever produced was accumulated in the natural environments or landfills, while about 12% was incinerated and only 9% was recycled.[1]

Once in the environment, larger plastic items can be fragmented into smaller debris by sunlight, mechanical

Department of Biosciences, University of Milan, Via Celoria 26, 20133 Milan, Italy. E-mail: andrea.binelli@unimi.it

† Electronic supplementary information (ESI) available. See DOI: 10.1039/d0en00961j

abrasion, salinity and temperature variations.[2] These modifications can profoundly change the fate and toxicity of plastics, being more easily ingested and accumulated in organisms. These smaller plastic pieces are called microplastics (MPs) and nanoplastics (NPs), which have been recently redefined as debris with a dimension between 1 μm to <1 mm and 1 nm to <1 μm, respectively.[3] Due to their smaller dimension, these plastic debris represents the most dangerous fraction, since they can be potentially ingested by all aquatic and terrestrial organisms. Indeed, there is much evidence of the negative effects caused by MPs and NPs at various levels of the biological organization.[4–10] The next challenge is represented by the joint effects due to the interaction between MPs, NPs and chemical pollutants present in the environment, which can be adsorbed on the surface of plastic debris. Indeed, their high surface/volume ratio increases the sorption of other contaminants present in the surrounding matrix, making MPs and NPs suitable as physical carriers for these pollutants through all the environmental compartments, biota included. Since MPs and NPs have properties similar to natural suspended matter, they possess a higher sorption capability for hydrophobic contaminants, such as polychlorinated biphenyls (PCBs), polycyclic aromatic hydrocarbons (PAHs) and other benzene-ring derivatives.[11] Many studies demonstrated the capability of MPs and NPs to be a carrier also for some hydrophilic pollutants due to the generation of oxidative groups during plastic debris weathering that increase their polarity, roughness and porosity,[12,13] as demonstrated for the adsorption on some MPs of perfluoro-octane-sulfonate (PFOS) and perfluoro-octane-sulfonamide (PFOA)[14] as well as of many antibiotics.[15,16] This means that smaller plastic debris can modify the overall bioavailability of the environmental contaminants for the organisms, magnifying or even decreasing the toxicity of pollutants bound together, as a consequence of the possible different relations in the chemical–plastic–organism ternary system.[17]

In this context, the aim of our study was the evaluation of the possible change in toxicity after the adsorption of triclosan (TCS) on 0.5 μm PS NPs (PNPs) in comparison with the effects evaluated after the exposure to single contaminants, by using zebrafish (*Danio rerio*) larvae as aquatic model organisms. TCS is one of the current most investigated environmental pollutants due to its wide use in many consumer products (soaps, toothpastes, deodorants, textiles, shoes, toys, cosmetics) and the increasing evidence of its negative effects on the health of organisms, including humans. Being a hydrophobic chemical ($\log K_{ow}$ = 4.76), TCS is a persistent environmental pollutant still present in natural environments in a concentration up to 5.2 μg L^{-1} in surface waters worldwide.[18] From the (eco)toxicological point of view, TCS and its by-products were reported to be endocrine disruptors in several model organisms, to affect immune responses, reactive oxygen species (ROS) production and also cardiovascular functions.[19] The ubiquitous presence of TCS in all the aquatic ecosystems worldwide makes this lipophilic contaminant prone to be transported by MPs and NPs, changing not only its environmental fate but also the intake, accumulation and probably toxicity towards organisms.

Since the possible interaction between MPs, NPs and environmental contaminants has been conducted up to now using only the chemicals described above, our study represents a novelty for TCS, whose adsorption on plastic debris (polyethylene) has already been detected by Wu *et al.*[20]

Our experimental design comprised three different steps: (1) we firstly planned the sample preparation in order to eliminate the interference caused by TCS and PNPs freely present in the water when in co-exposure, through a preliminarily adsorption of an environmental concentration of TCS (0.6 μg L^{-1}) on PNPs (200 μg L^{-1}); (2) we then evaluate the ingestion, uptake and accumulation of virgin and doped PNPs in tissues and organs of zebrafish larvae by confocal microscopy; (3) lastly, we exposed zebrafish larvae to PNPs and TCS administered alone and to the PNP–TCS complex for 7 days, measuring many endpoints belonging to different levels of the biological organization. The multi-tier approach was based on the evaluation of possible alterations in swimming behavior as the endpoint to assess the pollutants' effects at a whole organism level, while a biomarker suite and functional proteomics were carried out to investigate the effects at cellular and molecular levels.

To the best of our knowledge, this is the first multidisciplinary study aimed to assess the potential of NPs to be a carrier for this antibacterial chemical, evaluating at the same time the possible change in toxicity, since there is only the study by Syberg *et al.*[21] describing the combined effect of a mixture of TCS and polyethylene microbeads administered to the marine copepod *Acartia tonsa*, based however only on mortality as the measured endpoint.

2. Experimental

2.1 PNP characterization

PNPs within the nanosize range of 0.4–0.6 μm (10% w/v) and fluorescent pink PNPs (1% w/v) with a comparable size (0.5 μm) were purchased from Spherotech Inc. (Lake Forest, IL, USA). Fluorescent nanobeads were only administered to larvae designed for confocal microscopy observations. Detailed information about PNP characterization (size distribution, *Z*-potential, excitation and emission spectra) are shown in the ESI† (Table S1 and Fig. S1). Both PNP stock solutions contained sodium azide (0.02%) to prevent bacterial growth, whose concentration decreased to 0.00001% in the working solution used for the exposure assays. Nevertheless, we previously certified that this very low concentration of bacteriostatic additive did not affect the investigated endpoints.[9]

2.2 TCS adsorption on PNPs and selection of concentrations

Before the exposures, both the non-fluorescent and fluorescent PNPs were doped with TCS to obtain the TCS-

contaminated plastic suspensions, thus creating a PNP–TCS single complex which was then administered to zebrafish larvae. This experimental plan allowed the elimination from the PNP–TCS exposure solution of the two interfering fractions constituted by the TCS and PNPs alone.

TCS contamination was performed by adding PNPs (25 mg) and TCS (250 μg) in 3 glass bottles with 50 mL of deionized water and kept in constant mixing by a stirrer at 4 °C for 3 days in the dark. Then, the PNP–TCS suspension was centrifuged for 15 min at 3000*g* and 25 °C to precipitate the nanobeads. The supernatants were collected and used to evaluate the fraction of TCS not adsorbed on the PNPs, while the pellets containing the doped PNPs were gently dried under a nitrogen flow and kept in glass vials until the exposure assays.

In order to check the fraction of TCS adsorbed on PNPs, each pellet was resuspended in methanol and the suspension was ultrasonicated for 30 min to re-separate the adsorbed TCS from the PNPs. The solution was then filtered (mesh = 0.2 μm) to completely remove the remaining suspended PNPs. This solution, containing the TCS re-separated from PNPs, and the supernatants previously sampled, were analyzed by liquid–liquid extraction (isooctane/methanol 4 : 1 v/v and hexane/water 2 : 1 v/v) followed by a gas chromatographic analysis (TRACE GC coupled with a PolarisQ ion trap mass spectrometer, Thermo-Electron, Texas, USA). We calculated a concentration of 82 μg L^{-1} of TCS in the final solution, which was equal to 36% of the initial concentration (250 μg L^{-1}), representing the percentage of TCS adsorbed on PNPs. Therefore, to remain within the environmental concentrations of this chemical, the PNP amount for the exposure was set to 200 μg L^{-1}, following the calculation shown in Table 1. This concentration corresponded to 0.6 μg L^{-1} adsorbed TCS. Consequently, the same TCS concentration was used when the chemical was administered alone to zebrafish larvae.

2.3 Exposure of zebrafish larvae

AB strain adult zebrafish were reared in the facility at the Department of Biosciences, University of Milan, following Italian laws, rules and regulations (Legislative Decree no. 116/92). In accordance with the Italian Legislative Decree 26/2014, the project was carried out under the authorization of the Italian Ministry of Health (Aut. Min. no. 6/2019-PR).

We performed three independent experiments using different clutches of larvae from different fish to increase biological variability. Zebrafish larvae were exposed for 7 days, starting from the age of 4 days post fertilization (dpf) inside 800 mL glass beakers (approximately 100 larvae in 500 mL of zebrafish water in each beaker) and maintained at 28 °C on a 14 h light : 10 h dark cycle. The exposures were carried out under semi-static conditions, changing the medium every 24 h and maintaining the water in constant mixing. Larvae were fed with commercial artificial diets (particle size <100 μm) from 6 dpf. Control larvae (CTRL) were maintained in fish water (0.1 g L^{-1} Instant Ocean, 0.1 g L^{-1} $NaHCO_3$, 0.2 g L^{-1} $CaSO_4$ in deionized water with 0.1% methylene blue), while the three treatments consisted of (i) 0.6 μg L^{-1} TCS in zebrafish water, (ii) 200 μg L^{-1} PNPs (corresponding to about 3×10^9 nanobeads per L), and (iii) 200 μg L^{-1} of the complex PNP–TCS.

At the end of exposures, larvae were sacrificed in tricaine (300 mg L^{-1}) and immediately processed for the following microscopy observations, genotoxicity assessments and behavioral tests, or stored at −80 °C for further biomarker and proteomic analyses.

In the meantime, PNP–TCS suspensions and TCS solutions collected after 24 h in the exposure beakers were collected and analyzed in order to check for any TCS release from the particles as well as the eventual reduction in TCS concentration after 24 h of exposure. We used the same method applied for the quantification of TCS adsorption (liquid–liquid extraction in hexane/water 2 : 1 v/v followed by a gas chromatographic analysis).

2.4 Confocal microscopy

The ingestion and accumulation of fluorescent PNPs (alone and combined with TCS) in zebrafish larvae were investigated by confocal microscopy technique. At the end of exposures, 20 larvae for each independent experiment were sacrificed as described above and fixed in paraformaldehyde (4% in PBS), then stored at 4 °C. Larvae selected for whole-mount observations were treated with protease K (P2308, Sigma Aldrich), stained with DAPI (4′,6-diamidino-2-phenylindole) and directly mounted on microscope slides, while larvae designed for cryo-sectioning were washed in PBS (0.1 M) and sucrose (15% and 30%), included in the mounting medium (Bio Optica), frozen in dry ice and stored at −80 °C. Longitudinal and transversal sections (15 μm) were prepared using a Cryostat CM 1850 (Leica, Wetzlar, Germania) at −20 °C. Cell nuclei were stained with DAPI.

For each experimental group (CTRL, PNPs and PNP–TCS) we observed 10 whole-mount larvae and 10 slides of larval sections using a confocal microscope (laser scanning confocal microscope, Nikon A1) to localize the internalized fluorescent PNPs in the exposed organisms. Assessment of

Table 1 Concentrations of PNPs and TCS used for the preparation of TCS-contaminated particle suspensions

	Preparation solutions		Final concentration of solution	Exposure concentrations
	Stock solution	Working solution	Extract	
PNPs	100 g L^{-1}	2.5 g L^{-1}	—	200 μg L^{-1}
TCS	1 mg L^{-1}	250 μg L^{-1}	82 μg L^{-1}	0.6 μg L^{-1}

the orthogonal projections of *Z*-stack pictures guaranteed that PNPs were effectively inside the tissues and not a simple artefact due to the transport made by the blade of the cryostat.

2.5 Larval swimming activity

Potential behavioral alterations induced by the three different treatments were evaluated on 12 larvae for each experimental group (36 total larvae for each treatment) using the DanioVision™ tracking system (Noldus IT, Wageningen, Netherlands).

Each larva was put in a single well of a 24-multiwell plate and submitted to an alternating dark/light test based on 10 minutes of adaptation followed by 2 cycles of 20 min of dark and 10 min of light,[9] recording their swimming activity at 30 frames per s. During the entire test, the temperature was maintained at 28 °C by the DanioVision temperature control unit.

The acquired data were analyzed using the software EthoVision XT (Noldus IT, Wageningen, Netherlands) by measuring the following parameters: total distance moved (mm), turn angle (degree) and thigmotaxis (wall-hugging behavior). The software was also applied to create and visualize graphical representations of larval swimming activity, such as tracks (Fig. S3A†) and heatmaps (Fig. S3B†), where different colors represented the frequency of a specific position (hotspots) in the well.

2.6 Biomarker

Biomarker methods are thoroughly described in the ESI.† Briefly, cell viability was assessed by the trypan blue dye exclusion method before the genetic damage tests to guarantee a viability higher than 80%.[22] Genotoxicity assessments were performed according to Parolini *et al.*[23] by using pools of 7 larvae for each experimental group (3 pools of 7 individuals for each treatment). Genotoxicity was evaluated by measuring the frequency of apoptotic and necrotic cells as well as micronuclei (MN) which pointed out fixed and irreversible DNA damage.

The effects on detoxification systems were assessed by ethoxyresorufin-*O*-deethylase (EROD) and glutathione *S*-transferase (GST) activities, while the oxidative stress level was evaluated by superoxide dismutase (SOD), catalase (CAT) and glutathione peroxidase (GPx) activities and by the measurement of reactive oxygen species (ROS) production on pools of 35 larvae from each experimental group (3 pools of 35 individuals for each treatment).

Lastly, the presence of neurotoxic effects was assessed by the level of acetylcholinesterase (AChE) activity, using 5,5′-dithiobis-2-nitrobenzoic acid (DTNB) as reagent.[7] Due to the strong connection between neuronal alterations and behavior, for this test we pooled together larvae previously tested for behavioral changes (36 total larvae for each treatment).

All data resulting from enzymatic analyses and ROS evaluation were normalized to the protein total content of each sample measured by the Bradford method.[24]

2.7 Functional proteomics

The modulation of protein expression in control and treated larvae was investigated by the gel-free proteomic technique.[8] At the end of the exposure, pools of 20 larvae for each experimental group (3 pools of 20 individuals for each treatment) were homogenized in 300 μL of lysis buffer (described in the ESI†). Proteins were precipitated, reduced, alkylated and then digested by adding trypsin. Peptides were then purified by reverse phase chromatography, using Zip Tips (μ-C18; Millipore, Milan, Italy),[8] and analyzed with a mass spectrometer as reported by Magni *et al.*[8] with some modifications (described in the ESI†).

2.8 Statistical analysis

Statistical analyses on behavior and biomarker data were performed using STATISTICA 7.0 software. After having checked the normality and homoscedasticity of biomarker data, the significance was evaluated by one-way analysis of variance (ANOVA) followed by Duncan's multiple range *post hoc* test (DMRT), taking $p < 0.05$ as the significance cut-off. Regarding the proteomic results, a Student *t*-test was performed between control and treated samples.

3. Results

3.1 Check of the experimental conditions

The check of the possible release of TCS from the doped PNPs by gas chromatographic analyses showed the complete absence of the chemical in the exposure beakers after 24 h of exposure, pointing out that TCS did not detach from the particles. This means that the ecotoxicological effects due to the TCS–PNP complex presented below are certainly due to the combination of the two contaminants because our experimental design was able to eliminate the interference due to TCS and PNPs present alone in the exposure suspensions. Furthermore, the analyses of TCS concentration in the exposure solutions after 24 h revealed a decrease of about 30% (0.4 μg L^{-1}) in the beakers containing 0.6 μg L^{-1} TCS alone, confirming the need to perform the exposures under semi-static conditions by a daily renewal of chemical.

3.2 PNP uptake and accumulation in zebrafish larvae

Whole-mount observations by confocal microscopy confirmed the PNP uptake by larvae, both for virgin PNPs and the PNP–TCS complex (Fig. 1). On the other hand, the capability of PNPs to pass through biological membranes and accumulate in different tissues was already demonstrated also for zebrafish embryos.[9] Nevertheless, new findings have emerged from larval section observations, since we visualized PNPs both in the eye (Fig. 2) and in the trunk (Fig. 3). Furthermore, we did not observe any differences in the amount of ingested

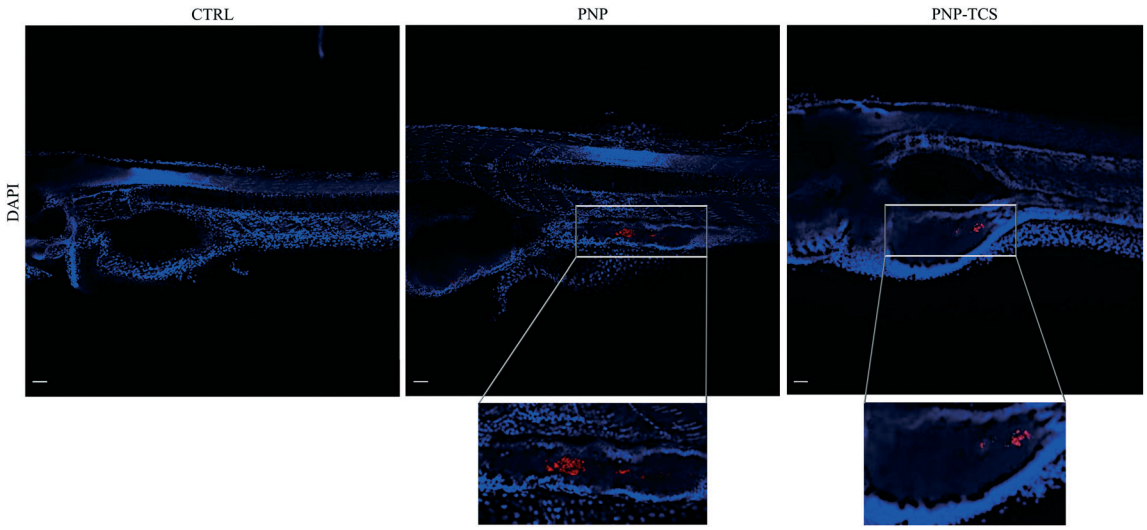

Fig. 1 Whole-mount images of larvae at the end of the exposure (scale bar 50 μm). Nanobeads are shown in red. Cell nuclei are stained with DAPI.

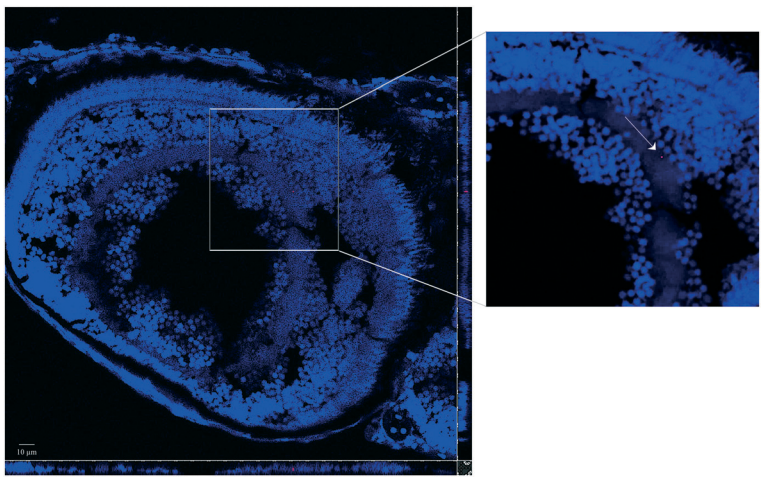

Fig. 2 Detail of a cryostat section (11 *Z*-steps of 1 μm) showing the eye of a zebrafish larva exposed to PNP–TCS. Nanobeads are shown in red. Cell nuclei are stained with DAPI. Orthogonal projections of *Z*-stack evidencing the nanobead at cellular level.

PNPs between virgin ones and the PNP–TCS complex, suggesting that TCS adsorption did not modify the particle intake.

3.3 Effects at individual level

At the end of exposures, the effects of the three treatments on fish behavior were evaluated by measuring their swimming activity. Results highlighted an opposite effect of TCS when administered alone or combined with PNPs. Indeed, we observed both a hypo- and a hyperactivity of zebrafish larvae compared to controls, respectively (Fig. 4A). In detail, the variation was significant both for the dark ($F_{3,156}$ = 21.28 and $p < 0.001$) and the light phase ($F_{3,74}$ = 50.15 and $p < 0.001$; Fig. 4B). By contrast, PNPs administered alone did not significantly affect the total distance travelled by larvae.

Regarding the other considered parameters, such as turn angle (Fig. S2A†) and thigmotaxis (Fig. S2B†), no significant differences were observed in all exposure conditions.

3.4 Effects at sub-organism level

Biomarker analyses pointed out significant variations of MN frequency ($F_{3,20}$ = 4.92 and $p < 0.05$), as well as GST ($F_{3,19}$ = 5.75 and $p < 0.01$) and GPx activities ($F_{3,20}$ = 3.64 and $p < 0.05$) (Fig. 5). In detail, we observed a significant increase ($p < 0.01$) of MN frequency due to TCS administered alone compared to controls, while a significant decrease was found in PNPs ($p < 0.05$) and PNP–TCS ($p < 0.05$) compared to TCS. Regarding oxidative endpoints, a significant increase of GST and GPx activity was detected in organisms exposed to TCS compared to controls ($p < 0.01$ and $p < 0.05$, respectively). The measured activities of these enzymes were

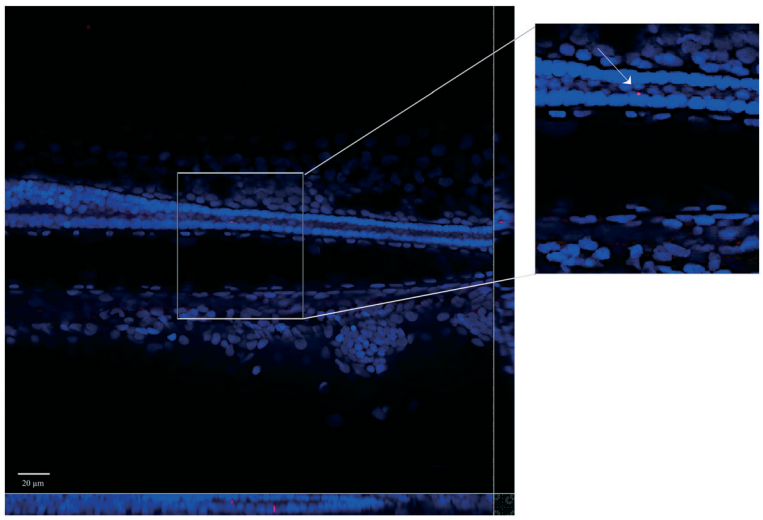

Fig. 3 Detail of a cryostat section (14 *Z*-steps of 1 µm) showing the tail of a zebrafish larva exposed to PNPs. Nanobeads are shown in red. Cell nuclei are stained with DAPI. Orthogonal projections of *Z*-stacks evidencing the nanobead at cellular level.

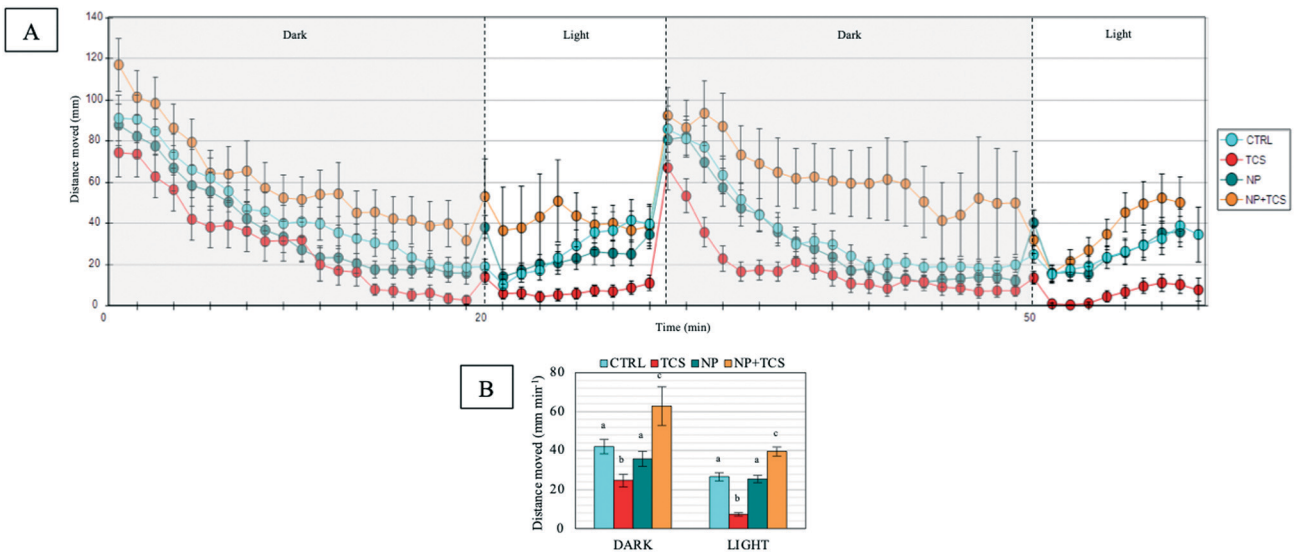

Fig. 4 Swimming activity (distance moved over time) measured in zebrafish larvae exposed to PNPs (200 µg L^{-1}), TCS (0.6 µg L^{-1}) and PNP–TCS, compared to control. (A) Total distance moved per minute (mean ± S.E.); (B) total distance moved during dark and light conditions (mean ± S.E.). Different letters correspond to values significantly different (one-way ANOVA and DMRT *post hoc* test, $p < 0.05$).

also significantly different between PNP-treated and TCS-treated groups. In detail, GST activity decreased in PNPs and PNP–TCS compared to TCS ($p < 0.01$ and $p < 0.05$, respectively), while GPx activity decreased in PNP–TCS compared to TCS ($p < 0.05$). Lastly, any significant effects of PNPs, both virgin and contaminated, were pointed out by biomarker analyses.

3.5 Effects on proteome

We identified 1807 proteins, 1480 of which were subsequently quantified. In detail, PNPs modified 43 proteins, 8 of which were significantly different ($p < 0.05$) from controls, but not above the 2-fold change threshold (Fig. S4A†). The remaining 35 proteins were quite equally divided between up-regulated (16) and down-regulated (19) proteins (Fig. 6A).

TCS was able to modulate 68 different proteins, 45 of which were significantly different ($p < 0.05$) from controls, but not above the 2-fold change threshold (Fig. S4B†). Then, we found 10 proteins up-regulated and 13 down-regulated (Fig. 6A).

The PNP–TCS complex modified a total of 29 proteins, all above the significance and the biological effect threshold of

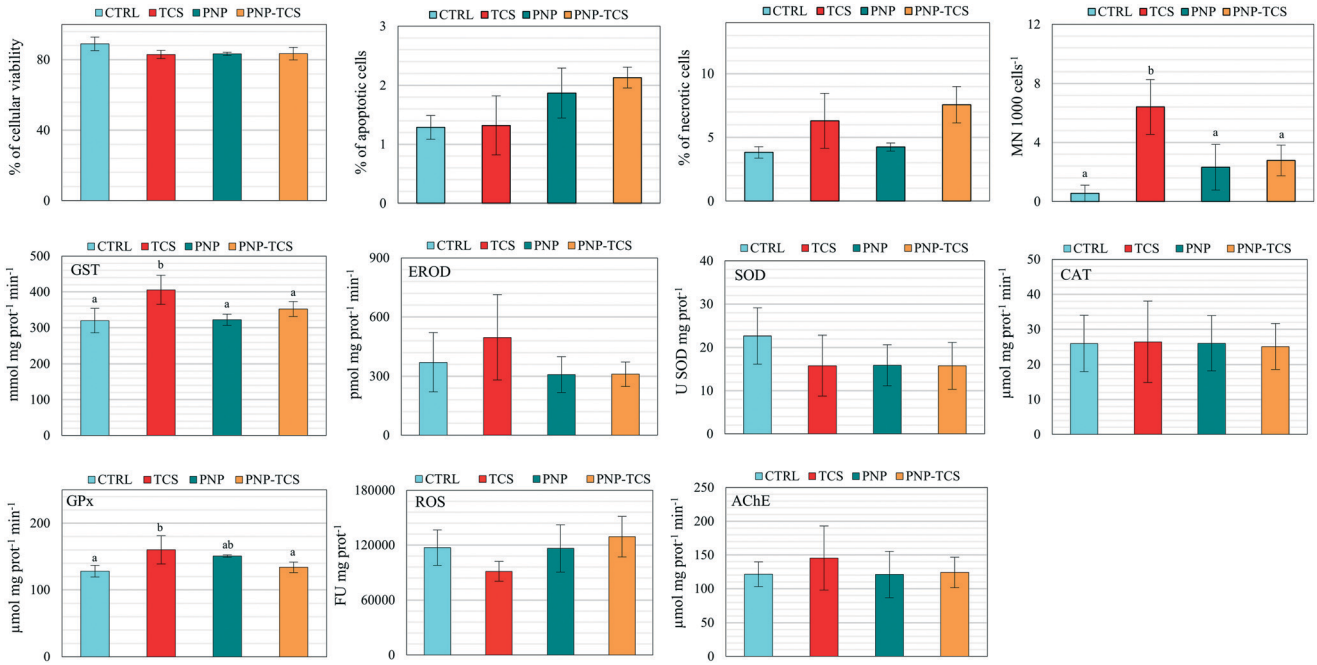

Fig. 5 Cellular effects measured in zebrafish larvae exposed to PNPs (200 μg L^{-1}), TCS (0.6 μg L^{-1}) and PNP–TCS, compared to control (pool of 3 independent experiments). Different letters correspond to values significantly different (one-way ANOVA and DMRT *post hoc* test, $p < 0.05$).

the 2-fold change (Fig. S4C†). In particular, we measured 11 up-regulated and 18 down-regulated proteins (Fig. 6A).

The entire proteomic data set revealed a number of proteins modulated by PNPs (35) higher than those changed by the PNP–TCS complex (29) and TCS (23), with different biological functions: PNPs mainly modified proteins involved in genetic processes, which represent 25% of the total changed proteins, followed by cytoskeleton (22%), energy (17%) and catalytic activity (11%). Calcium metabolism and transport accounted for 8%, while proteins involved in the immune system were only 3%. Six percent of all the misregulated proteins do not have known functions (Fig. 7A).

More than a quarter of proteins modulated by TCS belongs to the energy group (26%) followed by genetic processes (22%) and catalytic activities (18%), while cytoskeleton dropped to 13% only (Fig. 7B). The remaining 17% included proteins entangled in transport, development and the immune system, while 4% of identified proteins have no known annotated function.

The PNP–TCS complex modulated many proteins unrelated either to PNPs or TCS. The cytoskeleton proteins were the most affected by the complex (35%), while the second most modified group (genetic processes) accounted for 17% of the changed proteins (Fig. 7C). Catalytic activity (14%) and energy (10%) were less represented than in the other treatments, while modifications of structural proteins (7%) appeared.

The Venn diagram (Fig. 6B) confirmed the different effects due to pollutants, since only 7 proteins were in common among the three treatments (Table S2†), highlighting the lack of similar effects on common biological pathways. This is expected for the physical and chemical pollutants, with different routes of intake, accumulation and mechanism of actions (MoA), as confirmed by the only 3 proteins in common between these treatments (Fig. 6B). The MoA of the PNP–TCS complex seemed to be more similar to PNPs than TCS, as indicated by the 8 different proteins in common between the two treatments *versus* the only 4 changed proteins in common between TCS and the PNP–TCS complex (Fig. 6B).

4. Discussion

The aim of this study is a novelty in the NP scenario since we investigated both the role played by NPs as a vector for TCS and the possible ecotoxicological consequences of the intake of the PNP–TCS complex in relation to the administration of the two single pollutants.

4.1 TCS adsorption and microscopy observations

The first step to certify the following ecotoxicological results was the confirmation of the adsorption of TCS on PNPs and the intake of PNPs and the complex in the biological model.

The high amount of TCS adsorbed on PNPs, corresponding to 36% of the starting TCS concentration added in the suspension, confirmed the high sorption capability of PS for hydrophobic contaminants. This is due to the presence of several benzene rings in its polymeric structure, which increase the distance between the chains, thus facilitating contaminant attachment and integration.[25] On the other hand, the sorption behavior of TCS for PS was well described by Li *et al.*,[26] who showed that the proportion

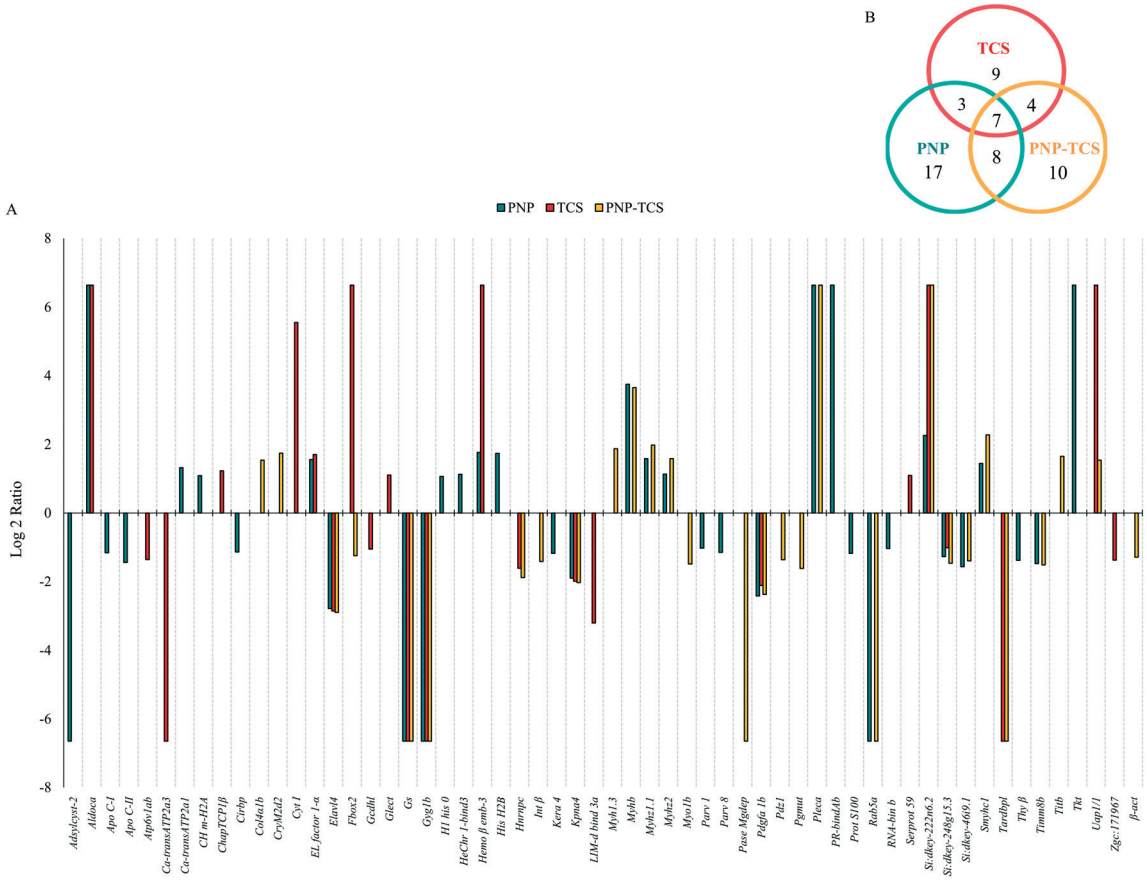

Fig. 6 (A) Protein modulation measured in zebrafish larvae exposed to PNPs (200 μg L^{-1}), TCS (0.6 μg L^{-1}) and PNP–TCS, compared to control. (B) Venn diagram. Adsylcyst-2: *S*-adenosylhomocysteine hydrolase-like 2; aldoca: fructose-bisphosphate aldolase; APO C-I: apolipoprotein C-I; APO C-II: apolipoprotein C-II; Atp6v1ab: ATPase H^+-transporting V1 subunit ab; CA-transATP2a3: calcium-transporting ATPase gn = ATP2a3; CA-transATP2a1: calcium-transporting ATPase gn = ATP2a1; ch m-h2a: core histone macro-h2a; ChapTCP1β: chaperonin containing TCP1, subunit 2 (beta); Cirbp: Cirbp protein; Col4α1b: collagen, type XIV, alpha 1b; CryM2d2: crystallin, gamma M2d2; Cyt i: type I cytokeratin; El factor 1-α: elongation factor 1-alpha; Elavl4: Elav-like protein; Fbxo2: F-box protein 2; Gcdhl: glutaryl-CoA dehydrogenase b; Glect: galectin; Gs: glutamine synthetase; Gyg1b: glycogenin 1b; H1 his 0: H1 histone family, member 0; Hechr 1-bind3: heterochromatin protein 1, -binding protein 3; hemo β Emb-3: hemoglobin beta embryonic-3; his H2b: histone H2b; Hnrnpc: heterogeneous nuclear ribonucleoprotein C1/C2; int β: integrin beta; Kera 4: keratin 4; Kpna4: importin subunit α; Lim-d bind 3a: Lim-domain binding factor 3a; Myh1.3: myosin, heavy polypeptide 1.3, skeletal muscle; Myhb: myosin, heavy chain b; Myhz1.1: myosin, heavy polypeptide 1, skeletal muscle; Myhz2: myosin, heavy polypeptide 2, fast muscle-specific; myo1b: myozenin 1b; Parv 1: parvalbumin 1; parv 8: parvalbumin 8; pase Mgdep: protein phosphatase, Mg^{2+}/Mn^{2+}-dependent, 1aa; Pdgfa 1b: Pdgfa associated protein 1b; Pdz1: Pdz domain-containing 1; Pgmut: phosphoglycerate mutase; pleca: plectin a; Pr-bindab: purine-rich element-binding protein ab; Prot S100: protein S100; Rab5a: Rab5a protein; RNA-bin b: cold-inducible RNA-binding protein b; Serprot 59: serine protease 59, tandem duplicate 2; Smyhc1: slow myosin heavy chain 1; Tardbpl: Tar DNA-binding protein, -like; thy β: thymosin beta; Timm8b: translocase of inner mitochondrial membrane 8 homolog b; Titb: titin b; TKT: TKT protein; Uap1/1: Udp-*n*-acetylhexosamine pyrophosphorylase-like protein 1; β-act: beta-actin.

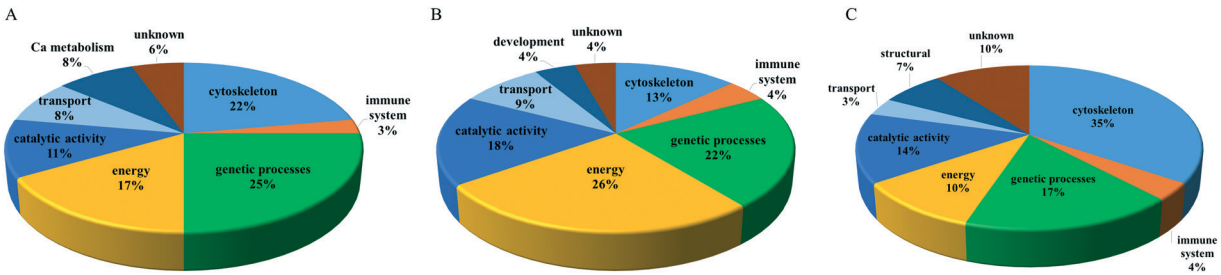

Fig. 7 Molecular functions of modified proteins in zebrafish larvae exposed to (A) PNPs (200 μg L^{-1}), (B) TCS (0.6 μg L^{-1}) and (C) PNP–TCS.

of the adsorbed TCS increases with decreasing PS particle size.

The smaller size of NPs not only increases their sorption capability but also enhances their ability to bioaccumulate

contaminants inside organism tissues.[27] Our study confirmed this behavior since we observed the presence of PNPs in the gastrointestinal tract of zebrafish larvae, yet an external compartment, but also discovered that some PNPs, both pristine and contaminated by TCS, were distributed in other organs, such as the eye (Fig. 2) and the trunk (Fig. 3).

The role played by NPs as a carrier for some environmental contaminants was already noticed in a study performed on adult zebrafish exposed to NPs (1 mg L^{-1}), bisphenol A (BPA; 1 μg L^{-1}) and their mixture, that showed the presence of both contaminants in the viscera, gills, head and muscles, leading also to a higher BPA accumulation in the brain, which was related to a dopaminergic neurotoxic effect.[28] Furthermore, an increased bioaccumulation of phenanthrene (0.1 mg L^{-1}) was observed in *Daphnia magna* when co-exposed to NPs (5 mg L^{-1}) for 14 days, highlighting their action as vectors of PAHs.[29]

4.2 Effects at organism level

It has been observed that zebrafish larvae, when exposed only to an alternating light/dark period, showed a pattern of increased movement in the dark phase, probably due to decreased predator threat, followed by a resting state in the light phase.[30] Thus, the possible alteration of this natural behavior has been used to assess the effects of any substance that might be able to generate neurotoxic effects, such as drugs, metals and nanoparticles.[31]

We applied this concept to our experiments, in which both TCS and the PNP–TCS complex significantly affected larval swimming activity, as opposed to PNPs administered alone (Fig. 4). Interestingly, we observed that TCS and the PNP–TCS complex had an opposite effect on larval swimming since the total distance moved significantly decreased during both dark and light phases in the larvae exposed to TCS, while it increased for those exposed to the PNP–TCS complex.

The alteration of locomotor behavior of zebrafish larvae caused by the exposure to environmental contaminants has been already observed. For instance, polybrominated diphenyl ethers (PBDEs) and their metabolites caused an altered swimming behavior, showing both an increased and decreased locomotion, depending on the molecules, concentrations and exposure conditions.[32,33] The evidence that diverse treatments can differently affect movements was also reported in a study by Ali *et al.*,[34] in which zebrafish embryos were exposed to a wide range of toxic compounds with different MoAs.

In our study, the TCS exposure induced significant larval hypoactivity, which could be attributable to affected locomotor system development,[35] while the hyperactivity observed in larvae exposed to the PNP–TCS complex could be attributed to visual defects[35] and/or an increased stress/anxiety level.[36]

Although these hypotheses should be in-depth investigated since the differences in behavioral patterns strictly depend on the neuronal targets of the tested contaminants,[37] some results from the proteomic approach seemed to explain the opposite swimming behaviour noticed after the TCS and PNP–TCS complex treatments, as shown below. Moreover, we might suggest that the opposite effect of TCS and the PNP–TCS complex can be attributable to the accumulation of the chemical in different body regions. Indeed, when TCS is administered alone, being a lipophilic compound, it bioaccumulates in lipid tissues, such as the yolk, but when adsorbed on PNPs, it is forced to follow the physical pollutants that accumulate in other tissues and organs, modifying its MoA against different cellular pathways, as previously demonstrated in our study.[38] This could not be confirmed in our experiments due to the small size of the zebrafish larvae. Another possible hypothesis could be related to the metabolization of TCS by the CYP 450 detoxification system, mainly present in the liver, producing the more toxic metabolite methyl-TCS.[39] Thus, the PNP–TCS complex might modify the accumulation pathway, eliminating or simply decreasing the amount of TCS that ends in the liver and, consequently, reducing the methyl-TCS production and changing its (eco)toxicological effects.

4.3 Effects at sub-organism level

The evaluation of sub-individual effects on exposed organisms was performed to further understand the different toxicity behaviors observed between TCS, PNPs and the PNP–TCS complex. The biomarker approach did not show any significant effect of the PNP treatment, both pristine and contaminated, pointing out only a few effects for TCS administered alone. On the other hand, our results are comparable to those shown in a recent study, in which the evaluation of biomarker responses was applied to test the effects of pristine PE fragments on zebrafish larvae, showing the lack of alteration on both the oxidative stress and the AChE activity.[40] However, the reported effects of NPs on aquatic organisms are varied and sometimes controversial, depending on particle concentration, physical and chemical properties, and composition.[41] Moreover, our data represent the first evidence concerning the effects of TCS-contaminated NPs on zebrafish, making it difficult to directly compare our results to those from other studies. The only existing studies reported an increased toxicity of NPs when combined with phenanthrene in *Daphnia magna*,[29] and Chen *et al.*[28] pointed out that a mixture of NPs and BPA led to an increase of neurotoxic effects in zebrafish compared to NPs and BPA alone.

Our results did not highlight any effects on AChE activity (Fig. 5), but the measurement of this unique endpoint is not sufficient to identify possible neurotoxic effects in the zebrafish cholinergic system, as also reported by Chen *et al.*[28] Thus, further analyses are needed to exclude the presence of neurological damage which could have been responsible for the locomotion alterations we observed.

Unlike PNPs, the slight and non-homogeneous effects caused by the TCS exposure on zebrafish larvae were only

related to a significant ($p < 0.05$) increase of GST, GPx and micronuclei formation (Fig. 5), confirming the results obtained in our previous study on zebrafish embryos in which we found that environmental concentrations of TCS (0.1–1 μg L^{-1}) were able to induce the activation of detoxification systems and generate cytotoxicity.[42] The lack of effects when TCS is bound to PNPs suggested a decrease of the toxicological profile of the complex that can be explained by two different hypotheses: (1) the chemical was not desorbed from PNPs, making it impossible to exploit its effect on the selected endpoints; (2) the complex formation decreased the bioavailability of TCS, reducing its concentration in *D. rerio* larvae.

As a final remark, the biomarker data set gave another evidence about the modification of the ecotoxicological effects for the 3 different exposures and the extreme complexity of the relationship between physical and chemical pollutants, as well as the need to measure many different endpoints along the biological organization able to obtain a wider ecotoxicological picture.

4.4 Effects on the proteome

The last step of the multi-tier approach was proteomics, a high-throughput technology which complements existing techniques on revealing the MoA of toxic substances. We focused the discussion only on the changed proteins whose functions can be related to results revealed by the other two applied approaches, while the description of the other classes of modulated proteins is shown in the ESI.†

4.4.1 Structural proteins. Unlike the other two treatments, the PNP–TCS complex treatment selectively modified two specific structural proteins (Fig. 6A), namely the crystallin γ M2d2 (CryM2d2) and collagen type XIV α1b (Col4α1b), confirming the zebrafish eye as a target for NPs, as also pointed out by microscopy (Fig. 2). This evidence is of particular interest as it may be closely related to the hyperactivity of zebrafish larvae observed after the exposure to the PNP–TCS complex (Fig. 4) since visual defects have been identified precisely as one of the possible causes of behavioral changes.[35]

CryM2d2 is a structural constituent of the vertebrate lens crystallin which is mainly composed by α-, β- and γ-crystallin proteins.[43] Although the γM-crystallin class represents more than 70% of the eye lens proteins in zebrafish,[44] their functional role is not completely clear. Interestingly, Pande *et al.*[45] reported that γ-crystallins are essential for maintaining lens transparency since their aggregation decreases the lens homogeneity and leads to cataract. Thus, the over-production of CryM2d2 noticed after the PNP–TCS complex exposure could be a signal of eye defects due to an increased crystallization of the γ-crystallins, whose deposits in the lens are typical in several non-genetic forms of cataract.[46]

A different function is related to Col4α1b, the other structural protein modulated only by the PNP–TCS complex, whose change can be related to eye function. Col4α1b belongs to the superfamily of fibril-associated collagens with interrupted triple helices (FACIT)[47] which is present in some connective tissues, such as the skin, tendons, and cornea.[48] Its main function is the regulation of the formation and size of the collagens fibrils to guarantee the stability and integrity of the extracellular matrix and its fibrillar collagen network.[49] Young *et al.*[50] found that type XIV collagen is highly expressed in the early stage of development of chicken embryos and it is involved in the regulation of fibrillogenesis in the corneal stroma.

The clear evidence that the two structural proteins modulated exclusively by the PNP–TCS complex are directly related to eye development and that they can be the possible reason for the hyperactivity noticed pointed out the need of future in-depth studies on the effect exerted by plastics and their adsorbed environmental pollutants in the early stages of eye development. This represents another proof about the change of the ecotoxicological behaviour when the two pollutants were administered bound together and probably due to the capability of PNPs to have the eye as a carrier, but at the same time to exert these specific effects only when in combination with TCS. On the other hand, previous studies identified the eye as one of the preferential targets for NPs: van Pomeren *et al.*[51] demonstrated the deposition of 25 and 50 nm PNPs in the zebrafish eye and Lee *et al.*[52] observed the accumulation of 50 nm PNPs in the retina of zebrafish embryos at 24 hours post-fertilization (hpf).

4.4.2 Proteins of energetic pathways. This was the biggest group of proteins modulated by TCS (Fig. 7), suggesting a direct effect of the chemical on the energy stock and energetic pathways able to determine the hypo-activity observed after the behavioral tests (Fig. 4).

The KEGG (Kyoto Encyclopedia of Genes and Genomes) PATHWAY database highlighted that 4 proteins (fructose-bisphosphate aldolase C-A, aldoca; glycogenin 1b, Gyg1b; glutaryl-CoA dehydrogenase, Gcdhl; ATPase H^+-transporting V1, Atp6v1ab) out of 6 modulated by TCS were involved in some energetic pathways. In detail, aldoca is directly involved in one of the essential sub-pathways of glycolysis that synthesizes D-glyceraldehyde 3-phosphate and glycerone phosphate from D-glucose. Since several previous studies on fish species[53–56] showed an up-regulation of aldoca during conditions reflecting a strong energy demand, the increased production of this glycolytic enzyme noticed in our experiments suggested the need of an energy over-production for zebrafish larvae through the formation of glycolytic ATP molecules, probably to counteract the effects due to TCS. One of the possible effects of TCS could thus be related to a rise of energy demand and the subsequent decrease in the energy stock available to other activities. Therefore, the hypo-activity revealed after the TCS exposure (Fig. 4) can be an indirect consequence of this energy lowering. This hypothesis seemed to be also confirmed by the downregulation of Gyg1b (Fig. 6A) which is involved in glycogen biosynthesis, fundamental as an energetic reserve. Unfortunately, no

previous studies are available for Gyg in *Danio rerio* but, from the ecotoxicological point of view, since the skeletal muscles use glycogen as the main source of energy for anaerobic metabolism to fuel short and intense activity, the downregulation of Gyg1b suggested once more a deficit in the energy storage at muscular level that could explain the movement decrease observed during the behavioral assays.

The functions of the other two proteins belonging to the energy group (Gcdhl and Atp6v1ab) that were downregulated by TCS also supported this hypothesis. Indeed, Gcdhl is a mitochondrial protein involved in the pathway of fatty acid degradation that catalyzes the transformation of glutaryl-CoA into crotonyl-CoA.[57] This is one of the final steps to produce acetyl-CoA, the entry molecule for the citric acid cycle that represents the main energy supply for animals. In humans, GCDH deficiency creates a neurodegenerative disease (glutaric aciduria type 1) characterized by an irreversible dystonic–dyskinetic movement disorder due to striatal neuronal death.[58]

Atp6v1ab, previously known as Atp6v1a, is indirectly related to glycolysis and pentose phosphate pathways involved in the ATP metabolic process and hydrogen ion transmembrane transport. Besides representing a proton transporter for all the steps of the energy pathways, this protein is also involved in the crucial role of ammonia excretion in zebrafish larvae. Indeed, Shih *et al.*[59] demonstrated that the H^+-ATPase of the apical membrane of the pump-rich cells (HRCs) of the *Danio rerio* gills contribute to more than 70% of skin acid secretion and that the knockdown of the H^+-pump gene Atp6v1a significantly decreased the NH_4^+ secretion.

4.4.3 Cytoskeleton proteins. Five out of the 8 modulated proteins in common between PNPs and the PNP–TCS complex belong to the cytoskeleton (myosin heavy polypeptide 1, skeleton muscle, Myhz1.1; myosin heavy polypeptide 2, fast muscle-specific, Myhz2; myosin heavy chain b, Myhb, slow myosin heavy chain 1, Smyhc1; plectin a, Pleca). These 5 up-regulated proteins are mainly related to the skeletal muscle system development and organization in zebrafish[60–63] (Table S2†). Very interestingly, the KEGG PATHWAY database revealed that three of them (Myhz2, Myhb and Smyhc1) are also functional elements of the paracellular tight junctions (TJs) of skeletal muscles that connect the absorptive epithelial cells at the apical membrane in the gastrointestinal tract.[64] TJs are multiprotein complexes whose main function is to assemble a paracellular barrier, allowing a selective diffusion on the basis of size and charge of ions and molecules.[65] According to most recent data, ions and molecules are hypothesized to permeate through the TJs by two different routes: pore and leak pathways.[66,67] The first one is the preferential pathway for molecules smaller than 0.4 nm,[68] while the leak pathway is a nonspecific way of entrance for macromolecules with a diameter up to 6 nm.[69] Although the PNPs administered to zebrafish in our study, with a size of 0.5 μm, should not enter through the TJs, they modified the amount of three of the structural proteins of this paracellular barrier which regulate actin in order to control the cell polarity. Thus, the same co-regulation noticed both for PNPs and the PNP–TCS complex might point out a possible alteration in the intercellular defence mechanism related just to PNPs.

At a more general level of discussion, the great impact on cytoskeleton proteins highlighted for PNPs and the PNP–TCS complex confirmed that the increase of oxidative stress is the main effect of these physical contaminants. Indeed, several studies have shown that the proteins of the cytoskeleton are one of the first targets of oxidative stress,[70–72] as also found in our previous study in which we administered two different mixtures of MPs to the freshwater bivalve *D. polymorpha*.[8]

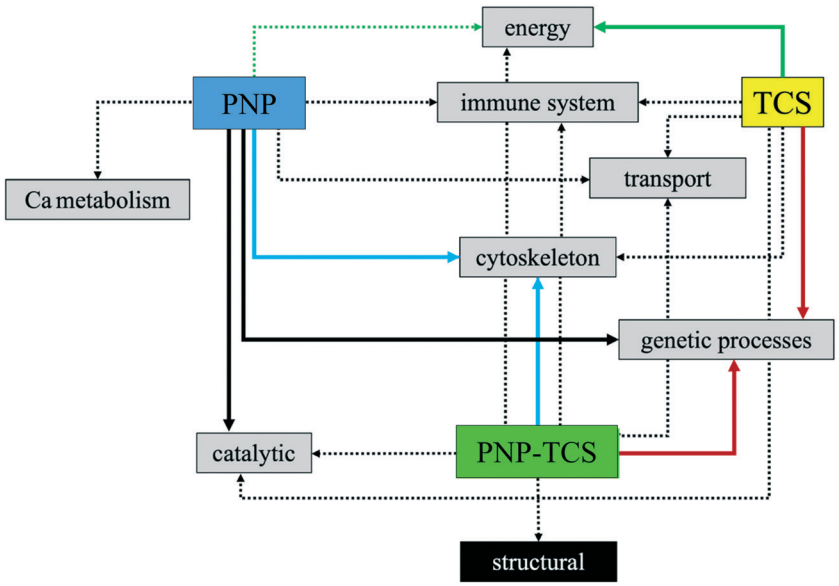

Fig. 8 Outline of proteomic results: dotted lines = low to medium effect of the contaminant; solid lines = high effect of the contaminant; same colour = similar effect of contaminants (high number of co-modulated proteins).

4.4.4 Final remarks for proteomics. Proteomics has proven to be a very useful and sensitive tool in the evaluation of ecotoxicity due to NPs, whose infiltration in the organism's tissues follows different pathways than chemicals, passing through the biological barriers and/or exploiting the transmembrane canals and TJs, depending on their size. The logical consequence is that the number of NPs that enters the organism tends to be lower than the number of chemicals which simply follow a concentration gradient, constraining the use of very sensitive analytical methodologies to observe the presence of NPs in the tissues and also to evaluate their toxicological effects. The high-throughput technology based on proteomics is surely one of the possible solutions because of its sensitivity that allows the evaluation of the impact made on different cellular pathways and suggests possible MoAs, as demonstrated in this study. Indeed, proteomics confirmed that the combined effect of chemical and physical pollutants should be considered more as a modification of toxicological behavior rather than a mere increase or decrease in toxicity, since the PNP–TCS complex not only modulated both proteins in common with TCS and PNPs but also changed several other proteins not modulated by the two contaminants administered alone. The most evident case is the one related to the two structural proteins up-regulated by the PNP–TCS complex alone, thus suggesting a complementary effect on the early stages of eye development only when the two contaminants were bound together.

Fig. 8 summarizes the network of proteins related to the same biological function and the relative effect of the three different contaminants. This toxicological behavior explains exactly what was said previously, namely that the PNP–TCS complex intrinsically possesses the ability to act both on protein targets modulated by PNP and TCS alone and to acquire new toxicological characteristics.

5. Conclusions

The purpose of this study was to open a new perspective on investigating the risk associated to the action of NPs as carriers of environmental pollutants. Overall, the whole data set obtained with the multi-step approach made a clear response to the main goal of this study, since it highlighted that the formation of the PNP–TCS complex heavily modified the toxicological behaviour of the single contaminants. It almost seems that the bond between chemical and physical compounds creates a kind of new pollutant with emerging and unpredictable characteristics that are able to change the toxicological pathways and targets. From the ecotoxicological point of view, our multiple results highlighted how the PNP–TCS complex showed a change in toxicological behavior with respect to individual contaminants instead of a simple decrease or increase of toxicity, suggesting the need to go beyond classical models based on additive, synergistic or antagonist effects that regulate interactions between chemical pollutants.

Another crucial result obtained is related to the need for a multilevel approach that covers many steps of biological organization. Indeed, differences found in the responses clearly showed that its application is critical, especially in this kind of studies, in which the relation between chemical and physical compounds is unknown and leads to unpredictable effects.

Ethical statement

All animal procedures were performed in accordance with the Guidelines for Care and Use of Laboratory Animals of the University of Milan and approved by the Animal Ethics Committee of the Italian Ministry of Health (Aut. Min. no. 6/2019-PR).

Conflicts of interest

There are no conflicts to declare.

References

1 R. Geyer, J. R. Jambeck and K. L. Law, Production, use, and fate of all plastics ever made, *Sci. Adv.*, 2017, **3**, e1700782.
2 T. O'Brine and R. C. Thompson, Degradation of plastic carrier bags in the marine environment, *Mar. Pollut. Bull.*, 2010, **60**, 2279–2283.
3 N. B. Hartmann, T. Huffer, R. C. Thompson, M. Hasselov, A. Verschoor, A. E. Daugaard, S. Rist, T. Karlsson, N. Brennholt, M. Cole, M. P. Herrling, M. C. Hess, N. P. Ivleva, A. L. Lusher and M. Wagner, Are we speaking the same language? Recommendations for a definition and categorization framework for plastic debris, *Environ. Sci. Technol.*, 2019, **53**, 1039–1047.
4 K.-W. Lee, W. J. Shim, O. Y. Kwon and J.-H. Kang, Size-dependent effects of micro polystyrene particles in the marin copepod *Tigriopus japonicus*, *Environ. Sci. Technol.*, 2013, **47**, 11278–11283.
5 Y. Lu, Y. Zhang, Y. Deng, W. Jiang, Y. Zhao, J. Geng, L. Ding and H. Ren, Uptake and accumulation of polystyrene microplastics in zebrafish (Danio rerio) and toxic effects in liver, *Environ. Sci. Technol.*, 2016, **50**, 4054.
6 L. Lei, S. Wu, S. Lu, M. Liu, Y. Song, Z. Fu, H. Shi, K. M. Raley-Susman and D. He, Microplastic particles cause intestinal damage and other adverse effects in zebrafish Danio rerio and nematode Caenorhabditis elegans, *Sci. Total Environ.*, 2018, **619–620**, 1–8.
7 S. Magni, F. Gagné, C. André, C. Della Torre, J. Auclair, H. Hanana, C. C. Parenti, F. Bonasoro and A. Binelli, Evaluation of uptake and chronic toxicity of virgin polystyrene microbeads in freshwater zebra mussel Dreissena polymorpha (Mollusca: Bivalvia), *Sci. Total Environ.*, 2018, **631–632**, 778–788.
8 S. Magni, C. Della Torre, G. Garrone, A. D'Amato, C. C. Parenti and A. Binelli, First evidence of protein modulation by polystyrene microplastics in a freshwater biological model, *Environ. Pollut.*, 2019, **250**, 407–415.
9 C. C. Parenti, A. Ghilardi, C. Della Torre, S. Magni, L. Del Giacco and A. Binelli, Evaluation of the infiltration of polystyrene nanobeads in zebrafish embryo tissues after

short-term exposure and the related biochemical and behavioural effects, *Environ. Pollut.*, 2019, **254**, 112947.
10 M. S. S. Silva, M. Oliveira, D. Lopéz, M. Martins, E. Figueira and A. Pires, Do nanoplastics impact the ability of the polychaeta Hediste diversicolor to regenerate?, *Ecol. Indic.*, 2020, **110**, 105921.
11 X. Liu, J. Xu, Y. Zhao, H. Shi and C. H. Huang, Hydrophobic sorption behaviors of 17ß-Estradiol on environmental microplastics, *Chem*, 2019, **226**, 726–735.
12 K. N. Fotopoulou and H. K. Karapanagioti, Surface properties of beached plastic pellets, *Mar. Environ. Res.*, 2012, **81**, 70–77.
13 F. Yu, C. Yang, Z. Zhu, X. Bai and J. Ma, Adsorption behavior of organic pollutants and metals on micro/nanoplastics in the aquatic environment, *Sci. Total Environ.*, 2019, **694**, 133643.
14 F. Wang, K. M. Shih and X. Y. Li, The partition behavior of perfluoro-octanesulfonate (PFOS) and perfluoro-octanesulfonamide (PFOA) on microplastics, *Chem*, 2015, **119**, 841–847.
15 X. C. Shen, D. C. Li, X. F. Sima, H. Y. Cheng and H. Jiang, The effects of environmental conditions on the enrichment of antibiotics on microplastics in simulated natural water column, *Environ. Res.*, 2018, **166**, 377–383.
16 J. Li, K. Zhang and H. Zhang, Adsorption of antibiotics on microplastics, *Environ. Pollut.*, 2018, **237**, 460–467.
17 B. Nowack and T. D. Bucheli, Occurrence, behavior and effects of nanoparticles in the environment, *Environ. Pollut.*, 2007, **150**, 5–22.
18 S. Jagini, S. Konda, D. Bhagawan and V. Himabindu, Emerging contaminant (triclosan) identification and its treatment: A review, *SN Appl. Sci.*, 2019, **1**, 640.
19 L. M. Weatherly and J. A. Gosse, Triclosan exposure, transformation, and human health effects, *J. Toxicol. Environ. Health, Part B*, 2017, **20**(8), 447–469.
20 C. Wu, K. Zhang, X. Huang and J. Liu, Sorption of pharmaceuticals and personal care products to polyethylene debris, *Environ. Sci. Pollut. Res.*, 2016, **23**, 8819–8826.
21 K. Syberg, A. Nielsen, F. R. Khan, G. T. Banta, A. Palmqvist and P. M. Jepsen, Microplastic potentiates triclosan toxicity to the marine copepod *Acartia tonsa* (Dana), *J. Toxicol. Environ. Health, Part A*, 2017, **80**(23–24), 1369–1371.
22 R. R. Tice, E. Agurell, D. Anderson, B. Burlinson, A. Hartmann, H. Kobayashi, Y. Miyamae, E. Rojas and Y. Sasaki, Single cell gel/Comet assay: guidelines for in-vitro and in-vivo genetic toxicology testing, *Environ. Mol. Mutagen.*, 2000, **35**, 206–221.
23 M. Parolini, A. Ghilardi, C. Della Torre, S. Magni, L. Prosperi, M. Calvagno, L. Del Giacco and A. Binelli, Environmental concentrations of cocaine and its main metabolites modulated antioxidant response and caused cyto-genotoxic effects in zebrafish embryo cells, *Environ. Pollut.*, 2017, **226**, 504–514.
24 M. M. Bradford, A rapid and sensitive method for the quantification of microgram quantities of protein using the principle of protein-dye binding, *Anal. Biochem.*, 1976, **72**, 248–254.
25 O. S. Alimi, J. F. Budarz, L. M. Hernandez and N. Tufenkji, Microplastics and nanoplastics in aquatic environments: Aggregation, deposition, and enhanced contaminant transport, *Environ. Sci. Technol.*, 2018, **52**, 1704–1724.
26 Y. Li, M. Li, Z. Li, L. Yang and X. Liu, Effects of particle size and solution chemistry on triclosan sorption on polystyrene microplastic, *Chemosphere*, 2019, **213**, 308–314.
27 J. P. da Costa, P. S. M. Santos, A. C. Duarte and T. Rocha-Santos, (Nano)plastics in the environment - Sources, fates and effects, *Sci. Total Environ.*, 2016, **566–567**, 15–26.
28 Q. Chen, D. Yin, Y. Jia, S. Schiwy, J. Legradi, S. Yang and H. Hollert, Enhanced uptake of BPA in the presence of nanoplastics can lead to neurotoxic effects in adult zebrafish, *Sci. Total Environ.*, 2017, **609**, 1312–1321.
29 Y. Ma, A. Huang, S. Cao, F. Sun, L. Wang, H. Guo and R. Ji, Effects on nanoplastics and microplastics on toxicity, bioaccumulation, and environmental fate of phenanthrene in fresh water, *Environ. Pollut.*, 2016, **219**, 166–173.
30 R. C. MacPhail, J. Brooks, D. L. Hunter, B. Padnos, T. D. Irons and S. Padilla, Locomotion in larval zebrafish: influence of time of day, lighting and ethanol, *Neurotoxicology*, 2009, **30**, 52–58.
31 R. M. Basnet, D. Zizioli, S. Taweedet, D. Finazzi and M. Memo, Zebrafish larvae as behavioural model in neuropharmacology, *Biomedicines*, 2019, **7**, 23.
32 L. J. Macaulay, J. M. Bailey, E. D. Levin and H. M. Stapleton, Persisting effects of a pbde metabolite, 6-oh-bde-47, on larval and juvenile zebrafish swimming behavior, *Neurotoxicol. Teratol.*, 2015, **52**, 119–126.
33 C. Y. Usenko, E. M. Robinson, S. Usenko, B. W. Brooks and E. D. Bruce, PBDE developmental effects on embryonic zebrafish, *Environ. Toxicol. Chem.*, 2011, **30**(8), 1865–1872.
34 S. Ali, D. L. Champagne and M. K. Richardson, Behavioral profiling of zebrafish embryos exposed to a panel of 60 water-soluble compounds, *Behav. Brain Res.*, 2012, **228**, 272–283.
35 S. Ali, D. L. Champagne, A. Alia and M. K. Richardson, Large-scale analysis of acute ethanol exposure in zebrafish development: a critical time window and resilience, *PLoS One*, 2011, **6**(5), e20037.
36 T. D. Irons, P. E. Kelly, D. L. Hunter, R. C. Macphail and S. Padilla, Acute administration of dopaminergic drugs has differential effects on locomotion in larval zebrafish, *Pharmacol., Biochem. Behav.*, 2013, **103**, 792–813.
37 L. D. Ellis, J. Seibert and K. H. Soanes, Distinct models of induced hyperactivity in zebrafish larvae, *Brain Res.*, 2012, **1449**, 46–59.
38 A. Binelli, L. Del Giacco, N. Santo, L. Bini, S. Magni, M. Parolini, L. Madaschi, A. Ghilardi, D. Maggioni, M. Ascagni, A. Armini, L. Prosperi, L. Landi, C. La Porta and C. Della Torre, Carbon nanopowder acts as a Trojan-horse for benzo(α)pyrene in Danio rerio embryos, *Nanotoxicology*, 2017, **11**(3), 371–381.
39 Y. Peng, Y. Luo, X. P. Nie, W. Liao, Y. F. Yang and G. G. Ying, Toxic effects of triclosan on the detoxification system and breeding of Daphnia magna, *Ecotoxicology*, 2013, **22**, 1384–1394.

40 A. Karami, B. D. Groman, S. P. Wilson, P. Ismail and V. K. Neela, Biomarker responses in zebrafish (Danio rerio) larvae exposed to pristine low-density polyethylene fragments, *Environ. Pollut.*, 2017, **223**, 466–475.

41 A. Haegerbaeumer, M.-T. Mueller, H. Fueser and W. Traunspurger, Impacts of micro- and nano-sized plastic particles on benthic invertebrates: A literature review and gap analysis, *Front. Environ. Sci.*, 2019, **7**, 17.

42 C. C. Parenti, A. Ghilardi, C. Della Torre, M. Mandelli, S. Magni, L. Del Giacco and A. Binelli, Environmental concentrations of triclosan activate cellular defence mechanism and generate cytotoxicity on zebrafish (Danio rerio) embryos, *Sci. Total Environ.*, 2019, **650**, 1752–1758.

43 H. Bloemendal, W. De Jong, R. Jaenicke, N. H. Lubsen, C. Slingsby and A. Tardieu, Ageing and vision: Structure, stability and function of lens crystallins, *Prog. Biophys. Mol. Biol.*, 2004, **86**, 407–485.

44 Y. R. Lin, H. K. Mok, Y. H. Wu, S. S. Liang, C. C. Hsiao, C. H. Huang and S. H. Chiou, Comparative proteomics analysis of degenerative eye lenses of nocturnal rice eel and catfish as compared to diurnal zebrafish, *Mol. Vision*, 2013, **19**, 623–637.

45 A. Pande, J. Pande, N. Asherie, A. Lomakin, O. Ogun, J. King and G. B. Benedek, Crystal cataracts: Human genetic cataract caused by protein crystallization, *Proc. Natl. Acad. Sci. U. S. A.*, 2001, **98**(11), 6116–6120.

46 A. Mumford, I. Cree, J. Arnold, M. Hagan, K. Rixon and J. Harding, The lens in hereditary hyperferritinaemia cataract syndrome contains crystalline deposits of L-ferritin, *Br. J. Ophthalmol.*, 2000, **84**, 697–700.

47 H. L. Bader, E. Lambert, A. Guiraud, M. Malbouyres, W. Driever, M. Koch and F. Ruggiero, Zebrafish collagen XIV is transiently expressed in epithelia and is required for proper function of certain basement membranes, *J. Biol. Chem.*, 2013, **288**, 6777–6787.

48 T. Manon-Jensen and M. A. Karsdal, in *Biochemistry of collagens, laminins and elastin: Structure, function and biomarkers*, ed. M. A. Karsdal, ScienceDirect, 2016, vol. 272.

49 J.-B. Oudart, J.-C. Monboisse and F. X. Maquart, Type XIX collagen: A new partner in the interactions between tumor cells and their microenvironment, *Matrix Biol.*, 2017, **57–58**, 169–177.

50 B. B. Young, G. Zhang, M. Koch and D. E. Birk, The roles of types XII and XIV collagen in fibrillogenesis and matrix assembly in the developing cornea, *J. Cell. Biochem.*, 2002, **87**, 208–220.

51 M. van Pomeren, N. R. Brun, W. J. G. M. Peijnenburg and M. G. Vijver, Exploring uptake and biodistribution of polystyrene (nano)particles in zebrafish embryos at different developmental stages, *Aquat. Toxicol.*, 2017, **190**, 40–45.

52 W. S. Lee, H.-J. Cho, E. Kim, J. H. Hu, H.-J. Kim, B. Kim, J.-S. Lee and J. Jeong, Bioaccumulation of polystyrene nanoplastics and their effect on the toxicity of Au ions in zebrafish embryos, *Nanoscale*, 2019, **11**, 3173.

53 S. A. M. Martin, O. Vilhelmsson, F. Médale, P. Watt, S. Kaushik and D. F. Houlihan, Proteomic sensitivity to dietary manipulations in rainbow trout, *Biochim. Biophys. Acta*, 2003, **1651**, 17–29.

54 O. T. Vilhelmsson, S. A. M. Martin, F. Mèdale, S. J. Kaushik and D. F. Houli-han, Dietary plant-protein substitution affects hepatic metabolism in rainbow trout (Oncorhynchus mykiss), *Br. J. Nutr.*, 2004, **92**, 71–80.

55 R. W. Smith, P. Cash, S. Ellefsen and G. E. Nilsson, Proteomic changes in the crucian carp brain during exposure to anoxia, *Proteomics*, 2009, **9**, 2217–2229.

56 P. Gómez-Requeni, L. E. C. Conceição, A.-E. O. Jordal and I. Rønnestad, A reference growth curve for nutritional experiments in zebrafish (Danio rerio) and changes in whole body proteome during development, *Fish Physiol. Biochem.*, 2010, **36**, 1199–1215.

57 K. S. Rao, M. Albro, T. M. Dwyer and F. E. Frerman, Kinetic Mechanism of Glutaryl-CoA Dehydrogenase, *Biochemistry*, 2006, **45–51**, 15853–15861.

58 J. Gao, C. Zhang and X. Luo, Effects of targeted suppression of glutaryl-CoA dehydrogenase by lentivirus-mediated shRNA and excessive intake of lysine on apoptosis in rat striatal neurons, *PLoS One*, 2013, **8**(5), e63084.

59 T.-H. Shih, J.-L. Horng, P.-P. Hwang and L.-Y. Lin, Ammonia excretion by the skin of zebrafish (Danio rerio) larvae, *Am. J. Physiol.*, 2008, **295**, 1625–1632.

60 M. Codina, J. Li, J. Gutiérrez, J. P. Y. Kao and S. J. Du, Loss of Smyhc1 or Hsp90alpha1 function results in different effects on myofibril organization in skeletal muscles of zebrafish embryos, *PLoS One*, 2010, **5**, e8416.

61 H. Nord, A. C. Burguiere, J. Muck, C. Nord, U. Ahlgren and J. von Hofsten, Differential regulation of myosin heavy chains defines new muscle domains in zebrafish, *Mol. Biol. Cell*, 2014, **25**, 1384–1395.

62 J. B. Buhrdel, S. Hirth, M. Kessler, S. Westphal, M. Forster, L. Manta, G. Wiche, B. Schoser, J. Schessl, R. Schroder, C. S. Clemen, L. Eichinger, D. O. Furst, P. F. van der Ven, W. Rottbauer and S. Just, In vivo characterization of human myofibrillar myopathy genes in zebrafish, *Biochem. Biophys. Res. Commun.*, 2015, **461**, 217–223.

63 K. Henke, J. M. Daane, M. B. Hawkins, C. M. Dooley, E. M. Busch-Nentwich, D. L. Stemple and M. P. Harris, Genetic screen for postembryonic development in the zebrafish (Danio rerio): Dominant mutations affecting adult form, *Genetics*, 2017, **207**, 609–623.

64 G. Asmonaite, H. Sundh, N. Asker and B. C. Almroth, Rainbow trout maintain intestinal transport and barrier functions following exposure to polystyrene microplastics, *Environ. Sci. Technol.*, 2018, **52**, 14392–14401.

65 J. Hou, in *The Paracellular Channel: Biology, Physiology and Disease*, Elsevier, 2019, vol. 248.

66 C. T. Capaldo and A. Nusrat, Claudin switching: Physiological plasticity of the tight junction, *Semin. Cell Dev. Biol.*, 2015, **42**, 22–29.

67 A. Tervonen, T. O. Ihalainen, S. Nymark and J. Hyttinen, Structural dynamics of tight junctions modulate the properties of the epithelial barrier, *PLoS One*, 2019, 0214876.

68 C. M. Van Itallie, J. Holmes, A. Bridges and J. M. Anderson, Claudin-2-dependent changes in noncharged solute flux are mediated by the extracellular domains and require attachment to the PDZ-scaffold, *Ann. N. Y. Acad. Sci.*, 2009, **1165**, 82–87.

69 M. M. Buschmann, L. Shen, H. Rajapakse, D. R. Raleigh, Y. Wang, Y. Wang, A. Lingaraju, J. Zha, E. Abbott, E. M. McAuley, L. A. Breskin, L. Wu, K. Andreson, J. R. Turner and C. R. Weber, Occludin OCEL-domain interactions are required for maintenance and regulation of the tight junction barrier to macromolecular flux, *Mol. Biol. Cell*, 2013, **24**, 3056–3068.

70 C. Riva, S. Cristoni and A. Binelli, Effects of triclosan in the freshwater Dreissena polymorpha: A proteomic investigation, *Aquat. Toxicol.*, 2012, **118–119**, 62–71.

71 C. Wilson and C. Gonzalez-Billault, Regulation of cytoskeletal dynamics by redox signaling and oxidative stress: Implications for neuronal development and trafficking, *Front. Cell. Neurosci.*, 2015, **9**, 381.

72 E. Belcastro, W. Wu, I. Fries-Raeth, A. Corti, A. Pompella, P. Leroy, I. Larteaud and C. Gaucher, Oxidative stress enhances and modulates protein S-nitrosation in smooth muscle cells exposed to S-nitrosoglutathione, *Nitric Oxide*, 2017, **69**, 10–21.

Supporting Information

2. EXPERIMENTAL

2.1 *PNPs characterization*

Table S1. Chemical parameters of PNPs measured by the Malvern Zetasizer Nano ZS instrument (Malvern instruments, UK) in the exposure medium. Data referred to a concentration of 1 mg/L. Size distribution is reported as average ± standard deviation of 3 measurements.

PNPs	Zeta-potential	Size distribution
No-fluo	*-36.27 ± 0.67 mV*	*716.13 ± 23.14 nm* 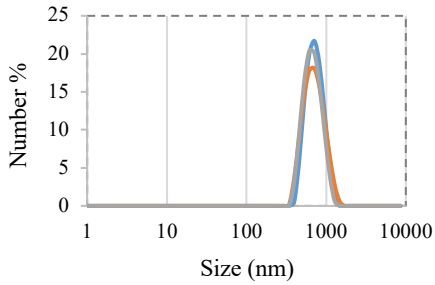
Fluo	*-33.77 ± 0.38 mV*	*474.73 ± 2.34 nm* 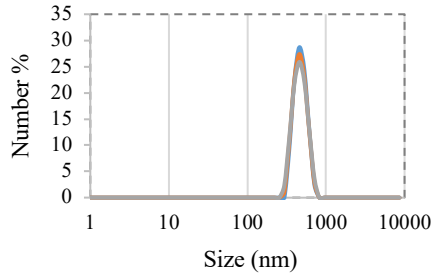

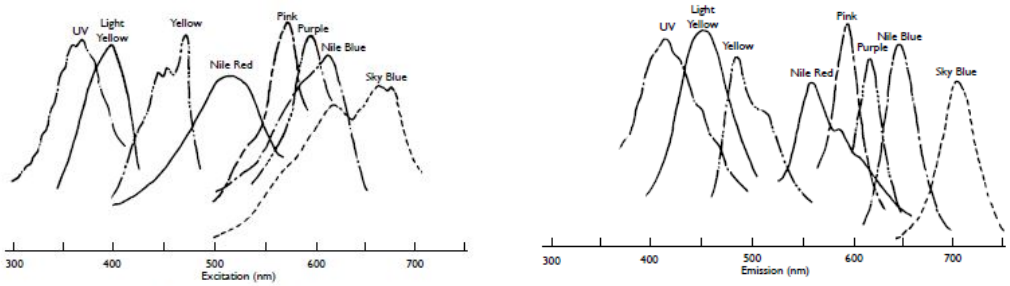

Fig. S1. Excitation and emission spectra of the fluorophore used in the fluorescent particles (Spherotech, Inc., Lake Forest, IL, USA).

2.2 *Biomarker*

To evaluate the levels of genotoxicity 7 larvae for each experimental group were pooled together and manually homogenized in PBS 0.01 M. First of all, cell viability was evaluated by the trypan blue dye exclusion method, mixing an aliquot of 10 µL of homogenates with 10 µL of 0.4% (w/v) trypan blue solution in PBS (three replicates per experimental group). Non-viable cells were stained deep blue. Later, the apoptotic and necrotic cell frequency (%) was assessed on 300 cells per slide (n = 9; three slides per pool), using a fluorescence microscope (Leitz DMR). An aliquot (10 µL) of homogenates was resuspended in LMA (Low Melting Agarose, 0.7% in PBS, pH 7.4), and distributed on slides pre-coated with a thin layer of NMA (Normal Melting Agorose, 1% PBS, pH 7.4). After fixation, slides were immersed in a lysis solution (NaCl 2.5 M, Na_2EDTA 100 mM, Tris-HCl 8 mM, pH 10) and maintained at 4°C in dark. Slides were then fixed in absolute ethanol. Before observations, cell nuclei were stained with DAPI. The frequency of micronuclei (MN ‰) was calculated on 400 cells per slide (n = 6; two slides per pool), using a fluorescence microscope (Leitz DMR). An aliquot (40 µL) of homogenates was distributed on slides and fixed for 15 min at real temperature (r.t). Slides were washed with glutaraldehyde solution (1% PBS) for 5 min, and PBS (0.01 M), and coloured for 5 min with bisbenzimide (Hoechst 33258, 1 µg/mL). In the end, samples were washed with a 1:1 glycerol:Mcllvaine solution (1:1).

The effects on detoxification and antioxidant systems were evaluated on pools of 35 larvae (3 pools for each treatment) homogenized in potassium phosphate buffer pH 7.4 (100 mM), with the addition of KCl (100 mM), EDTA (1 mM), protease inhibitors (1:100, v/v) and dithiothreitol (DTT; 1 mM). The homogenates were centrifuged at 15,000 *g* for 10 min at 4 °C and the recovered supernatants were used to measure the level of EROD, GST, SOD, CAT and GPx. EROD activity was evaluated by spectrofluorimetric analysis. Samples were added in a solution containing Tris (50 mM), BSA (5.32 g/mL in Tris), 7-ER (100 µM), and NADPH (3 mM). The reaction took place at 37°C in dark, in a thermostatic bath. After 20 min of incubation, samples were placed on ice and glycine (2 M) was added to terminate the reaction. A fast centrifugation at maximum speed was then applied to collect

the supernatants and fluorescence was read at $\lambda_{ex/em}$=535/590 nm using the EnSight™ multimode plate reader. Results were normalized using a resorufine standard curve (0.001-1 µM) and a blank (Tris 50 mM). The GST activity was measured by adding reduced glutathione (1 mM) in phosphate buffer (100 mM, pH 7.4) and using CDNB (1 mM) as substrate. The difference in absorbance (ΔOD) was measured for 1 min at 340 nm using the spectrophotometer (Jenway, UK). SOD activity was determined by measuring the degree of inhibition of cytochrome c (10 mM) reduction by the superoxide anion generated by the xanthine oxidase (1.87 mU/mL)/hypoxanthine (50 mM) reaction at 550 nm. The activity was given as SOD units (1 SOD unit = 50% inhibition of the xanthine oxidase reaction). The CAT activity was determined by measuring the consumption of H_2O_2 (50 mM) in potassium phosphate buffer (100 mM, pH 7), measuring the ΔOD for 2 at 240 nm using the spectrophotometer (Jenway, UK). The GPx activity was assessed monitoring the consumption of NADPH at 340 nm using 0.2 mM H_2O_2 as substrate in 50 mM potassium phosphate buffer (pH 7) including glutathione (2 mM), sodium azide (NaN_3; 1 mM), glutathione reductase (2 U/mL), and NADPH (120 mM). The quantification of ROS was calculated using dichlorofluorescein diacetate (DCFH-DA), a pigment that emits fluorescence when oxidized. Samples were transferred into a 96 multi-well plate and incubated at r.t. for 5 min. Then, PBS and DFCH-DA (10 mg/mL) were added and the plate was incubated again for 30 min at 37 °C. The ROS concentration was measured by fluorescence at 485/530 nm (excitation/emission) using the Ensight™ multimode plate reader.

To assess the presence of a neurotoxic effect on exposed organisms, pools of 12 larvae were homogenized as described above. Samples (three replicates per experimental group) were transferred into a 96 multi-well plate adding phosphate buffer (100 mM, pH 7.4), 5,5'-dithiobis-2-nitrobenzoic acid (DTNB, 5 mM) and acetylthiocholine (ASCh, 1 mM). The activity level of AChE was assessed measuring fluorescence at 412 nm for 15 min using the EnSight™ multimode plate reader.

2.3 *Functional proteomics*

Pools of 20 larvae for each experimental group (3 pools for each treatment) were homogenized in a lysis buffer composed of (4-(2-hydroxyethyl)-1-piperazineethanesulfonic acid (HEPES) 20 mM pH 7.5, sucrose 320 mM, ethylenediaminetetraacetic acid (EDTA) 1 M pH 8.5, (ethylene glycol-bis(β-aminoethyl ether)-N,N,N',N'-tetraacetic acid (EGTA) 5 mM pH 8.1, sodium orthovandate (Na_3VO_4) 1 mM, β-glycerophosphate 10 mM, sodium fluoride (NaF) 10 mM, sodium pyrophosphate (NaPPi) 10 mM, phenylmethylsulfonyl fluoride (PMSF) 1 mM in ethanol, dithiothreitol (DTT) 5 mM e protease inhibitors (Roche) in Milli Q® water[1]. Homogenates were centrifuged at 15,000 g for 10 min at 4 °C and proteins were quantified in the supernatant using the Bradford method[2]. Then, 200 µg of proteins for each group were precipitated in a procedure using methanol/chloroform/Milli Q® water (4:1:3 v/v). The pellets were suspended again in a solution of urea 8 M in Tris-HCl 50 mM, sodium chloride (NaCl) 30 mM pH 8.5 and protease inhibitors (Roche). Samples were centrifuged at 14,000 g for 30 min at 4 °C and proteins were re-quantified. Then, 10 µg of proteins were incubated in DTT 50 mM in ammonium bicarbonate (AMBIC) 50 mM for 30 min at 52 °C under stirring to reduce the disulphide bonds. Later, iodoacetamide (IANH2) 100 mM in AMBIC 50 mM was added and samples were incubated for 20 min at room temperature (r.t.) under stirring to alkylate the sulfhydryl groups. Proteins were then digested adding trypsin (Trypsin Sequencing Grade, Roche, Italy) in AMBIC 50 mM and samples were incubated over-night at 37 °C under stirring. Peptides were then purified by reverse phase chromatography, using Zip Tips (µ-C18; Millipore, Milan, Italy; Magni et al., 2019). In particular, peptides were purified and analysed at UNITECH OMICs (University of Milan, Italy) by the Dionex Ultimate 3000 nano-LC (Sunnyvale CA, USA) in connection with the Orbitrap Fusion™ Tribrid™ Mass Spectrometer (Thermo Scientific, Bremen, Germany). Proteins were identified using the Proteome Discoverer software 2.2 (Thermo Scientific) against the research database Uniprot-zebrafish.fasta and setting trypsin as digestive enzyme.

We measured the differences in abundance ratio (AR) between treatments and control for the total of identified proteins (minimum of two identified peptides). Two significance thresholds were applied

on the entire dataset to guarantee the goodness of data and the biological meaning, based respectively on the p value ($p<0.05$) and a minimum of 2-fold change difference in comparison with controls.

3. RESULTS

3.1 *Effects at individual level*

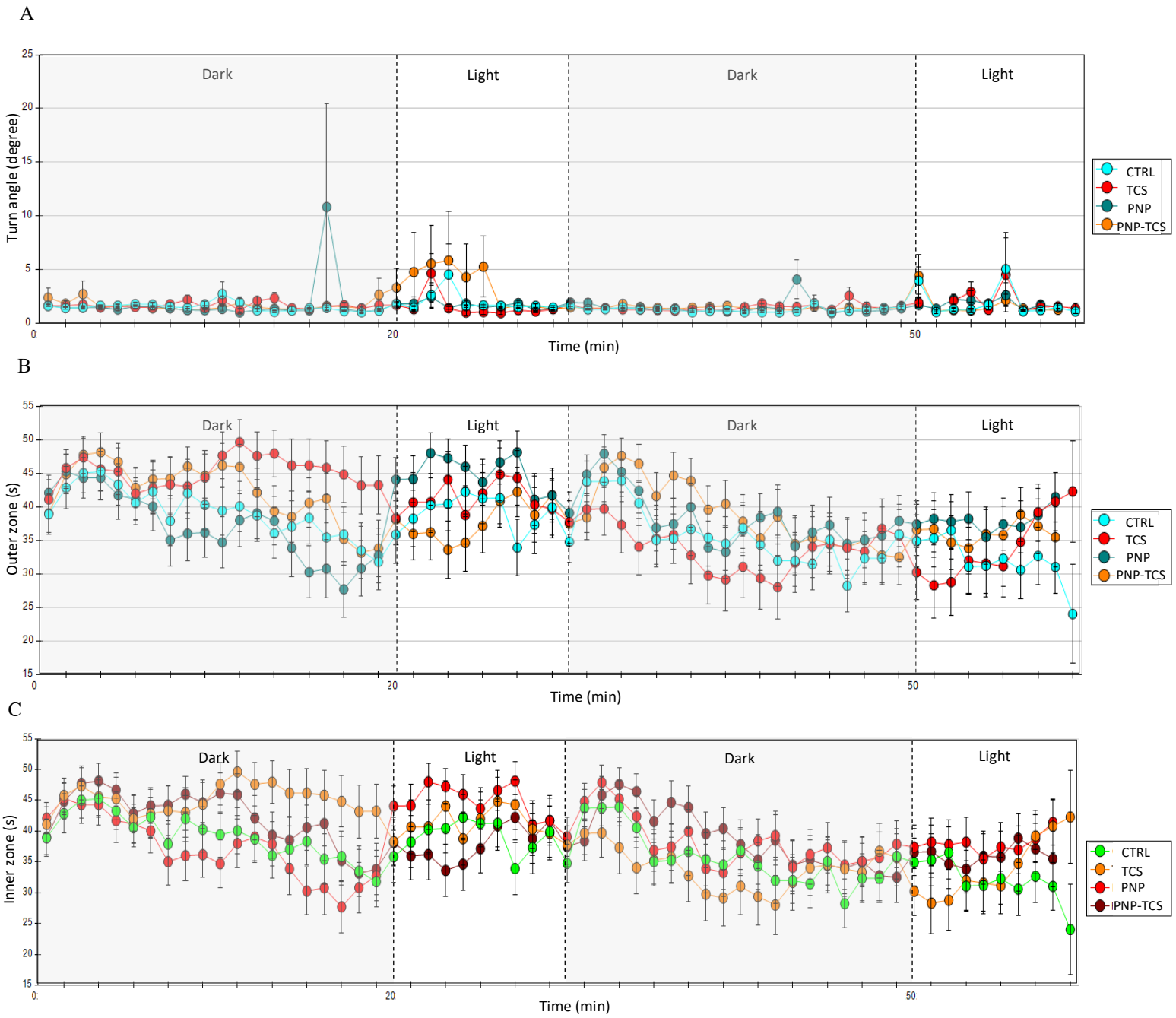

Fig. S2. Swimming activity measured in zebrafish larvae exposed to PNP (200 µg/L), TCS (0.6 µg/L) and PNP-TCS, compared to control. (A) Turn angle per minute (mean±S.E.); (B) Time spent in the outer zone per minute (mean±S.E.); (C) Time spent in the inner zone per minute (mean±S.E.).

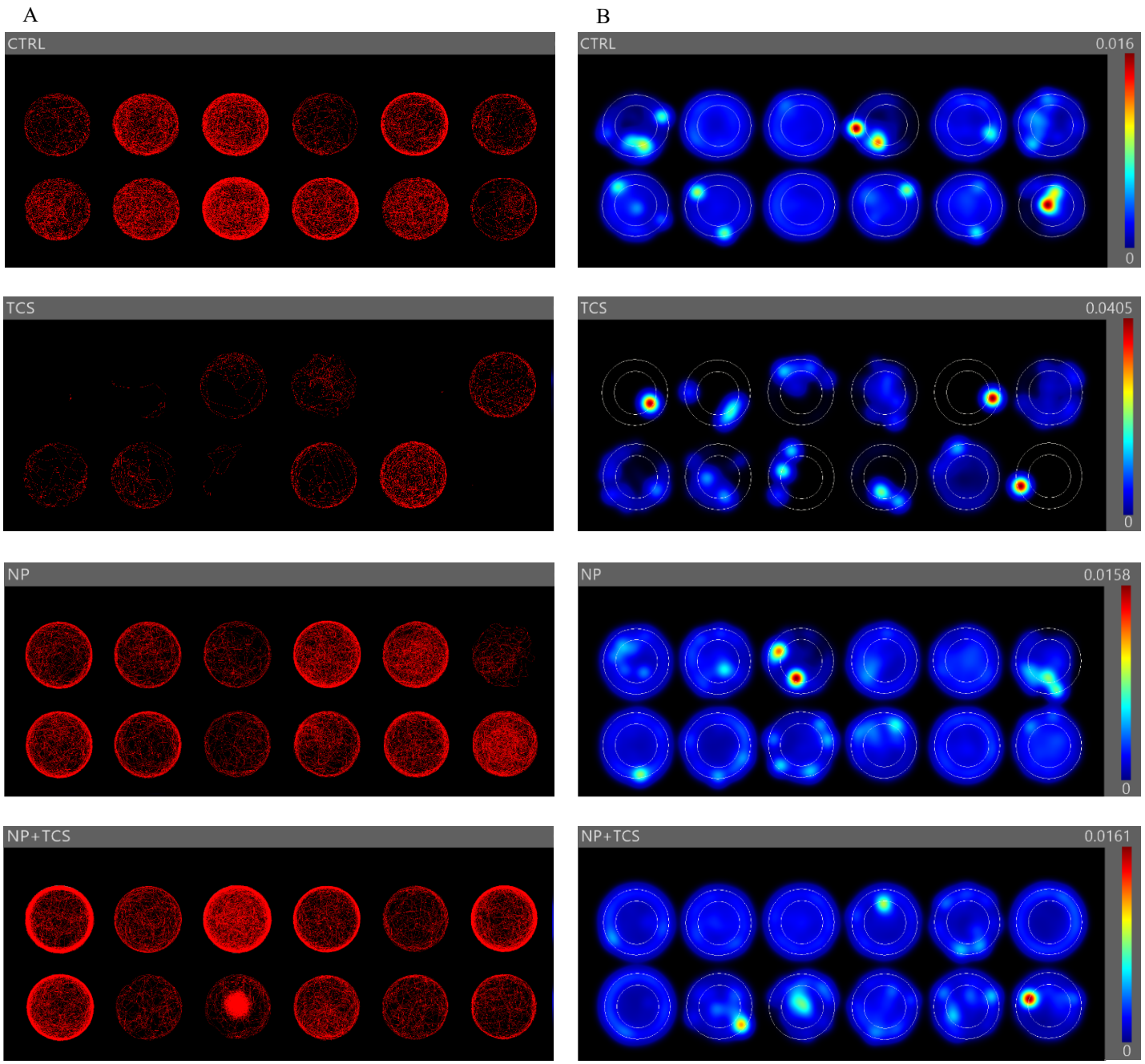

Fig. S3. Graphical representations of larval swimming activity, for each experimental group (data from one exposure). (A) Tracks; (B) Heatmaps.

4. DISCUSSION

4.1 *Effects on proteome*

4.1.1 *Proteins involved in genetic processes*

All the 5 proteins involved in genetic processes modified by the PNP-TCS complex (ELAV-like protein, *Elavl4*; TAR DNA-binding protein, *Tardbpl*; UDP-N-acetylhexosamine pyrophosphorylase-like protein 1, *Uap1/1*; heterogeneous nuclear ribonucleoprotein C1/C2, *Hnrnpc*; importin subunit α, *Kpna4*) were in common with TCS and were co-regulated in the same way (Fig. 6A). Three of them (*Elavl4*, *Tardbpl*, *Hnrnpc*) revealed also the same molecular function based on the RNA binding and belong to the RNA recognition motif (RRM) family that is known to selectively bind single-stranded RNAs[3]. RRM is one of the most abundant protein domains in eukaryotes and it is able to bind a multitude of RNA sequences and proteins. Eukaryotic RRM proteins are present in all post-transcriptional events, such as pre-mRNA processing, splicing and alternative splicing, mRNA stability and export, RNA editing, translation regulation and degradation[4].

Specifically, *Elavl4*, also known as *HuD*, is implicated in the early stage (from 14 hpf) of differentiation and specification of individual neurons in the development of zebrafish nervous system[5]. Akten et al.[6] pointed out a new interaction between *HuD* and the survival motor neuron (SMN) protein in spinal motor axons that selectively bind the cpg15-mRNA, whose transport and translation deficit are associated with some neurologic disorders, such as the fragile X syndrome and tuberous sclerosis[7,8]. The observed down-regulation of *Elavl4* can suggest a decreased capability to form the SMN-*HuD* complex with the consequence of negative effects on the development of motor axons and neuromuscular junctions due to TCS both alone and bound to PNPs.

The role played by *Tardbpl* in zebrafish is more complicated because it represents the homologue of *Tardbp*, whose orthologue *TARDBP* is implicated in the amyotrophic lateral sclerosis (ALS) in humans[9]. Very interestingly, Kabashi et al.[10] pointed out that the knockdown of *Tardbp* in zebrafish generated shorter and disorganized motor neuron axons and reduced coiling ability, while the knockdown of the homologue *Tardbpl* did not generate any defects. Hewamadduma et al.[11] showed

that *tardbp* mutation leads to the generation of a novel *tardbpl* splice form able of making a full-length *Tardbp* protein (*Tardbpl-FL*), which compensates for the loss of *Tardbp*. Since *Tardbpl* seems to be the product of alternative splicing able to block some neurogenerative disorders, its downregulation observed after the exposures to TCS and PNP-TCS complex could represent another signal of possible negative effects on the nervous system development in zebrafish, as also suggested by the modulation of *Elavl4*.

The role played by *Hnrnpc* is still little known. The KEEG PATHWAY Database highlighted that this protein is involved in the RNA binding and specifically belongs to the spliceosome protein complex that assemble on the mRNA precursor and help fold it for the subsequently transesterification.

The other two proteins co-modulated by TCS and PNP-TCS involved in genetic processes were the UDP-N-acetylhexosamine pyrophosphorylase-like protein 1 (*Uap1/1*) and importin subunit α (*Kpna4*) which are related to the nuclear import signal receptor activity and nuclear localization sequence binding, respectively.

4.1.2 *Catalytic proteins*

All the three contaminants impacted also on some proteins involved in catalytic activity, of which only the glutamine synthetase (*Gs*) are in common among the three treatments (Fig. 6A). *Gs* catalyzes several metabolic reactions, being a fundamental enzyme to maintain in fish the amino acid balance, neurotransmitter regulation and the biosynthesis of nucleotides and urea[12-14]. The simultaneous downregulation observed for *Gs* is particularly interesting in the light of its specific function related to the ammonia catalysis by the condensation of glutamate and ammonia into glutamine to counteract the ammonia increase in the body[15]. This means a possible disfunction in the ammonia elimination for zebrafish larvae mainly due to TCS exposure that downregulated also the above-mentioned *Atp6v1a* also related to this crucial function. Indeed, *Gs* activity is generally high in the brain of fish[16] to protect this organ from the harmful effect of ammonia, even if it is present also in other organs,

such as liver, muscle, kidney, stomach and intestine[15]. The need of the well-functioning of this enzyme is proven by the accumulation of ammonia in the extra- and intracellular compartments of fish exposed to high levels of this chemical in the aquatic ecosystems that can drive to convulsion, coma and death[17]. For instance, Wright et al.[18] found a significant ($p<0.05$) increase of *Gs* activity in brain and liver of rainbow trout (*O. mykiss*) exposed to high level of NH_4Cl for 48 h, while Dhanasiri et al.[15] demonstrated a rise of *Gs* enzyme activity in response to increased ammonia levels in zebrafish exposed to high level of ammonia in water during 72 h simulated transport. This impact on the ammonia elimination should be in-depth investigated because it is the first time that this very dangerous effect for fish larvae linked to both PNPs and TCS exposures has been identified.

The F-box protein 2 (*Fbox2*) was the other in common regulated protein belong to catalytic group, with a difference to the other changed ones because it was upregulated by TCS but downregulated by PNP-TCS complex (Fig. 6A). *Fbox2* is a neuron-enriched ubiquitin ligase substrate adaptor subunit that binds specifically glycoproteins containing high-mannose oligosaccharides, contributing to ubiquitination of N-glycosylated proteins through the endoplasmic reticulum-associated degradation (ERAD)[19]. This function is particularly important for the amyloid precursor protein (APP), a membrane glycoprotein whose degradation by-product showed the accumulation in Alzheimer disease[20]. However, APP is not only involved in the most common neurodegenerative disorder, but it has several roles in neuronal function and development, such as synapse formation, neurite outgrowth and neuronal survival[21,22]. Very intriguing, Atkin et al.[23] demonstrated as APP is not only a substrate for *Fbox2*, but also that it decreased in non-neuronal cells in the presence of *Fbox2*, while increased in hippocampal neurons and brain tissues in *Fbox2* knock-out mice. This opens interesting questions about the possible role played by TCS to affect this protein with the fundamental function of APP regulation and its possible implication in the Alzheimer disease. We have not a clear explanation for the opposite regulation of *Fbox2* due to TCS alone and PNP-TCS complex; one of the possible hypotheses could be due to the translocation of TCS in different neuron compartments mediated by the PNPs and the consequent different effect on this protein.

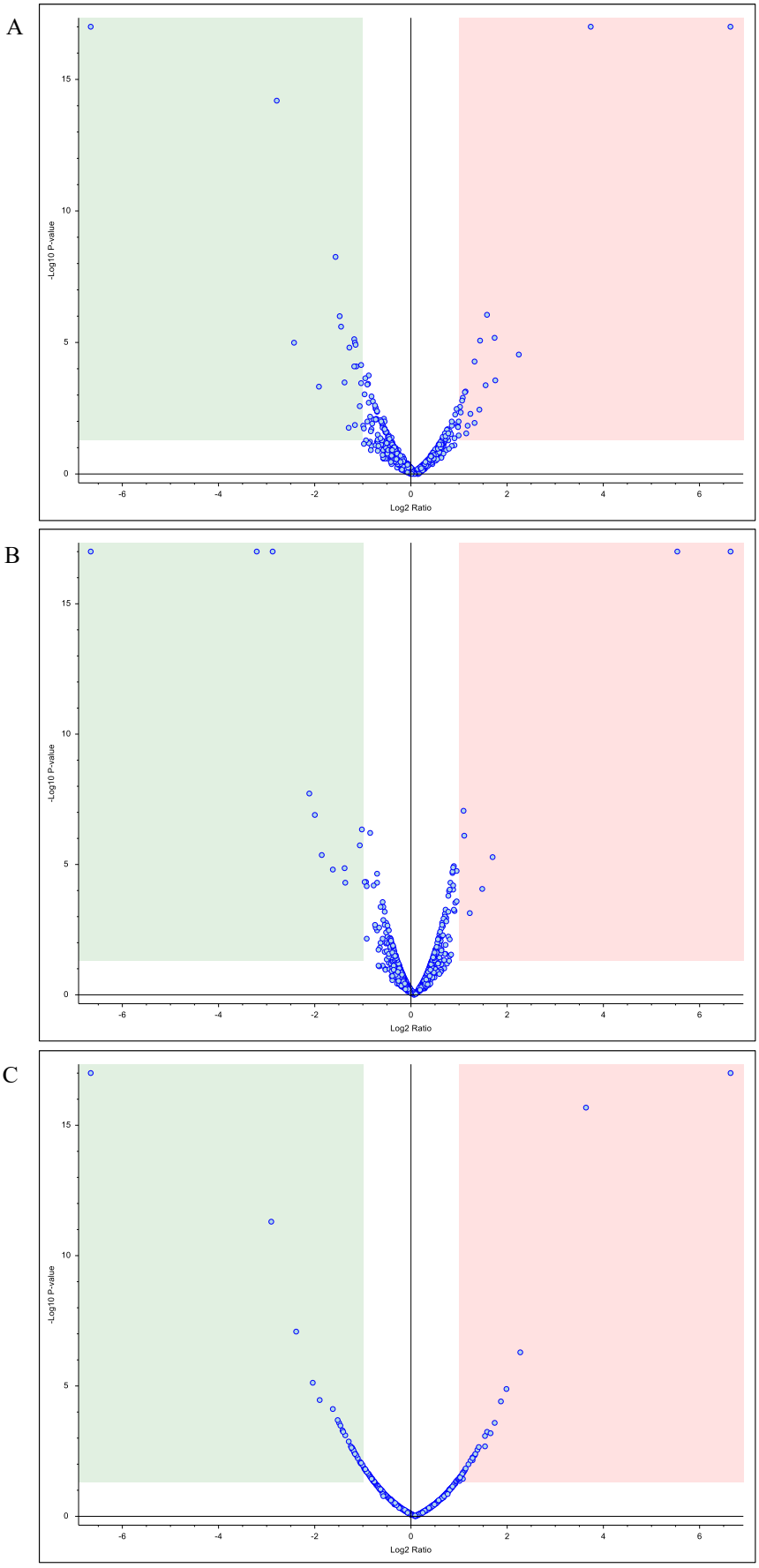

Fig. S4. Volcano plots illustrating significantly differentially modulated proteins in zebrafish larvae exposed to (A) PNP (200 µg/L), (B) TCS (0.6 µg/L) and (C) PNP-TCS. The green and red squares denote ±2-fold change and $p<0.05$, which are the significance thresholds (prior to logarithmic transformation).

Table S2. Description of modulated proteins in zebrafish larvae exposed to PNP (200 µg/L), TCS (0.6 µg/L) and PNP-TCS, compared to control. MW = Molecular Weight, pI = isoelectric point, AR = Abundance Ratio, a = not significant value (p>0.05).

Main Function	UniProt Accession	Description	Peptides	Unique Peptides	MW (kDa)	pI	AR: PNP/CTRL	AR: TCS/CTRL	AR: PNP-TCS/CTRL
Cytoskeleton structure									
	C5IG37	beta-actin	19	1	24.8	5.31	0.603[a]	0.641[a]	0.409
	A9JRS6	keratin 4	47	2	54.0	5.39	0.443	0.938[a]	0.489[a]
	Q7ZVD3	lim-domain binding factor 3a	5	2	31.6	9.04	0.557[a]	0.109	NOT FOUND
	F1QVX3	myosin, heavy chain b	64	3	222.5	5.90	13.419	0.780[a]	12.551
	B3DJM6	myosin, heavy polypeptide 1, skeletal muscle	165	7	222.0	5.67	3.010	0.943[a]	3.959
	B8A569	myosin, heavy polypeptide 1.3, skeletal muscle	161	6	222.1	5.69	2.031[a]	0.716[a]	3.673
	Q6IQX1	myosin, heavy polypeptide 2, fast muscle-specific	151	11	221.7	5.69	2.201	0.914[a]	3.007
	Q6DHF0	myozenin 1b	5	1	28.8	5.60	0.507[a]	0.953[a]	0.357
	A0A286YBE9	plectin a	4	2	543.8	7.03	100.000	1.226[a]	100.000
	F1Q4X3	si:dkey-222n6.2	4	2	44.1	5.41	4.782	100.000	100.000
	A0MQ61	slow myosin heavy chain 1	43	14	222.8	5.66	2.728	1.038[a]	4.834
	B8A6B8	thymosin beta	2	2	5.2	8.47	0.385	1.046[a]	0.772[a]
	A5X6X6	titin b	83	1	3198.2	6.33	2.229[a]	1.686[a]	3.152
	Q9PUB6	type i cytokeratin	32	1	46.7	5.49	1.944[a]	46.817	2.033[a]
Immune system									
	F1Q7P7	pdgfa associated protein 1b	3	1	19.9	9.19	0.187	0.231	0.193
Genetic processes									
	Q7ZUQ9	cirbp protein	10	1	19.2	9.31	0.455	0.618[a]	0.546[a]
	F1R6L3	cold-inducible rna-binding protein b	11	2	23.6	8.84	0.489	0.764[a]	0.450[a]
	Q4V914	core histone macro-h2a	10	10	39.8	9.83	2.129	0.875[a]	2.191[a]
	F1R133	elav-like protein	10	1	45.0	9.28	0.145	0.138	0.134
	Q6NYV3	h1 histone family, member 0	5	4	21.2	10.86	2.096	1.071[a]	1.796
	A0A140LGU1	heterochromatin protein 1,-binding protein 3	19	19	66.8	9.67	2.191	0.941[a]	1.837[a]
	X1WDH8	histone h2b	11	1	13.5	10.21	3.346	NOT FOUND	NOT FOUND
	Q6PUQ6	importin subunit α	2	1	59.0	5.24	0.268	0.252	0.245

	A0A0R4I9N0	purine-rich element-binding protein ab	3	2	31.3	7.49	100.000	0.823[a]	0.794[a]
	A0A2R8PYV5	tar dna-binding protein,-like	6	1	34.5	6.61	NOT FOUND	0.010	0.010
	A0A2R8RZT8	udp-n-acetylhexosamine pyrophosphorylase-like protein 1	2	1	56.3	5.94	0.878[a]	100.000	2.917
	A0A0R4IKH3	zgc: 55733 (heterogeneous nuclear ribonucleoprotein c1/c2)	2	1	32.5	5.66	0.408[a]	0.327	0.271
Energy source/production									
	E7FCD8	atpase h+-transporting v1 subunit ab	15	1	68.3	5.58	1.553[a]	0.391	0.573[a]
	A0A1L1QZG0	chaperonin containing tcp1, subunit 2 (beta)	6	1	11.2	5.01	2.688[a]	2.353	2.675[a]
	Q6P969	elongation factor 1-alpha	9	2	50.3	9.07	2.947	3.267	1.237[a]
	A0A2R8QMC2	fructose-bisphosphate aldolase	2	1	40.5	7.02	100.000	100.000	0.870[a]
	A0A0R4ISN6	glutaryl-coa dehydrogenase b	3	2	17.0	8.19	0.692[a]	0.483	0.571[a]
	Q6IQP1	glycogenin 1b	2	1	36.0	5.49	0.010	0.010	0.010
	Q6TNR9	phosphoglycerate mutase	8	1	28.8	7.18	0.675[a]	0.949[a]	0.326
	B2GTJ4	rab5a protein	4	1	23.4	8.13	0.010	NOT FOUND	0.010
	B2GRK9	tkt protein	21	1	68.0	7.20	100.000	0.800[a]	1.421[a]
Catalytic activity									
	E9QDI1	apolipoprotein c-i	4	4	9.9	5.41	0.448	0.862[a]	0.439[a]
	A0A286YAE3	apolipoprotein c-ii	3	3	12.7	5.90	0.368	0.776[a]	0.445[a]
	Q6TEP3	glutamine synthetase	2	1	42.0	6.84	0.010	0.010	0.010
	Q3YA99	integrin beta	2	1	86.5	5.66	1.093[a]	0.886[a]	0.376
	A0A2R8QDD8	protein phosphatase, mg2+/mn2+-dependent, 1aa	3	1	43.0	5.30	NOT FOUND	NOT FOUND	0.010
	Q6PC06	s-adenosylhomocysteine hydrolase-like 2	6	1	65.0	7.61	0.010	NOT FOUND	NOT FOUND
	F8W4J1	serine protease 59, tandem duplicate 2	6	6	28.0	5.03	1.082[a]	2.137	1.112[a]
	B0BLX4	zgc: 175088 (f-box protein 2)	5	1	20.0	4.44	0.511[a]	100.000	0.423
	B3DIZ3	zgc:171967	4	1	104.1	5.40	0.620[a]	0.386	0.449[a]
Transport									
	A0A2R8QJH4	calcium-transporting atpase	4	2	110.7	5.45	NOT FOUND	0.010	0.010[a]
	Q5BLF6	hemoglobin beta embryonic-3	6	1	16.6	8.44	3.403	100.000	1.339[a]
	B3DGI9	translocase of inner mitochondrial membrane 8 homolog b	2	2	10.7	5.80	0.360	0.733[a]	0.350

Calcium metabolism									
	Q804W0	parvalbumin 1	11	8	11.4	4.64	0.492	0.888[a]	0.531[a]
	Q5U3P2	parvalbumin 8	6	5	11.9	4.64	0.452	0.824[a]	0.654[a]
	Q6XG62	protein s100	9	4	10.4	5.21	0.442	0.841[a]	0.430[a]
Developmental processes									
	F8W2I6	galectin	5	1	15.3	7.94	0.885[a]	2.157	0.823[a]
Structural activity									
	A0A0R4IP59	collagen, type xiv, alpha 1b	5	5	84.5	5.35	1.436[a]	0.932[a]	2.918
	A0A2R8Q1I4	crystallin, gamma m2d2	9	1	21.4	7.81	0.986[a]	1.227[a]	3.350
Other									
	A7MBR3	pdz domain-containing 1	5	5	60.5	5.99	0.612[a]	1.121[a]	0.389
	X1WDJ4	si:dkey-248g15.3	2	2	7.8	8.50	0.414	0.497	0.363
	A0A0R4ITV0	si:dkey-46i9.1	2	2	7.3	5.45	0.338	0.675[a]	0.380

5. REFERENCES

1. A. Binelli, L. Del Giacco, N. Santo, L. Bini, S. Magni, M. Parolini, L. Madaschi, A. Ghilardi, D. Maggioni, M. Ascagni, A. Armini, L. Prosperi, L. Landi, C. La Porta and C. Della Torre, Carbon nanopowder acts as a Trojan-horse for benzo(α)pyrene in *Danio rerio* embryos, *Nanotoxicol.*, 2017, **11(3)**, 371-381.
2. M. M. Bradford, A rapid and sensitive method for the quantification of microgram quantities of protein using the principle of protein-dye binding, *Anal. Biochem.*, 1976, **72**, 248-254.
3. C. Maris, C. Dominguez, and F. H. T. Allain, The RNA recognition motif, a plastic RNA-binding platform to regulate post-transcriptional gene expression, *FEBS J.*, 2005, **272(9)**, 2118-2131.
4. E. Birney, S. Kumar and A. R. Krainer, Analysis of the RNA-recognition motif and RS and RGG domains: Conservation in metazoan pre-mRNA splicing factors, *Nucleic Acids Res.*, 1993, **21**, 5803-5816.
5. H. C. Park, S. K. Hong, H. S. Kim, S. H. Kim, E. J. Yoon, C. H. Kim, N. Miki and T. L. Huh, Structural comparison of zebrafish Elav/Hu and their differential expressions during neurogenesis, *Neurosci. Lett.*, **279**, 81-84.
6. B. Akten, M. J. Kye, L. T. Hao, M. H. Wertz, S. Singh, D. Nie, J. Huang, T. T. Merianda, J. L. Twiss, C. E. Beattie, J. A. J. Steen and M. Sahin, Interaction of survival of motor neuron (SMN) and HuD proteins with mRNA cpg15 rescues motor neuron axonal deficits, *PNAS*, 2011, **108**, 10337-10342.
7. H. Wang, Dynamic association of the fragile X mental retardation protein as a messenger ribonucleoprotein between microtubules and polyribosomes, *Mol. Biol. Cell.*, 2008, **19**, 105-114.
8. D. Nie, A. Di Nardo, J. M. Han, H. Baharanyi, I. Kramvis, T. Huynh, S. Dabora, S. Codeluppi, P. P. Pandolfi, E. B. Pasquale and M. Sahin, Tsc2-Rheb signaling regulates EphA-mediated axon guidance, *Nat. Neurosci.*, 2010, **13(2)**, 163-172.
9. M. Neumann, D. M. Sampathu, L. K. Kwong, A. C. Truax, M. C. Micsenyi, T. T. Chou, J. Bruce, T. Schuck, M. Grossman and C. M. Clark, L. F. McCluskey, B. L. Miller, E. Masliah, I. R. Mackenzie, H. Feldman, W. Feiden, H. A. Kretzschmar, J. Q. Trojanowski and V. M-Y. Lee, Ubiquitinated TDP-43 in frontotemporal lobar degeneration and amyotrophic lateral sclerosis, 2006, *Science*, **314**, 130-133.
10. E. Kabashi, L. Lin, M. L. Tradewell, P. A. Dion, V. Bercier, P. Bourgouin, D. Rochefort, S. Bel Hadj, H. D. Durham, C. Vande Velde, G. A. Rouleau and P. Drapeau, Gain and loss of function of ALS-related mutations of TARDBP (TDP-43) cause motor deficits in vivo, *Hum. Mol. Genet.*, 2010, **19(4)**, 671-683.

11. C. A. A. Hewamadduma, A. J. Grierson, T. P. Ma, L. Pan, C. B. Moens, T. Ramesh and P. J. Shaw, Tardbpl splicing rescues motor neuron and axonal development in a mutant tardbp zebrafish, *Hum. Mol. Genet.*, 2013, **22**, 2376-2386.
12. P. J. Walsh and T. P. Mommsen, in *Evolutionary considerations of nitrogen metabolism and excretion*, ed. P. Wright and P. Anderson, Academic Press, San Diego, 2001, Nitrogen excretion, 1-30.
13. P. Anderson, in *Urea and glutamine synthesis: environmental influences on nitrogen excretion*, ed. P. Wright and P. Anderson, Academic Press, San Diego, 2001, Nitrogen excretion, 239-277.
14. I. Suárez, G. Bodega and B. Fernández, Glutamine synthetase in brain: Effect of ammonia, *Neurochem. Int.*, 2002, **41**, 123-142.
15. A. K. S. Dhanasiri, J. M. O. Fernandes and V. Kiron, Glutamine synthetase activity and the expression of three glul paralogues in zebrafish during transport, *Comp. Biochem. Physiol.*, 2012, **163**, 274-284.
16. L. A. Sanderson, P. A. Wright, J. W. Robinson, J. S. Ballantyne and N. J. Bernier, Inhibition of glutamine synthetase during ammonia exposure in rainbow trout indicates a high reserve capacity to prevent brain ammonia toxicity, *J. Exp. Biol.*, 2010, **213**, 2343-2353.
17. D. J. Randall and T. K. N. Tsui, Ammonia toxicity in fish, *Mar. Pollut. Bull.*, 2002, **45**, 17-23.
18. P. A. Wright, S. L. Steele, A. Huitema and N. J. Bernier, Induction of four glutamine synthetase genes in brain of rainbow trout in response to elevated environmental ammonia, *J. Exp. Biol.*, 2007, **210**, 2905-2911.
19. Y. Yoshida, T. Chiba, F. Tokunaga, H. Kawasaki, K. Iwai, T. Suzuki, Y. Ito, K. Matsuoka, M. Yoshida, K. Tanaka and T. Tai, E3 ubiquitin ligase that recognizes sugar chains, *Nature*, 2002, **418**, 438-442.
20. L. Bertram, C. M. Lill, and R. E. Tanzi, The genetics of Alzheimer disease: Back to the future, *Neuron.*, 2010, **68**, 270-281.
21. D. Puzzo, L. Privitera, M. Fa', A. Staniszewski, G. Hashimoto, F. Aziz, M. Sakurai, E. M. Ribe, C. M. Troy, M. Mercken, S. S. Jung, A. Palmeri and O. Arancio, Endogenous amyloid-ß is necessary for hippocampal synaptic plasticity and memory, *Ann. Neurol.*, 2011, **69**, 819-830.
22. S. H. Tyan, A. Y. Shih, J. J. Walsh, H. Maruyama, F. Sarsoza, L. Ku, S. Eggert, P. R. Hof, E. H. Koo and D. L. Dickstein, Amyloid precursor protein (APP) regulates synaptic structure and function, *Mol. Cell Neurosci.*, 2012, **51**, 43-52.
23. G. Atkin, E. Minakawa, L. Sharkey, N. Tipper, W. Tennant and H. L. Paulson, *J. Biol. Chem.*, 2014, **289**, 7038-7048.

4. CONCLUDING REMARKS AND FUTURE PERSPECTIVES

The first part of the project provided an overview of the effects of PS micro- and nanoplastics on two of the most known freshwater model organisms. First of all, we demonstrated that zebrafish embryos can passively ingest a large number of plastic nanobeads (0.5 µm), which not only were able to accumulate in the intestinal tract, but also to pass through the intestinal barrier, moving to other organs, such as gills and neuromast. Concerning the effects of the exposure, the results highlighted the activation of the oxidative stress defense and the alteration of swimming behavior, which could be coupled with neurotoxic effects.

Furthermore, the uptake of plastic particles of greater dimensions (1 and 10 µm) was also assessed in freshwater zebra mussels, after only 6 days of exposure. In detail, microplastics were observed in the animal gut lumen, tissues and circulatory system. However, microplastic uptake did not seem to induce some alterations both of oxidative balance and neuro-genotoxicity in exposed mussels, at least for the selected endpoints. Nevertheless, subsequent functional proteomics analysis showed significant protein modulation in zebra mussels exposed to the same microbeads, which suggested the activation of the antioxidant machinery. Controversial responses clearly demonstrated that the application of a multi-tier approach is essential to investigate the potential toxicity of these physical contaminants.

The uptake and effects of nanoplastics (0.5 µm) were also investigated at terrestrial level, in the Lepidoptera *B. mori*. The obtained results demonstrated the capability of silkworm larvae to ingest nanobeads, which were able to pass the intestinal barrier, reaching the circulatory system and the internal tissues and organs. As previous studies, the slight and non-exhaustive results emerged from the measured endpoints confirmed the need to use several approaches that allow the comparison and integration of the entire dataset. Indeed, neither significant impact at cellular and molecular levels nor alteration of larval life cycle emerged from the bioassays, while the most relevant outcome emerged from the behavior observations, since nanoplastics affected silkworm locomotor activity, with potential negative indirect effects on survival and fitness.

Finally, the purpose of the conclusive study was to open a new perspective on investigating the risk associated to the action of nanoplastics as carrier of TCS. A preliminary study confirmed the toxicity of environmental concentrations of TCS on zebrafish embryos, evidencing the induction of oxidative stress response and significant cytotoxicity. In parallel, an adsorption experiment was conducted to assess nanoplastic capacity to adsorb TCS and to create artificially contaminated plastic nanobeads. TCS adsorption did not modify plastic particle intake, since both virgin and TCS-contaminated nanoplastics were ingested by zebrafish larvae and were visualized in their tissues. Moreover, the multi-tier approach has highlighted the importance of choosing the toxicity endpoints according to the experimental conditions. Indeed, our results demonstrated a different sensitivity degree among the used approaches, since biomarkers did not show neither an imbalance in the antioxidant response mechanism nor a genetic damage due to virgin and contaminated nanobeads, while the evaluation of the swimming behavior and proteomics seemed to be more prone to reveal the potential hazard made by these pollutants and their complex. Furthermore, the behavioural assays coupled with proteomics pointed out a shift in the toxicity made by the plastic particles and TCS administered alone compared to their complex, suggesting a much more complicated relation among them than a simple additive or synergic effect.

In summary, the entire project filled some gaps on plastic particle infiltration in organism tissues and on their potential toxicological effects, alone and combined with chemical contaminants, but it also highlighted the need for deeper investigations performing longer exposures and applying a multi-tiered approach. Furthermore, it pointed out the sensitivity and capability of proteomics to investigate the deepest effects due to micro- and nanoplastics, that might not emerge from other analyses. However, to correctly evaluate the environmental risks of micro- and nanoplastics, further efforts are absolutely needed for a better understanding of the fate and behavior of these physical contaminants, both through laboratory studies, but also by field surveys to better evaluate the complexity of this environmental problem.

5. REFERENCES

Alabi, O. A., Ologbonjaye, K. I., Awosolu, O., Alalade, O. E., 2019. Public and environmental health effects of plastic wastes disposal: A review. *J. Toxicol. Risk Assess.* 5, 021.

Al-Jaibachi, R., Cuthbert, R. N., Callaghan, A., 2018. Up and away: Ontogenic transference as a pathway for aerial dispersal of microplastics. *Biol. Lett.* 14(9).

Al-Thawadi, S., 2020. Microplastic and nanoplastic in aquatic environments: Challenges and threats to aquatic organisms. *Arabian J. Sci. Eng.* 45, 4419-4440.

Andrady, A.L., Neal, M.A., 2009. Applications and societal benefits of plastic. *Phil. Trans. R. Soc. B* 364, 1977-1984.

Andrady, A. L., 2011. Microplastics in the marine environment. *Mar. Pollut. Bull.* 62, 1596-1605.

Avery-Gomm, S., Provencher, J. F., Liboiron, M., Poon, F. E., Smith, P. A., 2018. Plastic pollution in the Labrador Sea: An assessment using the seabird northern fulmar *Fulmarus glacialis* as a biological monitoring species. *Mar. Pollut. Bull.* 127, 817-822.

Avio, C. G., Gorbi, S., Milan, M., Benedetti, M., Fattorini, D., d'Errico, G., Pauletto, M., Bargelloni, L., Regoli, F., 2015a. Pollutants bioavailability and toxicological risk from microplastics to marine mussels. *Environ. Pollut.* 198, 211-222.

Avio, C. G., Gorbi, S., Regoli, F., 2015b. Experimental development of a new protocol for extraction and characterization of microplastics in fish tissues: First observations in commercial species from Adriatic Sea. *Mar. Environ. Res.* 111, 18-26.

Barboza, L. G. A., Vieira, L. R., Guilhermino, L., 2018. Single and combined effects of microplastics and mercury on juveniles of the European seabass (*Dicentrarchus labrax*): Changes in behavioural responses and reduction of swimming velocity and resistance time. *Environ. Pollut.* 236, 1014-1019.

Barksby, N., Dormish, J. F., Haider, K. W. (2014). Polyurethane Synthesis. In S. Kobayashi & K. Müllen (Eds.), *Encyclopedia of Polymeric Nanomaterials*. Springer, Berlin, Heidelberg.

Batel, A., Linti, F., Scherer, M., Erdinger, L., Barunbeck, T., 2016. Transfer of benzo[a]pyrene from microplastics to *Artemia nauplii* and further to zebrafish via a trophic food web experiment: CYP1A induction and visual tracking of persistent organic pollutants. *Environ. Toxicol. Chem.* 35, 1656-1666.

Bhagat, J., Zang, L., Nishimura, N., Shimada, Y., 2020. Zebrafish: An emerging model to study microplastic and nanoplastic toxicity. *Sci. Total Environ.* 728, 138707.

Besseling, E., Foekema, E. M., Van Franeker, J. A., 2015. Microplastic in a macro filter feeder: Humpback whale *Megaptera novaeangliae*. *Mar. Pollut. Bull.* 95, 248-252.

Botterell, Z. L. R., Beaumont, N., Dorrington, T., Steinke, M., Thompson, R. C., Lindeque, P. K., 2019. Bioavailability and effects of microplastics on marine zooplankton: A review. *Environ Pollut.* 245, 98-110.

Browne, M. A., Dissanayake, A., Galloway, T. S., Lowe, D. M., Thompson, R. C., 2008. Ingested microscopic plastic translocates to the circulatory system of the mussel, *Mytilus edulis* (L.). *Environ. Sci. Technol.* 42(13), 5026-5031.

Brun, N. R., van Hage, P., Hunting, E. R., Haramis, A. P. G., Vink, S. C., Vijver, M. G., Tudorache, C., 2019. Polystyrene nanoplastics disrupt glucose metabolism and cortisol levels with a possible link to behavioural changes in larval zebrafish. *Commun. Biol.* 2(1), 1-9.

Catarino, A. I., Frutos, A., Henry, T. B., 2019. Use of fluorescent-labelled nanoplastics (NPs) to demonstrate NP absorption is inconclusive without adequate controls. *Sci. Total Environ.* 670, 915-920.

Chae, Y., An, Y. J., 2018. Current research trends on plastic pollution and ecological impacts on the soil ecosystem: A review. *Environ. Pollut.* 240, 387-395.

Chen, Q., Yin, D., Jia, Y., Schiwy, S., Legradi, J., Yang, S., Hollert, H., 2017. Enhanced uptake of BPA in the presence of nanoplastics can lead to neurotoxic effects in adult zebrafish. *Sci. Total Environ.* 609, 1312-1321.

Chen, G., Feng, Q., Wang, J., 2020a. Mini-review of microplastics in the atmosphere and their risks to humans. *Sci. Total Environ.* 703, 135504.

Chen, Y., Ling, Y., Li, X., Hu, J., Cao, C., He, D., 2020b. Size-dependent cellular internalization and effects of polystyrene microplastics in microalgae *P. helgolandica* var. *tsingtaoensis* and *S. quadricauda*. *J. Hazard. Mater.* 399, 123092.

Cole, M., Lindeque, P., Fileman, E., Halsband, C., Goodhead, R., Moger, J., Galloway, T. S., 2013. Microplastic ingestion by zooplankton. *Environ. Sci. Technol.* 47(12), 6646-6655.

Cole, M., Lindeque, P., Halsband, C., Galloway, T.S., 2011. Microplastics as contaminants in the marine environment: a review. *Mar. Pollut. Bull.* 62, 2588-2597.

Cole, M., Lindeque, P. K., Fileman, E., Clark, J., Lewis, C., Halsband, C., Galloway, T. S., 2016. Microplastics alter the properties and sinking rates of zooplankton Faecal Pellets. *Environ. Sci. Technol.* 50(6), 3239-3246.

Cole, M., Galloway, T. S., 2015. Ingestion of nanoplastics and microplastics by Pacific oyster larvae. *Environ. Sci. Technol.* 49, 24, 14625-14632.

d'Ambrières, W. (2019). Plastics recycling worldwide: current overview and desirable changes, *Field Actions Science Reports,* Special Issue 19, http://journals.openedition.org/factsreports/5102.

de Haan, W. P., Sanchez-Vidal, A., Canals, M., NUREIEV1 Shipboard Scientific Party, 2019. Floating microplastics and aggregate formation in the Western Mediterranean Sea. *Mar. Pollut. Bull.* 140, 523-535.

de Sá, C. L., Luís, L. G., Guilhermino, L., 2015. Effects of microplastics on juveniles of the common goby (*Pomatoschistus microps*): confusion with prey, reduction of the predatory performance and efficiency, and possible influence of developmental conditions. *Environ. Pollut.* 196, 359-362.

Ding, J., Zhang, S., Razanajatovo, R. M., Zou, H., Zhu, W., 2018. Accumulation, tissue distribution, and biochemical effects of polystyrene microplastics in the freshwater fish red tilapia (*Oreochromis niloticus*). *Environ. Pollut.* 238, 1-9.

Dris, R., Gasperi, J., Saad, M., Mirande, C., Tassin, B., 2016. Synthetic fibers in atmospheric fallout: A source of microplastics in the environment? *Mar. Pollut. Bull.* 104(1-2), 290-293.

Eerkes-Medrano, D., Thompson, R. C., Aldridge, D. C., 2015. Microplastics in freshwater systems: a review of the emerging threats, identification of knowledge gaps and prioritisation of research needs. *Water Res.* 75, 63-82.

Farrell, P., Nelson, K., 2013. Trophic level transfer of microplastic: *Mytilus edulis* (L.) to *Carcinus maenas* (L.). *Environ. Pollut.* 177, 1-3.

Fossi, M. C., Panti, C., Guerranti, C., Coppola, D., Giannetti, M., Marsili, L., Minutoli, R., 2012. Are baleen whales exposed to the threat of microplastics? A case study of the Mediterranean fin whale (*Balaenoptera physalus*). *Mar. Pollut. Bull.* 64(11), 2374-2379.

Franzellitti, S., Canesi, L., Auguste, M., Wathsala, R. H. G. R., Fabbri, E., 2019. Microplastic exposure and effects in aquatic organisms: A physiological perspective. *Environ. Toxicol. Pharmacol.* 68, 37-51.

Frias, J. P., Nash, R., 2019. Microplastics: Finding a consensus on the definition. *Mar. Pollut. Bull.* 138, 145-147.

Frias, J. P., Sobral, P., Ferreira, A. M., 2010. Organic pollutants in microplastics from two beaches of the Portuguese coast. *Mar. Pollut. Bull.* 60(11), 1988-1992.

Fytili, D., Zabaniotou, A., 2008. Utilization of sewage sludge in EU application of old and new methods - a review. *Renew. Sust. Energ. Rev.* 12(1), 116-140.

Galgani, F., Hanke, G., Maes, T. (2015). Global distribution, composition and abundance of marine litter. In M. Bergmann, L. Gutow & M. Klages (Eds.), *Marine Anthropogenic Litter*. Springer, Cham.

Gall, S. C., Thompson, R.C., 2015. The impact of debris on marine life. *Mar. Pollut. Bull.* 92(1-2), 170-179.

Gallo, F., Fossi, C., Weber, R., Santillo, D., Sousa, J., Ingram, I., Nadal, A., Romano, D., 2018. Marine litter plastics and microplastics and their toxic chemicals components: The need for urgent preventive measures. *Environ. Sci. Eur.* 30(1), 13.

Gerdes, Z., Ogonowski, M., Nybom, I., Ek, C., Adolfsson-Erici, M., Barth, A., Gorokhova, E., 2019. Microplastic-mediated transport of PCBs? A depuration study with *Daphnia magna*. PLoS One 14(2), e0205378.

GESAMP, (2015). Sources, fate and effects of microplastics in the marine environment: a global assessment. P. J. Kershaw (Eds). GESAMP (Joint Group of Experts on the Scientific Aspects of Marine Environmental Protection), 90-96.

Geyer, R., Jambeck, J. R., Law, K. L., 2017. Production, use, and fate of all plastics ever made. *Sci. Adv.* 3(7), e1700782.

Gray, A. D., Weinstein, J. E., 2017. Size- and shape-dependent effects of microplastic particles on adult daggerblade grass shrimp (*Palaemonetes pugio*). *Environ. Toxicol. Chem.* 36(11), 3074-3080.

Guilhermino, L., Vieira, L. R., Ribeiro, D., Tavares, A. S., Cardoso, V., Alves, A., Almeida, J. M., 2018. Uptake and effects of the antimicrobial florfenicol, microplastics and their mixtures on freshwater exotic invasive bivalve *Corbicula fluminea*. *Sci. Total Environ.* 622-623, 1131-1142.

Haegerbaeumer, A., Mueller, M. T., Fueser, H., Traunspurger, W., 2019. Impacts of micro- and nano-sized plastic particles on benthic invertebrates: A literature review and gap analysis. *Front. Environ. Sci.* 7, 17.

Hahladakis, J. N., Velis, C. A., Weber, R., Iacovidou, E., Purnell, P., 2018. An overview of chemical additives present in plastics: Migration, release, fate and environmental impact during their use, disposal and recycling. *J. Hazard. Mater*. 344, 179-199.

Hale, R. C., Seeley, M. E., La Guardia, M. J., Mai, L., Zeng, E. Y., 2020. A global perspective on microplastics. *J. Geophys. Res.: Oceans*, 125, e2018JC014719.

Harrison, R. M., Hester, R. E. (2018). Plastic and the Environment, Royal Society of Chemistry.

Hartmann, N. B., Huffer, T., Thompson, R. C., Hasselov, M., Verschoor, A., Daugaard, A. E., Rist, S., Karlsson, T., Brennholt, N., Cole, M., Herrling, M. P., Hess, M. C., Ivleva, N. P., Lusher, A. L., Wagner, M., 2019. Are we speaking the same language? Recommendations for a definition and categorization framework for plastic debris. *Environ. Sci. Technol.* 53, 1039-1047.

Hidayaturrahman, H., Lee, T., 2019. A study on characteristics of microplastic in wastewater of South Korea: Identification, quantification, and fate of microplastics during treatment process. *Mar. Pollut. Bull.* 146, 696-702.

Ho, B. T., Roberts, T. K., Lucas, S., 2018. An overview on biodegradation of polystyrene and modified polystyrene: the microbial approach. *Crit. Rev. Biotechnol.* 38(2), 308-320.

Horton, A. A., Walton, A., Spurgeon, D. J., Lahive, E., Svendsen, C., 2017. Microplastics in freshwater and terrestrial environments: Evaluating the current understanding to identify the knowledge gaps and future research priorities. *Sci. Total Environ.* 586, 127-141.

Huerta Lwanga, E., Gertsen, H., Gooren, H., Peters, P., Salánki, T., van der Ploeg, M., Basseling, E., Koelmans, A. A., Geissen, V., 2016. Microplastics in the Terrestrial Ecosystem: Implications for *Lumbricus terrestris* (Oligochaeta, Lumbricidae). *Environ. Sci. Technol.* 50(5), 2685-2691.

Huerta Lwanga, E., Gertsen, H., Gooren, H., Peters, P., Salánki, T., van der Ploeg, M., Basseling, E., Koelmans, A. A., Geissen, V., 2017a. Incorporation of microplastics from litter into burrows of *Lumbricus terrestris*. *Environ. Pollut.*, 220, 523-531.

Huerta Lwanga, E., Mendoza Vega, J., Ku Quej, V., Chi, J., Sanchez Del Cid, L., Chi, C., Escalona Segura, G., Gertsen, H., Salánki, T., van der Ploeg, M., Koelmans, A. A., Geissen, V., 2017b. Field evidence for transfer of plastic debris along a terrestrial food chain. *Sci. Rep.* 7(1), 14071.

Jabeen, K., Su, L., Li, J., Yang, D., Tong, C., Mu, J., Shi, H., 2017. Microplastics and mesoplastics in fish from coastal and fresh waters of China. *Environ. Pollut.* 221, 141-149.

Jahnke, A., Arp, H. P. H., Escher, B. I., Gewert, B., Gorokhova, E., Kühnel, D., Ogonowski, M., Potthoff, A., Rummel, C., Schmitt-Jansen, M., Toorman, E., MacLeod, M., 2017. Reducing uncertainty and confronting ignorance about the possible impacts of weathering plastic in the marine environment. *Environ. Sci. Technol. Lett.* 4, 85-90.

Jambeck, J. R., Geyer, R., Wilcox, C., Siegler, T. R., Perryman, M., Andrady, A., Narayan, R., Law, K. L., 2015. Marine pollution. Plastic waste inputs from land into the ocean. *Science* 347(6223), 768-771.

Jeong, C. B., Won, E. J., Kang, H. M., Lee, M. C., Hwang, D. S., Hwang, U. K., Zhou, B., Souissi, S., Lee, S. J., Lee, J. S., 2016. Microplastic size-dependent toxicity, oxidative stress induction, and p-JNK and p-p38 activation in the monogonont rotifer (*Brachionus koreanus*). *Environ. Sci. Technol.* 50(16), 8849-8857.

Jin, Y., Xia, J., Pan, Z., Yang, J., Wang, W., Fu, Z., 2018. Polystyrene microplastics induce microbiota dysbiosis and inflammation in the gut of adult zebrafish. *Environ. Pollut.* 235, 322-329.

Karbalaei, S., Golieskardi, A., Watt, D. U., Boiret, M., Hanachi, P., Walker, T. R., Karami, A., 2020. Analysis and inorganic composition of microplastics in commercial Malaysian fish meals. *Mar. Pollut. Bull.* 150, 110687.

Karbalaei, S., Hanachi, P., Walker, T. R., Cole, M., 2018. Occurrence, sources, human health impacts and mitigation of microplastic pollution. *Environ. Sci. Pollut. Res. Int.* 25(36), 36046-36063.

Kint, D., Munoz-Guerra, S., 1999. A review on the potential biodegradability of poly(ethylene terephthalate). *Polym. Int.* 48, 346-352.

Kiyama, Y., Miyahara, K., Ohshima, Y., 2012. Active uptake of artificial particles in the nematode *Caenorhabditis elegans*. *J. Exp. Biol.* 215, 1178-1183.

Koelmans, A. A. (2015). Modeling the role of microplastics in bioaccumulation of organic chemicals to marine aquatic organisms. Critical review. In M. Bergmann, L. Gutow & M. Klages (Eds.), *Marine Anthropogenic Litter*. (pp. 313-328), Berlin: Springer.

Kögel, T., Bjorøy, Ø., Toto, B., Bienfait, A. M., Sanden, M., 2020. Micro- and nanoplastic toxicity on aquatic life: Determining factors. *Sci. Total Environ.* 709, 136050.

Kooi, M., Besseling, E., Kroeze, C., van Wezel, A. P., Koelmans, A. A. (2018). Modeling the Fate and Transport of Plastic Debris in Freshwaters: Review and Guidance. In M. Wagner & S. Lambert (Eds.), *Freshwater Microplastics*, *The Handbook of Environmental Chemistry*, vol. 58, Springer, Cham.

Kowalski, N., Reichardt, A. M., Waniek, J. J., 2016. Sinking rates of microplastics and potential implications of their alteration by physical, biological, and chemical factors. *Mar. Pollut. Bull.* 109(1), 310-319.

Law, K. L., Thompson, R. C., 2014. Microplastics in the seas. *Science* 345(6193), 144-145.

Lee, K. W., Shim, W. J., Kwon, O. Y., Kang, J. H., 2013. Size-dependent effects of micro polystyrene particles in the marine copepod *Tigriopus japonicas*. *Environ. Sci. Technol.* 47(19), 11278-11283.

Lei, L., Wu, S., Lu, S., Liu, M., Song, Y., Fu, Z., Shi, H., Raley-Susman, K. M., He, D., 2018. Microplastic particles cause intestinal damage and other adverse effects in zebrafish *Danio rerio* and nematode *Caenorhabditis elegans*, *Sci. Total Environ.* 619-620, 1-8.

Li, Y., Zhang, H., Tang, C., 2020. A review of possible pathways of marine microplastics transport in the ocean. *Anthropocene Coasts* 3, 6-13.

Lusher, A. L., McHugh, M., Thompson, R. C., 2013. Occurrence of microplastics in the gastrointestinal tract of pelagic and demersal fish from the English Channel. *Mar. Pollut. Bull.* 67(1-2), 94-99.

Lu, K., Qiao, R., An, H., Zhang, Y., 2018. Influence of microplastics on the accumulation and chronic toxic effects of cadmium in zebrafish (*Danio rerio*). *Chemosphere* 202, 514-520.

Lu, Y., Zhang, Y., Deng, Y., Jiang, W., Zhao, Y., Geng, J., Ren, H., 2016. Uptake and accumulation of polystyrene microplastics in zebrafish (*Danio rerio*) and toxic effects in liver. *Environ. Sci. Technol.* 50(7), 4054-4060.

Magni, S., Binelli, A., Pittura, L., Avio, C. G., Della Torre, C., Parenti, C. C., Gorbi, S., Regoli, F., 2019. The fate of microplastics in an Italian Wastewater Treatment Plant. *Sci. Total Environ.* 652, 602-610.

Ma, J., Zhao, J. H., Zhu, Z. L., Li, L. Q., Yu, F., 2019. Effect of microplastic size on the adsorption behavior and mechanism of triclosan on polyvinyl chloride. *Environ. Pollut.* 254, 113104.

Mattsson, K., Hansson, L. A., Cedervall, T., 2015. Nano-plastics in the aquatic environment. *Environ. Sci. Process. Impacts* 17(10), 1712-1721.

Mattsson, K., Ekvall, M. T., Hansson, L. A., Linse, S., Malmendal, A., Cedervall, T., 2015. Altered behavior, physiology, and metabolism in fish exposed to polystyrene nanoparticles. *Environ. Sci. Technol.* 49(1), 553-561.

Mohamed Nor, N. H., Koelmans, A. A., 2019. Transfer of PCBs from microplastics under simulated gut fluid conditions is biphasic and reversible. *Environ. Sci. Technol.* 53(4), 1874-1883.

Munari, C., Infantini, V., Scoponi, M., Rastelli, E., Corinaldesi, C., Mistri, M., 2017. Microplastics in the sediments of terra nova bay (ross sea, Antarctica). *Mar. Pollut. Bull.* 122, 161.

Murray, F., Cowie, P. R., 2011. Plastic contamination in the decapod crustacean *Nephrops norvegicus* (Linnaeus, 1758). *Mar. Pollut. Bull.* 62(6), 1207-1217.

Nicholson, J. (2006). Polymers and The Environment, *The Chemistry of Polymers*, Royal Society of Chemistry.

Nicholson, J. (2017). *The Chemistry of Polymers*, Royal Society of Chemistry.

Ohishi T., Otsuka H. (2014) PET (Poly(ethylene terephthalate)) and PTT (Poly(trimethylene terephthalate)). In S. Kobayashi & K. Müllen (Eds.), *Encyclopedia of Polymeric Nanomaterials*. Springer, Berlin, Heidelberg.

Okamura T. (2014) Polyethylene (PE; Low Density and High Density). In S. Kobayashi & K. Müllen (Eds.), *Encyclopedia of Polymeric Nanomaterials*. Springer, Berlin, Heidelberg.

Oliveira, M., Almeida, M., Miguel, I., 2019. A micro(nano)plastic boomerang tale: A never ending story? *Curr. Trends Anal. Chem.* 112, 196-200.

Oliveira, M., Ribeiro, A., Hylland, K., Guilermino, L., 2013. Single and combined effects of microplastics and pyrene on juveniles (0+ group) of the common goby *Pomatoschistus microps* (Teleostei, Gobiidae). *Ecol. Ind.* 34, 641-647.

Ory, N. C., Sobral, P., Ferreira, J. L., Thiel, M., 2017. Amberstripe scad *Decapterus muroads*i (Carangidae) fish ingest blue microplastics resembling their copepod prey along the coast of Rapa Nui (Easter Island) in the South Pacific subtropical gyre. *Sci. Total Environ.* 586, 430-437.

Osborn, M., Stojkovic S., 2014. Marine microbes in the Plastic Age. *Microbiology Australia* 35, 207-210.

Pannetier, P., Cachot, J., Clérandeau, C., Faure, F., Van Arkel, K., de Alencastro, L. F., Levasseur, C., Sciacca, F., Bourgeois, J. P., Morin, B., 2019. Toxicity assessment of pollutants sorbed on environmental sample microplastics collected on beaches: Part I-adverse effects on fish cell line. *Environ. Pollut.* 248, 1088-1097.

Pannetier, P., Morin, B., Le Bihanic, F., Dubreil, L., Clérandeau, C., Chouvellon, F., Van Arkel, K., Danion, M., Cachot, J., 2020. Environmental samples of microplastics induce significant toxic effects in fish larvae. *Environ. Int.* 134, 105047.

Paul-Pont, I., Lacroix, C., Gonzalez Fernandez, C., Hegaret, H., Lambert, C., Le Goïc, N., Frere, L., Cassone, A. L., Sussarellu, R., Fabioux, C., Guyomarch, J., Albentosa, M., Huvet, A., Soudant, P., 2016. Exposure of marine mussels *Mytilus* spp. to polystyrene microplastics: toxicity and influence on fluoranthene bio-accumulation. *Environ. Pollut.* 216, 724-737.

Pedà, C., Caccamo, L., Fossi, M. C., Gai, F., Andaloro, F., Genovese, L., Perdichizzi, A., Romeo, T., Maricchiolo, G., 2016. Intestinal alterations in European sea bass *Dicentrarchus labrax* (Linnaeus, 1758) exposed to microplastics: Preliminary results. *Environ. Pollut.* 212, 251-256.

Peeken, I., Primpke, S., Beyer, B., Gütermann, J., Katlein, C., Krumpen, T., Bergmann, M., Hehemann, L., Gerdts, G., 2018. Arctic sea ice is an important temporal sink and means of transport for microplastic. *Nat. Commun.* 9.

Pitt, J. A., Kozal, J. S., Jayasundara, N., Massarsky, A., Trevisan, R., Geitner, N., Wiesner, M., Levin, E. D., Di Giulio, R. T., 2018a. Uptake, tissue distribution, and toxicity of polystyrene nanoparticles in developing zebrafish (*Danio rerio*). *Aquat. Toxicol.* 194, 185-194.

Pitt, J. A., Trevisan, R., Massarsky, A., Kozal, J. S., Levin, E. D., Di Giulio, R. T., 2018b. Maternal transfer of nanoplastics to offspring in zebrafish (*Danio rerio*): A case study with nanopolystyrene. *Sci. Total Environ.* 643, 324-334.

Plastics Europe (2019) Plastics – the facts 2019. An analysis of European latest plastics production, demand and waste data. http://www.plasticseurope.org/Document/plastics-the-facts-2019.aspx.

Prinz, N., Korez, Š. 2020. Understanding how microplastics affect marine biota on the cellular level is important for assessing ecosystem function: A review. In S. Jungblut, V. Liebich & M. Bode-Dalby M. (Eds.) *YOUMARES 9 - The Oceans: Our Research, Our Future*. Springer, Cham.

Qiang, L., Cheng, J., 2019. Exposure to microplastics decreases swimming competence in larval zebrafish (*Danio rerio*). *Ecotoxicol. Environ. Saf.* 176, 226-233.

Qiao, R., Lu, K., Deng, Y., Ren, H., Zhang, Y., 2019. Combined effects of polystyrene microplastics and natural organic matter on the accumulation and toxicity of copper in zebrafish. *Sci. Total Environ.* 682, 128-137.

Rainieri, S., Conlledo, N., Larsen, B. K., Granby, K., Barranco, A., 2018. Combined effects of microplastics and chemical contaminants on the organ toxicity of zebrafish (*Danio rerio*). *Environ. Res.* 162, 135-143.

Rehse, S., Kloas, W., Zarfl, C., 2016. Short-term exposure with high concentrations of pristine microplastic particles leads to immobilisation of *Daphnia magna*. *Chemosphere* 153, 91-99.

Rezania, S., Park, J., Md Din, M. F., Mat Taib, S., Talaiekhozani, A., Kumar Yadav, K., Kamyab, H., 2018. Microplastics pollution in different aquatic environments and biota: A review of recent studies. *Mar. Pollut. Bull.* 133, 191-208.

Rhodes, C. J., 2018. Plastic pollution and potential solutions. *Sci. Prog.* 101(3), 207-260.

Rist, S., Assidqi, K., Zamani, N. P., Appel, D., Perschke, M., Huhn, M., Lenz, M., 2016. Suspended micro-sized PVC particles impair the performance and decrease survival in the Asian green mussel *Perna viridis*. *Mar. Pollut. Bull.* 111(1-2), 213-220.

Rist, S., Baun, A., Hartmann, N. B., 2017. Ingestion of micro- and nanoplastics in *Daphnia magna* - Quantification of body burdens and assessment of feeding rates and reproduction. *Environ. Pollut.* 228, 398-407.

Rist, S., Hartmann, N. B. (2018). Aquatic Ecotoxicity of Microplastics and Nanoplastics: Lessons Learned from Engineered Nanomaterials. In M. Wagner & S. Lambert (Eds.), *Freshwater Microplastics, The Handbook of Environmental Chemistry*, vol. 58, Springer, Cham.

Rochman, C. (2015). The Complex Mixture, Fate and Toxicity of Chemicals Associated with Plastic Debris in the Marine Environment. In M. Bergmann, L. Gutow & M. Klages (Eds.), *Marine Anthropogenic Litter*. Springer, Cham.

Rochman, C., Kurobe, T., Flores, I., Teh, S. J., 2014. Early warning signs of endocrine disruption in adult fish from the ingestion of polyethylene with and without sorbed chemical pollutants from the marine environment. *Sci. Total Environ.* 493, 656-661.

Rochman, C., Tahir, A., Williams, S., Baxa, D. V., Lam, R., Miller, J. T., Teh, F., Werorilangi, S., Teh, S. J., 2015. Anthropogenic debris in seafood: Plastic debris and fibers from textiles in fish and bivalves sold for human consumption. *Sci. Rep.* 5, 14340.

Roch, S., Friedrich, C., Brinker, A., 2020. Uptake routes of microplastics in fishes: practical and theoretical approaches to test existing theories. *Sci. Rep.* 10, 3896.

Rodriguez-Seijo, A., Lourenço, J., Rocha-Santos, T. A. P., da Costa, J., Duarte, A. C., Vala, H., Pereira, R., 2017. Histopathological and molecular effects of microplastics in *Eisenia andrei* Bouché. *Environ. Pollut.* 220(A), 495-503.

Rummel, C. D., Löder, M. G., Fricke, N. F., Lang, T., Griebeler, E., Janke, M., Gerdts, G., 2016. Plastic ingestion by pelagic and demersal fish from the North Sea and Baltic Sea. *Mar. Pollut. Bull.* 102(1), 134-141.

Savoca, M. S., Tyson, C. W., McGill, M., Slager, C. J., 2017. Odours from marine plastic debris induce food search behaviours in a forage fish. *Proc. R. Soc. B* 284, 20171000.

Schür, C., Rist, S., Baun, A., Mayer, P., Hartmann, N. B., Wagner, M., 2019. When fluorescence is not a particle: The tissue translocation of microplastics in *Daphnia magna* seems an artifact. *Environ. Toxicol. Chem.* 38(7), 1495-1503.

Shen, M., Zhang, Y., Zhu, Y., Song, B., Zeng, G., Hu, D., Wen, X., Ren, X., 2019. Recent advances in toxicological research of nanoplastics in the environment: A review. *Environ. Pollut.* 252(A), 511-521.

Sjollema, S. B., Redondo-Hasselerharm, P., Leslie, H. A., Kraak, M. H. S., Vethaak, A. D., 2016. Do plastic particles affect microalgal photosynthesis and growth? *Aquat. Toxicol.* 170, 259-261.

Suaria, G., Avio, C. G., Mineo, A., Lattin, G. L., Magaldi, M. G., Belmonte, G., Moore, C. J., Regoli, F., Aliani, S., 2016. The Mediterranean Plastic Soup: Synthetic polymers in Mediterranean surface waters. *Sci. Rep.* 6, 37551.

Sussarellu, R., Suquet, M., Thomas, Y., Lambert, C., Fabioux, C., Pernet, M. E. J., Le Goïc, N., Quillien, V., Mingant, C., Epelboin, Y., Corporeau, C., Guyomarch, J., Robbens, J., Paul-Pont, I., Soudant, P., Huvet, A., 2016. Oyster reproduction is affected by exposure to polystyrene microplastics. *Proc. Natl. Acad. Sci. USA* 113(9), 2430-2435.

Su, Y., Zhang, Z., Wu, D., Zhan, L., Shi, H., Xie, B., 2019. Occurrence of microplastics in landfill systems and their fate with landfill age. *Water Res.* 164, 114968.

Takeoka Y. (2014) Poly(vinyl chloride) (PVC). In S. Kobayashi & K. Müllen (Eds.), *Encyclopedia of Polymeric Nanomaterials*. Springer, Berlin, Heidelberg.

Tanaka, K. Takada, H., 2016. Microplastic fragments and microbeads in digestive tracts of planktivorous fish from urban coastal waters. *Sci. Rep.* 6, 34351.

Terashima T. (2014) Polystyrene (PSt). In S. Kobayashi & K. Müllen (Eds.), *Encyclopedia of Polymeric Nanomaterials*. Springer, Berlin, Heidelberg.

Teuten, E. L., Saquin, J. M., Knappe, D. R. U., Barlaz, M. A., Jonsson, S., Björn, A., Rowland, S. J., Thompson, R. C., Galloway, T. S., Yamashita, R., Ochi, D., Watanuki, Y., Moore, C., Viet, P. H., Tana, T. S., Prudente, M., Boonyatumanond, R., Zakaria, M. P., Akkhavong, K., Ogata, Y., Hirai, H., Iwasa, S., Mizukawa, K., Hagino, Y., Imamura, A., Saha, M., Takada, H., 2009. Transport and release of chemicals from plastics to the environment and to wildlife. *Philos. Trans. R. Soc. Lond. B Biol. Sci.* 364, 2027-2045.

ter Halle, A., Ladirat, L., Gendre, X., Goudouneche, D., Pusineri, C., Routaboul, C., Tenailleau, C., Duployer, B., Perez, E. 2016. Understanding the fragmentation pattern of marine plastic debris. *Environ. Sci. Technol.* 50(11), 5668-5675.

Thompson, R. C., Moore, C. J., vom Saal, F. S., Swan, S. H., 2009. Plastics, the environment and human health: current consensus and future trends. *Philos. Trans. R. Soc. Lond. B Biol. Sci.* 364(1526), 2153-2166.

Van Cauwenberghe, L., Janssen, C. R., 2014. Microplastics in bivalves cultured for human consumption. *Environ. Pollut.* 193, 65-70.

van den Berg, P., Huerta-Lwanga, E., Corradini, F., Geissen, V., 2020. Sewage sludge application as a vehicle for microplastics in eastern Spanish agricultural soils. *Environ. Pollut.* 261, 114198.

van Pomeren, M., Brun, N. R., Peijnenburg, W. J. G. M., Vijver, M. G., 2017. Exploring uptake and biodistribution of polystyrene (nano)particles in zebrafish embryos at different developmental stages. *Aquat. Toxicol.* 190, 40-45.

von Moos, N., Burkhardt-Holm, P., Köhler, A., 2012. Uptake and effects of microplastics on cells and tissue of the blue mussel *Mytilus edulis* L. after an experimental exposure. *Environ. Sci. Technol.* 46(20), 11327-11335.

Wang, W., Ndungu, A. W., Li, Z., Wang, J., 2017. Microplastics pollution in inland freshwaters of China: A case study in urban surface waters of Wuhan, China. *Sci. Total Environ.* 575, 1369-1374.

Wang, J., Lu, L., Wang, M., Jiang, T., Liu, X., Ru, S., 2019. Typhoons increase the abundance of microplastics in the marine environment and cultured organisms: A case study in Sanggou Bay, China. *Sci. Total Environ.* 667, 191-198.

Zeng, E., 2018. Microplastic Contamination in Aquatic Environments: An Emerging Matter of Environmental Urgency. Elsevier.

Zhang, C., Chen, X., Wang, J., Tan, L., 2017. Toxic effects of microplastic on marine microalgae *Skeletonema costatum*: Interactions between microplastic and algae. *Environ. Pollut.* 220(B), 1282-1288.

Zhang, Q., Qu, Q., Lu, T., Ke, M., Zhu, Y., Zhang, M., Zhang, Z., Du, B., Pan, X., Sun, L., Qian, H., 2018. The combined toxicity effect of nanoplastics and glyphosate on *Microcystis aeruginosa* growth. *Environ. Pollut.* 243(B), 1106-1112.

Zhang, S., Ding, J., Razanajatovo, R. M., Jiang, H., Zou, H., Zhu, W., 2019. Interactive effects of polystyrene microplastics and roxithromycin on bioaccumulation and biochemical status in the freshwater fish red tilapia (*Oreochromis niloticus*). *Sci. Total Environ.* 648, 1431-1439.

Zhao, S., Zhu, L., Li, D., 2016. Microscopic anthropogenic litter in terrestrial birds from Shanghai, China: Not only plastics but also natural fibers. *Sci. Total Environ.* 550, 1110-1115.